

## Conversion of Polymeric Substrates by Aerobic Granular Sludge

Toja Ortega, S.

**DOI**

[10.4233/uuid:32c437c1-b0eb-48a5-8a42-cdf9fb396a7f](https://doi.org/10.4233/uuid:32c437c1-b0eb-48a5-8a42-cdf9fb396a7f)

**Publication date**

2023

**Document Version**

Final published version

**Citation (APA)**

Toja Ortega, S. (2023). *Conversion of Polymeric Substrates by Aerobic Granular Sludge*. [Dissertation (TU Delft), Delft University of Technology]. <https://doi.org/10.4233/uuid:32c437c1-b0eb-48a5-8a42-cdf9fb396a7f>

**Important note**

To cite this publication, please use the final published version (if applicable).  
Please check the document version above.

**Copyright**

Other than for strictly personal use, it is not permitted to download, forward or distribute the text or part of it, without the consent of the author(s) and/or copyright holder(s), unless the work is under an open content license such as Creative Commons.

**Takedown policy**

Please contact us and provide details if you believe this document breaches copyrights.  
We will remove access to the work immediately and investigate your claim.

# **Conversion of Polymeric Substrates by Aerobic Granular Sludge**

**Sara Toja Ortega**



# **Conversion of Polymeric Substrates by Aerobic Granular Sludge**

## **Dissertation**

for the purpose of obtaining the degree of doctor

at Delft University of Technology

by the authority of the Rector Magnificus, prof.dr.ir. T.H.J.J. van der Hagen,

chair of the Board for Doctorates

to be defended publicly on

Tuesday 30 May 2023 at 10:00 o'clock

by

**Sara TOJA ORTEGA**

Máster Universitario en Microbiología, Universidad Autónoma de Madrid, Spain

born in Galdakao, Spain



This dissertation has been approved by the promotor.

Composition of the doctoral committee:

Rector Magnificus,	chairperson
Prof.dr.ir. M.K. de Kreuk	Delft University of Technology, promotor
Dr. ing. M. Pronk	Delft University of Technology, copromotor

Independent members:

Prof.dr.ir. J.B.Van Lier	Delft University of Technology
Prof. dr. ir. E. Morgenroth	Swiss Federal Institute of Technology Zürich, Switzerland
Prof. dr. ir. D. Weissbrodt	Norwegian University of Science and Technology, Norway
Prof. dr. ir. I. Smets	KU Leuven, Belgium
Prof. dr. A. Mosquera Corral	University of Santiago de Compostela, Spain
Prof.dr.ir. D. van Halem	Delft University of Technology, reserve member

The research presented in this thesis was performed at the Sanitary Engineering Section, Department of Water Management, Faculty of Civil Engineering, Delft University of Technology, The Netherlands. The research was financially supported by the NWO VIDI grant 016.168.320.

Cover illustration: Confocal microscope image of a stained aerobic granule section. Blue=bacteria, Purple=GAO, Green=active microorganisms.

Copyright © 2023 by S. Toja Ortega

ISBN 978-94-6384-445-1

Printed by Proefschrift-aio.nl

An electronic version of this dissertation is available at <http://repository.tudelft.nl/>

---

# Contents

	Summary	vi
	Samenvatting	vi
Chapter 1	Introduction	1
Chapter 2	Effect of an increased particulate COD load on the AGS process	15
Chapter 3	Anaerobic hydrolysis of complex substrates in full-scale aerobic granular sludge	49
Chapter 4	Hydrolysis capacity of different sized granules in a full-scale AGS reactor	79
Chapter 5	Anaerobic uptake of monomers and polymers by full-scale aerobic granules	109
Chapter 6	Outlook	135
	References	145
	Acknowledgements	162
	Curriculum Vitae	164
	List of Publications	165

## Summary

Domestic wastewater is treated prior to its return to natural water bodies, to minimize its polluting effect. Biological wastewater treatment removes organic matter and nutrients from the wastewater, by employing the activity of microorganisms, which consume polluting compounds present in wastewater to grow. One of such technologies is aerobic granular sludge (AGS), which consists of self-immobilized microorganisms growing in spherical biofilms. The granular structure facilitates the separation between treated water and the biomass due to its excellent settling properties. This way, energy and space are saved in comparison to flocculent sludge-based treatment.

Despite its many advantages, the granular structure can pose some challenges too, particularly regarding the degradation of polymeric substrates. The higher mass-transfer resistance in granules compared to flocs challenges the degradation of these substrates, which have a size spanning from a few kDa to several micrometres. Polymeric substrates, furthermore, need to undergo hydrolysis before microorganisms can take them up, which is generally a slow process. Most AGS applications rely on microbial selection driven by the application of a sequencing batch reactor (SBR) cycle. The cycle consists of an anaerobic substrate feeding and a subsequent aerobic starvation period, which selects for intracellular polymer-storing organisms, such as polyphosphate accumulating organisms (PAO) and glycogen accumulating organisms (GAO). Substrates that experience high mass-transfer limitation and low degradation rates may interfere with the microbial selection strategy applied to AGS, especially when they are not (fully) taken up in the anaerobic feeding period and continue degrading aerobically in the next cycle phase. Some lab-scale studies have reported detrimental effects of polymeric substrates in AGS structure and activity, while others have managed to maintain a stable granule bed and suggest that the microbial utilization of polymeric substrates can contribute to good nutrient removal. The degradation of polymeric substrates by full-scale aerobic granules is still poorly understood.

To assess the effect of polymeric substrates in full-scale AGS, we monitored the treatment performance and sludge characteristics in a full-scale AGS installation fed with an increased particulate load (chapter 2). The sludge characteristics did not deteriorate during the four months of altered operation, while the large (>1 mm) granule fraction continued to increase in the reactors. Granules and flocs coexisted in the reactors, although granules were the main biomass fraction (>80%), and both fractions exhibited high hydrolytic capacities. During the experiment, excellent effluent quality was maintained, and denitrification rates increased. Combining these

observations, it appears that particulate substrates were not detrimental to granules and could be significantly utilized by microorganisms performing biological nutrient removal.

The hydrolytic capacity of the different components in an AGS reactor was further studied, and described in chapter 3. Here, we quantified the maximum protease, lipase and  $\alpha$ - and  $\beta$ -glucosidase activities in influent wastewater, reactor mixed liquor, bulk liquid, large granules (>1 mm), small granules (0.2-1 mm) and flocs (<0.2 mm). Our results showed that, even though flocs had the highest biomass-specific activity, granules contained most of the hydrolytic capacity in the AGS reactor. This was supported by a relatively high biomass-specific activity of granules, and the high abundance of this biomass fraction in the reactor. The high hydrolytic activities measured in large granules suggested that they can utilize a significant amount of polymeric substrate during anaerobic feeding.

In chapter 4, the location of hydrolysis is described in more detail. This study revealed that hydrolysis is strongly surface-limited in AGS. The surface-specific hydrolytic activity was similar for all granule sizes in an AGS reactor. Thus, no differentiation was found between granules of different sizes in terms of hydrolytic activity. Granules of different sizes did exhibit different enhanced biological phosphorus removal (EBPR) activity and microbial community composition. For practical applications, the available granule surface area will determine hydrolysis rates, more than the reported different microbial community composition of the granules of different sizes. Furthermore, the microorganisms below the outer 100  $\mu\text{m}$  of the granules are unlikely to utilize polymeric substrates from the wastewater.

Chapter 5 describes the anaerobic utilization of substrates that may be found in wastewater or result from hydrolysis of wastewater substrates, including volatile fatty acids (VFA), amino acids and carbohydrates. Substrate uptake, P release and PHA accumulation were measured. All studied substrates were consumed, most significantly VFA, glucose and a mixture of amino acids. Some of the substrates also induced significant P release indicating an involvement in EBPR. The uptake of proteins (particulate, colloidal and soluble casein) was further examined and compared to that of an amino acids mixture. Amino acids were taken up quickly and were associated to P release and PHA accumulation. Protein uptake was considerably slower; even the hydrolysis rate of soluble casein was too low to expect a significant amount of proteins to be stored during one hour of anaerobic feeding. However, the monomers derived from polymer hydrolysis can be relevant to supplement the VFA found in wastewater, especially when the wastewater has low or variable VFA content.

On the whole, this thesis demonstrates that aerobic granules can hydrolyse polymers on their surface or just below the surface, in higher or lower degree depending on the available surface area and contact time. Considering the substrate concentrations found generally in the influent of domestic wastewater treatment plants, hydrolysis rates are low, and hence the contribution of polymeric substrates to EBPR will be limited during a standard 1-hour anaerobic plug-flow feeding period. Aerobic hydrolysis by the AGS of the polymers left after the anaerobic feeding phase will also be slow, presumably slower than anaerobic hydrolysis since the wastewater pollutants are diluted by mixing with the reactor bulk liquid. The results of this study evidence that polymeric substrates are not a matter of concern in fully granulated AGS systems, and may be beneficial to the AGS process if specific conditions are applied to boost their anaerobic uptake.

# Samenvatting

Verontreinigingen in huishoudelijk afvalwater hebben een negatief effect op het milieu; daarom wordt afvalwater behandeld voordat het geloosd wordt op het oppervlaktewater. Biologische behandeling van afvalwater verwijdt organische stoffen en nutriënten uit het afvalwater door gebruik te maken van de activiteit van micro-organismen, die deze stoffen omzetten om te groeien. Eén van de technieken voor afvalwaterbehandeling is aeroob korrelslib (aerobic granular sludge, AGS), een slibvorm die bestaat uit zelf-geïmmobiliseerde micro-organismen die groeien in korrelvormige structuren. De korrelvormige structuur vergemakkelijkt de scheiding tussen behandeld water en biomassa door de uitstekende bezinkingskenmerken van het slib. Alle processen van de afvalwaterzuivering kunnen in één reactor plaatsvinden, zonder ingewikkelde recirculatiestromen. Hierdoor wordt energie en ruimte bespaard in vergelijking met de conventionele actief slib systemen.

Ondanks de vele voordelen kan de korrelstructuur ook voor uitdagingen zorgen, met name met betrekking tot de afbraak van polymeren, die een grootte hebben variërend van enkele kDa tot micrometers. De beperkte diffusie van deze stoffen in de korrel, zorgt voor een ander afbraak mechanisme dan in conventioneel vlokkig slib. Polymeren moeten bovendien gehydroliseerd worden voordat micro-organismen ze kunnen opnemen, wat een langzaam proces is. De meeste AGS-systemen maken gebruik van een sequencing batch-reactor (SBR). De SBR-cyclus bestaat uit het langzaam anaeroob voeden van het influent in een propstroom vanaf de bodem van de reactor en gelijktijdige effluent aflat, en een daaropvolgende aërobe reactie fase, gevolgd door een korte bezinkfase, waarna weer een nieuwe cyclus begint. Deze opbouw van de cyclus selecteert voor bacteriën die de snel afbreekbare organische stof anaeroob kunnen opslaan in hun cellen, zoals polyfosfaat-accumulerende organismen (PAO) en glycogeen-accumulerende organismen (GAO). Organisch substraat met een beperkte stof overdracht tijdens de anaerobe fase, en lage afbraaksnelheden, kunnen de korrelvorming verstoren; vooral wanneer ze niet (volledig) worden opgenomen tijdens de anaërobe voedingsperiode en tijdens de aërobe periode worden omgezet door snel groeiende heterotrofe organismen. Sommige studies op laboratoriumschaal hebben de negatieve invloed van polymeren op de korrelstructuur en -activiteit aangetoond, terwijl andere studies een stabiel korrelbed wisten te handhaven en een positieve invloed van polymeren op de nutriëntenverwijdering suggereerden. Echter, de rol van polymeren in AGS reactoren in praktijkinstallaties is nog steeds slecht begrepen.

Om het effect van polymeren in AGS praktijkinstallaties te begrijpen, hebben we de zuiveringsprestatie en slibkenmerken gemonitord in de AGS reactoren op RWZI Epe, die tijdelijk gevoed werden met een verhoogde belasting onopgelost substraat (hoofdstuk 2). De morfologie van het slib verslechterde niet gedurende het vier maanden durende experiment, terwijl de fractie van grote ( $>1$  mm) korrels toenam in de reactoren. Zowel korrels als vlokkelig slib kwamen samen voor in de reactoren, waarbij de korrels de belangrijkste biomassafractie vormden ( $>80\%$ ). Beide slibmorfologiën vertoonden een hoge hydrolytische capaciteit. Tijdens het experiment werd een uitstekende effluentkwaliteit gehandhaafd en nam de denitrificatiesnelheid toe. Deze waarnemingen suggereren dat onopgelost organisch substraat niet schadelijk was voor korrelvorming en gebruikt kan worden door de denitrificerende organismen.

De hydrolytische capaciteit van de verschillende slibfracties in een AGS-reactor werd verder onderzocht en resultaten zijn beschreven in hoofdstuk 3. Hier kwantificeerden we de maximale protease, lipase en  $\alpha$ - en  $\beta$ -glucosidase activiteiten in het influent en in de reactor. Daarnaast werden de bulkvloeistof, grote korrels ( $>1$  mm), kleine korrels (0,2-1 mm) en slibvlokken ( $<0,2$  mm) apart geanalyseerd. Resultaten lieten zien dat, hoewel de vlokken de hoogste biomassa-specifieke hydrolytische activiteit hadden, de korrels de grootste bijdrage vormden aan de totale hydrolytische capaciteit in de AGS-reactor. Dit kwam met name door de hoge fractie aan korrels in de reactor, gecombineerd met een relatief hoge biomassa-specifieke activiteit van de korrels. De hoge hydrolytische activiteiten gemeten in de grote korrels suggereert dat een aanzienlijke deel van de gevoede organische polymeren tijdens anaërobe voeding omgezet en opgenomen kan worden door het korrelslib.

In hoofdstuk 4 wordt de locatie van hydrolytische activiteit gedetailleerder beschreven. De oppervlakte specifieke hydrolytische activiteit was vergelijkbaar voor alle korrelgroottes in een AGS-reactor, en dus bepaalt de grootte van het oppervlak van de korrels de activiteit, en niet de totale biomassa in de korrels. Korrels van verschillende groottes hadden wel een verschillende microbiële samenstelling en vertoonden verschillen in de fosfaatverwijdering. In de praktijk zal echter het oppervlakte van de korrels bepalender zijn voor de hydrolysesnelheid, dan de verschillen in microbiële samenstelling van korrels van verschillende groottes. Bovendien zullen de polymere substraten niet meer beschikbaar zijn voor de micro-organismen die zich dieper dan 100  $\mu\text{m}$  in de korrel bevinden.

Hoofdstuk 5 beschrijft het de anaerobe opname van verschillende organische substraten, zoals vluchtige vetzuren (volatile fatty acids, VFA), aminozuren en koolhydraten. Deze substraten staan model voor de hydrolyse producten van de

polymeren die aanwezig kunnen zijn in afvalwater. Substraatopname, P-afgifte en PHA-ophoping werden gemeten. Alle onderzochte substraten werden anaeroob opgenomen: met name VFA, glucose en een mengsel van aminozuren vertoonden hoge opnamesnelheden. Sommige substraten veroorzaakten ook significante P-afgifte, wat wijst op het gebruik van deze substraten in de fosfaatverwijdering. De opname van eiwitten (onopgelost, colloïdaal en opgelost caseïne) werd verder onderzocht en vergeleken met de opname van een mengsel van aminozuren. Aminozuren werden snel opgenomen en waren geassocieerd met P-afgifte en PHA-ophoping, terwijl de opname van eiwitten aanzienlijk trager was. Zelfs de hydrolysesnelheid van opgelost caseïne was te laag om te verwachten dat een significante hoeveelheid eiwitten kan worden opgeslagen tijdens de anaerobe voeding, die gemiddeld ongeveer één uur duurt. Echter, monomeren, hydrolyse producten van de polymeren, kunnen wel relevant zijn om de biologische fosfaatverwijdering op peil te houden, vooral wanneer het afvalwater een laag of variabel VFA-gehalte heeft.

Over het geheel genomen laat het onderzoek in dit proefschrift duidelijk zien dat complexer organisch substraat wel degelijk potentie heeft om gebruikt te worden voor nutriënten verwijdering in aëroob korrelslib. Aërobe korrels kunnen polymeren op hun oppervlak of net onder het oppervlak hydrolyseren. De effectiviteit is afhankelijk van het beschikbare korreloppervlak en de anaërobe contacttijd tussen influent en de korrels. Over het algemeen zijn de substraatconcentraties van de polymere substraten in huishoudelijk afvalwater relatief laag, wat ook resulteert in relatief lage de hydrolysesnelheden. Daarom zal de bijdrage van dergelijke substraten aan de biologische P-verwijdering beperkt zijn. Vooral omdat de anaërobe voedingstijd over het algemeen relatief kort is. Echter, ook de aërobe hydrolyse van de polymeren die overblijven na de anaërobe voedingsfase zal ook traag zijn; vermoedelijk trager dan anaërobe hydrolyse, omdat de verontreinigende stoffen in het afvalwater worden verdund door menging van de reactortijdens de beluchting. Daarom zal het beschikbare substraat tijdens de beluchtingsfase beperkt zijn en weinig invloed hebben op de korrelmorfologie. Polymeren kunnen mogelijk zelfs gunstig zijn voor het AGS-proces als specifieke procescondities worden toegepast om de anaerobe hydrolyse en opname te stimuleren.





# 1

## Introduction

## 1.1 | AEROBIC GRANULAR SLUDGE FOR BIOLOGICAL WASTEWATER TREATMENT

Wastewater is an unavoidable by-product of many human activities. It originates in different contexts, such as domestic use or industrial processes, and often gets diluted with rainwater or groundwater (Henze and Comeau, 2008). Wastewater contains several components that make it potentially harmful for human health, such as pathogenic bacteria and/or toxic compounds, leading to a threat for public health upon direct disposal. Furthermore, wastewater is rich in organic matter and nutrients, such as phosphorus and nitrogen compounds. Microbial consumption of these compounds leads to oxygen depletion and eutrophication in the receiving water bodies (e.g. rivers), if their self-purifying capacity is exceeded (Chen et al., 2020; Metcalf & Eddy, 2003). In the current context of an increasing world population and expansion of cities, efficient wastewater treatment is essential to protect human health and the environment.

While until the 1970s wastewater treatment focused on particulate and pathogen removal, it progressively evolved to achieve higher quality standards and improve environmental protection (Jenkins and Wanner, 2014). Currently, most treatment plants combine several treatment steps to remove different types of pollutants from wastewater. Biological treatment is the core process in most plants, where organic matter, or chemical oxygen demand (COD), is removed by microorganisms cultivated in a reactor (Chen et al., 2020). Often, the microorganisms additionally remove nitrogen and phosphorus, which is known as biological nutrient removal (BNR). For many years, the preferred wastewater treatment system has been conventional activated sludge (CAS), an aerated treatment based on microorganisms growing in suspension (flocs) (Jenkins and Wanner, 2014). Even though the CAS process is an established technology, it has high energy and space requirements. Separating the microbial flocs from the treated wastewater requires a large surface of sedimentation tanks, and recirculation pumps that return the settled sludge back to the main reactor. In a global scenario of increasing concern about climate change, and decreasing space in the urban areas, alternative technologies to CAS are on demand (Bengtsson et al., 2018; Chen et al., 2020; de Bruin et al., 2004).

One of such technologies is aerobic granular sludge (AGS), a more compact version of CAS. AGS was described for the first time during the 1990s, and scaled up in the next decade in collaboration between TU Delft, Dutch water authorities, and the consulting and engineering firm Royal HaskoningDHV (de Bruin et al., 2004; De Kreuk, 2006; Mishima and Nakamura, 1991; Morgenroth et al., 1997; van der Roest et al., 2011).

Today, AGS is operated in full-scale plants under the tradename Nereda®. The basis of AGS are aerobic granules, a type of carrier-free biofilm with a similar microbial community as CAS, but with remarkably better settling properties (de Kreuk et al., 2007; Toh et al., 2003; van Dijk et al., 2020). This enables separating the treated water from the sludge within the biological reactor, eliminating the need for sedimentation tanks and a recycle system. As a result, AGS has a considerably lower footprint than CAS (33% lower), as well as a reduced energy demand (50-75% lower) (Pronk et al., 2015b). Furthermore, higher sludge concentrations can be maintained, which translate into high conversion rates. Accordingly, AGS can achieve very low COD, P and N effluent concentrations.



**Figure 1.1.** Aerobic granular sludge separated in different size ranges.

## 1.2 | BIOLOGICAL NUTRIENT REMOVAL AND SBR CYCLE

Nitrogen and phosphorus can be removed from wastewater by microorganisms, if different redox conditions are provided sequentially.

**Phosphorus** is removed from wastewater through enhanced biological phosphorus removal (EBPR). EBPR is achieved by combining anaerobic feast and aerobic famine conditions, promoting the growth of polyphosphate accumulating organisms (PAO) (Oehmen et al., 2007; Roy et al., 2021; Stokholm-Bjerregaard et al., 2017). During anaerobic feast conditions, PAO use polyphosphate as an energy source to take up COD and store it as intracellular storage polymers, such as poly-hydroxyalkanoates (PHA). During aerobic conditions, PAO consume intracellular storage compounds, and grow. They also take up phosphate from the medium to replenish their polyphosphate reserves. An EBPR system enriched in PAO can incorporate 0.06-0.15 mg P/mg VSS, compared to 0.02 mg P/mg VSS of a non-EBPR system (Chen et al., 2020). The net growth of PAO results in a net P removal from the medium.

**Nitrogen** is removed by transforming nitrogenous compounds to  $N_2$  and stripping  $N_2$  from the wastewater. The combined action of different microorganisms is needed for this (Ekama et al., 2020). First,  $NH_4^+$  is oxidized to  $NO_3^-$ , known as nitrification. Nitrifiers are aerobic autotrophs, which oxidize  $NH_4^+$  to  $NO_2^-$  (ammonia oxidizing bacteria, AOB) and  $NO_2^-$  to  $NO_3^-$  (nitrite oxidizing bacteria, NOB). The oxidation of  $NH_4^+$  to  $NO_3^-$  can also be performed directly by comammox bacteria (Koch et al., 2019). Then,  $NO_3^-$  is reduced to  $N_2$ , known as denitrification. Denitrifiers are anaerobic or facultative heterotrophs, which oxidize COD using  $NO_3^-$  as their final electron acceptor in the absence of oxygen. Hence, complete N removal requires the combination of aerobic and anoxic conditions.

CAS requires several reactor compartments with different redox conditions to remove COD, N and P. AGS, in contrast, can remove all these compounds in the same compartment, when operated in a sequencing batch reactor (SBR) mode. The typical SBR cycle consists of an anaerobic feeding phase, an aerobic reaction phase, settling, selection spill, and effluent discharge (Bengtsson et al., 2018; Derlon et al., 2016; Pronk et al., 2015b; van der Roest et al., 2011).

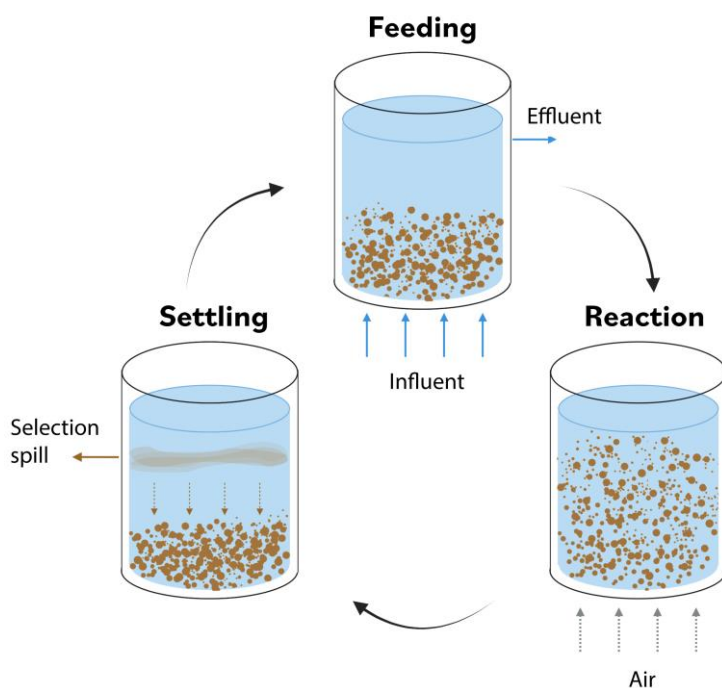


**Figure 1.2.** Typical SBR cycle employed for full-scale operation of AGS reactors.



**Anaerobic feeding.** In the anaerobic feeding period, the uptake of COD by PAO is promoted. Glycogen accumulating organisms (GAOs) also have the ability to store COD anaerobically, and are present in most plants. GAOs obtain energy from glycogen instead of polyphosphate, and therefore do not contribute to EBPR (Stokholm-Bjerregaard et al., 2017).

**Aeration.** In the aerobic phase, microbial growth occurs, and PAO take  $\text{PO}_4^{3-}$  up from the medium. Nitrification and denitrification also occur in this phase. The microorganisms in the surface of the granules consume oxygen, creating an oxygen concentration gradient throughout the granule. The coexisting anoxic and aerobic conditions in the granules allow simultaneous nitrification-denitrification (SND); denitrifiers in the granule core consume the  $\text{NO}_3^-$  produced by nitrifiers located in the outer layers. Once the  $\text{NH}_4^+$  concentration has reached the effluent consent, aeration can be turned off to promote denitrification, if some  $\text{NO}_3^-$  has built up in the medium due to incomplete SND. COD sources for denitrification can be PHA, in the case of denitrifying PAO and GAOs, or slowly biodegradable COD (sbCOD) left over.

**Settling and selection spill.** The settling phase is used to separate the granules from the treated effluent. Furthermore, settling velocity is used for biomass selection. The slow-settling sludge is selectively discharged in the spill.

**Effluent discharge.** The anaerobic feeding and effluent discharge are often combined: the influent is fed from the bottom of the reactor in a plug-flow, while the effluent is decanted from the top of the reactor. Plug-flow feeding serves a double purpose. Firstly, influent and effluent do not mix, keeping the effluent clean. Secondly, high substrate concentrations during feeding are reached around the sludge bed, settled at the bottom of the reactor. This promotes deeper substrate penetration into granules, higher substrate uptake rates and the enrichment of PAO in the granules close to the influent inlet.

## 1.3 | GRANULE STABILITY

Developing and maintaining stable granules is one of the major attention points in AGS treatment. A main strategy to ensure good granulation is the selection of slow-growing organisms, namely PAO and GAO, in the granules (de Kreuk et al., 2007; de Kreuk and van Loosdrecht, 2004). For that purpose, anaerobic substrate storage by PAO and GAO

is promoted, which is achieved by applying an anaerobic plug-flow feeding regime. When anaerobic feeding is applied, PAO and GAO have a competitive advantage over ordinary heterotrophic organisms (OHOs), due to their ability to store substrates and use them in the subsequent aerobic phase.

Granulation strategies are based on theoretical concepts on biofilm structure. Biofilm morphology is shaped by diffusion of the substrates into the biofilm, and the growth of the microorganisms that consume them. If substrate penetration into granules is limited and a diffusion gradient around the granules exists, microbial growth will occur towards the liquid, and protuberances will form. For granules to grow densely and smoothly, the formation of outgrowths on the granule surface has to be avoided or balanced by shear (Kwok et al., 1998; Tijhuis et al., 1996; van Loosdrecht et al., 1995). Moreover, the consumption rate of substrates will be low and the substrate can diffuse deeper in the granule and sustain biofilm growth there. When cells inside the biofilm reproduce, the biofilm density increases.

The diffusibility of the substrate is equally relevant for biofilm morphology. If the diffusion of a substrate is slow or consumption rate is high, steep substrate gradients originate at the granule-liquid interface. Then, different granule areas will have different exposure to the substrate (Picioreanu et al., 2000a). “Peaks” in the granule landscape experience higher substrate concentration than “valleys”. Microorganisms will grow faster in the peaks; especially if their maximum growth rate is high. Consequently, the granule surface will become more irregular over time, deteriorating the granule morphology (Picioreanu et al., 2000a). The filamentous outgrowths may ultimately break and lead to biomass loss and high effluent suspended solids.

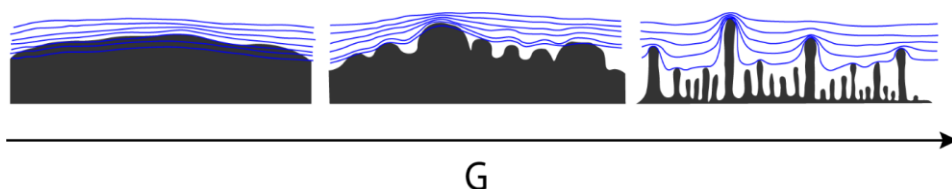


**Figure 1.3.** Representation of the effect of  $G$  (maximum biomass growth rate over maximum substrate diffusion rate) on biofilm structure (Adapted from Picioreanu et al., 1998). Lines of equal substrate concentration are depicted in blue. At low  $G$  values, smooth biofilms are formed. Substrate gradients are shallow and substrate is equally distributed throughout the biofilm surface. At high  $G$  values, steep substrate gradients lead to fast growth at the biofilm protuberances, enhancing the polarized substrate uptake and favouring more filamentous outgrowths and the development of an irregular granule surface.

In short, in a biofilm where substrate transport is diffusion-based, the rate between the maximum microbial growth rate and the substrate transport rate will determine the morphology of the biofilm (Picioreanu et al., 1998). This rate is represented by the parameter  $G$ , where a high  $G$  indicates a transport-limited regime and low  $G$  a growth-limited regime. A high  $G$  leads to irregular biofilms, while a low  $G$  favours smooth, dense biofilm growth. Hence, a large proportion of substrates with high diffusion coefficients in the wastewater is beneficial for biofilm stability. Especially, a high concentration of volatile fatty acids (VFA), such as acetate and propionate, is desirable. VFA, besides being small molecules with high diffusion coefficients, are the preferred substrates of many PAO and GAO. PAO and GAO have low growth rates, which further contributes to the formation of dense granules. Furthermore, the anaerobic substrate uptake by PAO will not only benefit granule stability, but also contribute to EBPR.

Diffusion rate can be further increased by applying high substrate concentrations during feeding, by means of a plug-flow feeding (Beun et al., 2002; de Kreuk and van Loosdrecht, 2004). Increased substrate penetration, besides avoiding filamentous outgrowths in the granule surface, also ensures that the core of the granules receives COD. This way, starvation and cell decay at the granule core are avoided, which lead to weakening of the granules and eventual breakage.

## 1.4 | AGS AND DOMESTIC WASTEWATER

### 1.4.1 | Domestic wastewater

Domestic wastewater has a complex composition compared to the synthetic wastewaters that were originally employed to develop AGS technology. The composition of domestic wastewater in general is highly variable, and affected by many factors, such as the origin of the wastewater, the amount of rainfall and infiltration, and the transformations in the sewer prior to the treatment plant.

**The origin** of the wastewater affects the size distribution and biodegradability of the pollutants. For example, many domestic wastewaters contain a proportion of industrial wastewater. Depending on the source of the industrial wastewater, a higher particulate COD can be expected, and the dominating biomolecule type will change. For instance, Sophonsiri et al. (2004) reported a large proportion of proteins in food processing wastewater, compared to municipal wastewater, and the percentage of particulate COD was higher too (Sophonsiri and Morgenroth, 2004).



**The type of sewer** has a strong impact on the composition of the wastewater arriving at the WTP too. For example, combined or separate sewers will result in very different pollutant concentrations. The wastewater will furthermore experience some conversions during its transport in the sewer. Sedimentation and resuspension affect the concentration of solids, and the amount of groundwater infiltration affects the pollutant concentration (Langeveld et al., 2003). In addition, the wastewater composition is modified by the action of microorganisms, which are transported with the wastewater particles or are present in a biofilm in the sewer walls. The conversions will be aerobic or anaerobic depending on the sewer configuration (Hvitved-Jacobsen et al., 2013, 1999). In gravity sewers the wastewater is transported aerobically most of the time, and hence COD will be consumed aerobically during transport. In contrast, in pressure mains anaerobic conditions are created. Anaerobic conversions can also result in COD consumption if alternative electron acceptors are present ( $\text{SO}_4^{2-}$ ,  $\text{NO}_x$ ), but generally less COD is consumed than in aerobic conditions (Hvitved-Jacobsen et al., 1999; Rudelle et al., 2011). Organic matter is then hydrolysed and fermented, increasing the concentration of VFA and other fermentation products. The degree of these conversions will vary depending on conditions such as the retention time in the sewer, and the temperature of the wastewater.

Despite its large variability, it can be generalised that domestic wastewater is low- to medium- strength, and contains a significant fraction of slowly biodegradable COD (sbCOD) (Henze et al., 1999). sbCOD includes substrates of a broad size range, from soluble ( $<0.45 \mu\text{m}$ ) to settleable ( $>100 \mu\text{m}$ ). The chemical nature of these substrates is also very diverse. Most sbCOD in the wastewater can be classified within either lipids, proteins or polysaccharides (Raunkjær et al., 1994; Sophonsiri and Morgenroth, 2004). However, each of these groups comprises biomolecules with very different properties; for example, cellulose and starch are both polysaccharides but differ in their structure, and different enzymes are needed for their degradation. The shared property of all these substrates is that they are polymeric, meaning that they need to be depolymerized prior to microbial uptake, through hydrolysis (Ferenci, 1980; Hollibaugh and Azam, 1983). Hydrolysis is a slow process, and has been repeatedly regarded as the rate-limiting step on the degradation of polymeric substrates (Morgenroth et al., 2002). Part of the hydrolysis can take place in the sewer, increasing the VFA concentration that reaches the wastewater treatment plant (Hvitved-Jacobsen et al., 1995; Yun et al., 2013). However, often, polymeric substrates are still a major COD fraction in the influent of the WTP, and are hydrolysed in the biological reactor. During hydrolysis, readily biodegradable COD (rbCOD) is slowly released, resulting in low rbCOD concentrations available throughout the treatment process.

### 1.4.2 | Domestic wastewater treatment with AGS

While much of the research on AGS has been done with simple substrates such as VFA or glucose, in the past few years more studies focused on granulation on real or synthetic complex wastewaters. The low VFA and high sbCOD concentrations of domestic wastewater make AGS-based treatment more challenging. First, low VFA availability and a slow release of rbCOD from the hydrolysis of sbCOD during the anaerobic phase, lead to low anaerobic COD storage by PAO, which could challenge granulation and EBPR performance. Second, the continuous release of hydrolysates, also during the aeration phase, will result in a significant rbCOD fraction available aerobically. The low rbCOD concentrations constantly released during aeration could favour the growth of OHOs, leading to irregular granules and high effluent suspended solids.

Aerobic availability of COD has led to morphological instability in a number of AGS studies. In reactors operated fully aerobically, granule morphology is compromised unless a high selection pressure is applied, as well as high shear rates and high dissolved oxygen (DO) conditions (Beun et al., 2000; Morgenroth et al., 1997; Mosquera-Corral et al., 2005). In reactors operated with anaerobic feeding, it is easier to maintain granule stability by promoting anaerobic COD storage. However, wastewaters with high particulate substrate concentrations can lead to the deterioration of granule morphology due to aerobic degradation of the particulates. Examples include reactors fed with domestic wastewater, starch, and synthetic faecal wastewater, where filamentous outgrowths were developed and the nutrient removal performance was reduced (Barrios-Hernández et al., 2020; de Kreuk et al., 2010; N. Schwarzenbeck et al., 2004; Wagner et al., 2015).

Nonetheless, aerobic COD consumption in AGS does not always lead to instability. Pronk et al. (2015) proposed that the location of the substrates during their aerobic degradation is essential to determine their effect on granule structure. So is the growth rate of the microorganisms involved in the aerobic COD uptake (Pronk et al., 2015a). If the substrates are adsorbed to the granules prior to their uptake, and if the maximum growth rate achievable for a substrate is low, a smooth granule morphology can be maintained.

Other studies also showed that stable granulation can occur in spite of aerobic COD consumption. A recently developed granulation model pointed that granulation could occur as long as sufficient COD was stored anaerobically by granules and proto-granules, and selective sludge wasting was provided (van Dijk et al., 2022). Lab-scale experiments also confirmed that enough anaerobic COD uptake and flocculent sludge wasting were

enough to counterbalance the detrimental effects of aerobically available COD (Haaksman et al., 2020).

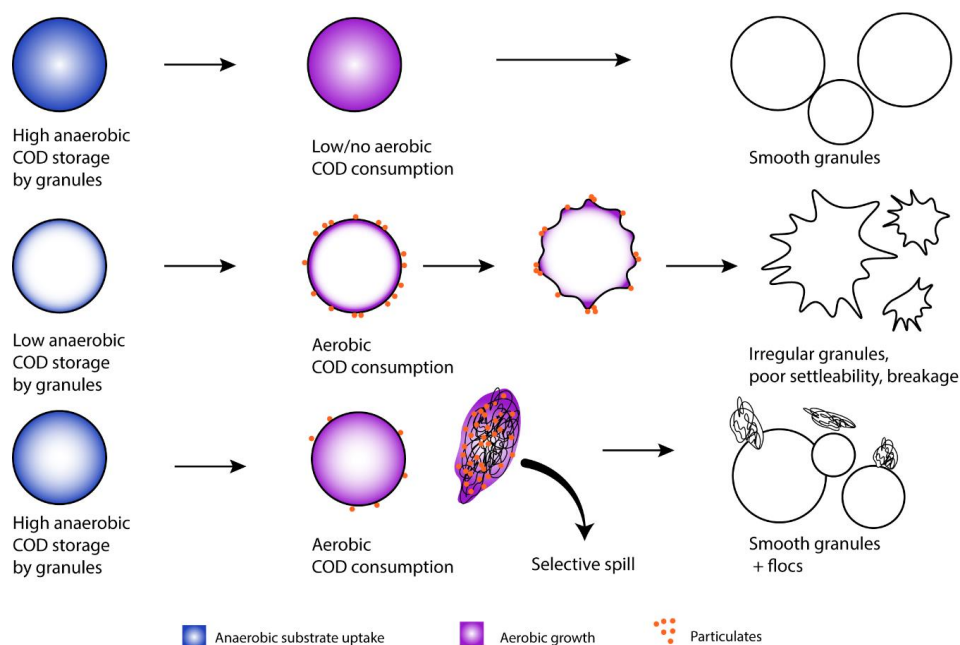


**Figure 1.4.** Representation of the effect of anaerobic and aerobic COD consumption in AGS morphology (Adapted from Pronk et al., 2015a). High anaerobic uptake, coupled with aerobic growth throughout the granule (sustained by intracellular storage compounds), leads to smooth granule growth. In the presence of sbCOD, low anaerobic substrate storage and high aerobic consumption in the granule surface supports the proliferation of heterotrophs in the granule surface, and leads to irregular granule morphology. If anaerobic COD storage is enhanced, then microbial growth occurs deeper in the granules; aerobic consumption of sbCOD leads to floc proliferation, which are discharged through the selective spill.

Furthermore, various lab and pilot-scale studies have explored different strategies to improve AGS stability with domestic wastewater-like influents (Cetin et al., 2018; Coma et al., 2012; Derlon et al., 2016; Layer et al., 2019; Ni et al., 2009; Rocktäschel et al., 2015; Wagner et al., 2015). Selective sludge withdrawal was identified as an important factor by various researchers (Derlon et al., 2016; Rocktäschel et al., 2015; Wagner et al., 2015). Several publications reported improved AGS operation with an extended anaerobic phase, and attributed it to an enhanced anaerobic COD storage originated from the hydrolysis of particulates (Barrios-Hernández et al., 2020; Campo et al., 2020; Sguanci et al., 2019; Yu et al., 2021). They suggested that anaerobic sbCOD uptake could be further promoted by mixing the reactor after plug-flow feeding, to distribute

particulates throughout the granule bed (Campo et al., 2020; Rocktäschel et al., 2015). Likewise, promoting anaerobic COD uptake by extending the anaerobic period and improving the particle-sludge contact via anaerobic mixing have been successfully applied to control filamentous bulking in CAS plants (Caluwé et al., 2022; Meunier et al., 2016). This strategy, besides limiting filamentous bulking, led to partial granulation in these systems.

The mentioned studies contribute to improving AGS operation, but still the mechanisms, location and rates of sbCOD consumption remain largely unknown. Given that the anaerobic and aerobic COD uptake impact the stability of the AGS process, a better understanding of the conversions of polymeric and particulate substrates on AGS reactors is needed.

## **1.5 | POLYMERIC SUBSTRATE UTILIZATION BY AGS MICROORGANISMS**

Elucidating the utilization of polymeric substrates by AGS microorganisms requires an improved understanding of hydrolysis and the subsequent hydrolysate uptake. The mechanisms pertaining the microbial conversion of polymeric substrates have been studied to a certain degree in activated sludge, and to a lower extent in AGS.

### **1.5.1 | Hydrolysis**

The rate of hydrolysis will determine what fraction of the polymeric COD is available to AGS microorganisms, anaerobically and aerobically. Most mathematical models used for wastewater treatment describe hydrolysis as a factor of enzyme concentration as well as substrate concentration, following first order or Michaelis-Menten kinetics (Morgenroth et al., 2002). These models are based on empirical data and can generally describe, among others, organic matter conversions observed in full-scale plants. The hydrolysis kinetics in aerobic granular sludge may differ from activated sludge kinetics, given that granule surface area may become an important factor influencing hydrolysis kinetics. CAS studies found enzymes to be mainly associated to the cells or their surrounding EPS, and therefore polymer hydrolysis requires direct contact between the substrates and the sludge. Granules are more rigid and present higher mass transfer resistance than flocculent sludge, which breaks and coagulates constantly. That is why it can be expected that hydrolysis rates will be lower in AGS compared to CAS, and especially particulates will be better captured in flocculent sludge. This has led to the

hypothesis that the flocculent sludge fraction in AGS reactors is important for the conversion of particulate substrates (Alves et al., 2022; Layer et al., 2019). Ranzinger et al. (2020) followed the distribution of particulates in the AGS bed during plug-flow feeding, concluding that the attachment of particulates to granules was limited, but it improved with mixing (Ranzinger et al., 2020). In a subsequent publication, they reported that particulate retention increased when flocs were present in the sludge bed, suggesting that the flocs captured particulates due to their open structure (M. Layer et al., 2020). Therefore, flocs are likely to be involved in sbCOD capture and hydrolysis, although their hydrolytic activity has not been quantified yet. Similarly, it is yet to be elucidated whether granules significantly contribute to the hydrolysis of polymeric substrates. Granule diameter could then be important for hydrolysis since it determines the relative granule surface area, which in turn influences mass transfer.

### 1.5.2 | Microbial uptake of hydrolysates

Following hydrolysis, the resulting hydrolysates may be utilized by different microorganisms. With a focus on EBPR and granule stability, anaerobic storage of hydrolysis products by PAO or GAO is desirable. Besides the classical PAO and GAO genera *Ca. Accumulibacter phosphatis* (from now on referred to as *Ca. Accumulibacter*) and *Ca. Competibacter phosphatis* (from now on referred to as *Ca. Competibacter*), in the last years other putative PAO and GAOs have been identified, such as *Tetrasphaera*, *Dechloromonas*, *Microlunatus*, *Propionivibrio*, *Defluviicoccus* or *Micropruina*, among others (Nielsen et al., 2019; Roy et al., 2021; Stockholm-Bjerregaard et al., 2017). The diversity of microorganisms able to anaerobically store substrates broadens the substrate uptake range of EBPR sludge, allowing the utilization of not only VFA but also other monomers derived from hydrolysis. For instance, glucose derived from polysaccharides or amino acids derived from proteins can be anaerobically utilized by a variety of PAO and GAO (Kristiansen et al., 2013; Nielsen et al., 2019; Stockholm-Bjerregaard et al., 2017). Since different microorganisms may be favoured in the presence of VFA or other monomers, the type of the rbCOD in the influent wastewater shapes the microbial community in AGS (Dockx et al., 2021; Layer et al., 2019). The composition and metabolism of the PAO and GAO community could have an impact on nutrient removal; for instance concerning denitrification or EBPR. The substrate uptake range in combination with the microbial community of full-scale aerobic granules have not been studied in detail yet, and deserve further attention.

## 1.6 | SCOPE OF THIS THESIS

As mentioned above, it is unclear how AGS utilizes polymeric substrates, and their effects on process performance and granule morphology are not well understood yet. To improve the understanding of the fate of this wastewater fraction in AGS reactors, this thesis explores the potential of full-scale aerobic granules to convert polymers.

Chapter 2 follows the effects of increasing the particulate COD load on full-scale AGS. This chapter explores if the added particulates result in increased granular sludge production, while monitoring the structural stability of granules. Furthermore, it assesses whether the sludge generates hydrolytic capacity when faced with increased polymeric substrate concentrations, and identifies shifts in the microbial community of granules and flocs upon the influent change.

Chapter 3 studies the distribution of the hydrolysis capacity in full-scale AGS reactors. Using polymeric substrates labelled with chromogenic molecules, the hydrolytic capacity of the reactor mixed liquor is quantified. The hydrolytic potential of the main fractions composing the mixed liquor is also assessed, by fractionating it into large granules (> 1 mm), small granules (0.2-1 mm), flocs and bulk liquid. The hydrolytic activity attached to the influent particulates is also quantified. The results of these analyses are used to evaluate the likelihood of different biomass fractions to consume polymeric substrates during the anaerobic feeding phase.

Chapter 4 focusses on hydrolysis on single granule level, studying its location and the surrounding microbial populations. To do so, fluorescently labelled casein and starch are dosed to granules, to subsequently visualize hydrolytically active areas through fluorescence microscopy. This chapter also compares the biomass-specific hydrolytic activity and the hydrolytically active locations in granules of different size sampled from the same reactor, ranging from 0.5 to 4.8 mm. The effects of relative surface area and biomass segregation on hydrolytic activity are evaluated.

Chapter 5 investigates anaerobic substrate uptake by AGS. This chapter explores the uptake of polymeric substrates and monomers (which may be present in wastewater or originate from the hydrolysis of polymers). The anaerobic substrate uptake range of granules is screened through batch tests first, by measuring the uptake of various organic compounds and the associated P release and PHA formation. Then, casein is chosen as a model substrate to study protein uptake. The uptake rate of soluble, colloidal and particulate casein is quantified, and compared with the uptake rate of amino acids and acetate. The results are used to make considerations about granule stability and EBPR in AGS grown in complex wastewater.

Finally, chapter 6 gives the concluding remarks of this thesis and suggests a prospective outlook for this research field.





# 2

## Effect of an increased particulate COD load on the AGS process

**Published as:** Toja Ortega, S., Pronk, M. & De Kreuk, M.K. (2021). Effect of an Increased Particulate COD Load on the Aerobic Granular Sludge Process: A Full Scale Study. *Processes*, 9(8), 1472. DOI: 10.3390/pr9081472



## ABSTRACT

2 High concentrations of particulate COD (pCOD) in the influent of aerobic granular sludge (AGS) systems are often associated to small granule diameter and a large fraction of flocculent sludge. At high particulate concentrations even granule stability and process performance might be compromised. However, pilot- or full-scale studies focusing on the effect of real wastewater particulates on AGS are scarce. This study describes a 3-month period of increased particulate loading at a municipal AGS wastewater treatment plant. The pCOD concentration of the influent increased from 0.5 g COD/L to 1.3 g COD/L, by adding an untreated slaughterhouse wastewater source to the influent. Sludge concentration, waste sludge production and COD and nutrient removal performance were monitored. Furthermore, to investigate how the sludge acclimatises to a higher influent particulate content, lipase and protease hydrolytic activities were studied, as well as the microbial community composition of the sludge. The composition of the granule bed and nutrient removal efficiency did not change considerably by the increased pCOD. Interestingly, the biomass-specific hydrolytic activities of the sludge did not increase during the test period either. Protease activity of the mixed liquor was  $0.015 \pm 0.005$  mmol Tyr eq gVS<sup>-1</sup> h<sup>-1</sup> before operation change, and  $0.015 \pm 0.003$  mmol Tyr eq gVS<sup>-1</sup> h<sup>-1</sup> after operation change; lipase activity was  $0.1 \pm 0.02$  mmol palmitate gVS<sup>-1</sup> h<sup>-1</sup> before operation change, and  $0.1 \pm 0.02$  mmol palmitate gVS<sup>-1</sup> h<sup>-1</sup> after the change. However, already during normal operation the aerobic granules and flocs exhibited a hydrolytic potential that exceeded the influent concentrations of proteins and lipids. Microbial community analysis also revealed a high proportion of putative hydrolysing and fermenting organisms in the sludge, both during normal operation and during the test period. The results of this study highlight the robustness of the full-scale AGS process, which can bear a substantial increase in the influent pCOD concentration during an extended period.

## 2.1 | INTRODUCTION

Aerobic granular sludge (AGS) technology is currently applied in more than 80 plants over the world treating domestic and industrial wastewater, under the tradename Nereda® (Royal HaskoningDHV, Amersfoort, The Netherlands). AGS offers various advantages in comparison to conventional activated sludge systems, including lower space and energy requirements (de Bruin et al., 2004). Furthermore, the granular sludge offers a number of resource recovery options (Amorim de Carvalho et al., 2021). The technology is operated as a sequencing batch reactor (SBR) consisting of simultaneous anaerobic plug-flow feeding and effluent withdrawal, followed by aeration and settling (Pronk et al., 2015b). The anaerobic feeding regime ensures anaerobic uptake of the readily biodegradable COD (rbCOD) by slow-growing organisms, which store this COD intracellularly and oxidise it in the subsequent aerobic phase (de Kreuk et al., 2005). This way, slow-growing organisms such as polyphosphate accumulating organisms (PAO) and glycogen accumulating organisms (GAO) are favoured over ordinary heterotrophic organisms (OHO), which results in smooth granule growth (de Kreuk and van Loosdrecht, 2004).

In addition to rbCOD, domestic wastewater and many industrial wastewaters contain a large fraction of slowly biodegradable, particulate COD (pCOD) (Karahan et al., 2006; Ravndal et al., 2018; Sophonsiri and Morgenroth, 2004). This COD fraction may provide additional substrate for nutrient removal and granular sludge production, from which resources could be recovered ultimately. On the other hand, it could challenge the stability of the AGS process, due to the inability of PAO and GAO to consume more complex COD directly; pCOD needs to be extracellularly hydrolysed to rbCOD, after which it can be assimilated by the microorganisms in the sludge (Morgenroth et al., 2002). Hydrolysis is often regarded as rate-limiting in the degradation of particulates (Gujer et al., 1999; Henze et al., 1986). It relies on contact between the substrate and hydrolytic enzymes, which are mainly reported to be biomass-bound (Frølund et al., 1995; Goel et al., 1998a; Karahan et al., 2006). In activated sludge, the open floc structure allows good contact between sludge flocs and pCOD, rendering a continuous and homogeneous release of rbCOD throughout the floc (Martins et al., 2011). In contrast, the dense biofilm structure of AGS limits the accessibility of pCOD to hydrolytic enzymes in the sludge. Such mass-transfer limitation has induced irregular granule growth and deterioration of granule stability in lab-scale reactors fed with high influent particulates (de Kreuk et al., 2010; Mosquera-Corral et al., 2003; Schwarzenbeck et al., 2005). This is attributed to hydrolysis of pCOD into rbCOD during the aeration phase on the granule surface, leading to substrate concentration gradients and aerobic rbCOD

consumption by fast-growing OHO (Picioreanu et al., 2000b). Nevertheless, AGS has been cultivated successfully on domestic wastewater (Cetin et al., 2018; Derlon et al., 2016), high-strength industrial wastewaters (Morales et al., 2013; Stes et al., 2021; Yilmaz et al., 2008) and faecal sludge-containing wastewater (Barrios-Hernández et al., 2020). Even though the influent to these reactors contained a high concentration of particulates, no filamentous outgrowth was observed. However, these studies reported much higher effluent suspended solids than generally achieved in the effluent of full-scale Nereda® reactors or found a flocculent sludge fraction accompanying the AGS. Overall, the sludge bed consisted of smaller granules compared to lab reactors fed with synthetic media containing solely rbCOD in all reported lab- and pilot-scale experiments. Layer et al. (2019) hypothesised that the flocculent sludge fraction benefitted the AGS process, by capturing influent pCOD and avoiding its aerobic degradation at the granule surface. Haaksman et al. (2020), similarly, proposed that rbCOD leakage to the aerobic phase mainly results in flocculent sludge growth, which has to be discharged regularly in order to maintain a stable granule bed. These studies suggest that AGS can adapt well to high concentrations of pCOD in the wastewater when suitable operating conditions are employed. Moreover, they suggest that granule stability is supported by an equilibrium between different biomass fractions within the AGS reactor. However, reports on full-scale AGS treating particulate-rich wastewater are scarce and they do not focus on the removal of pCOD. Thus, the effect of pCOD on granule stability and sludge bed composition at full-scale remains elusive. Furthermore, little is known about the enzymatic activity and microbial community of full-scale AGS cultivated on high influent pCOD concentrations.

To study the effect of particulates on AGS stability, a full-scale study was conducted at wastewater treatment plant (WWTP) Epe, the Netherlands, equipped with three 4500 m<sup>3</sup> reactors. The Nereda® reactors were operated with an increased influent COD load during a 4-month period (4 March–11 July 2019). The extra influent COD originated from the temporary discharge of untreated wastewater of a nearby slaughterhouse and consisted mainly of pCOD (71–86% of the total COD). During the experimental period, sludge growth, granule size and morphology and plant performance were monitored. Furthermore, the hydrolytic enzyme activity of the sludge was monitored to study its location (granular or flocculent sludge) and to compare the hydrolysis rates during operation with and without this additional untreated slaughterhouse wastewater. In this case, 16S rRNA gene amplicon sequencing was used to identify the main organisms in the sludge, and to detect shifts in the microbial community during increased pCOD loading. In this way, the present study aimed to assess the robustness of full-scale AGS

reactors faced with an increase in influent particulate content, while exploring the involvement of different sludge fractions in the removal of particulates.

## 2.2 | MATERIALS & METHODS

### 2.2.1 | Description of the plant and additional influent dosing

WWTP Epe, operated by the Water Authority Vallei en Veluwe, treats the wastewater of the municipality of Epe (The Netherlands) and its surroundings. The wastewater is pre-treated with 3 mm screens and grit removal and treated in three 4500 m<sup>3</sup> AGS reactors with a diameter of 25 m and a depth of 9.2 m, designed and built by Royal HaskoningDHV. The reactors are operated in SBR mode with simultaneous anaerobic feeding/effluent discharge, aeration and settling. The wastewater is fed from the bottom of the reactor in a plug-flow regime, at an average upflow velocity of approximately 1 m h<sup>-1</sup>. At the end of the settling phase, the slowest settling sludge is removed selectively. The influent of WWTP Epe is a mixture of domestic (70%), and industrial (30%) wastewater mainly originating from slaughterhouses. Wastewater composition is summarised in Table 2.1. The wastewater is treated to reach the effluent consents summarised in Table 2.2. The plant was designed to treat an average flow of 8000 m<sup>3</sup> d<sup>-1</sup>, and a load of 59,000 population equivalents (PE). Nevertheless, the conditions at the time of the study have not reached the design values: the average flow is approximately 5000 m<sup>3</sup> d<sup>-1</sup> and the load is 35000 PE.

In the period 4 March–11 July 2019, the wastewater of a nearby slaughterhouse was discharged untreated to the municipal sewer network leading to WWTP Epe. The additional influent increased the substrate loading to the Nereda<sup>®</sup> reactors, approaching the design values. The objective was to enhance the growth of granular sludge while maintaining good pollutant removal performance. In a regular situation, the slaughterhouse treats its own wastewater using a dissolved air flotation (DAF) system. The treatment involves addition of coagulants and removal of solids by flotation, removing 80–90% of the COD of the wastewater. The treated wastewater, mostly composed of soluble COD, is discharged to the municipal sewer network and arrives at WWTP Epe, at approximately 500 m distance. During the test period, in-house treatment was stopped and concentrated raw wastewater was discharged, with a high content of suspended solids (see Table 2.1). The wastewater was continuously discharged during 12 h per day, with an average flow of 300 m<sup>3</sup> d<sup>-1</sup> and a maximum flow of 50 m<sup>3</sup> h<sup>-1</sup>.

**Table 2.1** Influent composition of WWTP Epe during normal operation and during the test period. Values are expressed as average  $\pm$  standard deviation. Routine measurements: normal operation  $n = 79$ ; test period  $n = 21$ . Occasional miscellaneous analysis: normal operation  $n = 6$ ; test period  $n = 3$ . Asterisks denote significant changes (\* =  $p < 0.05$ ; \*\*\* =  $p < 0.001$ ).

	Normal Operation	Test Period	Significance
<b>Routine measurements</b>			
tCOD [g m <sup>-3</sup> ]	840 $\pm$ 254	1456 $\pm$ 692	***
TSS [g m <sup>-3</sup> ]	317 $\pm$ 123	633 $\pm$ 361	***
BOD <sub>5</sub> [g m <sup>-3</sup> ]	341 $\pm$ 109	537 $\pm$ 249	***
TN [g m <sup>-3</sup> ]	77 $\pm$ 21	101 $\pm$ 39	***
TP [g m <sup>-3</sup> ]	8 $\pm$ 2	13 $\pm$ 5	***
Q [m <sup>3</sup> /d]	4696 $\pm$ 2099	5229 $\pm$ 3418	
COD/N [g/g]	11 $\pm$ 3	14 $\pm$ 4	***
COD/P [g/g]	101 $\pm$ 15	117 $\pm$ 24	***
<b>Occasional miscellaneous analysis</b>			
tCOD [g m <sup>-3</sup> ]	864 $\pm$ 274	1713 $\pm$ 572	*
sCOD [g m <sup>-3</sup> ]	339 $\pm$ 129	386 $\pm$ 49	
Acetate [g COD m <sup>-3</sup> ]	82 $\pm$ 59	43 $\pm$ 37	
Propionate [g COD m <sup>-3</sup> ]	14 $\pm$ 12	16 $\pm$ 17	
Lipids [g COD m <sup>-3</sup> ]	45 $\pm$ 20	290 $\pm$ 77	*
Total carbohydrates [g COD m <sup>-3</sup> ]	274 $\pm$ 155	538 $\pm$ 125	
Total proteins [g COD m <sup>-3</sup> ]	90 $\pm$ 11	162 $\pm$ 53	
Soluble carbohydrates [g COD m <sup>-3</sup> ]	18 $\pm$ 1	21 $\pm$ 2	
Soluble proteins [g COD m <sup>-3</sup> ]	20 $\pm$ 7	33 $\pm$ 23	

### 2.2.2 | Sampling and sample handling

For this study, reactor mixed liquor samples and influent wastewater samples were collected. The samples were collected during two phases: before the test period (in a stretch of 5 months), and during the final week of the test period.

#### Influent wastewater

Influent wastewater was collected using a flow-proportional 24-hour sampler, after screening and grit removal. The samples were stored at 4 °C in the sampler chamber, and then transported to the lab for analysis. Part of the wastewater was filtered using a vacuum filter device to characterize the particulate size-fractions. Sequential filtering was performed using filters with the following pore sizes: 100  $\mu$ m, 10  $\mu$ m, 1  $\mu$ m and 0.1  $\mu$ m (Product details: 100  $\mu$ m: stainless steel mesh (Anglo Staal, Borne, The Netherlands); 10  $\mu$ m: Cyclopore®, polycarbonate [PC], 1  $\mu$ m: Whatman® GF/B, glass

fibre; 0.1  $\mu\text{m}$ : Cyclopore®, PC. Whatman, Buckinghamshire, UK). The filtrate of each step was collected and stored for analysis. A small sample was also filtered through 0.45  $\mu\text{m}$  for soluble COD (sCOD) analysis (Durapore® filters, PVDF. Merck, Darmstadt, Germany). Samples were preserved at 4 °C for short-term storage, and –20 °C for long-term storage.

### Reactor mixed liquor

Reactor mixed liquor was sampled to study hydrolytic activity and sludge characteristics. Mixed liquor samples were collected during the aeration phase, at least 40 min after the beginning of aeration to ensure a completely mixed sample. Sieve fractions of the mixed liquor were obtained by pouring the mixed liquor through a stack of sieves of 0.045, 0.2 and 1 mm, and gently rinsing with tap water. The fraction smaller than 0.045 mm was centrifuged and the supernatant was kept. The following fractions were collected: mixed sludge; bulk (<0.045 mm fraction, centrifuged); flocs (0.045–0.2 mm); and granules (>1 mm). The fraction between 0.2 and 1 mm was excluded from analysis due to its high amount of debris and heterogeneous composition.

### 2.2.3 | Analytical methods

Several measurements were performed on the influent and its size fractions, as well as the two samples of slaughterhouse wastewater. TSS and VSS were measured according to the Standard Methods (APHA, 2005). Volatile fatty acids (VFA) acetate and propionate were quantified using high performance liquid chromatography (HPLC) with an Aminex HPX-87H column from Bio-Rad (Hercules, CA, USA). tCOD was measured using photochemical test kits from Hach (Dusseldorf, Germany). sCOD was determined by measuring COD in the wastewater filtered through 0.45  $\mu\text{m}$ . Particulate COD (pCOD) was calculated as tCOD minus sCOD. Proteins were quantified using the modified Lowry method (Frølund et al., 1995). Carbohydrates were quantified using the anthrone-sulfuric acid method (DuBois et al., 1956). Lipids were measured by Merieux Nutrisciences (Resana, Italy) using the gravimetric method.

Sludge was inspected using a Keyence VHX-700F digital microscope (Mechelen, Belgium). The TS and VS of the sludge used in activity assays were determined according to the standard Methods (APHA, 2005).

### 2.2.4 | Hydrolytic enzyme activity tests

Lipase and protease enzyme activities of the sludge were assessed in the mixed sludge, granules, flocs and bulk liquid. The enzyme assays were performed within 8 h after sampling. The procedure of the assays is described in detail in Toja Ortega et al., 2021a.

In short, the sludge was incubated with chromogenic substrates, in anaerobic vials with a sampling port. The assay was conducted at 20 °C, pH 7.5 and at fully mixed conditions, using a Fisherbrand Seastar orbital shaker (Thermo Fisher Scientific, Waltham, USA) running at 120 rpm. The vials were flushed with N<sub>2</sub> gas for 2 min to provide anaerobic conditions. The substrates used were azocasein for the protease assays, and *p*-nitrophenyl-palmitate (*p*NP-palmitate) for the lipase assays (Sigma-Aldrich, Darmstadt, Germany). The assay vials were sampled every 15–30 min and the samples were filtered through 0.45 µm with a syringe filter to remove biomass. 1 mL sample was mixed with 1 mL TCA to stop enzyme activity. Samples were stored at –20 °C until analysed, and then thawed, centrifuged and filtered through 0.45 µm. The filtrate was mixed on a 1:1 proportion with NaOH 2M and its absorbance was measured, at 410 nm in the lipase assay and 440 nm in the protease assay. The increase in absorbance over time was translated to substrate hydrolysis rate, as described in Toja Ortega et al., 2021a. The sludge-specific activity was calculated considering the sludge concentration in the vials. Finally, the total activity contained in the reactor was calculated by multiplying the specific activity of each sludge fraction by its abundance in the reactor.

### 2.2.5 | Routine measurements

Routine influent and effluent measurements were conducted by a certified lab and provided by Water Authority Vallei en Veluwe. These included: COD, biological oxygen demand (BOD<sub>5</sub>), total nitrogen (TN), total phosphorus (TP), total suspended solids (TSS), ammonia nitrogen (NH<sub>4</sub>-N), nitrate/nitrite nitrogen (NO<sub>x</sub>-N) and flow. As were the excess sludge production, long-term reactor sludge concentration and granule size distribution measurements.

In addition to influent and effluent composition, key performance indicators (KPI) were used to follow reactor performance during the SBR cycle. Online samplers measure nutrient profiles during the AGS cycle (NH<sub>4</sub>-N, NO<sub>3</sub>-N, PO<sub>4</sub>-P, dissolved oxygen [DO]). Measurement data were retrieved from the Aquasuite Nereda® controllers (Royal HaskoningDHV, Amersfoort, The Netherlands) and provided by Royal Haskoning DHV.

### 2.2.6 | Microbial population analysis

#### Sludge processing and DNA extraction

The mixed sludge and sludge sieve fractions were homogenised using a Potter-Elvehjem tissue grinder to ensure a representative sludge sample for DNA extraction. The homogenized sludge was transferred to 1.5 mL Eppendorf tubes (Eppendorf, Hamburg,

Germany) and centrifuged in a microcentrifuge (Eppendorf, Hamburg, Germany) at 14,000 g for 5 min. Around 30 mg of pellet were added to extraction tubes from the FastDNA spin kit for soil (MP Biomedicals, Irvine, CA, USA). The DNA was extracted following the protocol optimized by Albertsen et al., (2015) for activated sludge samples. Each sample was extracted three times, to improve the recovery of the DNA of all microorganisms in the samples (Feinstein et al., 2009; Jones et al., 2011). The concentration of the extracted DNA was measured using a Qubit dsDNA HS assay kit (Thermo Fisher Scientific, Waltham, MA, USA).

### 16S rRNA gene amplicon sequencing and data analysis

The 16S rRNA gene was amplified and paired-end sequenced in an Illumina NovaSeq 6000 platform by Novogene (Beijing, China). The hypervariable regions V3–V4 were amplified and sequenced, using the primer set 341F [5'–CCTAYGGGRBGCASCAG–3'] and 806R [5'–GGACTACNNGGTATCTAAT–3']. The raw reads were deposited in the National Center for Biotechnology Information (NCBI) Sequence Read Archive (SRA) on BioProject PRJNA746138.

The trimmed and merged sequences provided by Novogene were processed using QIIME2, version 2020.2 (Bolyen et al., 2019). The sequences were quality-filtered using Deblur (Amir et al., 2017), trimming the sequences the 3' end at position 403 (parameter *p-trunc-len*). The remaining sequences were assembled into a phylogenetic tree to perform diversity analyses, using the *q2-phylogeny* plugin. Beta diversity metrics (Bray–Curtis and Unweighted Unifrac) were generated, and differences in beta diversity between sludge types and experimental conditions were analysed using PERMANOVA (Anderson, 2001). A *p*-value of 0.05 was used as cut-off for significance. Finally, taxonomic affiliation of the sequences was determined by aligning the sequences to the MiDAS 3.6 database (Nierychlo et al., 2020). Sample subsetting, visualization and further statistical analysis was performed in R, using the *Phyloseq* and *Ampvis2* packages (Andersen et al., 2018; McMurdie and Holmes, 2013). Abundant taxa were defined as taxa with 1% abundance or more. Per sludge type, significant differences in abundant taxa before and after the test period were determined through *t*-tests. A Bonferroni-corrected *p*-value was used, of 0.01 divided by the number of abundant taxa per sludge type.



## 2.3 | RESULTS

### 2.3.1 | Additional influent dosing and changes in influent composition

During the test period, the influent COD concentration almost doubled (from 840 to 1460 g m<sup>-3</sup>). The pCOD, in particular, increased from 525 to 1327 g m<sup>-3</sup>, along with the TSS content, which increased from 317 to 633 g m<sup>-3</sup>. Table 2.1 summarizes the characteristics of the influent to the wastewater treatment plant of Epe, before and during the addition of the untreated slaughterhouse wastewater. The VFA content in the influent was very variable, and the average VFA concentrations before and after the test period did not significantly change ( $p = 0.39$ ). The sCOD measurements did not indicate an increase in soluble compounds in the wastewater either. Furthermore, particle size measurements of the influent showed that the extra COD during the test period came in the fractions between 1 and 100  $\mu\text{m}$ , especially in the size fraction of 10 to 100  $\mu\text{m}$  (Supplementary information, Figure S2.1). The smallest COD fraction (<0.1  $\mu\text{m}$ ) had an average concentration of  $260 \pm 92$  g m<sup>-3</sup> before the test period, and  $331 \pm 61$  g m<sup>-3</sup> during the test period. However, the differences on this size fraction between both situations are not statistically significant ( $p = 0.11$ ). From the macromolecules quantified (proteins, carbohydrates and lipids), lipid concentration increased most, from 45 to 290 g m<sup>-3</sup>.

In short, there was a significant increase in the influent concentration of tCOD ( $p < 0.001$ ) and of TSS ( $p < 0.001$ ). sCOD and VFA concentrations, in contrast, were not significantly affected by the addition of the untreated slaughterhouse wastewater, since the location is only 500 m from the WWTP. Apparently, there was not enough residence time in the sewer for fermentation of this wastewater, despite the warm spring season. Even though sCOD did not increase, the BOD<sub>5</sub> was higher during the test period, indicating the presence of particulate substrates with high biodegradability in the added untreated slaughterhouse wastewater.

### 2.3.2 | Sludge production

The biomass concentration of the reactors increased during the 4 months of changed influent. On the year before the test, the average TS concentration of the reactors was  $5.8 \pm 1.7$  g TS/L. At the end of the test period, the average sludge concentration was  $8.3 \pm 0.6$  g TS/L. However, it should be noted that already the months before the test period the sludge concentration had started to increase (Supplementary information, Figure S2.2). The granule bed was composed of different sludge morphologies (size fractions).

The measured percentage of each sludge size fraction over the total sludge oscillated during the experimental period. Overall, the trend showed an increased large granule fraction (from 56 to 67%) and a decreased smaller granule fraction (from 23 to 18%) and floc fraction (from 20 to 15%). However, such tendency could not be attributed to the test period alone, because the change in sludge bed composition occurred during a longer time period and not only during the test itself (Supplementary information, Figure S2.2). Furthermore, protozoa growth was observed on granule surfaces (Figure 2.1), but this did not affect the settleability of the sludge; SVI<sub>5</sub> was maintained around 40–45 mL/g VS.

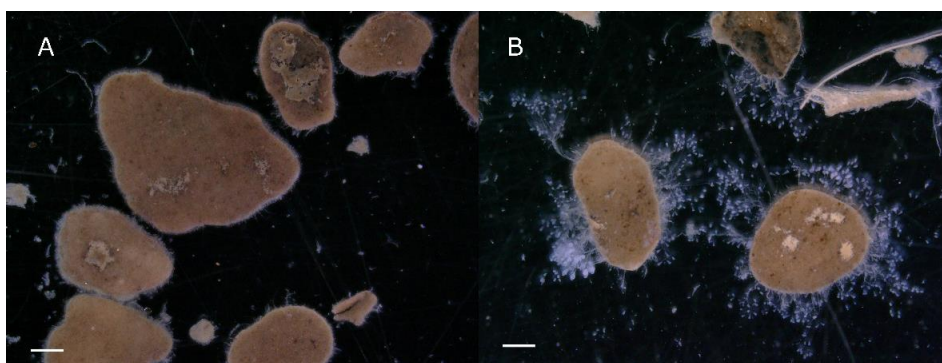


**Figure 2.1.** Micrographs of large granules (>1 mm): (a) on 23 January 2019 (normal operation); and (b) on 9 July 2019 (at the end of the test period). Size bar: 0.5 mm.

During the test period, the volume of the wasted sludge increased (Figure 2.2). The amount of wet sludge withdrawn doubled during the test period, from 870 to 1640 tonnes per month. The TS measurements of the waste sludge were lower during the test period than during normal operation ( $40 \pm 10$  g TS/L versus  $31 \pm 8$  g TS/L). Thus, in terms of dry weight the increase in wasted sludge was less pronounced: 48.8 tonnes TS per month instead of the normal 34.7 tonnes TS per month, or around 13 tonnes TS per month higher. These data show that the additional influent particulates were at least partly degraded during the process. If the particulates were removed non-degraded with the excess sludge, the sludge production would have been considerably higher during the test period. Considering the increase of 0.3 g TSS/L in the influent, sludge wasting would increase 50 tonnes TS/month instead of the observed 13 tonnes TS/month. The sludge production data should be interpreted with caution, though. The measurement of the dry solids content of the excess sludge was not very accurate, due to difficulties associated with full-scale monitoring. The operation of the sludge thickening unit was fluctuating, resulting on a variable spill concentration. Therefore, the TS measurements on weekly grab samples of the thickened sludge might not be fully representative of the

TS concentration of the spill over the whole period. Nevertheless, such a large gap between the expected and observed spill production still indicates that a fraction of particulate COD was likely to be consumed by the sludge. For a more detailed mass balance, check Supplementary information 5.

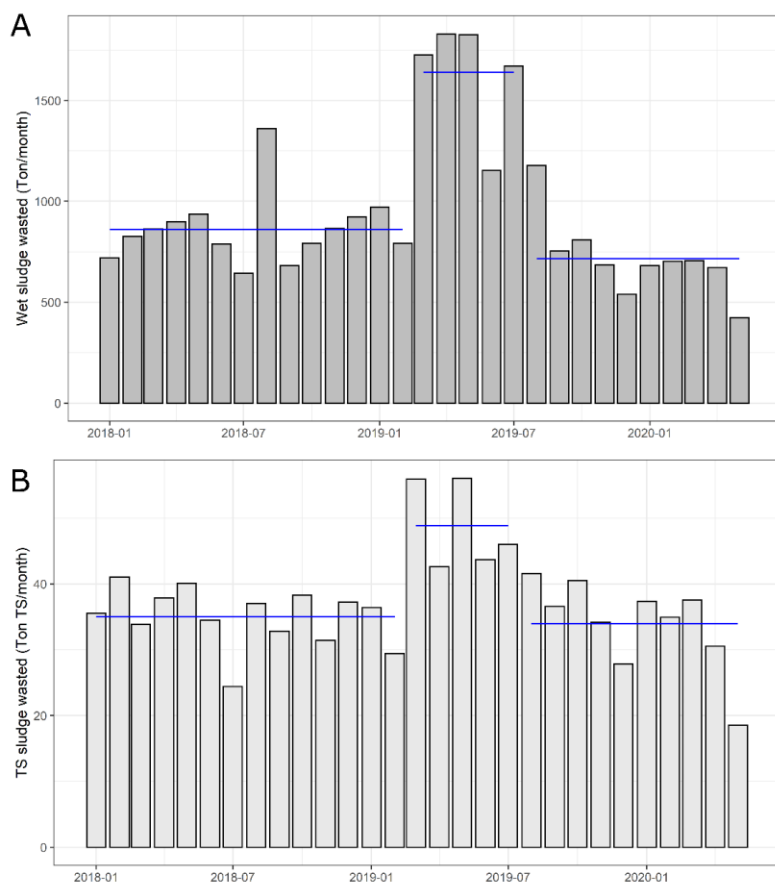


**Figure 2.2.** Monthly waste sludge production. (A) Tons of wet sludge produced (B) Tons of TS produced, based on the measured TS content of the waste sludge (40 g/L during normal operation and 31 g/L during the test period). The blue lines indicate the average sludge production in the periods before, during and after the test period.

### 2.3.3 | Hydrolytic enzyme activity tests

Hydrolytic enzyme activity assays showed that both granules and flocs have the ability to hydrolyze proteins and lipids (Figure 2.3). No protease and lipase activity was detected in the bulk liquid.

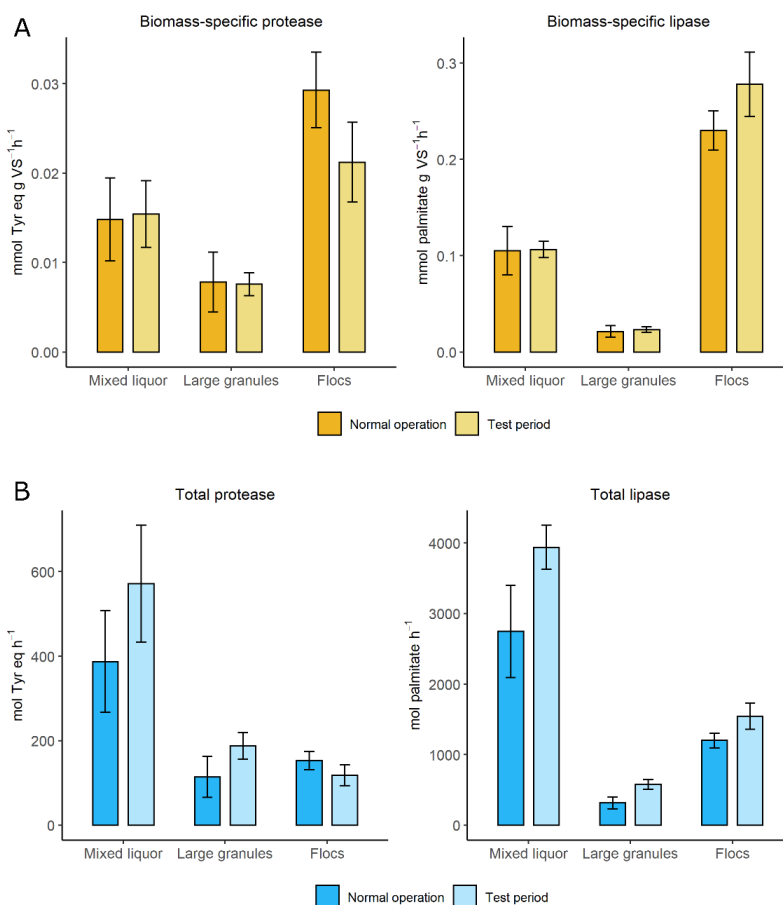


**Figure 2.3.** Hydrolytic activity of mixed sludge, granules and flocs. (A) Specific hydrolytic activities of the mixed liquor (Mix), and the sieve fractions large granules (>1 mm) and flocs (<0.2 mm); (B) Total hydrolytic activities at reactor-scale in the mixed liquor, and the total activity contributed by large granules and flocs. The fraction in the range 0.2 to 1 mm was not analysed but can be estimated by the difference between the mixed liquor and the sum of the other two fractions. Each bar represents the average of: 2 reactor samples and duplicate vials before the influent change ( $n = 4$ ); 3 reactor samples and duplicate vials at the end of the test period ( $n = 6$ ).

Before adding the particulate-rich influent stream, the specific protease activity (i.e., per gram of VS) of granules was about half of that of flocs. Nevertheless, due to the higher percentage of granular than flocculent sludge in the reactor, the total contribution to protease activity of the granule fraction in the reactor was as high as that of the flocculent fraction (Figure 2.3b). It is noteworthy that the large granule and floc activities

do not add up to the total activity in the mixed sludge. This can, at least partly, be explained by the activity of the small granule fraction (0.2–1 mm) which was not measured individually but is also part of the mixed liquor sample (Toja Ortega et al., 2021a). Increasing the influent pCOD did not significantly affect the biomass-specific protease activity of the mixed liquor and the granule fraction, and flocculent sludge activity decreased (Figure 2.3a). The total activity at reactor scale seemed to increase due to higher sludge concentration after the test period, although the large variation in activity in the mixed sludge fraction makes the difference statistically just not significant ( $p = 0.056$ ) (Figure 2.3b). The total protease activity contributed by large granules did increase significantly ( $p = 0.03$ ).

Regarding the hydrolysis of lipids, before the addition of the extra untreated slaughterhouse effluent the lipase activity was considerably higher in flocs than in granules (approximately 9-fold) (Figure 2.3a). Due to such a large difference in specific activity, also at a reactor level, the flocs contributed more to lipid hydrolysis than granules (three-fold). After the influent change, the specific lipase activity in flocculent sludge increased ( $p = 0.02$ ) and was approximately 10-fold of the specific lipase activity of granules. The biomass-specific lipase activity of granules, as with protease, did not change. On reactor-scale, the total mixed liquor lipase activity increased significantly due to the increased biomass concentration in the reactor ( $p = 0.009$ ). Regarding the contribution of each biomass fraction, the total lipase activity of granules increased due to the increased granular sludge concentration ( $p = 0.007$ ), so the activity of flocs became only twice as high as that of large granules at reactor scale. In any case, flocs seemed to be strongly involved in lipid hydrolysis, although granules also revealed measurable activity.

### 2.3.4 | Reactor performance and nutrient cycles

**Table 2.2.** Average effluent concentration of the main wastewater pollutants, in the months before the test period and during the test period. Standard deviation values are given between parentheses.

	COD [g m <sup>-3</sup> ]	BOD <sub>5</sub> [g m <sup>-3</sup> ]	TN [g m <sup>-3</sup> ]	NH <sub>4</sub> <sup>+</sup> -N [g m <sup>-3</sup> ]	NO <sub>x</sub> -N [g m <sup>-3</sup> ]	PO <sub>4</sub> -P [g m <sup>-3</sup> ]	TP [g m <sup>-3</sup> ]	TSS [g m <sup>-3</sup> ]
Effluent consent		7	5				0.3	30
Before test period	26 (±6)	1.5 (±0.5)	4.0 (±2.0)	0.3 (±0.2)	2.4 (±1.8)	0.04 (±0.01)	0.14 (±0.04)	5.2 (±1.6)
During test period	32 (±9)	2.4 (±1.3)	3.5 (±1.4)	0.3 (±0.3)	1.5 (±0.9)	0.07 (±0.09)	0.23 (±0.12)	5.5 (±1.2)

Effluent quality did not deteriorate during the test period (Table 2.2). Regarding reactor performance, several key performance indicators (KPI) were higher during the test period, including phosphate uptake rate, total phosphate release and ammonia uptake rate (nitrification) (Supplementary information 3). However, a similar trend was observed in the spring–summer period (April–July) of the years 2018 and 2020. Furthermore, the changes in the different KPI rate values can be theoretically coupled to temperature increase, so the increase was more likely attributed to seasonal variations than to the influent composition. Denitrification rate seems to be an exception. Denitrification rate was higher during the test period (Figure 2.4), and no similar increase was observed in the previous summer, except in reactor 2. In the following summer (2020) denitrification rate was higher than in the winter, but the change was not as pronounced as during the test period. Furthermore, changes in denitrification rate in previous years clearly followed increases in temperature, while during the test period the increase in denitrification rate was uncoupled from the increase in temperature. Nitrate uptake rates were determined during post-denitrification phases in all cycles. Simultaneous nitrification denitrification (SND) was not monitored through the KPI, because intermittent aeration was used, which did not allow a straightforward comparison of the produced and consumed nitrate.

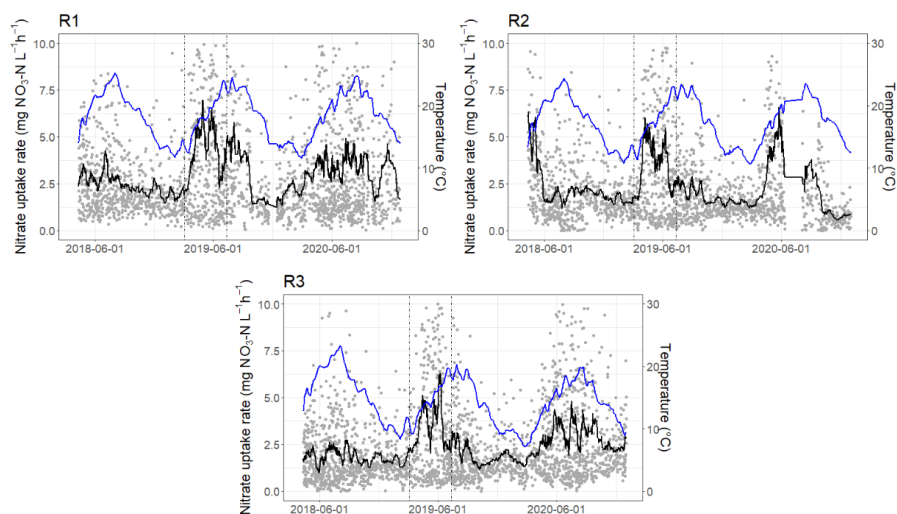


**Figure 2.4.** Denitrification rates measured during the post-denitrification period. R1, R2 and R3 indicate Nereda® reactors R1, R2 and R3 of WWTP Epe. Each dot represents the average rate in one SBR cycle. The continuous black line represents the moving average, with a sliding window of 7 days. The blue line indicates the temperature in the reactors. The test period is delimited by dashes.

### 2.3.5 | Microbial community composition: 16S rRNA gene amplicon sequencing results

The microbial community of the mixed liquor, large granules and flocs differed significantly, in terms of beta-diversity ( $p = 0.001$ ). Significant differences were observed too between the samples taken during normal operation and during the test period. The shift in microbial composition during the test period was most pronounced in flocculent sludge, and less in large granules. The distances between the analyzed samples are presented in Figure 2.5a.

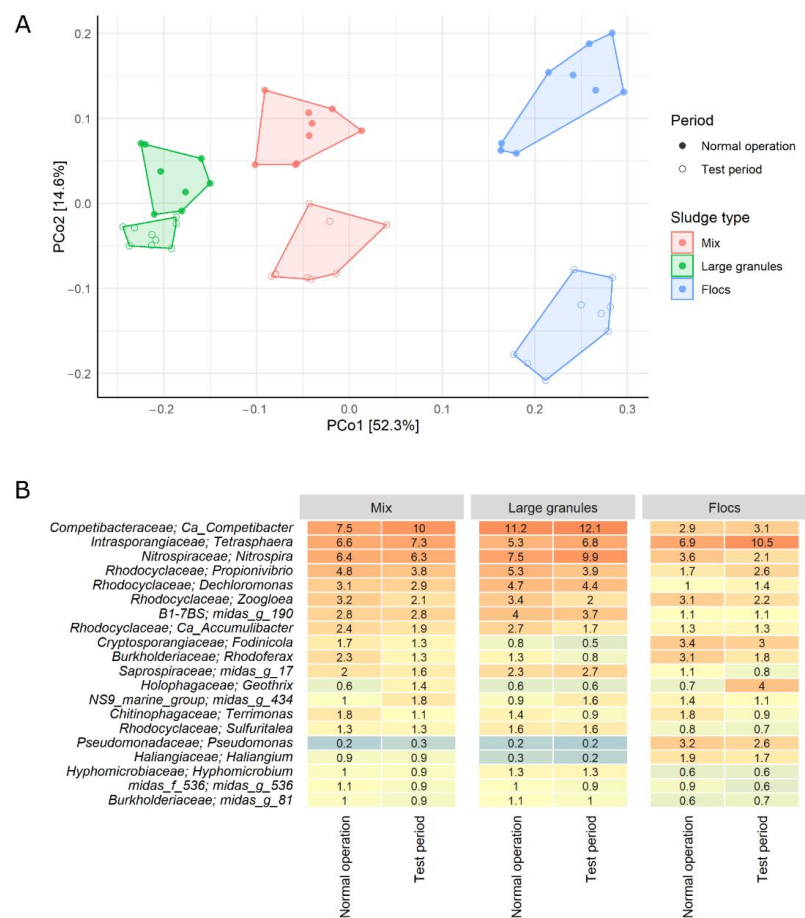


**Figure 2.5.** Microbial community composition of the sludge from WWTP Epe derived from 16S rRNA sequencing results. (A) Principal coordinates analysis (PCoA) plot based on the Bray-Curtis distance matrix between samples. (B) 20 most abundant genera and their families, in the mixed liquor sludge (Mix) and the large granule and floc fractions.

The 20 most abundant genera in the sludge are depicted in Figure 2.5b. Different genera of putative PAO and GAO were abundant in the sludge, such as *Ca. Accumulibacter*, *Tetrasphaera*, *Propionivibrio*, *Dechloromonas* and *Ca. Competibacter*. In the mixed sludge, a large proportion of the sequenced reads belonged to *Ca. Competibacter*, and the proportion increased during the test period from 7.5 to 10% of the reads. The genus *Tetrasphaera* was also abundant but did not significantly change over the test period in the mixed sludge. This PAO genus was predominant in the flocculent sludge fraction, where its proportion significantly increased during the test period. Large granules also had a considerably high percentage of *Tetrasphaera* (5.3–6.8%) and *Ca. Accumulibacter* (1.7–2.7%). The genus *Nitrospira* was also at high relative abundance in the sludge. Only a marginal percentage of *Nitrotoga* (0.002%) was detected, making *Nitrospira* the dominant nitrite oxidising bacteria (NOB). *Nitrospira* was mainly associated to large granules, where it also became more abundant during the test period. The AOB *Nitrosomonas* was detected but at low relative abundance (0.015%).

Microorganisms with a central role in hydrolysis and fermentation have been studied less than PAO, GAO and nitrifiers. This is partly due to the large array of organisms that can perform these functions. Several fermenting microorganisms were identified by Layer et al. in AGS reactors fed with complex wastewaters (Layer et al., 2019). The families *Saprospiraceae* and *Chitinophagaceae*, and the phylum *Chloroflexi* found in their study were at high relative abundances in Epe too (4.8–5.1%, 2.9–3.8% and 2–3.5%, respectively). Many members of these taxa can perform hydrolysis and fermentation (Xia et al., 2007). Between the abundant genera (>1% relative abundance) in Epe, there were several putative fermenters and hydrolysers: *Rhodoferax* (1.3–1.7%), *Fodinicola* (1.3–2.3%), *Terrimonas* (1.2–1.8%) and *Geothrix* (0.7–1.4%). *Rhodoferax* are denitrifying organisms and putative fermenters, which seem to be able to utilise carbohydrates, amino acids and short chain fatty acids. *Fodinicola*, in turn, are aerobic filamentous organisms that can hydrolyse proteins and carbohydrates. *Terrimonas*, too, are likely strictly aerobic hydrolysers. Last, *Geothrix* might play a role in lipid metabolism, as they can metabolise both short-chain and long-chain fatty acids, using nitrate as electron acceptor (Coates et al., 1999). However, the metabolism of these genera has not been systematically studied in situ and therefore it is difficult to infer their function in our system.



## 2.4 | DISCUSSION

### 2.4.1 | Changes in hydrolytic activity of the sludge

From the enzyme activities measured, none was detected in the bulk liquid. All lipase and protease activity were associated to the biomass, both to granules and to flocs. This observation is in line with previous biofilm and activated sludge studies that found hydrolytic activity to be predominantly associated to the biomass (Confer and Logan, 1998a; Frølund et al., 1995; Mosquera-Corral et al., 2003). Flocs had higher specific lipase and protease activity than granules, as observed in WWTP Garmerwolde (Toja Ortega et al., 2021a), most markedly in the case of lipase. The increased particulate load period had an effect on the biomass-specific activities of flocs, with a decrease in protease activity and an increase in lipase activity. This could be related to the increased influent lipid concentration in the test period, whereas the protein concentration did not change as sharply. That only the biomass-specific hydrolytic activities of flocs changed over the test period indicates that floc activity is more rapidly influenced by changes in the influent than granules. Furthermore, it seems from our results that flocculent sludge is actively involved in lipid hydrolysis and can increase the production of enzymes during a higher exposure to lipid substrates.

The change in influent composition did not affect the biomass-specific activity of granules. The total enzyme activity in the reactors mostly increased because of overall granule growth. The newly produced granules had the same biomass-specific activity, so the total hydrolytic activity increased. Under normal operation, the granular sludge already had, theoretically, enough potential to hydrolyse all the proteins and lipids from the more concentrated influent within one SBR cycle (Supplementary information 4). However, it would be unrealistic to assume that the rates measured in laboratory assays, based on kDa-size substrates with good biodegradability, are directly translatable to full-scale conditions. Nevertheless, the enzymatic activity of the granules does not seem to be a limiting factor for complete hydrolysis of influent pCOD. Similar results were obtained at the AGS reactors at WWTP Garmerwolde (Toja Ortega et al., 2021a). The hydrolysis rate apparently does not depend so much on enzyme content of the granules but on mass-transfer of the substrate into the biofilm (granule). In biofilm reactors, hydrolysis can be described using an areal hydrolysis rate ( $\text{g TOC}/\text{m}^2/\text{h}$ ), which accounts for the biofilm area in the reactor (Kommedal et al., 2006).

## 2.4.2 | Microbial community composition and shifts

### Microorganisms involved in P and N removal

In this section the most abundant taxa are discussed under the assumption that the relative abundances in the sequenced 16S rRNA genes reflect the abundance of their respective microorganisms in the sludge. This might not hold true in all cases, due to biases associated to 16S rRNA gene amplicon sequencing, including biases in the extraction and amplification of the DNA and differences in DNA copy number among microbial groups. For example, the relative abundances of *Ca. Accumulibacter* and *Tetrasphaera* are underestimated when determined by 16S sequencing compared to FISH, while *Dechloromonas* seems to be overestimated (Stokholm-Bjerregaard et al., 2017). However, the data can provide a glimpse of the main microbial components in the sludge. The sequencing results revealed a large proportion (~20% of the reads) of microorganisms related to enhanced biological phosphorus removal (EBPR) and nitrogen removal (Nielsen et al., 2010; Saunders et al., 2016). This is in line with the good nutrient removal performances that were achieved in the plant. The NOB *Nitrospira* was one of the most abundant microorganisms in the sludge, comprising 6.3–6.4% of the reads in the mixed sludge. Numerous studies have reported *Nitrospira* as the main NOB in full-scale EBPR plants, probably due to its high substrate *affinity*, which allows them to thrive under low oxygen and nitrite concentrations (Daims et al., 2001; Nielsen et al., 2010). The only detected AOB was *Nitrosomonas*, with low relative abundance (0.015%). Finding AOB at low relative abundances in 16S rRNA amplicon sequencing data does not necessarily imply a low AOB activity in the sludge (Weissbrodt et al., 2013). That was also the case in this study where no issues with nitrification were identified.

The classical PAO genus *Ca. Accumulibacter* was present in relatively high abundance (1.9–2.4%) in the mixed sludge. In general, at more complex influent composition fermentative PAO and GAO populations seem to be favoured (Ali et al., 2019; Campo et al., 2020; Layer et al., 2019; Nielsen et al., 2019), which is in line with the observations for the sludge in Epe. The fermentative PAO *Tetrasphaera* was found in high relative abundance, accounting for 6.6–7.3% of the reads in the mixed sludge samples. *Tetrasphaera* is often found in AS and AGS fed with complex wastewaters. They can use a wider range of substrates compared to *Ca. Accumulibacter*, including sugars and amino acids which they can utilise through a fermentative metabolism (Stokholm-Bjerregaard et al., 2017). The fermentative *Dechloromonas* was also abundant in the mixed sludge samples. Members of this genus seem to possess a PAO metabolism, but others behave as GAO (Nielsen et al., 2019). Therefore, their contribution to EBPR in our system is unclear. Overall, GAO were abundant in the sludge from Epe, the main genera

being *Ca. Competibacter* (7.5–10%) and the fermentative GAO *Propionivibrio* (3.8–4.8%). The high COD/P ratio of the wastewater (>100 mg COD/mg P) likely favoured the growth of GAOs. GAOs in most cases are not harmful to the EBPR process and indicate an excess of COD (Nielsen et al., 2019). In our study too, effective EBPR was observed regardless of the high GAO abundance.

Similar to previous studies, slow-growing microorganisms (PAO, GAO and nitrifiers) were enriched in the granular sludge in comparison with flocs, due to the longer solids retention time (SRT) of granules (Ali et al., 2019; Mari K.H. Winkler et al., 2012). Furthermore, granules have preferential access to influent substrates during the feeding phase, due to their localisation at the bottom of the reactor resulting from their higher settling velocity compared to smaller granules and flocs (van Dijk et al., 2020). This further enhances the access of PAO and GAO to the rbCOD in the influent. Interestingly, *Tetrasphaera* was more concentrated in flocculent sludge, and even increased during the test period, while previous studies reported higher *Tetrasphaera* abundances in granules than in flocs (Ali et al., 2019). The reasons for the discrepancy with our study might be related to the differences in substrate utilisation of both PAO. *Ca. Accumulibacter*, in granules, have preferential access to the VFA in the influent. Meanwhile, flocculent sludge has the ability to entrap more particulate substrates throughout the cycle, and also has a higher hydrolytic capacity, making monomers such as amino acids and monosaccharides available to *Tetrasphaera* throughout the cycle. However, this is a mere speculation that should be tested in more AGS plants and using more quantitative methods than 16S rRNA sequencing.

### Microbial community changes during the test period

The changes in microbial diversity during the test period were more pronounced in flocculent sludge than in large granules. The shorter SRT of flocculent sludge, and the higher immigration rates to this sludge fraction, can explain this observation (Ali et al., 2019). The new influent did not have a strong impact on the microbial communities in the more rigid and older granules, which relates to the stable performance of the plant and the minimal changes in the hydrolytic activity of granules. The larger shift in microbial community of flocs is also in line with the activity changes measured in this fraction.

In terms of changes in individual taxa, the GAO *Ca. Competibacter* proliferated during the test period, possibly due to the increased COD/P ratio. No clear increase was observed among the putative hydrolyser and fermenter taxa, even if the reactors received higher particulate contaminant concentrations. The abundance of *Chloroflexi*

and *Geothrix* increased, but *Saprospiraceae* and *Fodinicola* decreased, while *Tetrasphaera*, *Propionivibrio*, *Dechloromonas* and *Rhodoferax* did not change significantly. The sludge contained various organisms capable of metabolizing different types of organic matter already during normal operation, and at increased particulate loads there were shifts among these groups but no sharp increase in their relative abundances. The lack of a clear increase aligns with the results from the hydrolytic tests, as the specific hydrolytic activity of the sludge did not change either. Lipid metabolism in flocculent sludge was an exception; the specific lipase activity of flocculent sludge increased. In flocculent sludge, the abundance of *Geothrix* increased from 0.7 to 4.2%, which might be related to the increase in lipase activity. However, the metabolism of *Geothrix* in aerobic wastewater treatment systems has not been studied. Further analysis would be insightful to understand their role in this ecosystem. Filamentous microorganisms related to LCFA metabolism (*Ca. Microthrix*, *Gordonia*) were not abundant in the sludge, and *Ca. Microthrix* even decreased during the test period (from 0.5 to 0.09%). No foaming or bulking was observed in the reactors even if the lipid load increased considerably.

Protozoa were not studied through sequencing, as only the bacterial and archaeal 16S gene was targeted. However, microscopy revealed a protozoa bloom in the sludge during the test period (Figure 2.1). Protozoa are likely to take up particulates, although their contribution to pCOD removal was not quantified (Morgenroth et al., 2002; Norbert Schwarzenbeck et al., 2004). They did not deteriorate the settleability of the sludge and might contribute to granule stability by metabolizing particulates at the granule surfaces.

### 2.4.3 | Impact of particulates on the treatment and sludge growth

The treatment performance during the test period remained stable, in terms of COD, P and N removal. Effluent suspended solids did not increase either. Furthermore, during the test period the denitrification rates were higher than usual (on average, 4.0 mg NO<sub>3</sub>-N L<sup>-1</sup> h<sup>-1</sup> compared to 3.1 mg NO<sub>3</sub>-N L<sup>-1</sup> h<sup>-1</sup> during normal operation). Previous studies showed that the particulates could significantly contribute to denitrification in AS (Drewnowski and Makinia, 2014; How et al., 2020), as well as in biofilm reactors (Krasnits et al., 2014, 2013). In those studies, denitrification relied partly on intracellularly stored substrates, but mostly on particulates that remained entrapped in the sludge and kept hydrolyzing during the anoxic phase. In AGS reactors, this would mainly benefit post-denitrification, since simultaneous nitrification-denitrification (SND) requires the anaerobic storage of substrates and subsequently the coexistence of different redox zones during aeration. Particulates would have to be anaerobically hydrolyzed and

fermented by granules and diffuse below the granule surface in order to be stored as PHA and contribute to SND. This is likely a slow process due to mass-transfer limitation. Even if the anaerobic uptake of particulates by granules would be limited, SND can be enhanced by applying optimized aeration strategies. Layer et al. (2020) proposed to apply alternating aeration (intermittent switching on and off) or 2-step aeration (a pulse of high aeration followed by low DO for the rest of the reaction phase) to improve SND when AGS was fed with complex wastewater (Manuel Layer et al., 2020). This way, with an increased particulate COD load such as the one in the present study it is likely possible to enhance SND, as well as to reduce the post-denitrification phase length and achieve lower effluent N.

During the test period, sludge growth was observed in the reactors at WWTP Epe. The total sludge concentration of all three reactors increased (from 5.7 to 7.6 g TS/L in R1, 5.8 to 8.5 g TS/L in R2 and 5.9 to 8.7 g TS/L in R3), as well as the granule proportion (from 58 to 67%). Thus, granule growth was observed following the increase in influent COD. After the test period, the sludge concentration remained high but did not increase further. Nevertheless, the sludge concentration in the reactors, as well as the proportion of large granules, had started to increase before the test period and there were large oscillations in the measurements (Supplementary information, Figure S2.2). This makes it difficult to conclude whether granular sludge growth was supported by the added particulates. Part of these particulates were consumed in the reactor, but it is not clear if this was accomplished by the granules or by the flocculent sludge fraction. Nonetheless, the study does show that the sustained increased load of biodegradable influent particulates did not negatively impact granule growth. This holds for an influent particulate concentration of approximately 1.3 g COD/L (77% of the COD). The granule size did not decrease, as opposed to previous studies where with more complex wastewater the sludge bed was composed of smaller granule sizes (Derlon et al., 2016; Layer et al., 2019). The proportion of flocculent sludge did not increase either, probably due to increased sludge wasting (Figure 2.2). Furthermore, the higher influent particulate concentration did not result in filamentous outgrowths in the granules or disruption of granule stability as seen in previous studies (de Kreuk et al., 2010; Schwarzenbeck et al., 2005). Only a higher concentration of protozoa was observed on granule surfaces. According to our results, a moderate increase of influent suspended solids does not necessarily deteriorate granule integrity or size distribution. There might be a few reasons for this: (1) The granules can anaerobically hydrolyze part of the pCOD, as indicated by their relatively high hydrolytic activities. The available pCOD during aeration is therefore lowered; (2) protozoa at the granule surfaces might take up a considerable amount of particulates aerobically, limiting the creation of substrate

gradients at the granule surfaces (Norbert Schwarzenbeck et al., 2004); and (3) the flocculent sludge can capture and hydrolyze particulates, as indicated by its high specific hydrolytic activity, an observation in line with the hypothesis of Layer et al. (2019). An adjusted sludge wasting maintains the sludge bed composition avoiding a buildup of the flocculent sludge fraction and particulate material in the reactor.

## 2.5 | CONCLUSION

We studied a full-scale Nereda® plant faced with an increased influent pCOD concentration during a 3-month period. Doubling the influent pCOD concentration did not interfere with the smooth granule morphology and did not compromise nutrient removal efficiency. In line with this observation, the sludge exhibited high hydrolytic activity and a high proportion of putative hydrolysing and fermenting organisms. The exact contribution of pCOD to sludge growth and nutrient removal could not be clarified and deserves further research. Nonetheless, the results of this study point towards good performance stability of the AGS process operated with an increased influent particulate concentration. An increased COD could permit the achievement of more efficient N removal and meeting more stringent effluent discharge requirements, without adding external C sources or post-treatment steps. Therefore, adding a COD-rich wastewater stream, even with a high particulate content, can be a good solution when a higher COD load to AGS reactors is desired.

## SUPPLEMENTARY INFORMATION

**Supplementary information 1: Size-distribution of the influent COD, during normal operation and during the test period.**

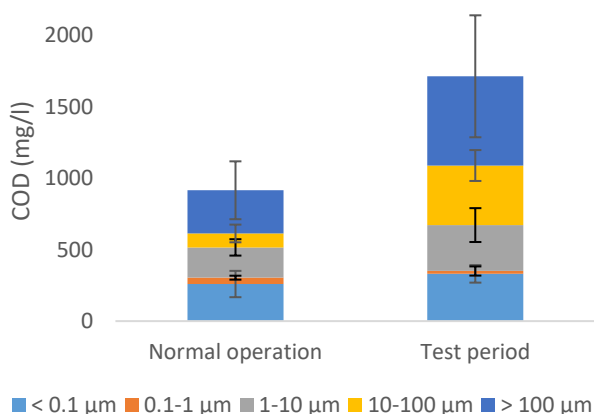


**Figure S.2.1.** Distribution of the influent COD in different size fractions, during normal operation and during the test period.  $n=3$ , in each scenario. Error bars represent standard deviation between the three measurements.

**Supplementary information 2: Sludge growth in the reactors during the test period and the months before and after.**

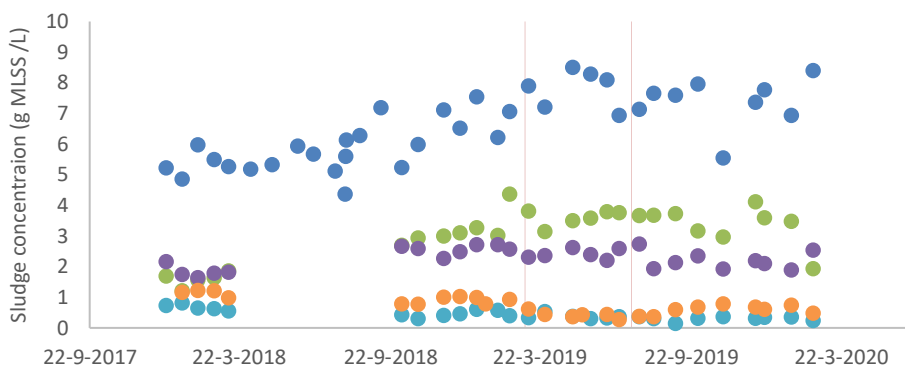


**Figure S.2.2.** Mixed liquor suspended solids (MLSS) concentration of the reactors at WWTP Epe, and the concentration of different granule size fractions. The values displayed are the average TS concentration from reactors 1, 2 and 3. The granule size distribution data from the period between April and November 2018 was not available, and therefore only the MLSS concentration is plotted on that period. The sludge growth data was measured and provided by Vallei en Veluwe. The vertical red lines delimit the test period.

### Supplementary information 3: Key performance indicators from reactors 1-3 of the WWTP Epe.

Figures S2.3.1-S2.3.5 show key performance indicators (KPI) recorded during each SBR cycle of the AGS reactors during a 3-year stretch of time. The data for each of the three reactors is represented in separate graphs.

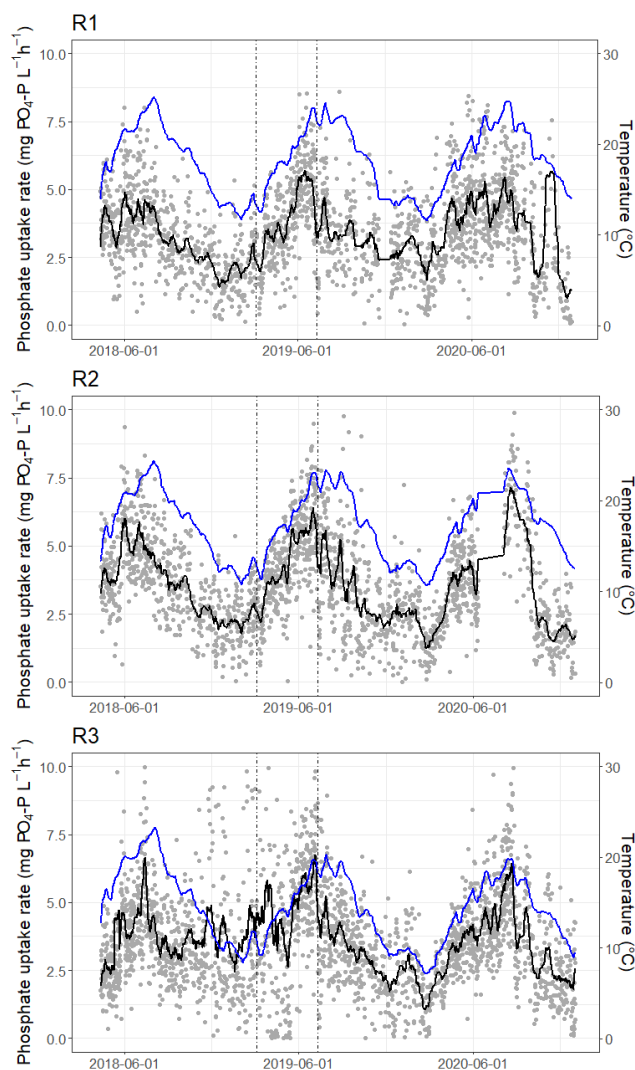


**Figure S2.3.1.**  $\text{PO}_3\text{-P}$  uptake rates measured in the reactors at WWTP Epe. Each dot represents the KPI value for a single SBR cycle, and the continuous black line represents the moving average with a sliding window of 7 days. Temperature is plotted in a blue line. The vertical lines indicate the test period, where a higher particulate COD load was fed to the reactors.



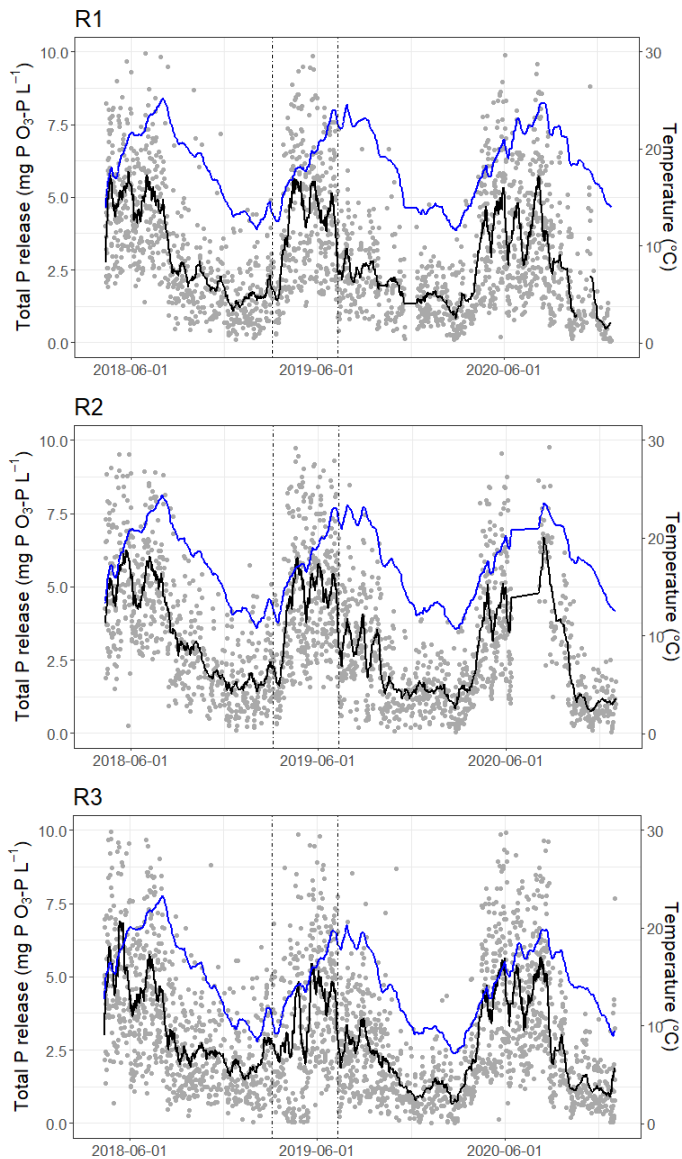


**Figure S2.3.2.** Total PO<sub>3</sub>-P release measured in the reactors at WWTP Epe. Each dot represents the KPI value for a single SBR cycle, and the continuous black line represents the moving average with a sliding window of 7 days. Temperature is plotted in a blue line. The vertical lines indicate the test period, where a higher particulate COD load was fed to the reactors.

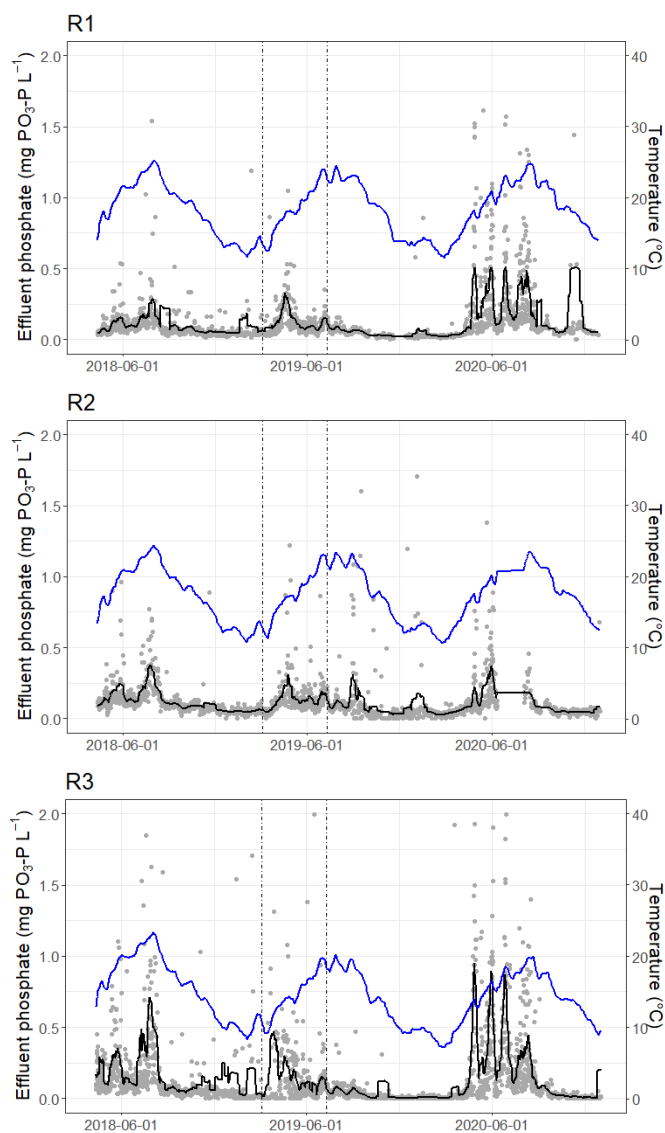


**Figure S2.3.3.** Effluent  $\text{PO}_3\text{-P}$  concentration measured in the reactors at WWTP Epe. Each dot represents the KPI value for a single SBR cycle, and the continuous black line represents the moving average with a sliding window of 7 days. Temperature is plotted in a blue line. The vertical lines indicate the test period, where a higher particulate COD load was fed to the reactors.

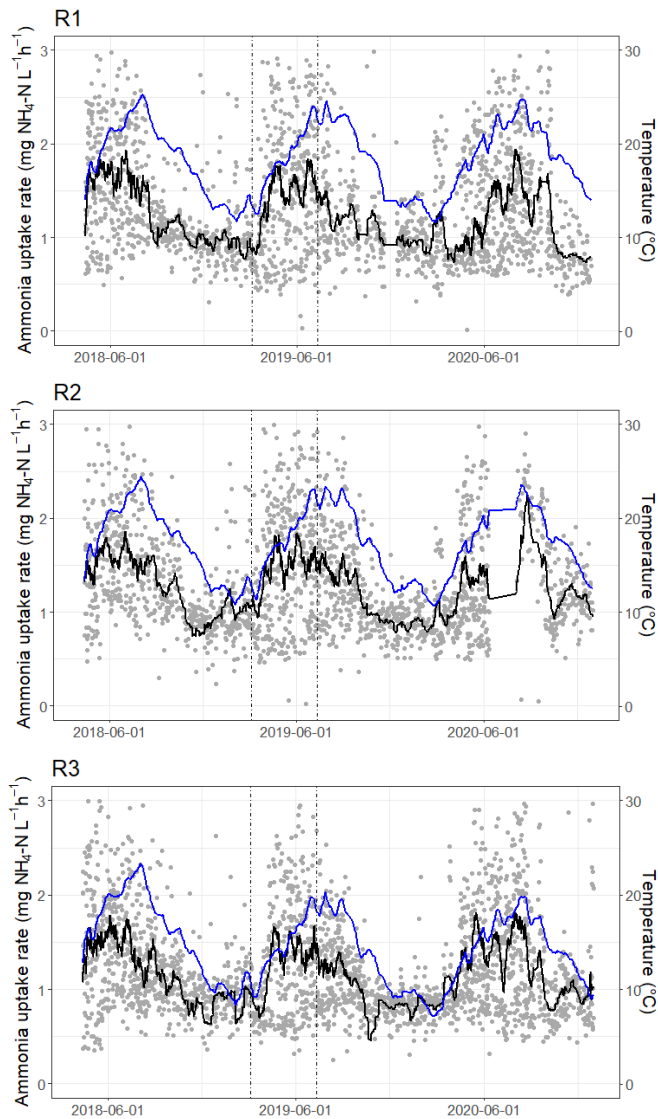


**Figure S2.3.4.** NH<sub>4</sub>-N removal rates measured in the reactors at WWTP Epe. Each dot represents the KPI value for a single SBR cycle, and the continuous black line represents the moving average with a sliding window of 7 days. Temperature is plotted in a blue line. The vertical lines indicate the test period, where a higher particulate COD load was fed to the reactors.

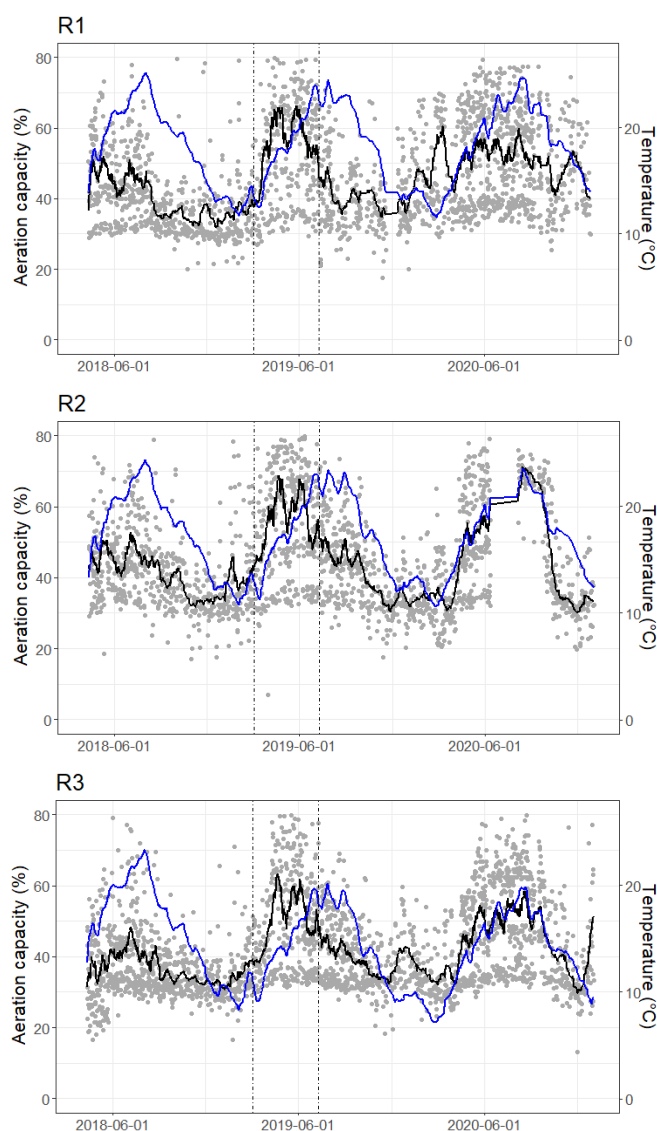


**Figure S2.3.5.** Aeration capacity used in the reactors at WWTP Epe. Each dot represents the KPI value for a single SBR cycle, and the continuous black line represents the moving average with a sliding window of 7 days. Temperature is plotted in a blue line. The vertical lines indicate the test period, where a higher particulate COD load was fed to the reactors.

### Supplementary information 4: Calculation of total hydrolytic activity during feeding.

The total hydrolytic activity during feeding is calculated by multiplying the specific hydrolytic activities measured in the enzyme assays by the weight of the settled sludge layer that is passed by the influent during plug-flow feeding. The volume of sludge “filled” with influent during feeding is considered to be the same as the feed batch volume. The total settled sludge bed volume is larger than the batch volume (Table S2.4.1), i.e. the volume fed per SBR cycle is smaller than the total settled sludge volume, which leads to the assumption that only large granules (at the bottom of the reactor) will be in contact with the influent during the plug-flow feeding. Hence, only large granule hydrolytic activity of the mass of sludge filled with influent is used to calculate the anaerobic hydrolysis during feeding. That is, the influent fed granule volume (=batch volume) divided by the  $SVI_5$ .

**Table S2.4.1.** Reactor sludge composition and SBR cycle characteristics, during normal plant operation.

Parameter	Value	Unit
TS (g/L)	6.4	g/L
VS (g/L)	4.9	g/L
$SVI_5$ (mL/g VS)	45	mL/g VS
Reactor vol (m <sup>3</sup> )	4500	m <sup>3</sup>
Sludge weight (kg VS)	22078	kg VS
Settled sludge bed volume (m <sup>3</sup> )	994	m <sup>3</sup>
Q (m <sup>3</sup> /d)	5066	m <sup>3</sup> /d
Batch volume/SBR cycle (m <sup>3</sup> )	422	m <sup>3</sup>
Granule mass in contact with influent	9381	kg
Specific protease activity large granules	26.77	mg protein g VS <sup>-1</sup> h <sup>-1</sup>
Specific protease activity mixed sludge	87.63	mg protein g VS <sup>-1</sup> h <sup>-1</sup>
Specific lipase activity large granules	8.13	mg lipid g VS <sup>-1</sup> h <sup>-1</sup>
Specific lipase activity mixed sludge	68.52	mg lipid g VS <sup>-1</sup> h <sup>-1</sup>

The bed volume filled with influent is divided in 10 segments, the activity of which is accounted for only once they are filled with influent, during a 2 hour plug-flow feeding. In table S2.4.2, the time during which each of the segments is active is displayed. Zero order kinetics is assumed for simplicity (substrate concentration >  $K_s$ ). It also shows the total activity contributed by that segment during the feeding time (its specific activity \* the granule mass in that segment \* time active).

**Table S2.4.2.** Hydrolytic activity contributed by each segment during feeding, during normal plant operation.

Segment #	Active (h)	Protease activity contributed (g protein)	Lipase activity contributed (g lipid)
segment 1	2	50233	15256
segment 2	1.8	45210	13730
segment 3	1.6	40187	12205
segment 4	1.4	35163	10679
segment 5	1.2	30140	9154
segment 6	1	25117	7628
segment 7	0.8	20093	6102
segment 8	0.6	15070	4577
segment 9	0.4	10047	3051
segment 10	0.2	5023	1526

**Table S2.4.3.** Comparison of the lipid and protein content in the influent (during normal operation and test period), and hydrolytic activity during feeding during normal plant operation.

Parameter	Protein	Lipid
Total activity in 2 h feeding (g substrate hydrolysed)	276282	83908
Influent substrate concentration hydrolysed in 2h feeding (mg/L)	654	199
Influent substrate concentration normal operation	76	45
Influent substrate concentration test period	135	290

As shown in Table S2.4.3, the sludge has enough hydrolytic capacity to (theoretically) hydrolyse all the influent proteins within the anaerobic feeding phase, both during normal operation and during the test period. However, the increased influent lipid concentration during the test period is higher than the sludge can hydrolyse during the feeding phase. Thus, the aerobic hydrolysis is estimated to assess whether the aerobic phase would allow complete lipid hydrolysis. During aeration, all the reactor sludge is in contact with the influent due to fully mixed conditions. Therefore, the specific activity of the mixed sludge is used for the calculations. Even if the assays only quantified anaerobic hydrolytic activity, the results were extended to aerobic conditions. This assumption was based on previous studies that proved hydrolysis rates to be unaffected by short-term (one SBR cycle) changes of redox conditions, when the hydrolytic activity was cell or biofilm associated (Boczar et al., 1992; Goel et al., 1998b). Considering the hydrolytic activity of the sludge in normal operation ( $68.52 \text{ mg lipid g VS}^{-1} \text{ h}^{-1}$ ), and the sludge mass in the reactor ( $22078 \text{ kg VS}$ ) the hydrolytic activity during aeration would be  $1370974 \text{ g lipid/h}$ , or if divided by the batch volume ( $422 \text{ m}^3$ ),  $305 \text{ mg/L}$  of influent lipids per hour of aeration. Therefore, the reactor has the capacity to hydrolyse the lipids remaining after the anaerobic feeding phase within the first hour of aeration.

### Supplementary information 5: Comparison of estimated and observed sludge production.

Sludge production was estimated from the COD and TN load to the reactors, and compared to the observed sludge production in order to explore the fate of the pCOD added in the test period. Equation 1 estimates the production of heterotrophic and nitrifying biomass, based on influent substrate (COD) and nitrogen (Metcalf & Eddy, 2003):

$$P_{X,VSS} = \frac{QY(S_i - S)}{1 + k_d SRT} (1 + f_d k_d SRT) + \frac{QY_n(NO_x)}{1 + k_{dn} SRT} + QnbVSS \quad [1]$$

where:

$P_{X,VSS}$  = Net waste sludge produced per day [kg VSS d<sup>-1</sup>]

$Q$  = Influent flow [m<sup>3</sup> d<sup>-1</sup>]

$Y$  = Biomass yield [kg VSS kg<sup>-1</sup> COD]

$Y_n$  = Nitrifying biomass yield [kg VSS kg<sup>-1</sup> COD]

$S_i$  = influent substrate concentration [kg COD m<sup>-3</sup>]

$S$  = effluent substrate concentration [kg COD m<sup>-3</sup>]

$NO_x$  = concentration of NH<sub>4</sub>-N in the influent that is nitrified [kg N m<sup>-3</sup>]

$k_d$  = endogenous decay coefficient [d<sup>-1</sup>]

$k_{dn}$  = endogenous decay coefficient for nitrifying organisms [d<sup>-1</sup>]

$SRT$  = theoretical average solids retention time [d]

$f_d$  = fraction of biomass that remains as cell debris

$nbVSS$  = non-biodegradable influent suspended solids [kg VSS m<sup>-3</sup>]

Sludge production was estimated considering biodegradable COD (bCOD) as substrate. Biodegradable COD was estimated from BOD, applying a factor of 1.6 (bCOD = 1.6 x BOD<sub>5</sub>) (Metcalf & Eddy, 2003). Since the non-biodegradable influent suspended solids (nbVSS) concentration was not known, sludge production was predicted based only on heterotrophic and nitrifying biomass growth, therefore excluding the last component of Equation 1 ( $Q \times nbVSS$ ). nbVSS was then estimated from the difference between the prediction and the observed sludge production. The values used in the calculation are listed in Table S2.5.1.

**Table S2.5.1.** values used in the prediction of sludge growth based on influent composition.

Parameter	Normal operation	Test period	Reference
Q [ $\text{m}^3 \text{d}^{-1}$ ]	4696	5229	This study
tCOD [ $\text{g COD m}^{-3}$ ]	840	1456	This study
BOD <sub>5</sub> [ $\text{g BOD m}^{-3}$ ]	341	537	This study
BOD <sub>5,eff</sub> [ $\text{g COD m}^{-3}$ ]	1,5	2,4	This study
bCOD [ $\text{g COD m}^{-3}$ ]	546	859	Calculated, this study
bCOD <sub>eff</sub> [ $\text{g COD m}^{-3}$ ]	2.4	3.8	Calculated, this study
TN [ $\text{g N m}^{-3}$ ]	77	101	This study
NO <sub>x</sub> [ $\text{g N m}^{-3}$ ]	62	81	Calculated, this study
k <sub>d</sub> [ $\text{d}^{-1}$ ]	0.12		(Metcalf & Eddy, 2003)
k <sub>dn</sub> [ $\text{d}^{-1}$ ]	0.08		(Metcalf & Eddy, 2003)
f <sub>d</sub>	0.15		(Metcalf & Eddy, 2003)
SRT [d]	25		(Ali et al., 2019)
Y [ $\text{kg VSS kg}^{-1} \text{COD}$ ]	0.4		(Metcalf & Eddy, 2003)
Y <sub>N</sub> [ $\text{kg VSS kg}^{-1} \text{N}$ ]	0.12		(Metcalf & Eddy, 2003)

The concentration of NH<sub>4</sub>-N in the influent that is nitrified (NO<sub>x</sub>) was assumed to be 80% of the TN. Based on the calculation above, the predicted sludge production is 381 kg VSS d<sup>-1</sup> during normal operation, and 665 kg VSS d<sup>-1</sup> in the test period. The actual sludge production, considering both the increase in reactor VSS concentration and spill production, was 1146 kg VSS d<sup>-1</sup> during normal operation and 1495 kg VSS d<sup>-1</sup> during the test period. From the difference between the prediction and the observed sludge production, an influent nbVSS concentration of around 160 g VSS m<sup>-3</sup> was calculated for both situations.

Several assumptions are made in the prediction of sludge production. For instance, the theoretical average SRT of our study was not measured, and it might not be the same for the normal operation and the pilot period. Moreover, the uncertainty of influent composition measurements decreases the accuracy of the values used in the balance. For example, instead of using different influent flows during normal operation and test period, an average flow of 4808 m<sup>3</sup> d<sup>-1</sup> could be considered for both situations, since the difference in flow was not significant between periods. In that case, the calculated nbVSS would be 157 g VSS m<sup>-3</sup> during normal operation and 184 g VSS m<sup>-3</sup> during the test period. This would be more in agreement with the higher nbCOD (tCOD-bCOD) during the pilot. This example illustrates that the limitations associated to full-scale monitoring do not allow to accurately estimate the fraction of pCOD consumed in the reactor during the higher load period. However, using typical growth and decay values it is possible to make a prediction of the sludge production that reasonably matches the observations.







# 3

## Anaerobic hydrolysis of complex substrates in full-scale aerobic granular sludge

**Published as:** Toja Ortega, S. Pronk, M. & de Kreuk, M.K. (2021). Anaerobic hydrolysis of complex substrates in full-scale aerobic granular sludge: enzymatic activity determined in different sludge fractions. *Applied Microbiology and Biotechnology*, 105(14-15), 6073-6086. DOI: 10.1007/s00253-021-11443-3

## ABSTRACT

Complex substrates, like proteins, carbohydrates and lipids, are major components of domestic wastewater, and yet their degradation in biofilm-based wastewater treatment technologies, such as aerobic granular sludge (AGS), is not well understood. Hydrolysis is considered the rate limiting step in the bioconversion of complex substrates, and as such it will impact the utilization of a large wastewater COD (chemical oxygen demand) fraction by the biofilms or granules. To study the hydrolysis of complex substrates within these types of biomass, this chapter investigates the anaerobic activity of major hydrolytic enzymes in the different sludge fractions of a full-scale AGS reactor. Chromogenic substrates were used under fully mixed anaerobic conditions to determine lipase, protease,  $\alpha$ -glucosidase and  $\beta$ -glucosidase activities in large granules (>1 mm diameter), small granules (0.2–1 mm), flocculent sludge (0.045–0.2 mm) and bulk liquid. Furthermore, composition and hydrolytic activity of influent wastewater samples were determined. Our results showed an overcapacity of the sludge to hydrolyse wastewater soluble and colloidal polymeric substrates. The highest specific hydrolytic activity was associated with the flocculent sludge fraction (1.5–7.5 times that of large and smaller granules), in agreement with its large available surface area. However, the biomass in the full scale reactor consisted of 84% large granules, making the large granules account for 55–68% of the total hydrolytic activity potential in the reactor. These observations shine a new light on the contribution of large granules to the conversion of polymeric COD, and suggest that large granules can hydrolyse a significant amount of this influent fraction. The anaerobic removal of polymeric soluble and colloidal substrates could clarify the stable granule formation that is observed in full scale installations, even when those are fed with complex wastewaters.

### 3.1 | INTRODUCTION

In recent years, aerobic granular sludge (AGS) technology has emerged as an alternative to the conventional activated sludge (AS) technology for the treatment of domestic wastewater (Bengtsson et al. 2018; Pronk et al. 2015). AGS is composed of granular microbial aggregates and can remove chemical oxygen demand (COD), phosphorus (P) and nitrogen (N) from wastewater (Bassin et al. 2012; Coma et al. 2012; de Kreuk et al. 2005; Layer et al. 2019). AGS requires less space and energy than AS, due to the granular morphology that improves the settling properties of the sludge, which leads to a smaller footprint and a simple reactor design. The technology is applied by Royal-Haskoning DHV at full-scale under the trade name Nereda®, based on a sequencing batch reactor (SBR) cycle consisting of simultaneous anaerobic feeding and effluent removal, aeration and settling (Giesen et al. 2013; Pronk et al. 2017). Full-scale AGS, fed with domestic wastewater, operates stable and can remove COD and nutrients efficiently (Giesen et al. 2014; Ni et al. 2009; Pronk et al. 2017). Still, some aspects of full scale operation of AGS need further study to optimize this novel process and understand the observations made in pilot and full scale applications. One main knowledge gap is the removal mechanism of influent particulate COD.

The composition of the influent is a main difference between full-scale practice and most lab-scale experiments. Substantial knowledge about AGS has been gained studying lab-scale reactors fed with simple influents, rich in volatile fatty acids (VFA) (Bassin et al. 2012; de Kreuk et al. 2005; Mosquera-Corral et al. 2005; Weissbrodt et al. 2014; Zeng et al. 2003). The conditions in these studies promoted the growth of slow-growing, storage polymer-forming microorganisms, such as polyphosphate accumulating organisms (PAO). Slow-growing microorganisms contribute to granule formation and stability (de Kreuk and van Loosdrecht 2004; Picioreanu et al. 1998). The selected PAO population additionally removes phosphorus and nitrate from the wastewater, therefore contributing to enhanced biological phosphorus removal (EBPR). Since acetate and propionate are the main substrates of PAOs, their loading rate is an important factor for EBPR treatment plant design and operation (Lopez-Vazquez et al. 2020).

VFA content of domestic wastewater is highly variable, ranging as much as from 1 to 50% of the total influent COD. The VFA concentration can be influenced by several parameters such as type of wastewater, sewer type, temperature and residence time in the sewer (Hvitved-Jacobsen et al. 1995; Narkis et al. 1980; Rudelle et al. 2011; Yun et al. 2013). Most domestic wastewaters contain 10 percent or less VFA-COD, while the

3 remaining COD is composed by complex substrates, such as proteins, carbohydrates and lipids (Levine et al. 1991; Raunkjær et al. 1994; Rudelle et al. 2011; Volcke et al. 2020). They are present in the wastewater as particulates (e.g. cellulose fibers, microbial cells) or as colloid and soluble polymers. In AGS systems, a large fraction of the particulate COD ends up in the flocculent sludge fraction in the reactor (Guo et al. 2020; Layer et al. 2019). This fraction has a relatively short solids retention time (SRT) (Ali et al. 2019) reducing the mineralization of the particulate COD (Guo et al. 2020). On the other hand, polymeric substrates could be used for EBPR and granule growth, which would be beneficial for AGS reactors treating wastewaters with a low or highly variable VFA content. During the anaerobic feeding phase easily degradable soluble COD can be stored cell-internally as poly-hydroxyalkanoates (PHA), while polymeric substrates can potentially be hydrolysed and fermented to VFA and stored sequentially. Hydrolysis has often been described as the rate-limiting step in biological degradation of organic matter (Balmat 1957; Ubukata 1997). Hence, in AGS reactors, the hydrolysis of polymeric substrates during the feeding phase will determine to a large extent the amount of substrate that is available for PHA storage and thus for the bio-P removal.

Moreover, incomplete uptake of polymeric substrates during the anaerobic phase, and their presence in the aerobic phase, is often associated with irregular sludge morphology, decreased settleability or smaller granule size (de Kreuk et al. 2010; Derlon et al. 2016; Layer et al. 2019; Wagner et al. 2015). Therefore, it is relevant for good AGS performance to have sufficient hydrolytic capacity for complete transformation of the polymeric substrates in the influent during the anaerobic phase. Although efforts have been made to characterize hydrolysis in biofilm systems at lab scale (Kommedal et al. 2006; Mosquera-Corral et al. 2003), and AS systems at lab and full-scale (Frølund et al. 1995; Goel et al. 1998; Morgenroth et al. 2002), hydrolysis in full-scale AGS reactors has not been extensively studied. Furthermore, the hydrolytic potential of aerobic granules, its accompanying flocculent biomass, and the activity in the bulk liquid is still unknown.

To evaluate the hydrolytic potential of polymeric substrates under the anaerobic feeding conditions, we measured the activities of specific hydrolytic enzymes of the sludge derived from a full scale Nereda® installation. In order to study the maximum hydrolysis capacity, we used soluble model substrates, rather than slowly biodegradable particulates. The sludge fractions were incubated with chromogenic lipase, protease and glucosidase substrates under anaerobic fully-mixed conditions and were sampled periodically to monitor hydrolysis rates. The hydrolytic activity of the mixed sludge, large (>1 mm) and small (0.2-1 mm) granules, flocculent sludge, influent wastewater, and bulk

liquid of the AGS reactor was determined and evaluated considering the composition of the incoming wastewater. Large granules were crushed and their activity was measured to study the effect of mass transfer limitation on hydrolysis. By studying anaerobic hydrolytic activity, this study aimed to elucidate the involvement of different types of biomass in the anaerobic conversion of polymeric COD, in AGS systems treating domestic wastewater.

## 3.2 | MATERIALS & METHODS

### 3.2.1 | Biomass sampling and separation

Biomass and influent were sampled at wastewater treatment plant (WWTP) Garmerwolde (The Netherlands) in the period from April 30 to May 9, 2019. Another sampling round was performed in February 2020 to measure granule size distribution and conduct additional enzyme assays. The stable operation of the plant and the low variability of the sludge volume index (SVI<sub>5</sub>) between the two sampling periods led to the assumption that the granule bed composition was comparable between both periods. The characteristics of WWTP Garmerwolde are described by Pronk et al. (2015). Two Nereda® reactors, designed by Royal Haskoning DHV (Amersfoort, The Netherlands), treat 35.000 m<sup>3</sup> d<sup>-1</sup> on average, half of the total flow to the wastewater treatment plant. The influent was sampled after screening and grit removal, and two types of influent samples were collected for different purposes: 1) Three representative 24-hour flow-proportional samples were collected, and used for physical-chemical characterization of the influent; 2) For each hydrolytic assay, influent grab samples were collected, to ensure that the influent sample used in the enzyme assays was as fresh as possible. The grab samples were used in the hydrolytic assays, and not characterized in terms of chemical composition. The sludge samples were taken from the AGS reactor at least 40 minutes after the start of the mixed aeration phase to ensure a homogeneous sample. Samples were preserved at 4°C, and the activity tests were performed within 8 hours after the sample was taken.

For the hydrolytic activity tests, 7 sample types were prepared: mixed sludge, large granules, crushed large granules, small granules, flocs, bulk liquid and influent. The sludge was washed over a stack of sieves by applying tap water with moderate pressure. The following fractions were collected: large granules (>1000 µm diameter), small

3 granules (200–1000  $\mu\text{m}$  diameter), and flocs (45–200  $\mu\text{m}$  diameter). A lower limit was used for flocs to separate them from the bulk liquid. Crushed granules were obtained by dispersing 15 g of large granules using a Potter-Elvehjem-type tissue grinder. The bulk liquid fraction was obtained by settling the sludge for 2 hours and collecting the supernatant. Mixed sludge was diluted to approximately 4 g/L using 20 mM Tris-HCl buffer. All the other fractions were also buffered with 20 mM Tris-HCl and diluted to a final approximate concentration of 4 g mixed liquor suspended solids (MLSS)/L. The activity of the influent, on  $\alpha$ - and  $\beta$ -glucosidase assays, was determined using a raw influent sample. For the protease and lipase assays, the influent particles were concentrated by settling: 2 liters of influent were settled and the supernatant was discarded to keep a final volume of 250 mL. This concentration step was needed to increase the signal in the protease assay, which was less sensitive than the other assays. The influent used in lipase assays was also settled, because the same samples as for protease assays were used for lipase assays, since they were performed in the same days. Complementary experiments were performed in February 2020 to compare the activity of the settled and non-settled influent. The pH of all the samples was set to 7.5 for the assay.

### 3.2.2 | Hydrolytic activity tests

The substrates used for hydrolytic activity tests were *p*-nitrophenyl (*p*NP) conjugates (*p*NP-palmitate, *p*NP- $\alpha$ -glucopyranoside and *p*NP- $\beta$ -glucopyranoside), and azocasein. These substrates target lipase,  $\alpha$ -glucosidase,  $\beta$ -glucosidase and protease activities, respectively. All used chemicals were purchased from Sigma-Aldrich (Darmstadt, Germany). Excess concentrations of substrate were used in the assay to ensure zero order kinetics and thus to measure maximum hydrolytic activity. *p*NP- $\alpha$ -glucopyranoside, *p*NP- $\beta$ -glucopyranoside and azocasein solutions were prepared by dissolving the powder substrates in Tris-HCl. These substrates were fully dissolved. *p*NP-palmitate, however, was insoluble in Tris-HCl buffer, so an emulsion was prepared in an isopropanol - Tris-HCl mixture (Supplementary information: Figure S3.1). The tests were performed in 40 ml vials with air-tight stoppers equipped with a sampling port. On each assay, all the sample types derived from one sampling were run in parallel. The vials were flushed with  $\text{N}_2$  for one minute to create anaerobic conditions. The temperature of the assays was between 18 and 20°C. Biomass was incubated with the chromogenic substrates on a Fisherbrand Seastar orbital shaker from Thermo Fisher Scientific (Waltham, MA USA) at 120 rpm, and samples were taken regularly throughout the length of the experiment. The samples were sieved through a 100  $\mu\text{m}$  mesh to remove

biomass. Immediately after, 1 ml of sample was mixed with 1 ml of 30% (w/v) trichloroacetic acid (TCA), to stop the enzymatic reaction. Samples were stored at -20°C until analyzed. The frozen samples were thawed at room temperature, centrifuged and filtered through 0.45  $\mu\text{m}$ . 1 mL of sample was mixed with 1 mL of 2 M NaOH. Finally, absorbance was measured in a spectrophotometer Genesys 10S UV-Vis from Thermo Fisher Scientific (Waltham, MA USA) at the corresponding wavelength (Table 3.1).

**Table 3.1.** Chromogenic substrates and assay conditions used for the different enzyme assays.

Assay	Substrate	Concentration	Assay length	Absorbance
Lipase	<i>p</i> NP-palmitate	20 mM	1 h 15 min	410 nm
$\alpha$ -Glucosidase	<i>p</i> NP- $\alpha$ -glucopyranoside	1 mM	1 h 15 min	400 nm
$\beta$ -Glucosidase	<i>p</i> NP- $\beta$ -glucopyranoside	1 mM	1 h 15 min	400 nm
Protease	Azocasein	0.2 % (w/v)	2 h 30 min	440 nm

### 3.2.3 | Calculation of hydrolytic activity

Absorbance was plotted over time and the data was analyzed through linear regression. Samples with an  $R^2$  value lower than 0.7 were discarded (Lundstedt et al. 1998), considering that the activity was below the detection limit of the method. Samples with less than 4 data points (due to sample loss or problems in sample analysis) were also discarded. Triplicate samples were averaged and the standard deviation was calculated aggregating the standard deviation between triplicates and the standard deviation of the fits. The slope of the regression was used to calculate the hydrolytic activity of the samples.

To couple increase in absorbance to moles of substrate hydrolyzed, substrate characteristics were taken into account. *p*NP-conjugated substrates release one *p*NP mol per mol of substrate hydrolyzed, and therefore the activity is expressed as  $\mu\text{mol } p\text{NP h}^{-1}$ . A calibration curve with known *p*NP concentrations was used to translate absorbance values to  $\mu\text{mol } p\text{NP}$ . Protease activity is generally reported in terms of tyrosine equivalents: 1 U protease = 1  $\mu\text{mol Tyr/min}$  (under certain T and pH). To express protease activity as  $\mu\text{mol tyrosine equivalents per hour}$  ( $\mu\text{mol Tyr eq h}^{-1}$ ), a correlation was made between absorbance at 440 nm and Tyr equivalents, for azocasein (Supplementary information: Figure S3.2). The Tyr content of azocasein is 6.9 Tyr per mol of protein, and therefore 1 mol Tyr equivalent would translate to 0.14 moles of protein hydrolyzed.



The specific hydrolytic activity of the different types of sludge was calculated by dividing the measured activity by the amount of biomass used in the assay. Total activity at reactor level contributed by the different sludge fractions was calculated by multiplying the specific activity by the amount of each type of sludge in the reactor. For influent and bulk fractions, the specific activity was expressed per volume unit. Their total enzyme activity at reactor level was calculated by multiplying the specific activity by the volume of influent fed per cycle, and the volume of bulk in the reactor. Bulk volume was calculated as follows:

$$V_b = V_r \times (1 - TS \times SVI_{30} \times (1 - \varepsilon)),$$

where  $V_b$  is the volume of bulk,  $V_r$  is the reactor volume, TS is the concentration of sludge in the reactor and  $\varepsilon$  the porosity of the packed sludge bed, which is assumed to be 0.52 based on van Dijk et al. (2020).

The total amount of substrate that could be degraded during a 1-hour anaerobic feeding was calculated simplifying the plug-flow into 10 CSTRs (continuous stirred-tank reactors) over the total fed influent volume. The following assumptions were made: 1) The influent fills up the reactor according to the feeding flow, and the hydrolytic activity of each CSTR segment is only considered once the influent reaches it. 2) The settled sludge bed occupies the volume corresponding to its  $SVI_5$  of 40 ml/g. This is around 3830 m<sup>3</sup> of sludge, while the average feed batch is 3870 m<sup>3</sup> based on the average flow and a feeding of one hour. Thus, at the end of the feeding the whole sludge bed is filled with influent. 3) The sludge bed is stratified due to differences on settling velocity of the different granule sizes (van Dijk et al. 2020). Considering the composition of the sludge bed (see Results: Biomass composition), the first 9 segments only contain large granules, and the last segment is a mixture of large granules, small granules and flocculent sludge. The total hydrolytic activity calculated this way was translated from  $\mu\text{mol } p\text{NP h}^{-1}$  and  $\mu\text{mol Tyr eq h}^{-1}$  to mg COD substrate hydrolyzed. To do so, we considered the molecular weight of the substrates, the ratio of dye released to moles of substrate hydrolyzed mentioned above, and the COD per mg substrate for each biomolecule type based on Sophonsiri and Morgenroth (2004).

### 3.2.4 | Analysis of the biomass

Total solids (TS) and volatile solids (VS) of the biomass were measured following Standard Methods (APHA 2005). Granule size distribution measurements were performed sieving 1.5 L of sludge through the following mesh sizes: 1000  $\mu\text{m}$ , 200  $\mu\text{m}$ ,

and 45  $\mu\text{m}$ . The total solids and volatile solids of the resulting sludge fractions were determined as described in the Standard Methods. The weight percentage of each fraction respect to the total was calculated.

A VHX-700F digital microscope from Keyence (Mechelen, Belgium) was used to take micrographs of the biomass used for the experiments. The dimensions of the large granules were determined via image analysis using the built-in software of the microscope. The average granule diameter values given by the software were used to calculate the sphere equivalent volume of the granules. Particle size distribution of the flocculent sludge and crushed granules was measured using a Bluewave light-scattering particle size analyzer from Microtrac (Montgomeryville, USA).

### 3.2.5 | Analysis of the influent wastewater

24-hour flow-averaged influent wastewater samples were preserved at 4°C for up to 24 hours. Biological oxygen demand ( $\text{BOD}_5$ ) was measured using photochemical test-kits, with product number LCK 555, from Hach (Düsseldorf, Germany). Total suspended solids (TSS) and volatile suspended solids (VSS) of the influent were measured as described in the Standard Methods (APHA 2005). Part of the influent was filtered applying positive pressure through a 0.45  $\mu\text{m}$  pore size, using a cross-flow filter, to keep a soluble influent fraction. The raw and filtered influent were stored at -20°C until further use.

The stored influent samples were thawed at room temperature in closed vials. Soluble and total COD were analyzed using photochemical test-kits, product number LCK514, from Hach (Düsseldorf, Germany). Soluble and total protein concentration was measured using the modified Lowry method (Frølund et al. 1995) which distinguishes proteins and humic compounds. Soluble and total carbohydrate concentration was measured using the anthrone-sulfuric acid method (DuBois et al. 1956). Lipid content was measured using the gravimetric determination method by Merieux Nutri-Sciences (Resana, Italy). The measured concentration of proteins, lipids and carbohydrates was converted to COD based on Sophonsiri and Morgenroth (2004).

Long-term measurements of total COD,  $\text{BOD}_5$ , TSS, total phosphorus (TP), phosphate ( $\text{PO}_4^{3-}\text{-P}$ ), total nitrogen (TN), and ammonium ( $\text{NH}_4^+\text{-N}$ ) in the wastewater were performed by a certified lab, and provided by the water authority Noorderzijlvest (Groningen, The Netherlands).

### 3.3 | RESULTS

#### 3.3.1 | Influent wastewater composition

Several influent parameters were analyzed on three sampling days. The results of the analyses are summarized in Table 3.2. In addition, long-term measurements of the wastewater composition are shown, as provided by the water authority Noorderzijlvest. These averaged values were obtained from the regular plant monitoring in the period between 1 April 2019 and 6 February 2020.

**Table 3.2.** Composition of the influent wastewater to the Nereda® reactor. Long term measurement results were provided by the water authority and resulted from regular plant monitoring (April 2019 to February 2020).

	Measurements during sampling campaign					Long-term measurements	
	1-5-19	7-5-19	8-5-19	26-2-20 <sup>a</sup>	Average	Low - high	Average
tCOD (g m <sup>-3</sup> )	567	703	587	301	619	260-800	544
sCOD (g m <sup>-3</sup> )	143	133	127	-	134	-	-
BOD <sub>5</sub> (g m <sup>-3</sup> )	129	238	283	-	217	100-370	231
TSS (g m <sup>-3</sup> )	393	445	384	-	407	140-380	248
VSS (g m <sup>-3</sup> )	220	308	172	-	233	-	-
TP (g m <sup>-3</sup> )	-	-	-	-	-	2.5-12	6.6
PO <sub>4</sub> <sup>3--</sup> P (g m <sup>-3</sup> )	-	-	-	-	-	1.6-5.9	4
TN (g m <sup>-3</sup> )	-	-	-	-	-	21-73	49
NH <sub>4</sub> <sup>+</sup> -N (g m <sup>-3</sup> )	-	-	-	-	-	16-59	41
Soluble proteins (g COD m <sup>-3</sup> )	13	18	21	-	17	-	-
Total proteins (g COD m <sup>-3</sup> )	66	86	52	-	68	-	-
Soluble carbohydrates (g COD m <sup>-3</sup> )	13	9	8	-	10	-	-
Total carbohydrates (g COD m <sup>-3</sup> )	110	210	109	-	143	-	-
Soluble humics (g COD m <sup>-3</sup> )	99	65	67	-	77	-	-
Total humics (g COD m <sup>-3</sup> )	157	101	148	-	135	-	-
Lipids (g COD m <sup>-3</sup> )	22	-	-	17	20	-	-
VFA (g COD m <sup>-3</sup> )	58	9	40	-	29	-	-

The rounded average flow to the two Nereda® reactors during the experimental period was 31000 m<sup>3</sup> d<sup>-1</sup>. With a biological reactor volume of 9500 m<sup>3</sup> per reactor, the volumetric loading rate of each reactor was 1.6 m<sup>3</sup> (m<sup>3</sup> d)<sup>-1</sup>. The average sludge loading approximated 0.07 kg COD (kg TS d)<sup>-1</sup>. The reactor was operated at an average volumetric exchange ratio (VER) of 40%.

### 3.3.2 | Biomass composition

The biomass concentration of the reactor during the sampling period was between 12 and 15 g TS/L. The VS/TS ratio of the sludge was 80 ± 1%. The SVI<sub>5</sub> during this period was 30–40 mL/g. The proportion of large granules (> 1 mm) in the reactor was remarkably high in this plant; they accounted for 84% of the VS. Small granules were 7% of the VS and flocculent sludge 9%. The distribution of diameters of large granules (>1 mm) is shown in Figure 3.1. The average diameter of the large granule fraction is 3.6 mm. However, it should be noted that when accounting for the volume occupied by the granules of the different sizes, the distribution shifts towards larger diameters.

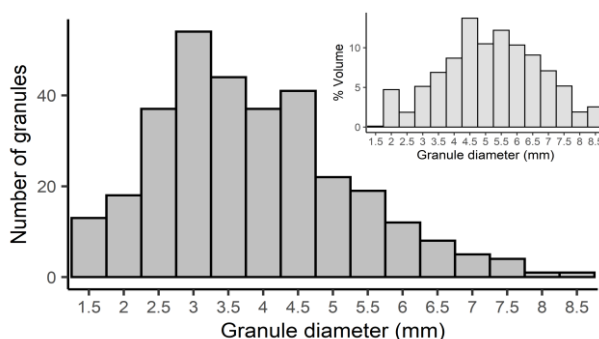


**Figure 3.1.** Granule size distribution of the large granule fraction measured by image analysis. N = 317 granules. On the top right corner, calculated volume distribution of large granules (sphere-equivalent volume).

The separation of the biomass using sieves did not render perfect separation of the biomass fractions (Supplementary information: Figure S3.3). The small granule fraction (0.2–1 mm) was highly heterogeneous, and consisted of a fiber/cellulose matrix that entrapped biomass and inorganic particles of different sizes. This made it impossible to determine the granule size of this sludge fraction using the image analysis software.

Flocculent sludge (0.045–0.2 mm) and crushed granules had a comparable particle size distribution (Supplementary information: Figure S3.4), showing that large granules were thoroughly homogenized.

3.3.3 | Hydrolytic enzyme activity distribution in the sludge

All mixed sludge samples showed hydrolysis activity on all substrates tested. The specific activities for the enzymes measured are summarized in

Table 3.3. It should be taken into account that the dye released per substrate hydrolyzed

	Hydrolytic activity ( $\mu\text{mol } p\text{NP (g VS h)}^{-1}$ ; $\mu\text{mol Tyr eq (g VS h)}^{-1}$ )	stdev	n
$\alpha$ -Glucosidase	13	2	9
$\beta$ -Glucosidase	17	5	8
Lipase	34	26	5
Protease	10	6	9

is not equal for all assays (see Methods), and therefore the hydrolysis rates of the different substrates cannot be compared directly.

Table 3.3. Specific hydrolytic activities of the mixed sludge sample.

	Hydrolytic activity ( $\mu\text{mol } p\text{NP (g VS h)}^{-1}$ ; $\mu\text{mol Tyr eq (g VS h)}^{-1}$ )	stdev	n
$\alpha$ -Glucosidase	13	2	9
$\beta$ -Glucosidase	17	5	8
Lipase	34	26	5
Protease	10	6	9

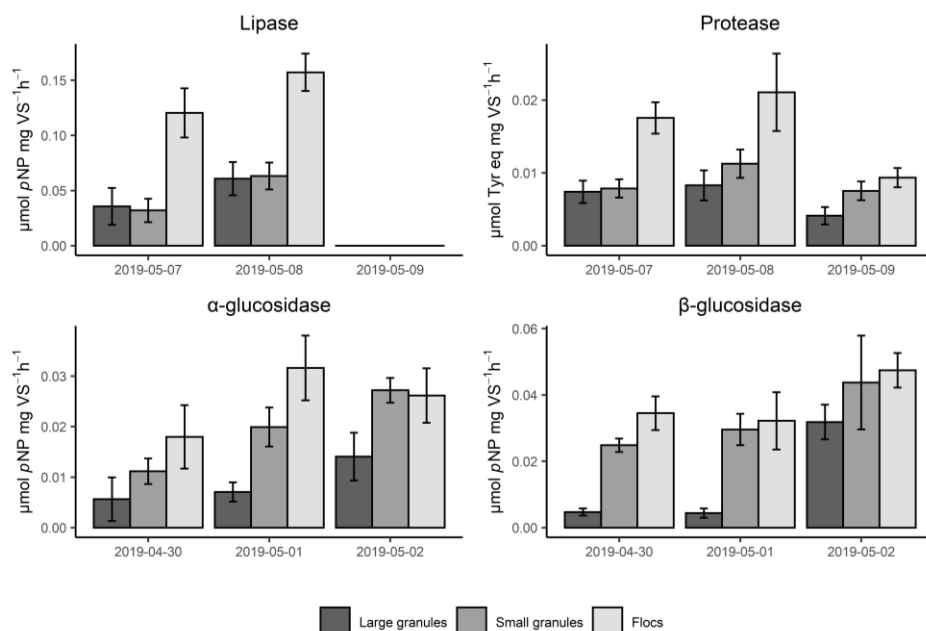


**Figure 3.2.** Specific hydrolytic activities measured in the different sampling days. Note that lipase samples from the 9th of May had to be discarded due to poor fit of the linear regression. Each bar represents triplicate samples and error bars represent standard deviation of the triplicates.

The distribution of the activity of hydrolytic enzymes in the different sludge fractions is shown in Figure 3.2. The maximum hydrolyzed amounts during an anaerobic feed of one hour, estimated with the measured hydrolytic activities, would be 570 mg COD/L of protein, 650 mg COD/L of lipid, 80 mg COD/L of  $\alpha$ -glycosides and 160 mg COD/L of  $\beta$ -glycosides (240 mg COD/L of carbohydrates). The biomass specific activity of all the hydrolytic enzymes tested was highest in the flocculent sludge fraction, while granules exhibited lower hydrolytic activity per gram VS. The difference between these fractions differed per type of enzyme and sampling day. Flocculent sludge activity was 1.5 to 7.5 times higher than large granule activity. Depending on the enzyme group and sampling day, the activity of the small granule fraction was comparable to the larger granules, between that of flocculent sludge and large granules, or comparable to the flocculent sludge.

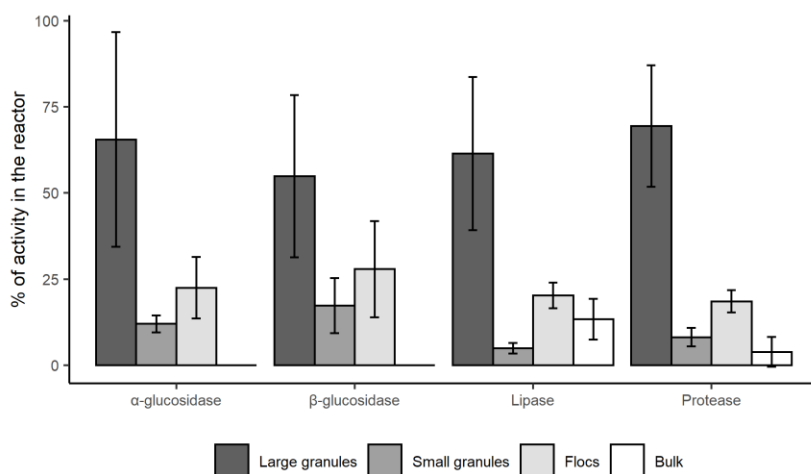


**Figure 3.3.** Percentage of hydrolytic activity contributed by large granules, small granules, flocs and bulk liquid with respect to the total reactor activity. The values represented in the graph are averaged over three days of sampling (2 days in the case of lipase). Error bars represent standard deviation.

The hydrolytic activity of each sludge fraction at reactor level was calculated by multiplying the hydrolytic activity per gram VS by the total VS mass of that fraction within the reactor. The bulk liquid activity was determined as activity per mL, and multiplied by the total volume of the bulk liquid in the reactor. Figure 3.3 shows the percentage of enzyme activity contributed by each of the biomass fractions, averaging the data from all the sampling days. The data for each of the days can be found in Supplementary information: Figure S3.5. Considering the total mass of large granules in the reactor, the total enzyme activity of the large granule fraction was higher than that of flocs and small granules. Reactor level hydrolytic activity of the granule fraction was 2–3.8 times higher than that of the flocculent fraction for all the substrates. It is noteworthy that flocculent sludge still had relatively high hydrolytic potential on a reactor scale (18–28% of the total), even though flocculent sludge occupied only a small fraction of the VS in the reactor.

Glucosidase activities were not detected in the bulk liquid. Bulk protease activity was detected but contributed only 4% of the total protease activity in the reactor. Besides, there were large differences in the bulk protease activity measured per day (Supplementary information: Figure S3.5). Lipase activity was rather high in the bulk liquid, accounting for 13% of the activity in the reactor. Upon the observation of high

bulk lipase activities, an additional experiment was conducted centrifuging the bulk liquid at 12000 rpm for 15 minutes, to ensure that all the cells and other particles were removed from the sample. The centrifuged bulk still contained high lipase activity, although it was 20% lower than the activity of the non-centrifuged bulk. This result indicated that indeed the bulk activity measured in the assays was mainly due to enzymes in solution and not due to cell-bound enzymes.

### 3.3.4 | Hydrolytic activity of the influent

All the enzymes measured showed activity in the influent too (Figure 3.4a). Considering an average influent feed of 3870 m<sup>3</sup>/cycle, the influent hydrolytic activity that is fed to the reactor per cycle was calculated. In comparison to the sludge activities measured, the activity carried by the influent was rather high in the case of  $\alpha$ - and  $\beta$ -glucosidase (Figure 3.4b). The  $\alpha$ -glucosidase activity brought by the influent was, on a reactor level, nearly as high as that of small granules.

Lipase activity was underestimated in the assays where the influent particles were concentrated by settling. An assay comparing the non-settled influent to the settled influent showed that the activity contributed by the settled influent fraction was only 43% of the total activity of the wastewater. Therefore, more than half of the lipase activity in the wastewater was in the supernatant. Thus, concentration of the influent by settling should be avoided when determining its hydrolytic potential, since the soluble activity can be quite significant. The protease activity of the total influent could not be measured due to lower sensitivity of the protease assays, and thus it is unclear if influent protease assays also neglected the activity in the supernatant.



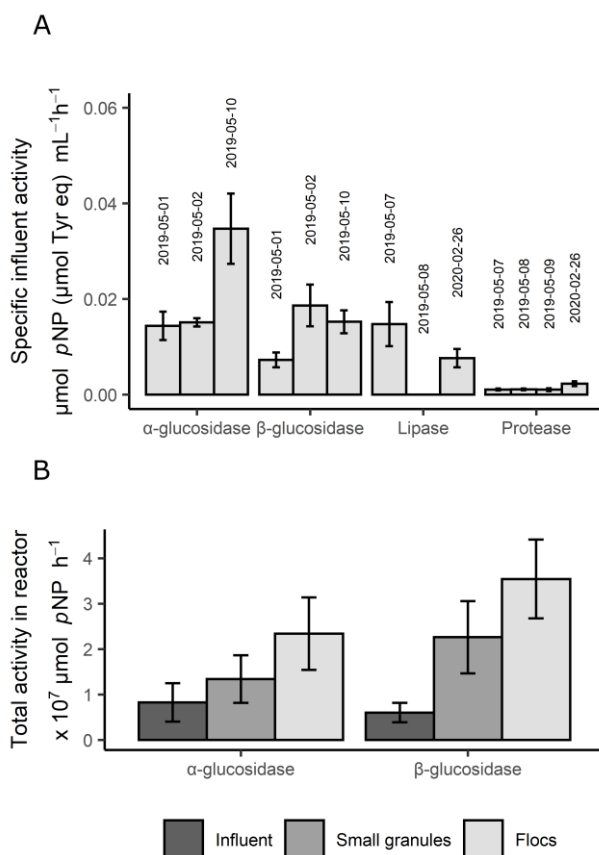


**Figure 3.4.** a) Specific influent hydrolytic activities (activity/mL) measured in different sampling days. Lipase and protease activities were measured in a settled influent sample; the activity shown in the graph is the calculated activity per mL of the original influent, taking the settling step into account. Each bar represents triplicate samples. Error bars represent standard deviation of the triplicates. b) Comparison of glucosidase activities contained in one feed batch (3870 m<sup>3</sup>) with the total activity present in the small granules and flocculent sludge in the reactor. Each bar represents the average activity during the different sampling days, and error bars represent standard deviation. Values for large granules and bulk liquid are not included in this figure, but their activity relative to small granules and flocs can be found in Figure 3.3.

### 3.3.5 | Enzyme activity in dispersed sludge

Comparison of the enzymatic activity of intact and crushed granules was used to account for diffusion limitation of the substrates towards the inside of the granules (Figure 3.5). The activity of crushed granules was higher than that of full granules. This difference

was larger in the case of lipase and protease; intact granules only exhibited 40 to 44% of the protease and lipase activity measured in the crushed granules.

A higher variability was observed in lipase activity than in the other enzyme activities, which might be due to differences in the level of solubilization of the *p*NP-palmitate solution used in each assay. A poorly dissolved palmitate would render higher observed differences between intact and crushed granules. The absorbance values of the  $t_0$  samples highly differed per day, showing high heterogeneity during substrate preparation.

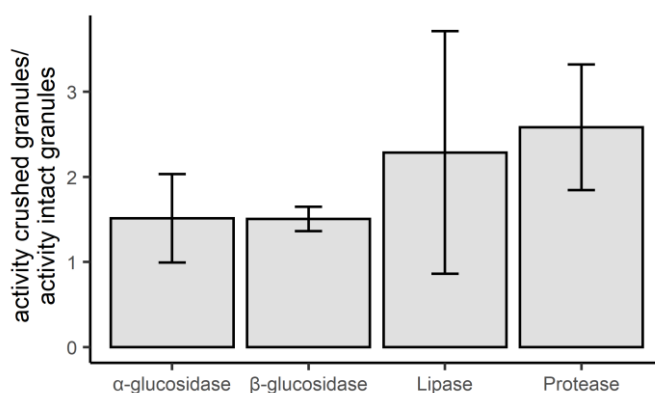


**Figure 3.5.** Activity of crushed granules over activity of intact large granules. Each bar represents three experiments performed in triplicate (except in lipase where the data is from two experiments, also in performed in triplicate). Error bars represent standard deviation.

## 3.4 | DISCUSSION

### 3.4.1 | Sample heterogeneity and daily variations

The present study disclosed high variability in the determination of hydrolytic activity of AGS fractions and influent wastewater. This could be for several reasons. One of them is the substrate preparation procedure, which in the case of *p*NP-palmitate is laborious. The other substrates were directly prepared in Tris-HCl and there were no problems with solubilization. With *p*NP-palmitate, however, the slightest difference in preparation conditions (e.g. stirring speed, time and speed of addition of the reagents to the solution) affected the characteristics of the final substrate solution, resulting in

inconsistent degrees of solubilization. Different concentrations of soluble substrate on different assays might be a reason behind the high variability of the measured lipase activity between days. Apart from the implications on measurement reproducibility, this also indicates that the form in which the substrate is found in the wastewater (i.e. particulate or soluble) will greatly affect its hydrolysis rate.

Another source of variability was the heterogeneity of the sludge. The standard deviations of the triplicate samples were significantly high, in some cases reaching 30–40% of the average value. The differences between triplicates were highest in the large granule fraction. Taking a representative sample of aerobic granules is challenging, due to difficulties in sampling fast-settling granules, and also due to the size heterogeneity of the granule fraction. As shown in Figure 3.1, the large granule fraction consisted of a large range of diameters. Considering the relatively low volumes of sludge used in the assay (40 mL per vial), the different granule diameters might have not been equally represented in all replicates. Therefore, the use of high granule quantities is advisable to diminish this variability between samples, as well as setting an upper size limit for large granules, in order to keep surface to volume ratios of the granules in the sample similar. The quantity of crushed granules prepared was 500 mL, making sure a representative granule size distribution was used for these experiments.

Lastly, daily fluctuations in the influent composition and concentration added most likely to the variability of the measurements. Hydrolytic activities tend to vary due to differences in influent composition, environmental conditions and reactor operation (Nybroe et al. 1992). Large variations between days were observed on the measured hydrolytic activity, as shown in Figure 3.2 and Figure 3.4. Similarly to our observations, high long-term variations in enzyme activities of AS have been previously reported (Frølund et al. 1995). The relative contributions of the different types of sludge to the total activity fluctuated less than the individual activities of the fractions. This enabled us to draw general conclusions about the enzyme activity distribution in the AGS reactor studied. Other studies have reported different sludge bed compositions, with smaller granule size and higher concentrations of flocculent sludge fractions (Cetin et al. 2018; Derlon et al. 2016; Layer et al. 2019; van Dijk et al. 2018). Based on our results, it is clear that the proportions of the different granules and floc sizes affect the overall hydrolytic activity of the reactor, and therefore these fractions need to be reported to be able to compare different reactor performance datasets.

### 3.4.2 | Biomass-bound activity

This study showed that different sludge fractions from a full-scale AGS reactor have the potential to hydrolyze influent polymers under anaerobic conditions. Most of the hydrolyzing potential was found to be biomass-bound for all the substrates, but lipase activity was also rather high in the reactor bulk liquid (13% of the total activity). Since the bulk liquid was separated from its suspended solids by settling, low density or buoyant lipid aggregates might have been retained in the bulk liquid sample, including the attached lipases.

For proteins and carbohydrates, hydrolytic activity in the reactor is mainly bound to the biomass. Larsen and Harremoës (1994) reported high bulk liquid hydrolysis of carbohydrates, but most AS and biofilm studies assigned the main contribution to biomass-associated hydrolysis and particle removal (Boczar et al. 1992; Boltz and La Motta 2007; Confer and Logan 1998; Frølund et al. 1995; Karahan et al. 2006; Mosquera-Corral et al. 2003). Frølund et al. (1995) described AS flocs as a matrix of immobilized enzymes. This allows the retention of enzymes inside the reactor, and due to the lifetime of enzymes they can be active in a different phase of the cycle than they were synthesized (Boczar et al. 1992; Goel et al. 1998). The retention of enzymes would support the hypothesis that aerobic and anaerobic hydrolysis occur at similar rates. This would justify using one hydrolytic constant while modelling AGS, regardless of the redox conditions in the reactor, as proposed in the Activated Sludge Model No. 3 (ASM3) (Gujer et al. 1999). Yet degradation of polymers by protozoa or other predators should be considered separately, since their activity was not researched in this work and might differ during anaerobic and aerobic conditions.

Having enzyme activity predominantly in the (granular) biomass fraction also implies that contact between the polymeric substrates and biomass is necessary for their hydrolysis. Recent studies employing magnetic resonance imaging (MRI) and mass balancing explored the substrate-sludge interaction during a plug flow passage of influent through a settled bed of AGS (Layer et al. 2020; Ranzinger et al. 2020). Ranzinger et al. (2020) concluded that colloidal substrates are evenly distributed throughout the granular sludge bed during plug-flow feeding, but that the interaction between particulates larger than 1  $\mu\text{m}$  and AGS was limited. Even though it is difficult to extrapolate small scale flow experiments to full scale reactors that are 45 m in diameter, we could argue that colloidal and polymeric (soluble) substrates, like the substrates used in our assays, are accessible to the granule bound enzymes in the granules during

anaerobic plug-flow feeding. In contrast, the fate of larger particulate substrates in full scale systems remains unclear. The high hydrolytic potential in granules found in the present study encourages further research on how different types and sizes of organic particles exactly interact with granular biomass during feeding, and to what extent they are available to the hydrolytic enzymes. This insight could increase the effectiveness and duration of the anaerobic period, increasing the overall reactor efficiency.

### 3.4.3 | Surface-dependent hydrolysis

Large granules (>1 mm diameter) were able to hydrolyze all substrates tested. Their specific activity, however, was lower than that of small granules (0.2-1 mm) and flocculent sludge (0.045-0.2 mm). A lower specific activity of large granules was expected due to their low surface area to volume ratio. The diffusion of polymeric substrates in biofilms is highly reduced or even negligible (Carlson and Silverstein 1998), and therefore their hydrolysis will be influenced by the biofilm surface area. As reported by previous studies, polymer degradation is restricted to the first few micrometers of biofilm surface (de Kreuk et al. 2010; Kommedal et al. 2006). Since azocasein is a polymer with a molecular weight of approximately 23 kDa, the lower specific protease activity of large granules compared to other sludge types can be explained by transport limitation. *p*NP-palmitate is a smaller substrate (378 Da). Nonetheless, the *p*NP-palmitate substrate was an emulsion due to the poor solubility of palmitate in water. (Supplementary information 1). Moreover, palmitate has been reported to adsorb to the surface of anaerobic granules, hindering its diffusion (Palatsi et al. 2012). Therefore, a similar dependency of the surface area to volume ratio for its hydrolysis could be expected. The  $\alpha$ - and  $\beta$ -glucosidase substrates used in these assays had a molecular weight of 301 Da. Substrates of this size (smaller than sucrose), can diffuse into biofilms rather easily (Stewart 1998). Nevertheless, flocculent sludge had higher  $\alpha$ - and  $\beta$ -glucosidase activity than large granules, and crushed granules had 1.5 times the activity of intact granules. This suggests that even for small, soluble substrates, the observed hydrolysis rate is strongly affected by transport of the substrates into the granules. The surface area available for hydrolysis will thus be crucial for the hydrolysis of most substrates, but most importantly for substrates of larger size which cannot diffuse into granules.

The results of lipase and protease assays with crushed granules also evidence surface-limited hydrolysis in large granules. By dispersing the granules and removing the resistance to substrate diffusion, the hydrolysis rate increased considerably. The hydrolytic enzymes made available by crushing might be located in deeper layers of the

granule and only have access to the assay substrates upon crushing. Therefore, they are likely not involved in the degradation of influent substrates *in situ*. These enzymes could be degrading complex substrates in the granule matrix, such as polymers embedded in the granules or products from cell decay (Adav et al. 2009). Alternatively, the enzymes released when crushing granules could be mainly located close to the surface and hydrolyze influent substrates, but at reduced rates, due to limiting substrate concentrations below the surface induced by mass transfer resistance. Knowing more specifically where hydrolyzing enzymes are located in granules would help to understand the processes happening inside the granule, and approximate which layer of the granules, and thus fraction of the biomass, contributes to the conversion of complex influent substrates.

### 3.4.4 | Hydrolytic activity of the influent

The influent contained  $\alpha$ - and  $\beta$ - glucosidase activities in the same order of magnitude as the sludge fractions; for example,  $\alpha$ - glucosidase activity of the influent was about 1/3 of that of flocs. Besides, soluble carbohydrate concentrations in the influent were low: readily biodegradable carbohydrates were probably hydrolyzed in the sewer prior to the arrival to the plant. The remaining particulate carbohydrates might keep hydrolyzing during feeding to the reactor; during a 1-hour feeding period a maximum of 10% of the total carbohydrates could be degraded by the enzymes in the influent. A previous study suggested that the hydrolysis of influent suspended solids would be mainly performed by microorganisms in the influent (Benneouala et al. 2017). Besides, a recent study on the microbial composition of the wastewater treatment plant of Garmerwolde identified several hydrolyzing microorganisms in the influent (Ali et al. 2019). Nevertheless, in contrast to AGS, the influent microorganisms have a short retention time in the reactor. Large granules share few taxa with the influent; they are composed by a highly specialized, and stable, microbial community with a very high SRT, while the microbial composition of the flocculent sludge fraction is fluctuating and more affected by the changes in influent composition (Ali et al. 2019). This indicates that the hydrolyzing bacteria coming with the influent are likely to end up in flocs when the sludge bed is mixed during the aeration phase; hence, the hydrolytic activity contained in influent particles would be partly discharged with the selection spill and partly stay at the top of the granule bed due to stratification during sludge settling (van Dijk et al. 2020). It is thus unlikely that this layer with flocs would contribute to the hydrolysis of the particles under the anaerobic feeding conditions, during which the influent is fed from the bottom of the reactor, especially considering the applied VER of 40%.

### 3.4.5 | Full-scale hydrolysis and implications for practice

This study demonstrated that aerobic granules have the potential to significantly contribute to overall reactor hydrolysis. The hydrolytic potential of the large granules determined in this study would be enough to anaerobically degrade much higher concentrations of soluble protein and carbohydrates than those present in the influent (45 and 25 times higher, respectively). The granular sludge also had an overcapacity to hydrolyse the total lipid, protein and carbohydrates concentrations that were measured in the influent during the anaerobic phase. However, it should be noted that the rates in this study are maximum rates: they were measured at excess substrate conditions, and the complex substrates present in domestic wastewater likely have an overall lower biodegradability than the four model substrates used here. Therefore, the hydrolysis rates measured in this study are not directly applicable to granular sludge models. These hydrolysis rates reflect the enzyme concentration in the different biomass fractions, but not the in-situ hydrolysis rate. The hydrolysis constant in granular sludge models should be derived from measurements of the hydrolysis rate of a specific influent by a specific biomass fraction.

In full-scale AGS, during the anaerobic feeding phase influent is fed through the settled sludge bed from the bottom of the reactors in a plug-flow regime (Pronk et al. 2015; van Dijk et al. 2020). The settling velocity of granules is heavily influenced by their size (Liu et al. 2008; Winkler et al. 2012). Consequently, the settled sludge bed is stratified with larger granules at the bottom and smaller ones on top (van Dijk et al. 2020). Due to the lack of mixing during feeding, it is most likely that the products of hydrolysis will only be available close to where hydrolysis takes place. These conditions highlight the importance of having hydrolytic activity associated with the large granules. PAOs from large granules would then have preferential access to the already present VFA in the influent, but also to the VFA that are formed in the anaerobic phase. This would mean that higher P removal efficiencies could be achieved than based solely on influent VFA. Knowing that the sludge has the ability to hydrolyze polymers, the length of the anaerobic phase can be adjusted to enhance EBPR performance in AGS reactors with low influent VFA. Our results encourage further in-situ research linking hydrolysis rates with anaerobic uptake of substrates in domestic wastewater. Still, the hydrolytic activity in aerobic granules measured in this study suggests that they would have access to more COD during anaerobic feeding than only influent VFA, supporting granule formation and EBPR.

Anaerobic hydrolysis and uptake of the hydrolysis products is beneficial for the granule morphology too (de Kreuk et al. 2010). If polymeric substrates are present during aeration, hydrolysis will continue and substrate will slowly be released during this phase, creating local substrate gradients at the surface of the granules and favoring fast growing heterotrophs. This can result in irregular outgrowth of biofilm surfaces, and deteriorate the settleability of the sludge (de Kreuk et al. 2010; Mosquera-Corral et al. 2003). Considering the hydrolytic activities measured in this study, most of the soluble and colloidal polymeric substrates will likely be degraded by granules during the anaerobic phase, and will not be present during aeration. This rests on the assumption that soluble and colloidal substrates have sufficient interaction with granules (Ranzinger et al. 2020). The hydrolysis of larger particulate substrates during plug-flow feeding might be limited by their contact with the sludge, as discussed before. Their aerobic hydrolysis will only provide residual readily biodegradable COD (rbCOD) concentrations during aeration. A slow supply of rbCOD during the aerobic phase is mostly linked to flocculent sludge growth, with minimal impact on granule structure given appropriate selective sludge removal is applied (Haaksman et al. 2020). Previous works also observed that reactors fed with non-diffusible substrates developed a fraction of flocculent sludge (Derlon et al. 2016; Layer et al. 2019; Wagner et al. 2015), and Layer et al. (2019) hypothesized that the co-existence of the two morphologies was beneficial for AGS stability. The particles that are not degraded in the aerobic phase but are incorporated in the floc structure can be used during the (optional) anoxic phase as substrates for denitrification. Tougher particles (e.g. cellulose fibers) will not be fully degraded within the SRT of flocs (<7 days) (Ali et al. 2019) and will be removed with the excess sludge during the sludge selection spill (Guo et al. 2020; Pronk et al. 2015). A high content of influent particles in the excess sludge could be related to its high biogas potential due to low mineralization of the spill sludge discharge (Guo et al. 2020). Hydrolysis of easily biodegradable polymers by large granules during the anaerobic phase, and selective removal of the excess sludge containing the more hardly biodegradable substrates, would explain the fairly regular granule growth observed in Garmerwolde (Supplementary information: Figure S3.3), and other AGS reactors fed with municipal wastewaters (Cetin et al. 2018; Derlon et al. 2016; van Dijk et al. 2020).



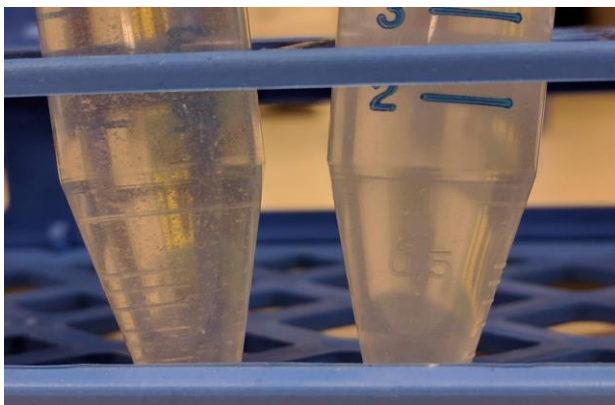
## SUPPLEMENTARY INFORMATION

### Supplementary information 1: Preparation of *p*NP- palmitate solution.

The *p*NP- palmitate solution was prepared in isopropanol due to its poor solubility in water, based on Gupta et al. (2002) and Winkler and Stuckmann (1979). The protocol was adapted to prepare a higher concentration *p*NP-palmitate solution, increasing the isopropanol and Triton X-100 concentrations. To prepare 100 mL of a substrate solution of 30 mM *p*NP-palmitate, the following procedure was followed:

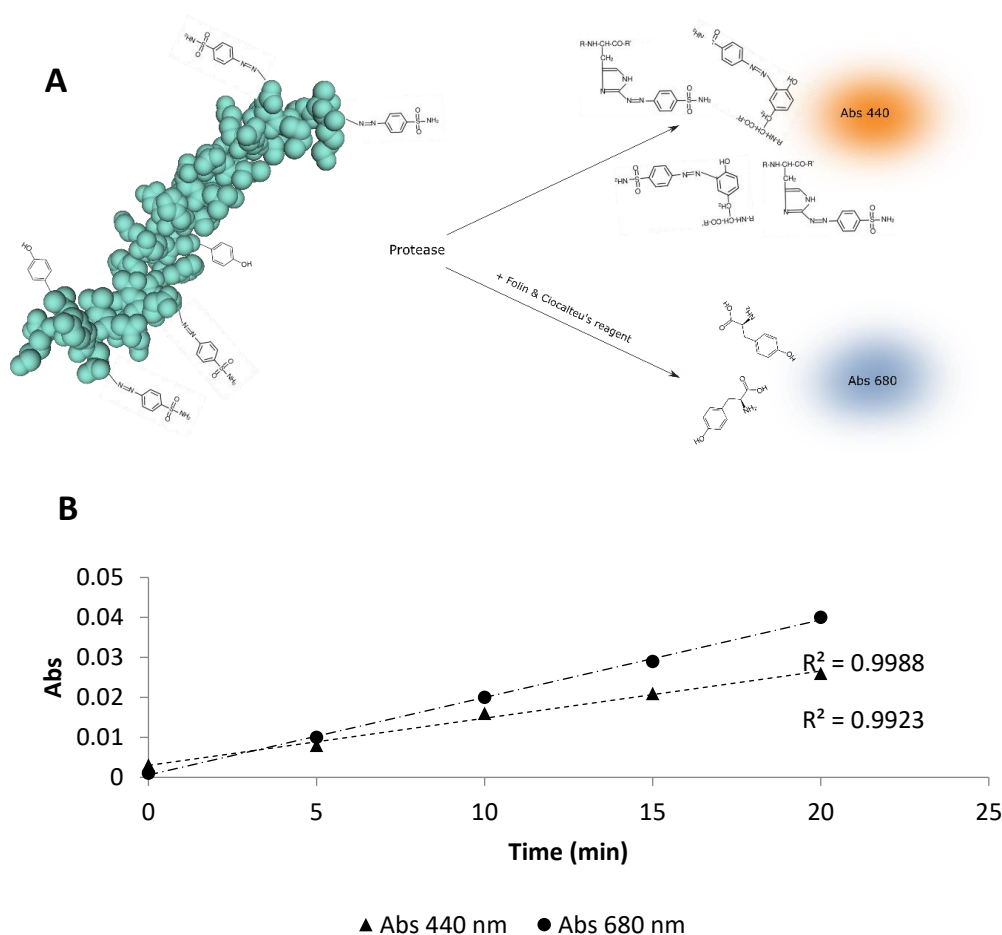
1. 0.74 g of sodium deoxycholate (Sigma-Aldrich, Darmstadt, Germany. Product number D6750) were dissolved in 35.8 mL of isopropanol, stirring vigorously using a magnetic stirrer. It is essential to provide sufficient turbulence during this step. The solution should be kept stirring until a dense, white emulsion is reached.
2. 1.01 g *p*NP- palmitate were added to the solution. The solution was kept vigorously stirring until no *p*NP- palmitate flakes are observed.
3. 0.3 g gum Arabic were added to the solution and stirred until dissolved.
4. When a homogeneous suspension was achieved, the solution was transferred to a magnetic stirrer with a heating plate and heated to 35 °C.
5. 53.3 mL Tris-HCl (20 mM, pH 7.5) was slowly added to the suspension, while stirring.
6. 10.7 mL Triton X-100 were added to the final solution.

The resulting *p*NP-palmitate solution was a cloudy solution, as shown in Figure S3.1.



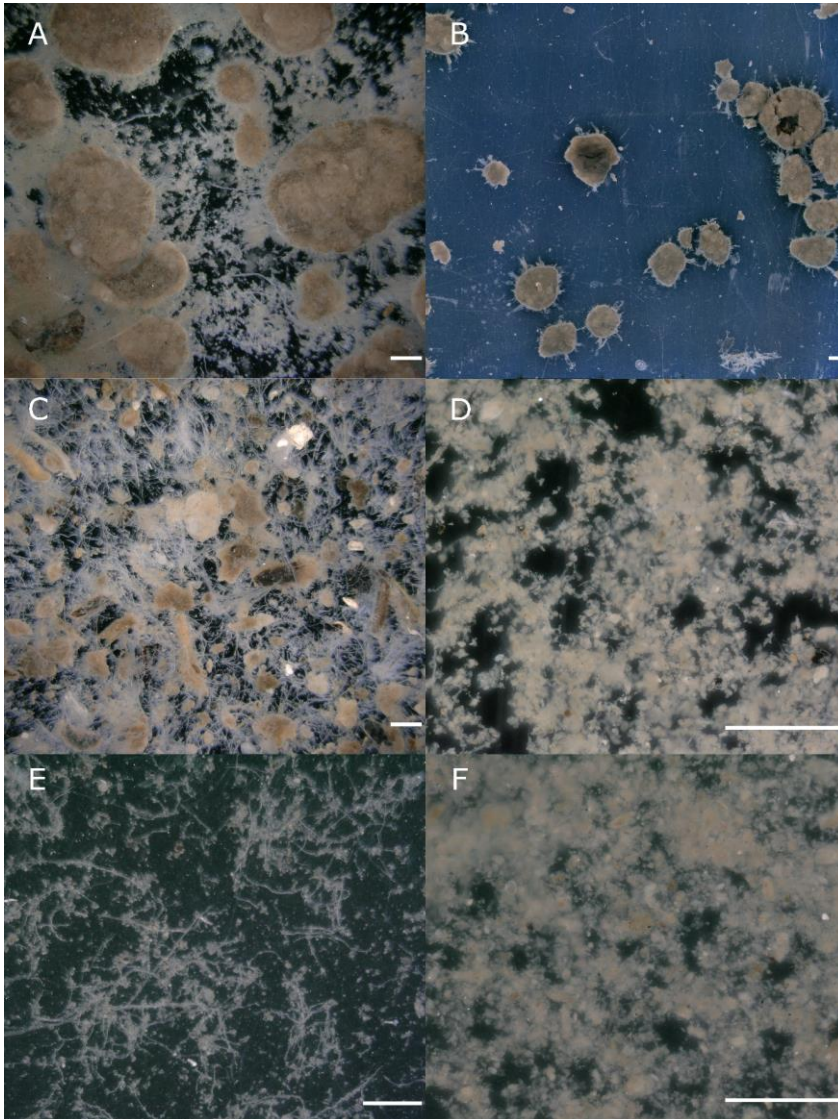
**Figure S3.1.** *p*NP-palmitate solutions, prepared without temperature control (left) and at 35 °C (right). Notice the difference between the cloudy emulsion in the right, and the clear solution with palmitate precipitates in the left.

## Supplementary information 2: Protease assays – translation from Absorbance 440 to Tyrosine equivalents.

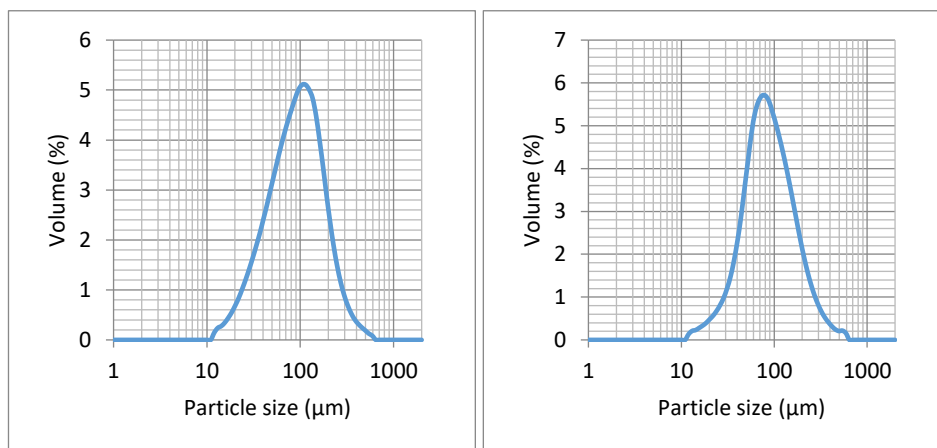


**Figure S3.2.** Procedure to translate Abs 440 to Tyrosine equivalents. A) Azocasein was hydrolysed using a commercial protease (Sigma-Aldrich, Darmstadt, Germany. Product number P4630). The release of tyrosine and azo dye during hydrolysis was measured in parallel. Duplicate samples were taken at several points through time. In one of the samples, absorbance at 440 nm was measured, to detect the azo dye released. The other sample was treated with Folin & Ciocalteu's reagent, which reacts with tyrosine residues making them detectable at Abs 680. Abs 680 was then translated to Tyr equivalents using a calibration curve with L-Tyrosine (Sigma-Aldrich, Darmstadt, Germany. Product number T3754) B) Plot of Abs 440 and Abs 680 through time during the enzymatic reaction. The slopes of Abs 440 vs time and Abs 680 vs time were used to translate from Abs 440 to Abs 680, and later to Tyr equivalents.

**Supplementary information 3: Micrographs of the sludge and influent fractions used in the enzyme assays.**



**Figure S3.3.** Microscope images of the biomass fractions used in the assay: A) Mixed sludge, B) Large granules, C) Small granules, D) Flocculent sludge, E) Influent, and F) Crushed large granules. Size bars: 1000  $\mu\text{m}$ . Note that the small granule fraction consists of a complex fiber matrix and different sizes of granules, which doesn't allow to determine the average granule diameter of this fraction.

**Supplementary information 4: Results of the dispersion of large granules.**

**Figure S3.4.** Output of particle size distribution measurements of flocculent sludge and crushed large granules. A) Crushed granules; B) Flocculent sludge. The average particle size in the crushed sludge fraction was  $105.1 \pm 0.9 \mu\text{m}$ , and in the floc sludge fraction,  $101.5 \pm 0.6 \mu\text{m}$ .

### Supplementary information 5: Daily variations of the percentage of the total reactor activity contributed by the different biomass fractions.

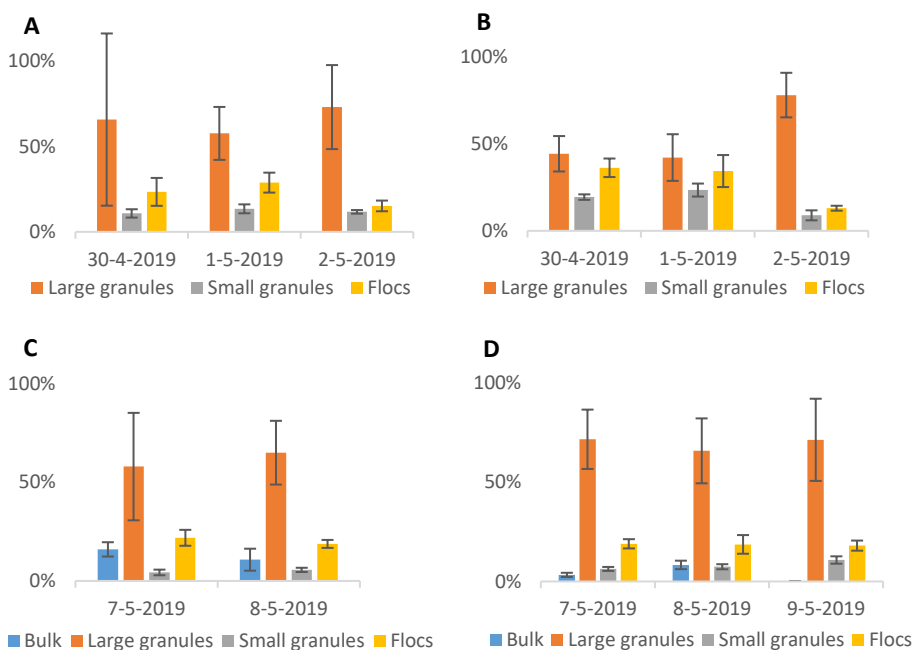


**Figure S3.5.** Percentage contributions of enzyme activity per sludge type, in the different sampling days. a)  $\alpha$ -Glucosidase, b)  $\beta$ -Glucosidase, c) Lipase, d) Protease. Note the differences in bulk activity between days for protease, and activity of granules in the case of  $\beta$ - glucosidase.









# 4

## Hydrolysis capacity of different sized granules in a full-scale AGS reactor

**Published as:** Toja Ortega, S., Van den Berg, L., Pronk, M., & de Kreuk, M. K. (2022). Hydrolysis capacity of different sized granules in a full-scale aerobic granular sludge (AGS) reactor. *Water Research X*, 16, 100151. DOI:10.1016/j.wroa.2022.100151



## ABSTRACT

In aerobic granular sludge (AGS) reactors, granules of different sizes coexist in a single reactor. Their differences in settling behaviour cause stratification in the settled granule bed. In combination with substrate concentration gradients over the reactor height during the anaerobic plug flow feeding regime, this can result in functional differences between granules sizes. In this study, we compared the hydrolytic activity in granules of 4 size ranges (between 0.5 and 4.8 mm diameter) collected from a full-scale AGS installation. Protease and amylase activities were quantified through fluorescent activity assays. To visualise where the hydrolytic active zones were located within the granules, the hydrolysis sites were visualized microscopically after incubating intact and sliced granules with fluorescent casein and starch. The microbial community was studied using fluorescent in situ hybridization (FISH) and sequencing. The results of these assays indicated that hydrolytic capacity was present throughout the granules, but the hydrolysis of bulk substrates was restricted to the outer 100  $\mu\text{m}$ , approximately. Many of the microorganisms studied by FISH, such as polyphosphate and glycogen accumulating organisms (PAO and GAO), were abundant in the vicinity of the hydrolytically active sites. The biomass-specific hydrolysis rate depended mainly on the available granule surface area, suggesting that different sized granules are not differentiated in terms of hydrolytic capacity. In this chapter, we discuss the possible reasons for this and reflect about the implications for AGS technology.

## 4.1 | INTRODUCTION

Aerobic granular sludge (AGS) is an advanced wastewater treatment technology, which uses granular biofilms for removing pollutants from the wastewater. Besides removing COD, AGS can perform enhanced biological phosphorus removal (EBPR) and biological nitrogen removal (Bengtsson et al., 2018; de Kreuk et al., 2005; Pronk et al., 2015b). In most full-scale applications, the treatment involves anaerobic uptake of COD followed by aerobic/anoxic biomass growth. This is achieved by applying a sequencing batch reactor (SBR) cycle that consists of three phases: anaerobic feeding, reaction and settling (Bengtsson et al., 2018; Derlon et al., 2016; Pronk et al., 2015b). At the end of the settling phase, slow settling sludge is selectively discharged (referred to as selection spill). The treated water is discharged during the next feeding phase, displaced by the influent volume fed from the reactor bottom. Plug-flow feeding is important to avoid mixing of the untreated influent and treated effluent, and to provide high local substrate concentrations (de Kreuk and van Loosdrecht, 2004; Pronk et al., 2015a).

The employed SBR cycle, besides ensuring adequate wastewater treatment, influences biomass differentiation. AGS reactors are usually composed of granules of different sizes and flocs. In AGS literature, a range of granule diameters has been reported, varying from 0.2 mm to more than 6 mm (Coma et al., 2012; Lanham et al., 2012; Layer et al., 2019; Stes et al., 2021; Toja Ortega et al., 2021a). The selection spill wastes mainly flocs and small granules, which creates biomass fractions with different SRTs in the same reactor (Ali et al., 2019; Guo et al., 2020). Large granules can have an SRT of months, while on the opposite end flocculent sludge is retained for only a few days (Ali et al., 2019). In addition, plug-flow feeding results in higher substrate concentrations at the bottom of the sludge bed. Larger granules, with a higher settling velocity, are more likely to end up in the bottom of the settled bed during feeding, experiencing higher substrate concentrations than small granules (van Dijk et al., 2022). These conditions could result in functional differences between the granules of different sizes, coupled to their differences in mass-transfer resistance. For instance, in the full-scale AGS plant of Garmerwolde, the Netherlands, polyphosphate-accumulating organisms (PAO) and glycogen-accumulating organisms (GAO) were more concentrated in the larger granules (Ali et al., 2019). Such selection was attributed to the long retention of large granules and their preferential uptake of volatile fatty acids (VFA) during feeding. Moreover, larger granule sizes are more suitable for simultaneous nitrification-denitrification (SND) because of their larger anoxic volume during the reaction phase (Manuel Layer et al., 2020). In smaller granules, on the other hand, nitrifying organisms are enriched due to a larger relative aerobic volume (Nguyen Quoc et al., 2021). Similarly, granule size could

be important for the hydrolysis of slowly biodegradable substrates. However, biomass differentiation regarding hydrolysis has not been studied in detail yet.

Hydrolysis is a key process to consider when studying the fate of polymeric substrates during wastewater treatment. These substrates make up the largest COD fraction in municipal wastewater, and must be extracellularly hydrolysed to compounds of smaller molecular weight (<1 kDa) to be assimilated by microorganisms (Ferenci, 1980; Hollibaugh and Azam, 1983). Previous experimental work found hydrolysis to be mainly biomass-bound, rather than occurring in the reactor bulk liquid (Confer and Logan, 1998b; Goel et al., 1998b; Janning et al., 1998, 1997; Mosquera-Corral et al., 2003). In full-scale AGS, aerobic granules showed significant hydrolytic activity, suggesting that wastewater polymers can be utilized by granules (Toja Ortega et al., 2021a). However, the limited diffusion of polymers into the granules affects their hydrolysis, resulting in lower biomass-specific hydrolysis rates in granules compared to flocculent sludge. Moreover, several studies suggest that most of the particulates are captured by flocculent sludge, and the granules are only accessible for polymeric substrates of smaller size (i.e. colloidal and soluble) (M. Layer et al., 2020; Ranzinger et al., 2020). Those polymeric molecules can be present in the wastewater or originate from the conversion of the particulate COD. Thus, it is still uncertain how relevant granules are for hydrolysing influent polymers and which granule volume is hydrolytically active. Those points should be addressed to clarify the contribution of polymeric COD to nutrient removal processes and stable granule growth.

4

In addition, it is not known whether all granules within an AGS reactor have a similar hydrolysis capacity. Smaller granules would presumably hydrolyse influent substrates at a higher rate due to their higher available surface area (Toh et al., 2003). Nevertheless, the hydrolytic activity of granules of different sizes might be influenced by factors other than mass transfer of the substrate. For instance, the abovementioned SRT differences and substrate concentration gradients in the sludge bed during feeding could support the enrichment of hydrolysing organisms and enzymes in some specific granule sizes. Exploring differences in hydrolytic activity along the AGS bed would add to the current knowledge of biomass differentiation in AGS reactors. Furthermore, the distribution of hydrolytic activity may reflect the removal mechanism of particulate substrates in AGS. Understanding the differences in microbial activity on different granule size ranges can ultimately aid process control.

In this study we explored the location of hydrolysis in AGS on granule level. First, we studied whether granules of different sizes within an AGS bed are differentiated in terms of their hydrolytic potential. We compared the biomass-specific hydrolysis rate of

granules of different sizes, focussing on protease and amylase activities. These enzyme groups were targeted based on previous studies that showed significant protease and  $\alpha$ -glucosidase activities on AGS (Toja Ortega et al., 2021a, 2021b). In addition, we investigated the location of hydrolysis within granules, to gain insight into substrate penetration depth and the distribution of enzymes throughout the granules. Microbial groups of interest were identified via fluorescence in situ hybridization (FISH) to study their localization relative to the hydrolysis sites. The hydrolytic activity results from each granule size fraction were finally evaluated in relation to other granule characteristics, such as granule density and settling velocity, substrate uptake rate, and microbial community composition. Based on these observations, we reflect on the implications of our findings for particulate hydrolysis in AGS and full-scale operation.

## 4.2 | MATERIALS & METHODS

### 4.2.1 | Sludge sampling and processing

Aerobic granules were harvested in wastewater treatment plant (WWTP) Utrecht, the Netherlands. The plant treats domestic wastewater in 6 Nereda<sup>®</sup> reactors of 12000 m<sup>3</sup>, designed by Royal HaskoningDHV and operated by the Dutch district water authority Hoogheemraadschap de Stichtse Rijnlanden. The average flow during the sampling period was 74,700 m<sup>3</sup> d<sup>-1</sup>, and the reactors are operated with a sludge loading of 0.05 kg COD kg VSS<sup>-1</sup> d<sup>-1</sup>. The full-scale reactors were sampled after at least 20 minutes of aeration to ensure a homogeneous mixed liquor sample.

The granules were separated into four size fractions by sieving the reactor mixed liquor through different mesh sizes. The resulting granule size fractions consisted of the following diameter ranges: 0.5-1 mm, 1.6-2 mm, 2.5-3.15 mm, and 4-4.8 mm. Non-overlapping fractions were used in the study to facilitate the comparison between granules of different size. The granule fractions derived from sieving were cleaned based on settling to remove non-granule material, like husk and fibres. To do so, granules were transferred to a beaker and tap water was added. The content of the beaker was mixed by stirring. After a few seconds of settling time, granules were at the bottom of the beaker and the liquid only contained the non-granular fraction that was subsequently discarded. The process was repeated for 5-10 times until the discarded liquid was clean. The resulting granule size fractions were stored at 4°C until use, for a maximum of 2 days. Before the assays, the granules were acclimatized for half an hour in 10mM Tris-HCl buffer (pH 7.8) at room temperature (20°C).

### 4.2.2 | Protease and amylase assays

Protease and amylase activities of the granules were quantified using fluorogenic substrates. These substrates enable studying the activity on a single granule scale, in a 96-well-plate reader. Furthermore, studying the hydrolysis of real wastewater polymeric substrates is extremely challenging due to their complexity and variability. Therefore, surrogates were used to provide a reproducible experimental setup and study the hydrolytic capacity of granules in detail. The hydrolytic activity assays were based on the protein hydrolysis assay described by Van Gaelen et al., 2020. Protease activity was measured using the BODIPY® FL casein substrate (EnzChek Protease Assay Kit E6638, Thermofisher scientific, Waltham, Massachusetts, USA). Amylase activity was measured using the BODIPY® FL DQ™ starch substrate (EnzChek™ Ultra Amylase Assay Kit E33651, Thermofisher scientific, Waltham, Massachusetts, USA). The substrates were prepared following kit instructions, rendering a protease solution of 10 mg BODIPY® casein/L and an amylase substrate of 200 mg BODIPY® starch/L. There was a modification: amylase substrate was prepared using the digestion buffer provided in the protease assay (10 mM Tris-HCl, pH 7.8, 0.1 mM sodium azide), in order to keep the same assay conditions. The digestion buffer used in the assay was also the 200 mM Tris-HCl provided in the protease assay.

## 4

Two types of sample were studied per granule size fraction: intact granules and crushed granules. The latter were used to determine the hydrolytic capacity of the sludge minimizing mass transfer limitation. Each granule size fraction was studied on a separate run, using a 96-well plate. In each run, hydrolysis rates were monitored in 4 wells containing crushed sludge, as well as in 20 wells containing one intact granule per well. For the intact granule samples, 100 µl of digestion buffer and one granule were added to the assay wells. The crushed granules were prepared by using a Potter-Elvehjem tissue grinder, and diluted to an approximate concentration of 1 g TSS/L using digestion buffer. Then, 100 µl of crushed sludge sample were added to the assay wells. To start the assay, 50 µl of substrate was added to all the samples. Besides the samples, controls were added in each assay. Blanks were prepared for each type of sludge, by adding digestion buffer instead of substrate. Standard samples were also included for each type of sludge, by adding a known concentration of hydrolysed substrate (standard) instead of fresh substrate. The standards were prepared by hydrolysing an aliquot of the substrate solution with commercial enzyme (P5985 and 10065, Sigma-Aldrich, St. Louis, MO, USA).

Hydrolytic activity was monitored in a 96-well plate reader (FLUOstar Galaxy Multi-functional Microplate Reader, BMG LABTECH, Ortenberg, Germany). The reader

measures the fluorescence intensity in each of the 96 wells in defined time intervals. Each experiment ran for approximately 1.5 h, with fluorescence readings every 5 minutes. For both substrates, the Ex/Em wavelengths 485/538 nm were used. The experiments were performed with acclimatised granules at room temperature, with linear mixing. Per hydrolytic activity assay, all the granules were fractionated from the same mixed liquor sample batch and their activities were measured on the same day.

### 4.2.3 | Calculation of hydrolysis rates

The fluorescence intensities from the individual wells were analysed through linear regression. The fluorescence intensities of each well were normalized with the fluorescence intensity of the standards. The linear range of the time-resolved fluorescence curve was visually selected to calculate the hydrolysis rate, expressed as fluorescence (arbitrary units) per hour. The activity per g VSS was calculated by estimating the amount of biomass in each well. In the crushed sludge samples, the VSS concentration of the samples was directly measured following Standard Methods (APHA, 2005). For the granule samples, the amount of biomass per well was variable, and therefore the VSS per well was estimated, instead of measured directly. The estimation was done as follows. First, granule volume was estimated through light microscopy. The plate was placed under a digital microscope (VHX-700F, Keyence, Mechelen, Belgium) and an image of each granule was captured. The images were analysed using the microscope software, to extract the circle equivalent diameter of the granules. The granule volume was then calculated from this diameter, assuming spherical granules. Finally, the granule volume was translated to VSS using granule biomass density, determined separately (see Materials & Methods, Additional characterization of the granule fractions). Hydrolytic activity was also expressed relative to granule surface area. The surface area, too, was calculated based on the circle equivalent diameter determined via image analysis of each granule separately. The obtained biomass-relative and surface-relative rates were normalized against the highest measured rate to simplify visualizations, given that the fluorescence units were by definition arbitrary.

### 4.2.4 | Enzyme staining and microscopic examination

#### Identification of hydrolytically active sites

BODIPY® FL casein and BODIPY® FL DQ™ starch were also used for localizing hydrolytically active sites in the granules. The objective of these experiments was to assess the location within the granule at which polymers from the bulk can be hydrolysed. The

procedure was based on the enzyme staining method described for activated sludge (Xia et al., 2008b, 2008a, 2007). We modified the protocol to stain the biofilm instead of flocculent sludge. Substrate solutions of 100 mg/L were prepared diluting the substrates in Tris-HCl buffer (10 mM, pH 7.8). The substrate concentration and incubation time were chosen based on preliminary assays (Supplementary information, Table S4.1). Granules were incubated with fluorescent substrates in 2 mL sample tubes (Eppendorf, Hamburg, Germany). Approximately 120 mg of fresh granules (5 mg TS) were added to 500 µl of digestion buffer and 250 µl of substrate solution. That rendered a substrate to sludge ratio of 5 µg substrate per g TS. Samples were incubated for two hours, in the dark and with orbital shaking at 120 rpm (Fisherbrand Seastar, Thermo Fisher Scientific, Waltham, USA).

After incubation with fluorescent substrates, the granules were transferred to freeze-drying medium (Neg-50™, Thermo Fisher Scientific, Waltham, USA) and stored at 4°C overnight, protected from light. Then, the granules were sectioned in a Leica CM1900 cryostat (Leica microsystems, Nussloch, Germany). The temperature of the blade and the sample holder was -22°C, and the granules were sectioned in 20 µm-thick coupes. Granule sections were spread on poly-lysine coated slides and air-dried in the dark. Finally, the sections were examined using a Zeiss Axioplan 2 epifluorescence microscope (Zeiss, Oberkochen, Germany). The fluorescent signals from the hydrolysed BODIPY® FL casein and BODIPY® FL DQ™ starch were visualized and captured using a FLUOS filter (excitation 485 nm, emission 515-565 nm).

### **Distribution of hydrolytic enzymes throughout the granule**

A variation of the above described method was used to explore the distribution of enzymes throughout the granule. Fresh granules were sliced using a scalpel, mounted in a microscope slide, and incubated with the fluorogenic substrates. The granule sections were covered with 10 µl of a 2:1 buffer:substrate solution and incubated in the dark for 2 hours. Then, the substrate solution was replaced by digestion buffer and the slides were observed on the fluorescence microscope.

#### **4.2.5 | Fluorescent *in situ* hybridization (FISH)**

After inspecting the activity staining, the granule sections were fixed in ethanol (50%) for 2 hours. Ethanol fixing was used independently of the microbial group targeted by FISH (Gram negative or Gram positive), as described in Xia et al., 2007 (Xia et al., 2007).

The following probes were used: EUBmix, staining most bacteria (a mixture of EUB338, EUB338-II and EUB338-III) (Amann et al., 1990; Daims et al., 1999); PAOmix, targeting

*Ca. Accumulibacter*-related polyphosphate accumulating organisms (PAO) (a mixture of PAO462, PAO651, and PAO846) (Crocetti et al., 2000); GAOmix, targeting glycogen accumulating organisms (GAO) (a mixture of GAOQ431 and GAOQ989 probes) (Crocetti R. et al., 2002); Actino-221, targeting actinobacterial PAO related to genus *Tetrasphaera* (Kong et al., 2005); CFX1223 (Björnsson et al., 2002) and GNSB-941 (Gich et al., 2001), targeting most members of the phylum *Chloroflexi*; and Bac111 targeting activated sludge clones of the family *Saprospiraceae* (Kong et al., 2007). Detailed information of all these probes is given in probeBase (Loy et al., 2003). All the probes were Cy3 or Cy5 labelled.

FISH staining was performed as described in Bassin et al., 2011 (Bassin et al., 2011). Samples were incubated for 2 hours with the FISH probes. The stained slides were mounted with VECTASHIELD® antifade mounting medium (Vector laboratories, Burlingame, CA, USA), and inspected on the epifluorescence microscope. The hybridised cells were visualized using the filters Cy3 (excitation 546 nm, emission 575-640 nm) and Cy5 (excitation 575-625 nm, emission 660-710 nm).

#### 4.2.6 | Microbial diversity analysis

Three sludge samples were collected at different points of each of the studied reactors (R1, R3 and R4). Each of the triplicate samples was sieved separately using the same procedure as described in section 2.1. 15 mL of the sieved granules (roughly 300 mg TSS) of each size fraction were homogenized using a tissue grinder. The homogenized samples were centrifuged at 14,000 g for 5 minutes and approximately 2 mg TS of the resulting pellet were added to the extraction tubes. DNA was then extracted as described in Toja Ortega et al., 2021b.

The V3-V4 regions of the 16S rRNA gene was amplified and paired-end sequenced in an Illumina NovaSeq 6000 platform by Novogene (Beijing, China). The primer set 341F [5'–CCTAYGGGRBGCASCAG–3'] and 806R [5'–GGACTACNNGGGTATCTAAT–3'] was used. The raw reads were deposited in the National Center for Biotechnology Information (NCBI) Sequence Read Archive (SRA) on BioProject PRJNA837281.

The trimmed and merged sequences provided by Novogene were processed using QIIME2, version 2020.2 (Bolyen et al., 2019). The sequences were quality-filtered using Deblur (Amir et al., 2017), trimming the sequences the 3' end at position 237 (parameter p-trim-length). With the remaining sequences, alpha and beta diversity metrics were generated, and differences in diversity between granule sizes were assessed using PERMANOVA (Anderson, 2001). A *p*-value of 0.05 was used as cut-off for significance. Finally, taxonomic affiliation of the sequences was determined by aligning the



sequences to the MiDAS 3.6 database (Nierychlo et al., 2020). Sample subsetting, visualization and further statistical analysis was performed in R, using the Phyloseq and Ampvis2 packages (Andersen et al., 2018; McMurdie and Holmes, 2013). Differences in the relative abundance of the 20 most abundant genera were studied performing a Wald test. The relative abundances in the smallest and largest granules were compared. Differences were considered significant with a  $p$  value below the Bonferroni-corrected  $p$  value of 0.05 ( $p = 0.05/\text{number of comparisons}$ ).

## 4.2.7 | Additional characterization of the granule fractions

### PAO activity

The activity of PAO was assessed in the four granule size fractions through batch tests. The assay was performed in triplicate. The granules, which had been stored anaerobically overnight, were acclimated by aerating for 35 min. Then, they were crushed using a Potter-Elvehjem tissue grinder and buffered with 20 mM Tris-HCl (pH 7.5). The assays were conducted in 500 mL bottles, with a final sludge concentration of approximately 3 g VSS/L. Sodium acetate was added to a final concentration of 170 mg COD/L. The bottles were sealed with rubber stoppers and flushed with N<sub>2</sub> for two minutes to provide anaerobic conditions. The samples were incubated for two hours in a Fisherbrand Seastar orbital shaker at 120 rpm, taking samples regularly (every 6-10 minutes). Samples were filtered using 0.45 µm PES syringe filters. The acetate concentration of the samples was measured in a gas chromatographer equipped with an FID detector (7890A GC; Agilent Technologies, Santa Clara, CA, USA). Phosphate concentration was determined colorimetrically using the USEPA method 365.1, in an AQ400 discrete analyser (Seal analytical, Mequon, WI, USA). The TSS and VSS concentration of the sludge solutions used in the assay were determined following standard methods (APHA, 2005).

### Settling tests

The terminal settling velocity of granules was studied in a measuring cylinder with an internal diameter of 7.94 cm and a height of 42.1 cm, filled with tap water. Granules were placed individually at the top of the cylinder and their settling was recorded using a camera (GoPro Hero Session 4, San Mateo, CA, USA). Around 50 granules were examined per size fraction.

### Granule biomass density measurements

Granule biomass density was measured using the modified dextran blue method, as described in Van den Berg et al., 2021 (van den Berg et al., 2022a). The density measurements were performed in 200 mL samples, and each granule size fraction was measured in triplicate.

## 4.3 | RESULTS & DISCUSSION

### 4.3.1 | Granule size effect on hydrolysis rate

The hydrolysis capacity of different sized aerobic granules was studied using fluorescent protease and amylase assays. Biomass-specific hydrolytic activity (fluorescence  $[\Delta F]/g$  VSS/h) was inversely proportional to granule diameter (Figure 4.1). This relationship can be explained by the changes in surface/volume ratio with respect to granule diameter, ( $SA/V \propto d^{-1}$ , for a perfect sphere). The areal hydrolysis rate ( $\Delta F/m^2/h$ ) somewhat decreased with increasing granule size too (Figure 4.1). Hence, the smaller granules had a higher biomass-specific hydrolytic activity, supported mainly by their proportionally higher available surface area and enhanced by a higher activity per surface area. According to these results, the hydrolytic capacity that potentially could degrade influent particulates can be doubled by halving the average granule diameter in an AGS reactor.

The different biomass-specific rates indicated that hydrolysis was, as described previously, conditioned by mass transfer. In WWTP Garmerwolde, crushed granules and flocs showed roughly twice as high hydrolytic activity as intact granules (e.g., protease rates were 0.016 and 0.017  $\mu\text{mol product mg VS}^{-1} \text{ h}^{-1}$  on crushed granules and flocs, and 0.007  $\mu\text{mol product mg VS}^{-1} \text{ h}^{-1}$  on intact granules) (Toja Ortega et al., 2021a). Activated sludge studies using similar methods also generally reported higher hydrolysis rates than those measured in granules, although hydrolysis rates differed between studies and plants up to two orders of magnitude (e.g. protease activities reported in AS range from 0.015 to 2.1  $\mu\text{mol product mg VS}^{-1} \text{ h}^{-1}$ ) (Frølund et al., 1995; Nybroe et al., 1992). In this study too, the available surface area determined the activity of the sludge, and the hydrolysis rates increased upon granule crushing (data not shown). The starch and proteins used in the assays were soluble substrates: the molecular weight of the labelled starch was lower than 1 kDa; and casein has a molecular weight of around 24 kDa.

Considering that the hydrolysis rate of even the small starch molecules was determined by the available granule surface area, the same could be expected for larger substrates.

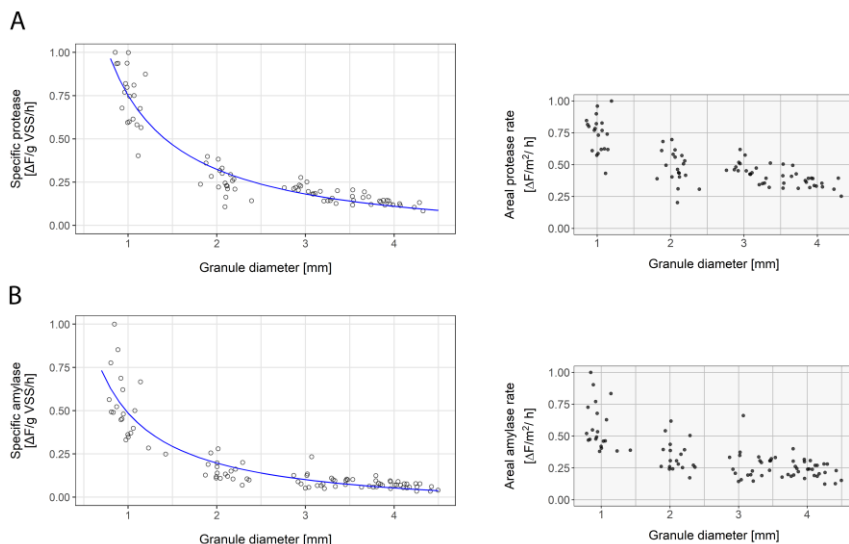


**Figure 4.1.** Hydrolysis rates measured in granules between 0.5 and 4.8 mm. a) Protease activity as a function of granule diameter; and b) amylase activity as a function of granule diameter. In the left graphs, biomass specific activity is shown, as increase in fluorescence per gram VSS per hour. In blue, the inverse proportional fit of the data is shown ( $y = k / x$ ). The right graphs show the surface-specific hydrolytic activity, as increase in fluorescence per granule surface (m<sup>2</sup>) per hour. Each data point represents one granule.

### 4.3.2 | Hydrolysis sites and hydrolytic capacity distribution within granules

#### Mass-transfer limited hydrolysis of polymeric substrates occurs at the granule surface

The sites of hydrolysis were microscopically visualized in granules incubated with fluorescent substrates; intact granules were incubated for 2 hours and cryosectioned afterwards. Figure 4.2 shows the micrographs of granules of 4 different sizes incubated with BODIPY-casein. Amylase assays rendered similar results which can be found in the Supplementary information, as well as additional protease images (Figures S4.3-S4.5). All the granule sizes revealed a hydrolytically active layer in the outer part of the granules. The thickness of this layer varied depending on the zone of the granule, and

rarely reached further than the outer 100  $\mu\text{m}$  of granule. Granule size did not appear to impact the thickness of the hydrolytically active layer.

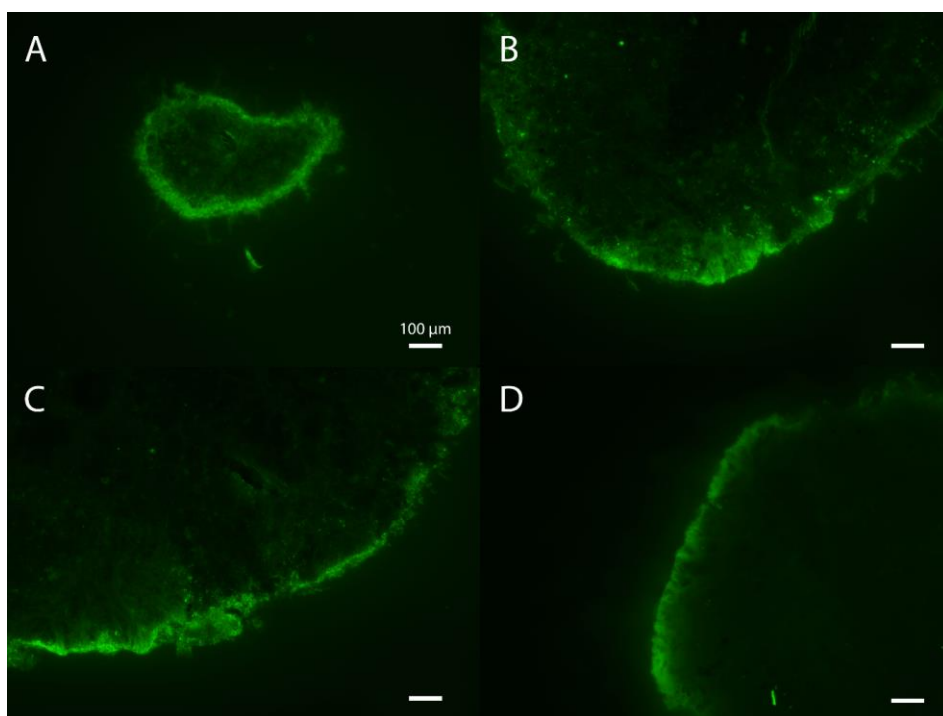


**Figure 4.2.** Fluorescence microscope images of sections of intact granules incubated with BODIPY-casein. a) 0.5-1 mm granule; b) 1.6-2 mm granule; c) 2.5-3.15 mm granule; d) 4-4.8 mm granule. All size-bars indicate 100  $\mu\text{m}$ . The areas where BODIPY-casein is hydrolysed appear bright green.

Protease active sites were generally arranged in a thin layer close to the surface of the granules, within the outer 100  $\mu\text{m}$ . In some spots along the granule surface, larger fluorescent patches could be observed which exceeded the 100  $\mu\text{m}$  of depth. Those areas were generally more fluffy (Supplementary information; Figure S4.4.2). With protease staining, it was seldom possible to distinguish individual stained cells, but rather a cloudy background was observed, as if hydrolysis products were distributed throughout the extracellular space. For amylase, on the contrary, distinct cells were discernible, even though a fluorescent background was observed too (Supplementary information; Figure S4.5). Nevertheless, the granule depth at which hydrolysis occurred was similar for both substrates.

### Hydrolytic potential is also present deeper inside the granule

The distribution of hydrolytic potential in granules was further inspected by eliminating mass transfer limitation, that is, slicing granules before incubating them with fluorescent substrates in order to expose the full sectional plane to the fluorescent substrate. The result of these experiments differed for both substrates: while proteases seemed to be distributed throughout the whole granule, amylase activity was still restricted to the outer parts of the granules, although in a thicker layer than when incubating intact granules (Figure 4.3).

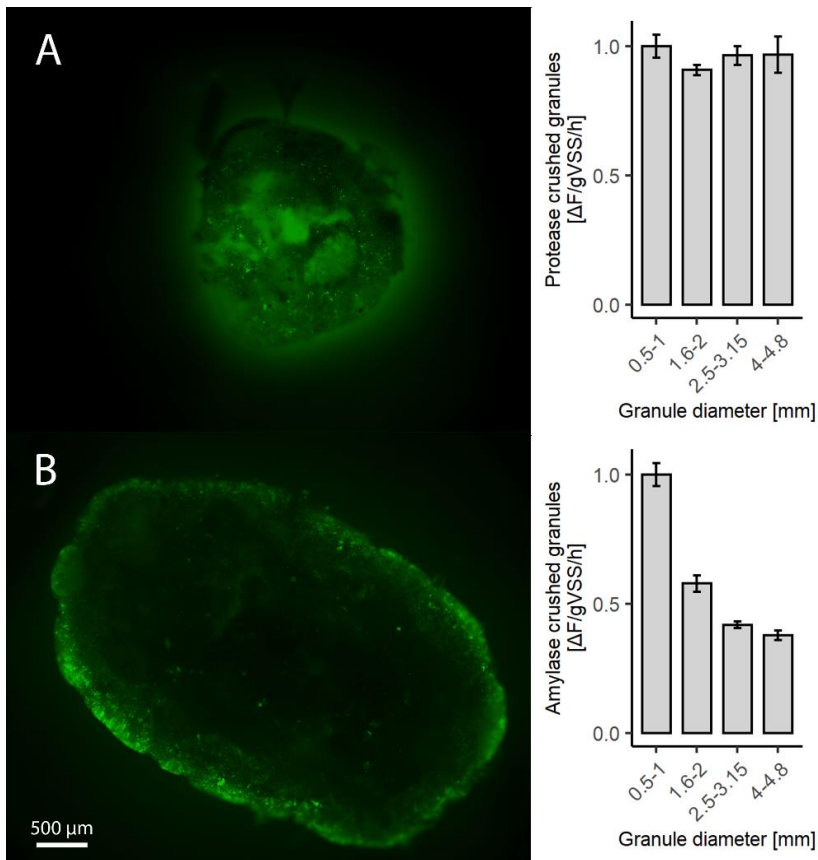


**Figure 4.3.** Micrographs of granules incubated with labelled substrate after sectioning, showing the incubated sectional plane. Top = granule incubated with Bodipy-casein; bottom = granule incubated with Bodipy-starch. The hydrolytically active granule areas appear bright, due to the fluorescence emitted by hydrolysed BODIPY. On the right, the hydrolytic activity of the crushed granules of different sizes is plotted; each bar represents the average of 4 samples (error bars = standard deviation).

The activity distribution observed under the microscope related to the hydrolysis rates measured in crushed granules (Figure 4.3). When the granule structure was disrupted by crushing, all the granule sizes had the same protease activity, suggesting that the inner parts of the granules had similar hydrolytic capacities across granule sizes. On the contrary, the amylase activity of crushed granules decreased with granule size. Based on the microscopic observations, this could be due to low or no amylase activity in the inner volume of granules, and the larger proportion of such volume in larger granules.

The difference in protease and amylase enzyme distribution might be related to the distribution of different macromolecules in the granule matrix. Previous studies investigating the distribution of extracellular polymeric substances (EPS) in lab-grown AGS reported that  $\alpha$ -polysaccharides were mainly present close to the granule surface (Adav et al., 2008; McSwain et al., 2005). Proteins, on the other hand, were distributed throughout the granule, and the granule core was mainly composed of protein. The distribution of proteins and polysaccharides in full-scale granules was not studied yet, but might be similar to the reported observations in lab-grown granules. The different distribution of proteases and amylases throughout the granules might reflect the distribution of their potential substrates, proteins and alpha polysaccharides, on the granule matrix. In spite of these differences in granule-wide distribution of protease and amylase activity, the hydrolysis of both casein and starch in intact granules was restricted to the granule surface, indicating that hydrolysis is mass-transfer limited.

### 4.3.3 | Microorganisms in the vicinity of the hydrolytically active layer

Microorganisms surrounding the hydrolytically active layer were identified by FISH. PAO, GAO, and putative starch and protein hydrolysers were targeted via FISH probes. GAO and *Ca. Accumulibacter*-related PAO were abundant in all granule sizes. PAO were most concentrated in the outer granule layers, while GAO were abundant in the core too. These microorganisms were often intercalated with hydrolytically active cells (Figure 4.4a).

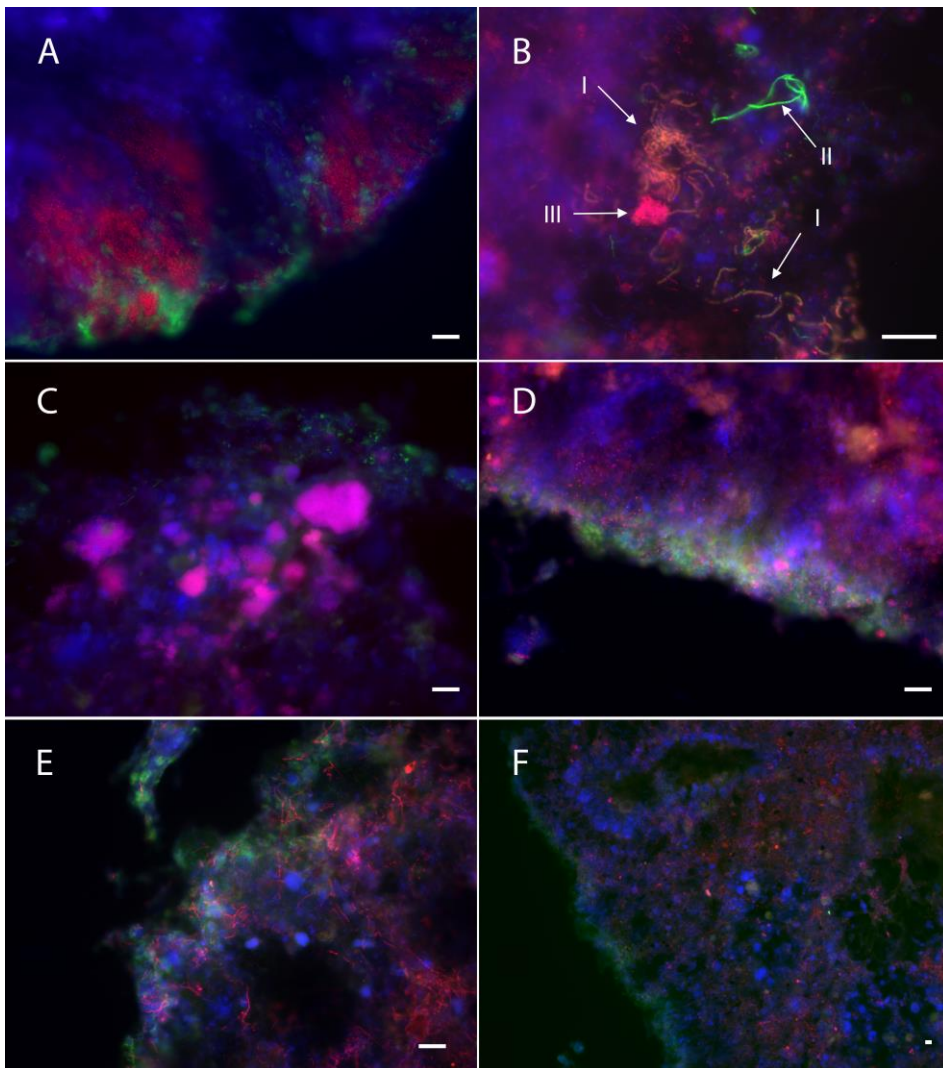


**Figure 4.4.** Fluorescence microscope images of aerobic granules stained with fluorescent substrates followed by FISH. Blue = EUB; Green = activity staining (amylase in a-c; protease in d-f); Red = specific microbial groups: a) PAOmixon; b) Actino-221 (*Tetrasphaera*); c) GAOmix; d) Bac111 (*Saprospiraceae*); e-f) CFX1223 + GNSB-941 (*Chloroflexi*), at two different magnifications to visualize granule surface and granule-wide distribution. Size-bar = 20  $\mu$ m. The arrows in b indicate individual stained cells (I: starch hydrolysing *Tetrasphaera*; II: non-*Tetrasphaera* starch hydrolyser; III: non-starch hydrolysing *Tetrasphaera*).

The amylase-staining was still visible after the FISH hybridization procedure, making it possible to identify some of the starch hydrolysing organisms. Some of the starch hydrolysers hybridized with the probe Actino-221 (targeting *Tetrasphaera*), specifically some of the filamentous starch hydrolysers (Figure 4.4b, arrows I). Some of the

*Tetrasphaera* members can hydrolyse starch, and they are overall regarded as dominant glucose fermenters in EBPR plants (Nielsen et al., 2012; Xia et al., 2008a). Despite some of the amylase stained cells were identified as *Tetrasphaera*, most of the starch hydrolysing organisms remained unidentified. In general, the abundance of *Tetrasphaera* was high, as in previous AS and AGS studies (Ali et al., 2019; Nguyen et al., 2011; Stokholm-Bjerregaard et al., 2017; Toja Ortega et al., 2021b).

Since individual cells were seldom stained with protease substrates, protein hydrolysing organisms could not be identified. Nevertheless, it was possible to observe the microorganisms in the vicinity of the active protease sites. Phylum *Chloroflexi* and family *Saprospiraceae* were targeted as putative hydrolysers (Xia et al., 2007). The probes targeting these taxa hybridized with a significant amount of organisms in the sludge. Some of the *Chloroflexi* or *Saprospiraceae* hybridized cells were located close to the hydrolysis sites; however, their distribution was not restricted to those sites, and they were most abundant further from the granule surface. Therefore, their relevance for protein hydrolysis could not be determined. *Saprospiraceae* were rod-shaped, often arranged in colonies, and located mostly in the outer part of the granules. *Chloroflexi* were filamentous and widely distributed throughout the granules. *Chloroflexi*-hybridized cells were specially abundant in the granule core, where they might be subsisting on cell decay products and other recalcitrant compounds (Figure 4.4f) (Kragelund et al., 2007). Interestingly, the *Chloroflexi* genus *Kouleothrix* was identified by 16S as one of the abundant genera (Figure 4.5b). This genus is considered a major indicator of bulking in AS (Nittami et al., 2017). However, it did not seem to have detrimental effects on aerobic granules. *Chloroflexi* filaments did not result in filamentous outgrowths or irregular granule surfaces (Supplementary information, Figure S4.6). They rather constituted a filamentous network inside the granules (Figure 4.4 e, f). A similar observation was made by De Graaf et al. (2020), who cultivated aerobic granules with a high abundance of the filamentous *Thiothrix*. The high proportion of filamentous organisms in the granules did not deteriorate granule morphology or cause operation issues, showing that operating conditions rather than bacterial morphology determine granule stability (de Graaff et al., 2020). This interpretation is supported by our observation of filamentous organisms thoroughly distributed in stable full-scale granules.

#### 4.3.4 | Additional comparison of the different granule size fractions

The microbial composition of granules of different sizes was compared, based on 16S rRNA amplicon sequencing results. Figure 4.5b shows the average abundance of the main 20 genera. The abundances of the main microorganisms showed some variation



between reactors; for the composition per reactor, check Supplementary information (Figure S4.7). Nevertheless, the main genera were shared between all samples. The microbial community composition differed significantly between the different granule size fractions. When studying the Bray-Curtis dissimilarity between samples, one can appreciate that samples cluster according to granule size (Figure 4.5a). The distance between samples grows with increasing granule size difference.

In all granule sizes, the microorganisms targeted by FISH were found in high relative abundance in NGS results. However, the differences in relative abundance between granule sizes were small. An increase in *Ca. Competibacter* and *Ca. Accumulibacter* can be noticed with increasing granule size, but the relative abundance differences are not significant ( $p < 0.05/\text{number of comparisons}$ ). The relative abundance of the family *Saprospiraceae* did significantly increase from the largest to smallest granule sizes. Other genera that were at significantly higher concentrations in the smaller granules were the nitrifying *Nitrosomonas* and *Nitrospira*, as described previously (Nguyen Quoc et al., 2021). To check other significant abundance differences on the most abundant microorganisms, see Supplementary information (Tables S4.8.1 and S4.8.2).

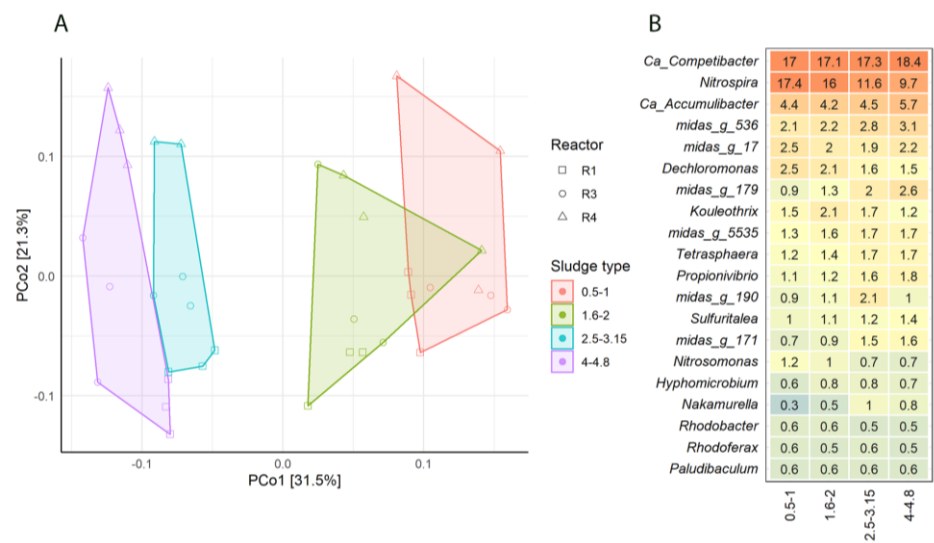


**Figure 4.5.** Microbial differences between aerobic granules of different sizes. A) PCoA plot of the Bray-Curtis dissimilarity between samples. Each point represents one DNA sample. B) Heatmap showing the most abundant genera identified by 16S rRNA amplicon sequencing. The values in the heatmap signify percent of reads of an OTU in three reactors and triplicate samples. All samples were taken in the same day.

Activity batch tests revealed an increasing specific anaerobic acetate uptake and P release with increasing granule size (Table 4.1). The terminal settling velocity was also higher in the largest granules, as expected due to their larger size (Liu et al., 2008; van Dijk et al., 2020) (Table 4.1). These results are in agreement with the observations at Garmerwolde WWTP and the hypothesis that the higher settling velocity of larger granules favours PAO enrichment (Ali et al., 2019; van Dijk et al., 2022). Granule density decreased with increasing granule size, which could be explained by a reduced substrate availability at the granule core due to diffusion limitation leading to biomass decay. The large granules (>4 mm), older and with a larger core volume, were the least dense, in line with results reported by Toh et al. (2003) (Toh et al., 2003).

**Table 4.1.** Granule characterization results. Acetate uptake rate, P release rate and granule density were measured in triplicate. Terminal settling velocity was measured for 49-55 granules of each size range. Average values  $\pm$  standard deviation are shown.

	Acetate uptake rate [mgAcH/gVSS/h]	P release rate [mg P/g VSS/h]	Terminal settling velocity [m/h]	Granule density [g VSS/L]
4-4.8 mm	33 $\pm$ 5	10.9 $\pm$ 0.8	112 $\pm$ 11	55 $\pm$ 8
2.5-3.15 mm	23 $\pm$ 2	8.9 $\pm$ 1.0	86 $\pm$ 10	60 $\pm$ 4
1.6-2 mm	25 $\pm$ 2	8.4 $\pm$ 1.2	56 $\pm$ 12	71 $\pm$ 5
0.5-1 mm	18 $\pm$ 1	5.9 $\pm$ 0.6	29 $\pm$ 11	76 $\pm$ 10

#### 4.3.5 | General discussion

Our results showed a similar distribution of hydrolytic activity in all the granules ranging from 0.5 to 4.8 mm from a full-scale AGS reactor. All the granules had an active hydrolytic layer at their outer part and its thickness did not seem to depend on granule size. The hydrolysis rates measured in the different sized granules also indicated that hydrolysis is largely surface-area related. This makes small granules more suitable to degrade polymeric substrates; not because of a specific microbial community composition or higher enzyme concentration, but mainly due to their high available surface area. Their activity was enhanced by a somewhat higher surface-related activity, although a significant trend could not be identified.

There was, nonetheless, microbial differentiation between granules of different sizes. The microbial community of the granules shifted with the changes in granule size. Since most hydrolysers remained unidentified, it was not possible to assess their abundance

changes in the different size fractions. The abundances of the PAO *Ca. Accumulibacter* and the GAO *Ca. Competibacter* did not differ significantly between granule size fractions. Nonetheless, activity tests did show differences in acetate uptake and P release rates. The largest granules exhibited higher acetate uptake and P release activities, reflecting a higher EBPR activity. This higher activity can be explained by the differences in substrate availability during full-scale operation. Due to stratification during settling, larger granules will be located closer to the influent inlet at the bottom of the reactor than the small granules (van Dijk et al., 2020, 2022). Large granules thus spend most of the anaerobic period in contact with the influent, while smaller granules are only in contact with the influent during the final stages of the feeding phase, when the influent level reaches the upper part of the settled bed (van Dijk et al., 2022). VFAs are taken up at high rates, and hence, the position of granules in the sludge bed during feeding impacts their access to VFA significantly (de Kreuk and van Loosdrecht, 2004; Pronk et al., 2015a). In this way, anaerobic COD storage is promoted in granules at the bottom of the settled granule bed, that is, in the largest granules (van Dijk et al., 2022). This may lead to PAO and GAO enrichment as previously reported by Ali et al. (2019) in the full-scale AGS from WWTP Garmerwolde (Ali et al., 2019).

In contrast, hydrolysis potential was similar, yet surface-bound, across granule sizes. One reason could be that the position of the granules in the settled bed has little effect on their interaction with polymeric substrates. Granule-substrate interaction is greatly influenced by the size of the substrate and by mixing. The majority of polymeric substrates in domestic wastewater are in the particulate form. Polymeric substrates can also be soluble and colloidal, but these forms are generally less abundant in domestic wastewater; likely due to biodegradation during transport in the sewer. Reported soluble protein and carbohydrate concentrations in domestic wastewater range between 3 and 100 mg COD/L, and between 5 and 110 mg COD/L, respectively. Their particulate counterparts range between 3 and 161 mg COD/L for proteins and between 5 and 200 mg COD/L for carbohydrates (Narkis et al., 1980; Raunkjær et al., 1994; Ravndal et al., 2018; Toja Ortega et al., 2021a, 2021b). During plug-flow feeding, while soluble and colloidal substrates penetrate the granules easily, particulates are trapped within the voids of the granule bed, but their attachment to the biomass appears to be low (M. Layer et al., 2020; Ranzinger et al., 2020). Most of the particulate COD is thus likely resuspended in the aerobic phase, where the reactor volume is fully mixed. Aeration creates a turbulent flow which promotes collision between granules and particulate substrates (Boltz and La Motta, 2006; M. Layer et al., 2020); Layer et al. (2020) reported a retention of 60-85% of the particulate COD in AGS after 3 hours of aeration. Hence, the aerobic phase probably determines the biomass fraction

particulates can attach to, including both the granular and flocculent fractions that usually constitute the AGS bed. In this context, the development of hydrolytic capacity would be driven by the interactions taking place during the aerobic phase, where there is no sludge stratification, and a large surface area is advantageous to enhance collision chances.

Furthermore, the synthesis of hydrolytic enzymes within the granule matrix might be triggered by compounds in the EPS rather than by substrates in the bulk liquid. Studies on the EPS composition of AGS found proteins widespread through the granules, and  $\alpha$ -polysaccharides only in the outer layers (Adav et al., 2008; McSwain et al., 2005). The granule-wide distribution of hydrolytic activity determined in our study also showed protease activity all through the granule, while amylase was restricted to the surface. High protease activities have been measured previously in the granule core, and related to EPS turnover and biomass decay (Adav et al., 2009). Therefore the hydrolytic enzymes could be mainly degrading EPS and cell decay components, although they also allow granules to hydrolyse polymeric substrates from the influent, at the surface of the AGS or within the granules in case of diffusible polymers. The combined FISH and activity staining results showed that PAO and GAO localized close to the hydrolysis sites, and they could potentially take up the hydrolysates generated during the anaerobic phase. Furthermore, some of the actinobacterial PAO (*Tetrasphaera*) in this study could hydrolyse starch, also suggesting that polysaccharides can be used for EBPR. However, the contribution of polymeric COD to EBPR remains a topic for further research.

Evident from our study is that granule surface area will determine the potential of aerobic granules to degrade polymeric COD, both aerobically and anaerobically. If boosting the anaerobic uptake of polymeric COD is desired, due to a wastewater with low VFA for example, a smaller average granule size might be beneficial. The length of the anaerobic phase could be regulated too to promote hydrolysis. Smaller granules will also increase nitrification rates, and overall improve mass-transfer (Nguyen Quoc et al., 2021). If, on a different scenario, there are enough VFA in the influent for effective EBPR, larger granules might be preferred for an improved simultaneous nitrification-denitrification (SND) and a decreased degradation of polymeric substrates. Lower aerobic COD degradation would then decrease aeration costs and enhance the recovery of energy from the sludge spill (Guo et al., 2020).

## 4.4 | CONCLUSION

The main conclusions of this study are:

- The stratification of the AGS granule bed during feeding drives microbial differentiation in granules of different sizes, based on their proximity to the influent inlet during feeding. As a result, large granules have higher PAO concentrations and acetate uptake rates, reflecting their preferential access to influent VFA. Nevertheless, this differentiation is not evident from the distribution of hydrolysis capacity. All granule sizes exhibited a similar hydrolytic activity per surface area, and thus the development of hydrolytic activity does not appear to be conditioned by the position of granules in the settled bed during feeding.
- Hydrolysis of polymers occurred in the outer 50-100  $\mu\text{m}$  of the granules. PAOs and GAOs were observed in the vicinity of the hydrolytically active granule sites, but their anaerobic uptake of hydrolysates was not demonstrated and deserves further research.
- Small granules returned higher specific hydrolysis rates due to their larger specific surface area. Thus, small granules are preferred when anaerobic COD storage from polymeric substrates needs to be maximized. However, the hydrolysis kinetics of polymeric substrates should be studied further to evaluate how significantly these substrates can contribute to anaerobic COD storage in AGS.

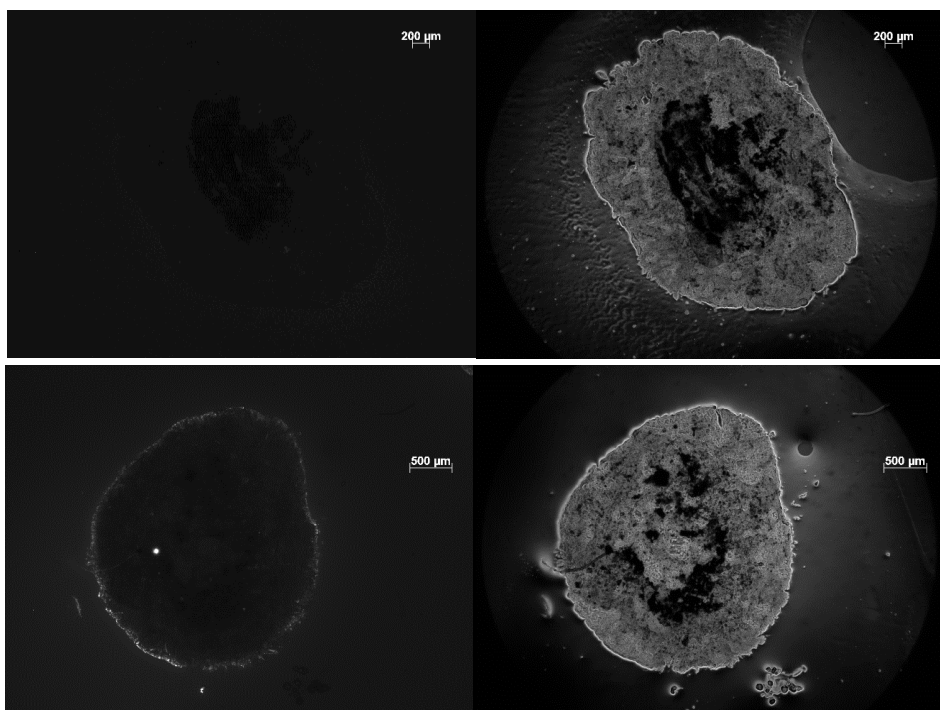
## SUPPLEMENTARY INFORMATION

### Supplementary information 1: Determination of substrate concentration and incubation times for hydrolytic activity staining assays.

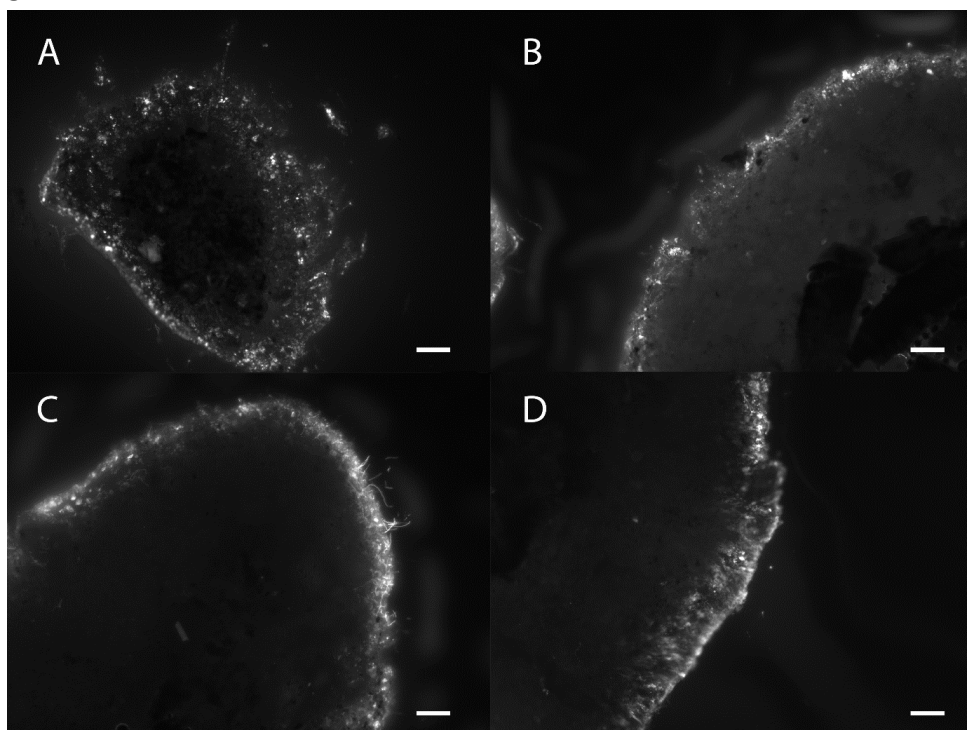
The incubation time and assay conditions for the hydrolytic activity assays were determined during preliminary assays. The tested conditions are summarized in table S1, next to the observed results.

**Table S4.1.** Summary of the incubation conditions during preliminary experiments of fluorescent activity staining.

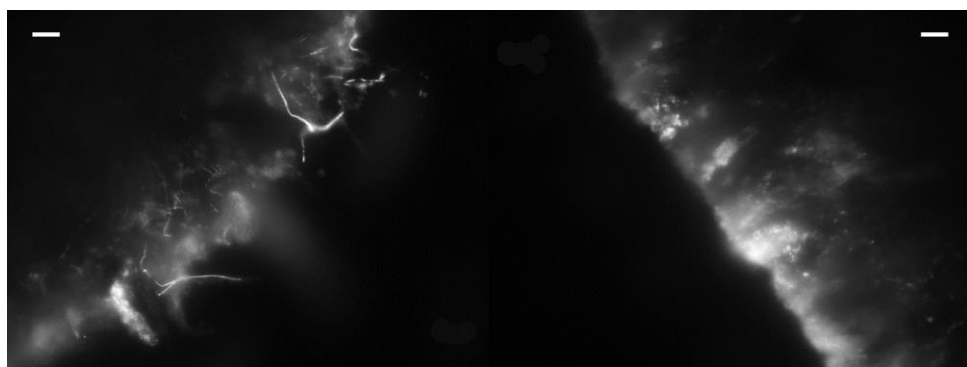
Trial #	Substrate concentration (mg S/g VS)	Incubation time	Washing	Fixing before microscopy?	Observable fluorescence?
1	0.7	15 min	1 wash PBS	No	No
2	0.3	15 min	1 wash PBS	No	No
3	0.7	15 min, 28 min, 1 h	No washing	No	No
4	0.5	3 h	No washing	No	Yes, low
5	0.5	3 h	10 min in PBS	No	Yes, weaker signal
6	0.5	3 h	10 min in PBS	Yes	No
7	0.5	2 h	No washing	No	Yes, low
8	0.5	6 h	No washing	No	Yes, low
9	5	2 h	No washing	No	Yes, higher signal
10	5	6 h	No washing	No	Yes, higher signal

**Supplementary information 2: Controls of hydrolytic activity staining**

**Figure S4.2.** Comparison between control and sample granules. A granule incubated with BODIPY (top) is compared against a granule incubated with BODIPY-starch (bottom). For each granule, two microscope images are shown: FITC channel (left) and phase contrast channel (right). The control granule does not show any fluorescently labelled granule areas. Only when the polymeric substrate is hydrolysed and taken up by microorganisms, a fluorescent signal can be observed on the microscope.

**Supplementary information 3: Supplementary figures of amylase stained granules**

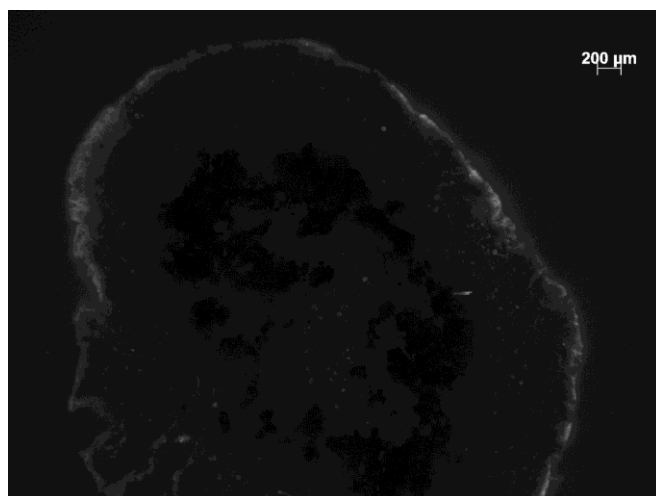
**Figure S4.3.1. Amylase-stained granules.** The hydrolytically active granule areas appear bright, due to the fluorescence emitted by hydrolysed BODIPY. a) 0.5-1 mm; b) 1.6-2 mm; c) 2.5-3.15 mm; d) 4-4.8 mm. Size bars = 100  $\mu$ m.



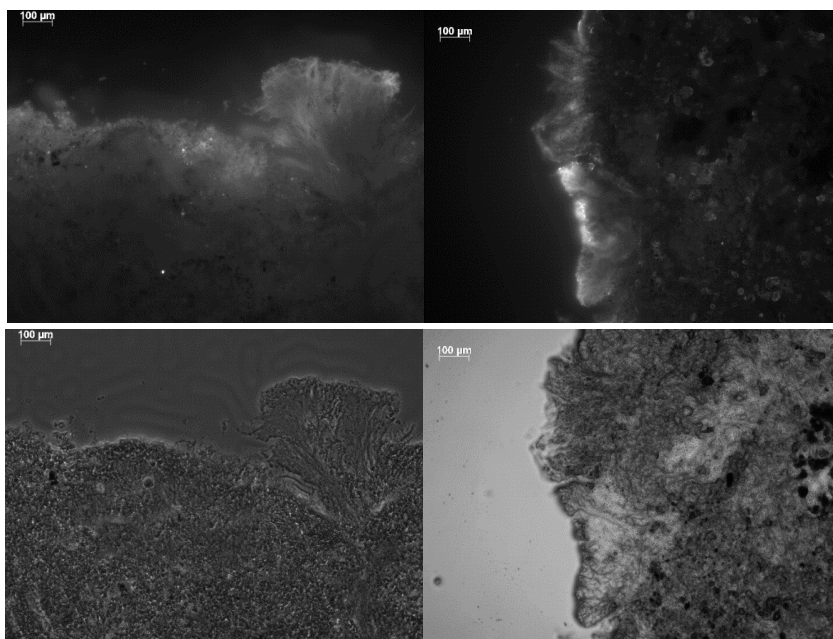
**Figure S4.3.2. Amylase-stained microorganisms.** On the left, filamentous hydrolysers. On the right, non-filamentous hydrolysing colonies. Size bars= 20  $\mu$ m.



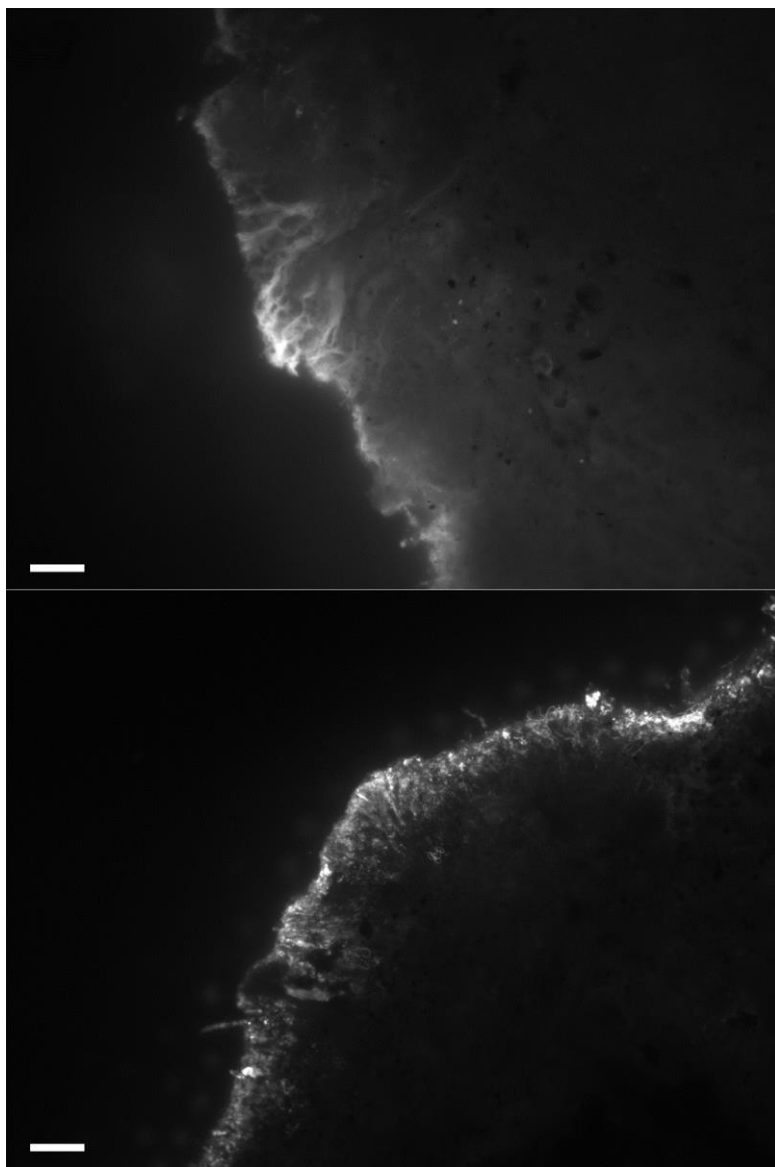
#### Supplementary information 4: Additional images of protease-stained granules.



**Figure S4.4.1. 4-4.8 mm granule observed at low magnification (2.5X).** The hydrolytically active granule areas appear bright, due to the fluorescence emitted by hydrolysed BODIPY. Some areas of the granule appear with a thin stained area, while others are thicker (reaching up to 200  $\mu\text{m}$ ).



**Figure S4.4.2. Larger protease active sites on the surface of large granules (4-4.8 mm).** The top images show the fluorescent signals indicating protease activity; at the bottom, phase-contrast images of the same sections are shown.

**Supplementary information 5: Comparison between amylase and protease staining.**

**Figure S4.5.** Comparison between protease (top) and amylase (bottom) staining. The hydrolytically active granule areas appear bright, due to the fluorescence emitted by hydrolysed BODIPY. Protease stained areas are cloudy while amylase staining allows higher cell-level resolution. Size bars = 100  $\mu\text{m}$ .

**Supplementary information 6: Light microscope images of granules of different sizes**

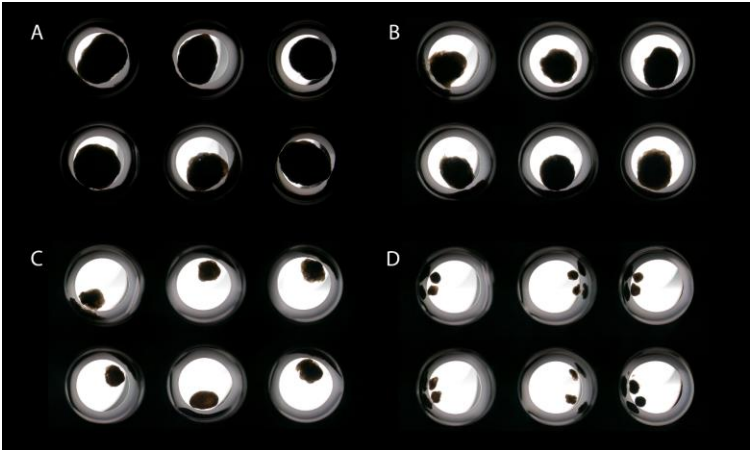


**Figure S4.6.** Transmitted light images of granules of different sizes. A) granules between 4-4.8 mm; B) granules between 2.5-3.15 mm; C) granules between 1.6-2 mm; D) granules between 0.5-1 mm.

**Supplementary information 7: Variation in the relative abundance of the most abundant species across sampled reactors.**

	R1				R3				R4			
<i>Proteobacteria; Ca_Competibacter</i>	17.5	16.6	15.4	18.4	16.9	20.5	21.5	23.5	16.6	14.2	14	13.1
<i>Nitrospirae; Nitrospira</i>	17.1	17.6	13	12.3	17.2	14.7	11.5	9.5	18	15.7	9.4	7.4
<i>Proteobacteria; Ca_Accumulibacter</i>	3.5	3.9	3.9	4.1	3.5	3.6	3.5	4.7	6.1	5.1	6.8	8.2
<i>Bacteroidetes; midas_g_536</i>	2.3	1.9	2.1	2.1	1.7	2	2.8	2.6	2.4	2.8	4	4.6
<i>Bacteroidetes; midas_g_17</i>	2.3	2.2	1.6	2.2	2.4	2.2	1.7	2.3	2.8	1.6	2.7	2.2
<i>Proteobacteria; Dechloromonas</i>	2.1	1.9	1.4	1.2	2.2	2	1.6	1.8	3	2.5	2	1.4
<i>Bacteroidetes; midas_g_179</i>	1.2	1.3	1.8	2	0.9	1.5	2.5	3.4	0.7	1	1.7	2.5
<i>Chloroflexi; Kouleothrix</i>	1.4	1.5	1.3	1.3	1.6	2.5	2.3	1.3	1.6	2.1	1.3	1.1
<i>Proteobacteria; midas_g_5535</i>	1.3	1.6	1.8	1.8	1.1	1.7	1.6	1.7	1.5	1.5	1.9	1.6
<i>Actinobacteria; Tetrasphaera</i>	1.4	1.4	1.6	1.9	1.2	1.3	1.8	1.5	1.1	1.4	1.6	1.5
<i>Proteobacteria; Propionivibrio</i>	0.9	1.2	1.5	1.5	0.9	1.2	1.4	1.8	1.4	1.2	2.2	2
<i>Proteobacteria; midas_g_190</i>	0.7	1	1.9	0.8	0.8	1	1.8	1	1.1	1.3	2.7	1.1
<i>Proteobacteria; Sulfuritalea</i>	0.9	1	1.2	1.6	0.9	1.2	1.1	1.3	1.2	1.1	1.2	1.4
<i>Bacteroidetes; midas_g_171</i>	0.7	0.9	1.4	1.4	0.7	0.9	1.5	1.3	0.7	0.9	1.8	2
<i>Proteobacteria; Nitrosomonas</i>	1.2	1	0.7	0.7	1.3	1	0.7	0.6	1.1	1	0.7	0.7
<i>Proteobacteria; Hyphomicrobium</i>	0.6	0.6	0.6	0.6	0.6	0.8	1.1	0.7	0.4	1.1	0.8	0.9
<i>Actinobacteria; Nakamurella</i>	0.4	0.7	1.6	1.7	0.2	0.4	0.8	0.4	0.2	0.3	0.5	0.4
<i>Proteobacteria; Rhodobacter</i>	0.6	0.6	0.5	0.6	0.7	0.6	0.6	0.4	0.5	0.7	0.5	0.6
<i>Proteobacteria; Rhodoferrax</i>	0.6	0.5	0.9	0.6	0.6	0.6	0.4	0.5	0.6	0.6	0.6	0.5
<i>Acidobacteria; Paludibaculum</i>	0.6	0.6	0.6	0.6	0.5	0.6	0.6	0.5	0.5	0.5	0.5	0.5
	0.5-1	1.6-2	2.5-3.15	4-4.8	0.5-1	1.6-2	2.5-3.15	4-4.8	0.5-1	1.6-2	2.5-3.15	4-4.8

**Figure S4.7.** Relative abundances of the main 20 genera identified by 16S rRNA amplicon sequencing in the 3 reactors studied. All three reactors are from WWTP Utrecht and were sampled on the same dry weather flow day. Each of the values represents the average relative abundance measured in triplicate samples.

Supplementary information 8: Significant relative abundance differences on the 20 main taxa between small (0.5-1 mm) and large (4-4.8 mm) granules.

Table S4.8.1. Differences on genus level						
Enriched in	pvalue	Kingdom	Phylum	Class	Order	Family
Large granules	1.11E-09	k__Bacteria	p__Proteobacteria	c__Gammaproteobacteria	o__Betaproteobacteriales	f__Rhodocyclaceae
Small granules	1.80E-08	k__Bacteria	p__Proteobacteria	c__Gammaproteobacteria	o__Betaproteobacteriales	f__Rhodocyclaceae
Small granules	7.48E-15	k__Bacteria	p__Proteobacteria	c__Gammaproteobacteria	o__Betaproteobacteriales	f__Nitrosomonadaceae
Small granules	4.66E-05	k__Bacteria	p__Bacteroidetes	c__Bacteroidia	o__Chitinophagales	f__Saprospiraceae
Small granules	2.44E-10	k__Bacteria	p__Nitrospirae	c__Nitrospira	o__Nitrospirales	f__Nitrospiraceae
Large granules	1.54E-12	k__Bacteria	p__Bacteroidetes	c__Ignavibacteria	o__SJA-28	f__midas_f_31
Large granules	1.01E-11	k__Bacteria	p__Bacteroidetes	c__Ignavibacteria	o__Ignavibacteriales	f__PHOS-HE36
Large granules	6.93E-05	k__Bacteria	p__Proteobacteria	c__Gammaproteobacteria	o__Betaproteobacteriales	f__Rhodocyclaceae

Table S4.8.2. Differences on family level						
Enriched in	pvalue	Kingdom	Phylum	Class	Order	Family
Small granules	2.22E-13	k__Bacteria	p__Proteobacteria	c__Gammaproteobacteria	o__Betaproteobacteriales	f__Nitrosomonadaceae
Small granules	9.34E-06	k__Bacteria	p__Bacteroidetes	c__Bacteroidia	o__Chitinophagales	f__Saprospiraceae
Small granules	7.95E-09	k__Bacteria	p__Nitrospirae	c__Nitrospira	o__Nitrospirales	f__Nitrospiraceae
Large granules	1.1E-06	k__Bacteria	p__Chloroflexi	c__Anaerolineae	o__SBR1031	f__A4b
Large granules	5.94E-13	k__Bacteria	p__Bacteroidetes	c__Ignavibacteria	o__SJA-28	f__midas_f_31
Large granules	4.56E-16	k__Bacteria	p__Bacteroidetes	c__Ignavibacteria	o__Ignavibacteriales	f__PHOS-HE36



# 5

## **Anaerobic uptake of monomers and polymers by full-scale aerobic granules**

**Manuscript in preparation:** Toja Ortega, S., Pronk, M., & de Kreuk, M. K. Anaerobic uptake of monomers and polymers by full-scale aerobic granules.

## ABSTRACT

Municipal wastewater is characterized by its complex composition, containing diverse organic compounds that may be used as carbon source by microorganisms. In aerobic granular sludge (AGS), wastewater treatment relies on the anaerobic uptake of substrates by slow-growing organisms, such as polyphosphate accumulating organisms (PAO) and glycogen accumulating organisms (GAO). The stored substrates may be used by the PAO to perform enhanced biological phosphorus removal (EBPR) in the subsequent aerobic phase. In this study, we assessed the anaerobic uptake capacity of different monomeric and polymeric substrates by aerobic granules that were obtained from a Nereda® municipal wastewater treatment plant (WWTP). We also measured the uptake rates of particulate, colloidal and soluble casein, and compared them to the uptake rate of hydrolysed amino acids. Anaerobic batch tests show that AGS microorganisms can store a wide variety of substrates, including volatile fatty acids (VFA), amino acids, and carbohydrates. The highest uptake capacities were measured for acetate and propionate ( $43 \pm 15$  and  $46 \pm 8$  mg COD/g VSS), which were coupled with P release ( $0.34 \pm 0.08$  and  $0.41 \pm 0.03$  P-mol/ C-mol) and PHA production. The uptake capacity for carbohydrates, especially glucose, was high ( $26 \pm 2$  mg COD/g VSS). Carbohydrates were stored as PHA, but induced low P release (0.06-0.08 P-mol/C-mol). The contribution of carbohydrates to EBPR seems thus negligible, but they can contribute to granule formation given their anaerobic uptake and intracellular storage. Other monomers, including butyrate, lactate and amino acids, were taken up too and were accompanied by phosphorus release and PHA formation, indicating these substrates may contribute to both EBPR and granule formation. The hydrolysis rate of soluble proteins (1 mg COD/g VSS/h, at a substrate concentration of 200 mg COD/L) was too low to expect significant anaerobic carbon storage, and the uptake of particulate proteins was even slower. Aerobic consumption of proteins does not seem to be a threat for granule stability either, given the their limited hydrolysis.

## 5.1 | INTRODUCTION

In aerobic granular sludge (AGS), stable granule formation and nutrient removal are achieved by promoting the growth of polyphosphate-accumulating organisms (PAOs) and glycogen-accumulating organisms (GAOs) (de Kreuk and van Loosdrecht, 2004). Most full-scale AGS applications employ an SBR cycle that promotes the anaerobic storage of carbon sources by PAOs and GAOs (Bengtsson et al., 2018; Pronk et al., 2015b). An anaerobic feeding is followed by an aerobic starvation phase in which stored substrates are used for microbial growth. The canonical PAOs and GAOs have a very limited substrate uptake range; mostly only volatile fatty acids (VFAs). As a consequence, influent VFA concentration is considered important for AGS reactor design.

Most domestic wastewaters contain a low or variable VFA concentration, mainly depending on the sewer system (Henze and Comeau, 2008; Hvitved-Jacobsen et al., 1995; Narkis et al., 1980; Rudelle et al., 2011). This COD concentration would have to be supplemented with other substrates to explain the granule growth and nutrient removal observed in full-scale AGS. Roughly 20 mg COD/L of VFAs are needed to remove 1 mg P from wastewater (Abu-Ghararah and Randall, 1991). Furthermore, to obtain stable granulation, it is essential to have a large enough fraction of the influent COD stored anaerobically and low availability of external substrates during aeration (de Kreuk and van Loosdrecht, 2004; van Dijk et al., 2022). Van Dijk et al. (2022) predicted that decreasing the anaerobically available COD concentration from 40% to 20% of the substrate would significantly hinder granulation, extending the start-up period to more than one year. VFAs are rarely such a high proportion of the influent COD in domestic sewage, and therefore the anaerobic uptake of other C-sources is needed to explain the successful granulation obtained in full-scale plants. Models like ASM2d consider a fermentable COD fraction and hydrolysable COD fraction, which would release VFAs during the anaerobic feeding phase (Henze et al., 1999). Moreover, in activated sludge (AS) reactors, C-sources other than VFAs can be taken up anaerobically too. This is partly due to the presence of different genera of PAOs and GAOs, which have different substrate utilization capabilities (Nielsen et al., 2019; Qiu et al., 2019; Roy et al., 2021; Stokholm-Bjerregaard et al., 2017). Full-scale AGS reactors, including WWTP Utrecht sampled for this study, also contain different genera of PAOs and GAOs, including *Ca. Accumulibacter*, *Tetrasphaera*, *Dechloromonas*, *Ca. Competibacter*, and *Propionivibrio* (Ali et al., 2019; Kleikamp et al., 2022; Toja Ortega et al., 2021b). Hence, full-scale AGS is also expected to harbour the metabolic potential to utilize different C-sources for granule growth and nutrient removal.



Most of the biodegradable compounds in wastewater are in one of three large macromolecule groups: proteins, carbohydrates and lipids (Raunkjær et al., 1994; Sophonsiri and Morgenroth, 2004). Among these, proteins are frequently found in relatively high concentrations and are good candidates for being used for EBPR. Some PAOs, such as *Tetrasphaera* and clade IIF of *Ca. Accumulibacter*, are able to take up most amino acids (Kristiansen et al., 2013; Qiu et al., 2020). Furthermore, aerobic granules have been cultivated successfully in lab-scale reactors with amino acids as the only C source (Dockx et al., 2021). EBPR activity was unstable when amino acids were the only C-source, but when dosed in combination with VFA, stable COD and P removal were maintained. Other AGS reactors have also been stably operated with a fraction of amino acids or peptides, but their uptake kinetics and contribution to EBPR was not studied specifically (Layer et al., 2019; Wagner et al., 2015). Proteins have also been used as the sole substrate in an airlift biofilm reactor, where they were completely taken up and led to smooth biofilm formation (Mosquera-Corral et al., 2003). The reactor was operated under fully aerobic conditions and therefore the suitability of proteins as C-source for EBPR was not assessed. In full-scale AGS too, granules exhibit protease activity consistently across plants (Toja Ortega et al., 2021a, 2021b). Therefore, the aerobic granules have the potential to hydrolyse proteins and utilize their amino acids as C-source. However, the *in situ* protein conversion rates and their contribution to EBPR remain unknown to the authors' knowledge.

In this work, we studied the anaerobic substrate uptake by AGS of full-scale origin (WWTP Utrecht). A range of C-sources was tested in anaerobic batch tests to explore the substrate uptake spectrum of aerobic granules. The uptake of proteins was further studied through anaerobic uptake rate tests using casein as a model substrate. The uptake rate of monomers (i.e. amino acids), was compared with that of casein of different sizes (soluble, colloidal and particulate). The observed substrate uptake profile and protein uptake rates were examined next to the composition of municipal wastewater, and we hypothesize about the fate of different influent compounds in full-scale AGS treatment.

## 5.2 | MATERIALS & METHODS

### 5.2.1 | Granule and wastewater source

Aerobic granular sludge was sampled in the municipal wastewater treatment plant of Utrecht, the Netherlands. The plant consists of 6 Nereda® reactors with a volume of 12000 m<sup>3</sup> each, treating an average flow of 75167 m<sup>3</sup>/day. The reactors are operated with biological phosphorus removal and with a sludge loading rate of 0.05 kg COD (kg TS d)<sup>-1</sup>.

Mixed liquor samples were collected during aeration. The sludge was stored at 4°C for a maximum of 24 hours before the assays. Just before performing the assays, the sludge was aerated for about 45 min to replenish the intracellular poly-P and acclimatize the sludge. The mixed liquor, containing granules of different sizes and flocs, was sieved to retain the granules with a diameter between 1 and 2 mm. The resulting granules were washed with tap water to remove the worse settling material retained in the sieves. The granules were suspended in tap water, and after letting them settle for a short time the supernatant was removed. The process was repeated several times until the supernatant was clear. The clean granules were stored in effluent overnight until the assay.

Influent wastewater was sampled in two plants: Utrecht WWTP and Harnaspolder WWTP, both in the Netherlands. 24-hour flow-proportional samples were collected and stored in a cooling chamber until transport. Both wastewaters were fractionated on the sampling day into different size fractions. Sequential filtration was performed in an Amicon stirred cell (Merck Millipore, USA), applying positive pressure, through 10 µm, 1 µm, 0.1 µm and 1 kDa filters (10 µm, 0.1 µm: polycarbonate [PC], Cyclopore® Whatman, UK; 1 µm: PC, GVS, Italy; 1 kDa: Ultracell regenerated cellulose, Merck Millipore, USA). The resulting size fractions were: raw wastewater, <10 µm, <1 µm, <0.1 µm and <1 kDa.

### 5.2.2 | Anaerobic uptake capacity tests

Anaerobic uptake capacity tests were performed by dosing a range of soluble substrates to the granules and incubating them anaerobically for two hours. The two-hour period was chosen to reflect an extended anaerobic feeding phase. The assays were performed with sludge sampled on different days, and each day a blank sample (no substrate, only buffer) and a positive control (acetate) were included in the assay. The acetate standard and blank test at each experiment made the assays performed on different days comparable, despite fluctuations in the biomass activity.

The granules were buffered with 0.1 M sodium bicarbonate (pH 7.8) and used in the assays at a concentration of around 4 g TS/L. All substrates were dosed at a final concentration of 500 mg COD/L. The following substrates were used (all purchased from Merck, USA, unless specified). VFA and fermentation products: sodium acetate trihydrate, sodium propionate, sodium butyrate, sodium lactate, succinic acid, and ethanol; carbohydrates: D-glucose, D-maltose monohydrate, xylose, and starch; amino acids and proteins: L-glutamic acid, L-aspartic acid, glycine, L-leucine (Carl Roth, Germany), casein hydrolysate (Carl Roth, Germany), and casein from bovine milk; lipids: sodium oleate (Carl Roth, Germany), and high-oleic oil (de Nieuwe Band, NL).

To start the assays, the substrates were dosed to the granules in 40 mL vials. The working volume was 30 mL. The samples were flushed with N<sub>2</sub> gas for 2 minutes and incubated at room temperature (20°C) for 2 hours, fully mixed. Mixing was provided by a Fisherbrand Seastar orbital mixer at 120 rpm (Thermo Fisher Scientific, USA). A sample was taken from the vials at the beginning and the end of the assays. Both bulk liquid and granules were collected. The bulk liquid was filtered through 0.45 µm PES syringe filters and stored at 4°C until further processing. Granules were immediately deactivated after sampling, by mixing 1 mL of granules with 1 mL of 4% formaldehyde solution (Merck, USA), and stored in ice. At the end of the assay, the granules were washed, crushed with the aid of a pipette tip, and stored at -80°C until PHA extraction.

### 5.2.3 | Anaerobic uptake rate tests

Uptake rate tests followed a similar procedure as the uptake capacity tests. The difference was that periodic samples were taken throughout the experiment to measure C uptake and P release rates. The assays studied the anaerobic uptake of casein of different sizes: particulate (>10 µm), colloidal (0.1-1 µm) and soluble (<0.1 µm). The uptake of proteins was compared to that of hydrolysed amino acids (casein hydrolysate, Carl Roth, Germany). Blank and acetate control samples were included in the assays too.

Casein solutions of different size distributions were all prepared with the same substrate (casein from bovine milk, Merck, USA), but following different preparation procedures. The soluble and colloidal casein solutions were prepared in an alkaline solution (5 g/L sodium carbonate, pH 11.6), to enhance the solubility of casein. The soluble fraction was prepared by mixing for 2 hours, then filtering the solution through a 0.1 µm PC filter (Cyclopore® Whatman, UK) using an Amicon stirred cell, and harvesting the permeate. To prepare the colloidal fraction, the casein-sodium carbonate solution was stirred for 30 minutes. Then, the solution was filtered through a 1 µm PC filter (GVS, Italy) and the permeate was further processed by diafiltration, using a 0.1 µm filter. For diafiltration, tap water and casein solution were dosed simultaneously to the Amicon stirred cell,

maintaining a constant volume and a low concentration of casein during filtration. Three volumes of tap water were flushed per volume of casein solution, washing out the substrates smaller than 0.1  $\mu\text{m}$ , and the retentate was collected (0.1-1  $\mu\text{m}$ ). The particulate casein fraction was prepared directly in a bicarbonate buffer (pH 7.8) to minimize the solubilisation of casein. The solution was stirred for 1 hour and then washed by diafiltration, as described above. In this case a PC filter with a pore size of 10  $\mu\text{m}$  was used (Cyclopore® Whatman, UK), to wash out particles smaller than 10  $\mu\text{m}$ .

After preparation, the pH of all the solutions was adjusted to pH 7.8. The substrates were dosed to the granules to an initial substrate concentration of 200 mg COD/L. The granules were incubated anaerobically, fully mixed, and sampled regularly. The duration of the assays varied depending on the expected uptake rates: acetate and casein amino acid assays were monitored for 3 hours, while protein assays and blanks were monitored for 7.5 hours. Bulk liquid samples were collected throughout the assays and filtered through 0.45  $\mu\text{m}$  PES syringe filters, to measure  $\text{PO}_4\text{-P}$ ,  $\text{NH}_4\text{-N}$ , and COD concentrations. The COD uptake of the colloidal and particulate protein assays could not be measured directly since the dosed COD was not soluble, and casein particles could not be distinguished from particles derived from the sludge. Hence, the COD uptake was calculated from  $\text{PO}_4\text{-P}$  release, assuming the same P release/COD uptake ratio as with free amino acids.

#### 5.2.4 | Analytical methods

$\text{PO}_4\text{-P}$  and  $\text{NH}_4\text{-N}$  were quantified colorimetrically on a Discrete Analyser (Seal AQ400, Seal analytical, USA), using the methods USEPA 365.1 and USEPA 350.1, respectively. COD and TOC concentrations were determined using photochemical test kits (LCK514 and LCK387, Hach, Germany). Total suspended solids (TSS) and volatile suspended solids (VSS) were determined following Standard methods (APHA, 2005). PHA was extracted following the method described by Lanham et al., 2013 (Lanham et al., 2013). Shortly, the crushed granules preserved at  $-80^\circ\text{C}$  were freeze dried and weighed in a high-precision balance. 60-80 mg of biomass were used for PHA extraction. 1.5 mL of propanol:HCl (4:1) and 1.5 mL of dichloroethane were added and the samples were incubated at  $100^\circ\text{C}$  for 2 hours, with intermittent mixing. Ultra-pure water was added to aid phase separation. The organic phase was collected and filtered through sodium sulphate to eliminate residual water. The extracts were collected in glass vials and analysed via gas chromatography to quantify 3-hydroxybutyrate (3HB) and 3-hydroxyvalerate (3HV) concentrations. The chromatography equipment used was a 6890N system (Agilent, USA) with a FID detector, and a HP-INNOWax column (Agilent, USA).

Proteins and phenolic compounds were quantified using the modified Lowry method (Frølund et al., 1995). Carbohydrates were quantified using the anthrone-sulfuric acid method (DuBois et al., 1956). The resulting protein and carbohydrate concentrations were converted to COD based on Sophonsiri et al., 2004 (Sophonsiri and Morgenroth, 2004). Cellulose was extracted from wastewater samples following the procedure described by Pereira Espíndola et al., 2021 (Espíndola et al., 2021), omitting the bleaching step. The extracted pulp was weighed and used as an estimate of the cellulose content of Utrecht influent wastewater. VFA were quantified via high-performance liquid chromatography (HPLC) using an Aminex HPX-87H column (Bio-Rad, USA) in a Prominence-i system (Shimadzu, Japan) equipped with a SPD-20A UV index detector (Shimadzu, Japan). 5 mM sulphuric acid in ultrapure water was used as eluent. The resulting concentrations of different VFA were converted to COD and combined into a total VFA concentration.

## 5.3 | RESULTS

### 5.3.1 | Anaerobic uptake capacity tests

#### Variations on the acetate uptake capacity of the sludge

The acetate uptake capacity of the granules and the P release associated to it were measured in every sludge sampling to monitor the variations in sludge activity. The measured acetate uptake capacities and P/C ratios of the sludge sampled on different days are shown in Figure 5.1. P release to acetate uptake ratio ranged from 0.23 to 0.46 P-mol/C-mol, with an average of  $0.34 \pm 0.08$  P-mol/C-mol. The PHA content of the sludge before incubation with all different carbon sources was below 1% of the TS. Such low PHA concentration is expected because of the full-scale origin of the sludge; only part of the biomass is PAO/GAO, the influent is domestic wastewater, and the sludge is sampled after aeration. A similar PHA concentration was measured in domestic wastewater-fed AS with EBPR activity (Lanham et al., 2013). Furthermore, in WWTP Utrecht a significant fraction of granules larger than 1-2 mm exists (Toja Ortega et al., 2022). The larger granules likely have preferential access to influent VFA, limiting the VFA available for smaller granules located higher up in the granule bed.

The variation in the acetate uptake and P release was expected due to variations in wastewater composition, temperature and operation history. These result in differences in the poly-P pool and the intracellular polymers of the sludge, which influence substrate

uptake. Moreover, the reactors were sampled over a period of one year, during which the relative abundance of PAO may have varied, resulting in differences in activity. To allow comparing the substrate uptake in different sampling days, we normalized the observed COD uptake and P/C ratios of each of the tested substrates relative to the acetate uptake and associated P release ratio of their corresponding assay day, given that the highest carbon uptake and P release was always observed with acetate. The same was done for the PHA production. The P released by the blank (endogenous P release) also varied between samplings, and was subtracted from the test samples in each sampling (Supplementary information, Table S5.1).

### Monomeric substrates

The AGS was able to take up all the substrates tested, in a larger or smaller extent. The highest COD uptake capacity was observed with the VFAs acetate and propionate. The uptake capacity for acetate was  $43 \pm 15$  mg COD/g VSS, and it was stored mostly as PHB (0.79 C-mol PHB/C-mol substrate uptake) and partly as PHV (0.28 C-mol PHV/C-mol substrate) (Figure 5.1, Figure 5.2). Propionate is also a known EBPR substrate and both its uptake ( $46 \pm 8$  mg COD/g VSS) and associated P release ( $0.41 \pm 0.03$  P-mol/C-mol) were high. Propionate uptake was accompanied by PHV production (0.82 C-mol PHV/C-mol substrate), as described previously (Oehmen et al., 2005). With butyrate there was considerable uptake capacity ( $33 \pm 6$  mg COD/g VSS), although lower than with acetate and propionate, and the associated P/C ratio was somewhat lower too ( $0.23 \pm 0.03$  P-mol/C-mol) (Figure 5.1c). Both PHB and PHV were formed with butyrate (0.12 C-mol PHB and 0.15 C-mol PHV/C-mol substrate). Lactate, succinate and ethanol represent other common fermentation products, and were also consumed by the AGS. Lactate uptake capacity was  $21 \pm 2$  mg COD/g VSS, with a high P/C ratio ( $0.15 \pm 0.03$  P-mol/C-mol) and PHA formation (0.6 C-mol PHA/C-mol substrate) (Figure 5.2). A lower uptake capacity was observed for succinate ( $11 \pm 2$  mg COD/g VSS) and ethanol ( $13 \pm 2$  mg COD/g VSS), and also a low P/C ratio ( $0.04 \pm 0.03$  P-mol/C-mol for succinate;  $0.05 \pm 0.02$  P-mol/C-mol for ethanol). PHA formation with succinate and ethanol was 0.15 and 0.66 C-mol PHA/C-mol substrate, respectively.

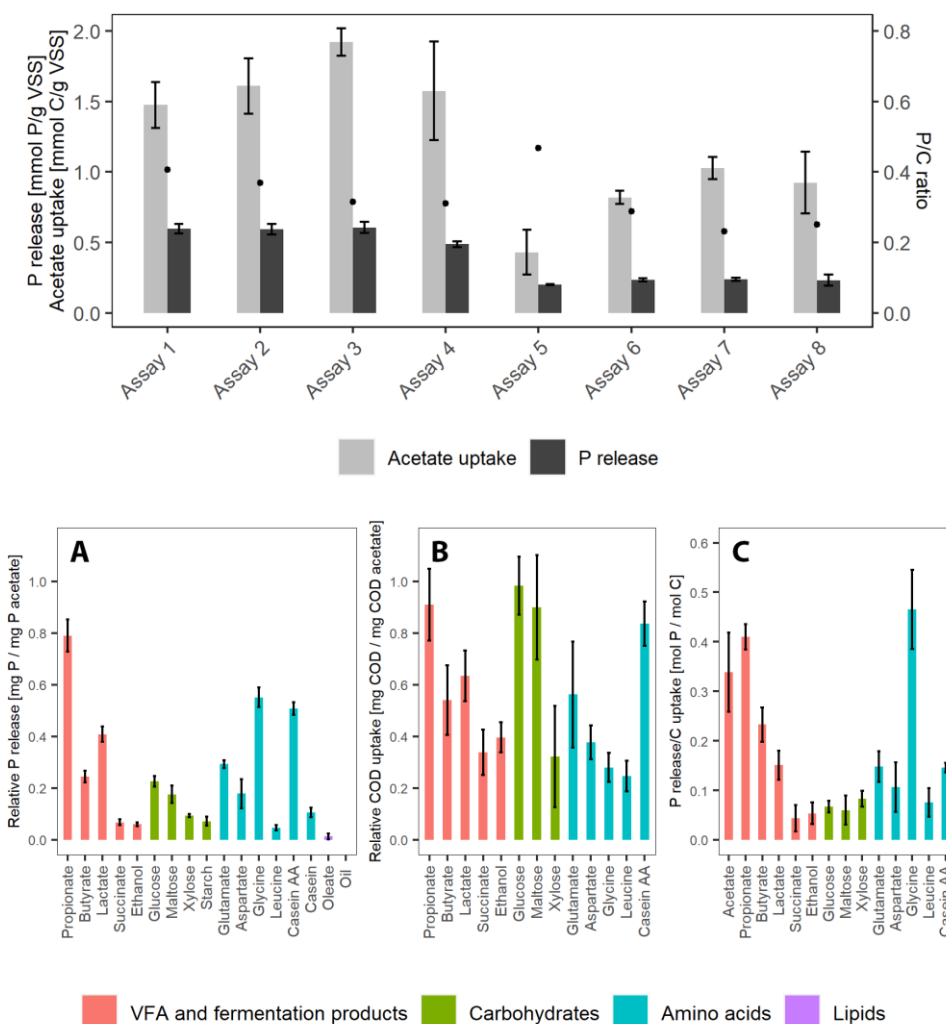


**Figure 5.1.** Results of anaerobic uptake test results. The top graph shows the biomass-specific acetate uptake and P release of the granules sampled on different days, as a measure of the variability of the sludge activity. The dots indicate the P/C ratio measured in each day. The bottom graphs present the a) biomass-specific P release, b) biomass-specific COD uptake and c) P release to C uptake ratio of the granules incubated with different substrates. The measured COD uptake and P release for each substrate are normalized against the COD uptake and P release of the acetate control from the same day. The P and COD released by the blank are subtracted from all the samples. Each bar represents the average of triplicate samples, with error bars indicating standard deviation of the triplicates. The absolute C uptake capacity and P release values per unit biomass can be found in the supplementary materials (Table S5.1, Fig S5.1.1).

Carbohydrate uptake resulted in a relatively low P/C ratio (0.06–0.08 P-mol/C-mol). However, the total uptake capacity was remarkably high in the case of glucose ( $26 \pm 2$  mg COD/g VSS) and maltose ( $24 \pm 2$  mg COD/g VSS). Granules in glucose and maltose-dosed samples produced mainly PHV (0.35 and 0.12 C-mol PHV/C-mol substrate, respectively), and also a low amount of PHB. The uptake capacity for xylose was lower ( $8 \pm 3$  mg COD/g VSS).

Amino acids were also considerably taken up by the sludge, especially when dosed as an amino acid combination, casein amino acids (Casein AA in short) ( $36 \pm 23$  mg COD/g VSS). The P/C ratio was high and also the PHA pool increased (0.27 C-mol PHA/C-mol substrate). When different amino acids were dosed individually, their uptake was more modest. The measured uptake capacities were  $15 \pm 3$ ,  $28 \pm 5$ ,  $12 \pm 2$ , and  $12 \pm 7$  mg COD/g VSS for leucine, glutamate, aspartate and glycine, respectively. The uptake of the amino acids resulted in PHA production (0.18, 0.06, 0.19 and 0.73 C-mol PHA/C-mol substrate, for leucine, glutamate, aspartate and glycine, respectively). An unusually high P release to C uptake ratio (0.47 mol-P/mol-C) was measured for glycine.

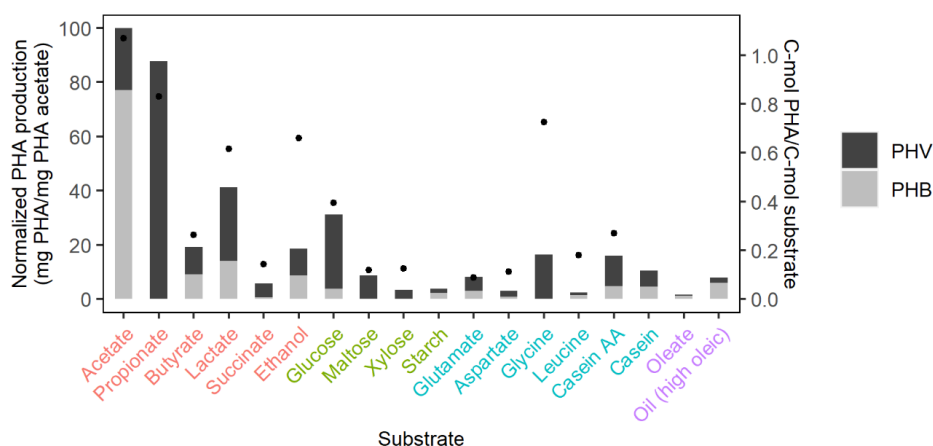


**Figure 5.2.** PHA production per gram VSS for each of the tested substrates. The bars represent the measured PHA production for each substrate, normalized against the PHA production in the acetate control from the same day. The absolute PHA production values per unit biomass can be found in the supplementary materials (Table S5.1, Fig S5.1.2). The average PHA composition of all the acetate samples is plotted in the first position. The dots indicate the C-mol PHA produced per C-mol substrate consumed for each of the substrates. Axis text colours indicate the biomolecule type (red = VFA and fermentation products; green = carbohydrates; blue = amino acids and proteins; purple = lipids).



### Polymeric substrates

A few polymeric substrates were also studied in these batch tests. The COD uptake was not measured in those substrates because of their polymeric/colloidal nature – non-soluble COD is not distinguishable from COD derived from the sludge. However, their P release and PHA accumulation were measured. Oil (composed of triglycerides with at least 80% oleate) did not induce P release, but some PHB production was observed (0.06 mmol PHB/g VSS). Oleic acid alone did not result in PHA accumulation, so it might be that the observed PHB accumulation in the oil sample resulted from the glycerol that is contained in triglycerides. Starch and casein, the polymeric version of glucose and casein amino acids, induced P release and also PHA formation (0.05 and 0.11 mmol PHA/g VSS, for starch and casein respectively). However, in a lower degree than in their monomeric counterparts. This is probably related to a slower uptake of the polymers, which require a hydrolysis step before being consumed. During the 2 hours of anaerobic assay, the maximum polymeric substrate uptake capacity of the sludge is probably not reached.

### 5.3.2 | Anaerobic uptake rate tests

After observing the lower P release and PHA accumulation with polymeric substrates, the uptake rate of casein was studied, and compared to the uptake rate of casein amino acids (Table 5.1, Figure S5.2). The differences in uptake rate were attributed to the hydrolysis step required to convert the protein into its free amino acids. Acetate uptake rate was also measured as a reference.

**Table 5.1.** Maximum COD uptake, P release and N release rates in anaerobic uptake rate tests. Mean  $\pm$  standard deviation values are shown.

Substrate	COD uptake rate [mg COD (g VSS h) <sup>-1</sup> ]	P release rate [mg PO <sub>4</sub> -P (g VSS h) <sup>-1</sup> ]	NH <sub>4</sub> -N release rate [mg NH <sub>4</sub> -N (g VSS h) <sup>-1</sup> ]
Acetate	23.3 $\pm$ 2.4	9.3 $\pm$ 0.8	-0.014 $\pm$ 0.03
Casein amino acids	9.7 $\pm$ 0.8	2.9 $\pm$ 0.3	0.070 $\pm$ 0.008
Soluble casein	1.0 $\pm$ 0.1*	0.93 $\pm$ 0.06	0.020 $\pm$ 0.004
Colloidal casein	1.0 $\pm$ 0.1*	0.99 $\pm$ 0.06	0.013 $\pm$ 0.002
Particulate casein	n.a.	0.72 $\pm$ 0.08	0.010 $\pm$ 0.001
Blank	n.a.	0.76 $\pm$ 0.07	0.007 $\pm$ 0.003

\* Calculated from P release/COD uptake ratio of casein amino acids

n.a.: Blank has no COD uptake due to no substrate addition. Particulate casein: COD uptake was not calculated since P and N release were at level of the blank.

Acetate uptake rate was highest at  $23.3 \pm 2.4$  mg COD (g VSS h)<sup>-1</sup>. Casein amino acids were taken up relatively quickly in the first hour of assay ( $9.7 \pm 0.8$  mg COD (g VSS h)<sup>-1</sup>), where after the uptake continued at a lower rate. Soluble and colloidal casein were both taken up one order of magnitude slower than amino acids ( $1.0 \pm 0.1$  mg COD (g VSS h)<sup>-1</sup>), and at a constant rate during the 7.5 hours of assay. In a reactor with 8 g VSS/L of granules, that would translate into 8 mg COD/L of protein taken up in 1 hour of anaerobic feeding, considering a 200 mg COD/L bulk liquid soluble protein concentration. Up to 17 mg COD/L could be hydrolysed a plug-flow is considered, where all the biomass is concentrated at the bottom of the reactor. It should be noted that the uptake of proteins was monitored through PO<sub>4</sub>-P and NH<sub>4</sub>-N release. Even if soluble proteins could also be measured *via* COD, the changes in COD between time points were too small for an accurate analysis.

The sludge incubated with particulate proteins behaved very similarly to the blank both in terms of P and N release. With the substrate concentration used in the assay (200 mg COD/L), uptake of particulate casein was undetectable.

### 5.3.3 | Influent composition

The influent wastewater of two plants was analysed, to assess the abundance and size distribution of different types of organics in wastewater. The COD of the sampled wastewaters was  $482 \pm 17$  and  $632 \pm 89$  mg COD/L in the plants of Utrecht and Harnaschpolder, respectively. Carbohydrates constituted the largest COD fraction in both wastewaters (Figure 5.3). They accounted for  $23 \pm 4\%$  (Utrecht) and  $22 \pm 15\%$  (Harnaschpolder) of the total COD.

Soluble (<0.1 µm) carbohydrates and proteins were very scarce. In both studied plants, less than 10 mg COD/L were soluble carbohydrates, and less than 15 mg COD/L were soluble proteins. Since a single influent sample was collected per plant, the variability in wastewater composition was not captured in this study. Raunkjaer et al. 1994 reported high variability in the soluble carbohydrate fraction, attributing it to their high biodegradability and differences in the retention in the sewer. Soluble carbohydrates and proteins, anyhow, have not been found in high concentrations in most domestic wastewater samples (Table 5.2). The soluble COD consisted mostly of VFA (27 and 61 mg COD/L in Utrecht and Harnaschpolder), and phenolic compounds. The VFA-COD from Utrecht was divided between acetate (12 mg COD/L) and butyrate (15 mg COD/L). The wastewater from Harnaschpolder contained mainly acetate (40 mg COD/L) and the rest of the VFA was propionate and butyrate (5 and 16 mg COD/L, respectively).

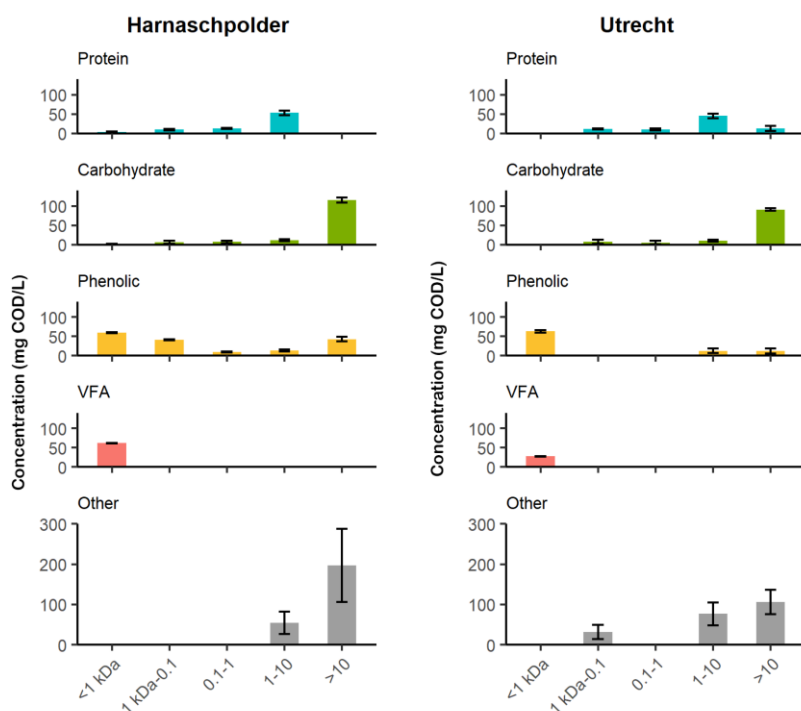


**Figure 5.3.** Influent composition of the plants Utrecht and Harnaspolder. The wastewater was fractionated and each of the size fractions was analysed in triplicate. The difference between the total COD in each fraction and the sum of the quantified compounds is shown as “Rest”.

The carbohydrates were most concentrated in the largest influent size fractions; over 80% of the carbohydrates were larger than 100  $\mu\text{m}$  in both plants. Alkaline extraction performed in the wastewater of Utrecht yielded around 50 mg/L of fibrous cellulosic material, contributing about half of the carbohydrates larger than 100  $\mu\text{m}$ . Proteins were 17% (Utrecht) and 13% (Harnaspolder) of the COD. Most of the proteins were in the supracolloidal range (1-10  $\mu\text{m}$ ), contributing 56 and 67% of the total proteins in Utrecht and Harnaspolder, respectively. Few proteins were quantified in the particulate fraction (>100  $\mu\text{m}$ ), and this fraction contained a large proportion of unidentified COD.

## 5.4 | DISCUSSION

### 5.4.1 | Wastewater composition and anaerobic C uptake range of aerobic granules

Our batch tests reveal a similar uptake spectrum in AGS as in AS, reflecting the capacity of AGS to anaerobically utilize a variety of substrates present in municipal wastewater. The VFAs acetate and propionate, known substrates of PAO and GAO, exhibited the highest uptake and P release. Butyrate was also taken up with P release but to a lower extent, as described previously (Begum and Batista, 2014; Wang et al., 2021).

Substrates that cannot be directly stored by the classical PAO *Ca. Accumulibacter*, like glucose, were taken up anaerobically by granules and induced P release too, indicating that carbohydrates were at least partly used by PAO. Glucose uptake by the PAO *Tetrasphaera* has been described (Kristiansen et al., 2013), but also carbohydrates may be fermented and the products taken up by *Ca. Accumulibacter*. Furthermore, the anaerobic uptake of carbohydrates is coupled to PHV storage. The prevalence of PHV is not surprising; the pyruvate generated by glycolysis can be fermented to acetate and propionate to balance the redox potential in the cell, and both VFA combined form PHV (Hollender et al., 2002; Wang et al., 2002). The uptake and storage of glucose as PHV might be done by GAO. Some *Ca. Competibacter* species are able to take up glucose and store it as PHV, and some species also partly ferment it to lactate (McIlroy et al., 2014). The GAO *Micropruina* can also ferment glucose to a range of products and store it as PHV (McIlroy et al., 2018). The glucose fermentation products released by *Tetrasphaera* or GAO (e.g. lactate, propionate, acetate or succinate) might be taken up by *Ca. Accumulibacter* too, resulting in PHV production and P release. Nonetheless, the low P/C ratio observed with carbohydrates indicates that these substrates will be more important for granule formation than for EBPR. Similarly, small amounts of succinate and ethanol were taken up and stored intracellularly but induced low P release, indicating that they may be suitable granule-forming substrates but not relevant for EBPR.

Amino acids were identified as suitable EBPR substrates, as in previous CAS studies (Nielsen et al., 2019; Qiu et al., 2019; Roy et al., 2021; Stokholm-Bjerregaard et al., 2017). The amino acid mix, casein amino acids, was consumed by the granules at relatively high rates (9.6 mg COD/g VSS/ h), inducing P release and PHA accumulation. Given that protein hydrolysis would produce a mixture of amino acids, proteins appear as suitable substrates for EBPR. The individual amino acids were consumed to a lower extent when

dosed in isolation. The low uptake capacity for leucine was in line with that reported in previous studies (Dockx et al., 2021; Nguyen et al., 2015). Glutamate and aspartate were taken up more, likely because these amino acids are readily converted to TCA cycle components, which makes them an attractive substrate for many microorganisms (Dockx et al., 2021; Nguyen et al., 2015; Qiu et al., 2019). The PHA production per C uptake of glutamate, however, was notably low (0.08 C-mol PHA/C-mol glutamate). A similar observation has been reported before; in *Ca. Accumulibacter* enrichments, glutamate is taken up fast and with P release, but little PHA is formed (Qiu et al., 2020). It was hypothesized that glutamate can be stored intracellularly as poly-glutamate (PGA) instead. The high P/C ratio observed with glycine in our study also resembles previous observations. A recent study reported that glycine was not used by most PAO, and these PAO hydrolysed poly-P to pump glycine out of the cell (Tian et al., 2022). This resulted in a high P release that was not accompanied by COD uptake. Despite the high P release in our study, some glycine was taken up too ( $12 \pm 7$  mg COD/g VS) accompanied by PHV accumulation. *Tetrasphaera* can take up glycine, which would explain the observed uptake, but most *Tetrasphaera* do not produce PHV. The observed PHV formation might be explained by the release of fermentation products (acetate, succinate, alanine, glyoxylate) released upon glycine uptake by *Tetrasphaera*, and their subsequent consumption by other organisms.

Our assays explore the array of substrates that can be taken up anaerobically by AGS granules, cultivated with municipal wastewater. One should be cautious when translating these results to situations where a particular substrate is very dominant in the influent. For instance, in AS fed with glucose-rich industrial wastewater, EBPR can deteriorate in the long term, and lab-grown AGS fed with glucose has been reported to not perform EBPR at all (Dockx et al., 2021; Zengin et al., 2010). A similar effect has been observed when using lactate as the sole carbon source (Rubio-Rincón et al., 2019). Lactate can be transported by cells and converted to propionate leading to PHV formation. Rubio-Rincón et al (2019) showed that during long-term feeding of lactate as sole carbon source, PAO seem to switch to a GAO-like metabolism given that the uptake and storage of this substrate does not rely on poly-P hydrolysis. However, when combined with other substrates (like VFA) lactate and glucose may be stored anaerobically while maintaining good EBPR (Hollender et al., 2002; Rubio-Rincón et al., 2019; Zengin et al., 2010). Some other studies have maintained good EBPR in the long term with influents lacking VFA, by applying suitable operating conditions (Elahinik et al., 2022; Marques et al., 2017).

### 5.4.2 | Anaerobic conversion of proteins and contribution to EBPR

Monomers like the ones studied in our presented batch tests, were scarce in the analysed wastewaters of Utrecht and Harnaschpolder. Nonetheless, monomers could originate during treatment from the hydrolysis of polymeric substrates, such as proteins or carbohydrates. Hence, the concentration of those compounds was determined in both analysed wastewaters using colorimetric methods. The limitations of these methods should not be ignored. For instance, a number of factors interfere with the Lowry method used for protein quantification, even when it is modified to account for phenolic substances. First, protein quantification results depend on the protein used to make the calibration curve (Felz et al., 2019). Moreover, at low protein concentrations, the modified Lowry method tends to underestimate proteins and overestimate phenolic compounds (Avella et al., 2010). Furthermore, the Lowry assay does not digest the sample and therefore the proteins aggregated in particles are not quantified reliably. Hence, part of the COD now unidentified or assigned to phenolic substances could be proteins too. Even though some deviation on the actual protein concentrations should be expected, these analyses provided a general description of domestic wastewater composition.

The analysed wastewaters contained low concentrations of soluble proteins and carbohydrates, and similarly low concentrations were reported in previous wastewater characterization studies (Table 5.2). Therefore, the polymeric COD that could potentially contribute to anaerobic COD storage was mostly in the form of colloids or particulates. Most carbohydrates in our study were large particulates (>100  $\mu\text{m}$ ), from which around half was cellulose fibres. These end up almost entirely in the excess sludge with minimal degradation (Espíndola et al., 2021; Guo et al., 2020). Proteins were most concentrated in the size fraction between 10 and 100  $\mu\text{m}$ . Thus, the protein-derived COD that can be stored anaerobically by the granules will be largely determined by the rate at which particulate proteins can be hydrolysed by AGS.

**Table 5.2.** Domestic wastewater composition, determined in various locations. sProt = soluble proteins; pProt = particulate proteins; sCarb = soluble carbohydrates; pCarb = particulate carbohydrates.

Location	tCOD	VFA	sProt	pProt	sCarb	pCarb	Ref
Utrecht WWTP (NL)	482	27	11	69	7	105	This study
Harnaschpolder WWTP (NL)	631	61	14	65	6	134	This study
Garmerwolde WWTP (NL)	619	9-58	17	68	10	143	(Toja Ortega et al., 2021a)
Epe WWTP (NL)	864	16-124	20	70	18	256	(Toja Ortega et al., 2021b)
Aalborg West (DK)	330-800		38-107	55-98	7-88	46-103	(Raunkjær et al., 1994)
Hjallerup (DK)	230-560		38-74	36-95	5-23	13-83	(Raunkjær et al., 1994)
Aalborg East (DK)	480-550		59-63	85-108	7-32	47-94	(Raunkjær et al., 1994)
Aabybro (DK)	280-640		14-66	26-114	3-20	26-90	(Raunkjær et al., 1994)
Urbana-Champaign (USA)	309		15	22	5	14	(Sophonsiri and Morgenroth, 2004)
Haifa (IL)	604-1180	89-104	10-42	23-161	5-12	5-82	(Narkis et al., 1980)
Neveh Shaanan (IL)	352-443	22-48	45-61	32-50	7-10	6-57	(Narkis et al., 1980)

The anaerobic conversion of proteins observed in this study was low. Soluble and colloidal proteins were taken up faster than their particulate counterparts, and yet roughly 10 times slower than their respective hydrolysed amino acids. A typical full-scale SBR cycle consists of 1 hour anaerobic feeding and approximately 4 hours of aeration (van Dijk et al., 2022). With the measured rates, in a reactor with a granule concentration of 8 g VSS/L, 200 mg COD/L of soluble proteins would only supply an extra 8 to 17 mg COD/L during 1 hour of anaerobic feeding. In domestic wastewater, the soluble protein concentration is considerably lower than 200 mg COD/L (Table 5.2), and therefore hydrolysis rates would be lower based on first order kinetics. Most proteins found in the analysed wastewaters were between 10 and 100  $\mu\text{m}$ , although they were still less

concentrated than 200 mg COD/L. These particulate proteins might contribute some COD during the anaerobic phase, but their hydrolysis is even slower than that of soluble proteins. The hydrolysis of particulates was undetectable in our assays, which were performed at fully mixed conditions. Depending on the protein-granule interaction during plug-flow feeding applied in full-scale installations, anaerobic hydrolysis of particulate proteins could differentiate from our findings.

Even though amino acids are theoretically suitable EBPR substrates, their contribution to EBPR in AGS systems treating domestic sewage will be modest, simply because their concentration in the influent is very low, and they are also slowly released during hydrolysis of proteins. Similarly, negligible concentrations of soluble carbohydrates were measured in domestic sewage. As a result, carbohydrate uptake will rely on the generally low hydrolysis rate of larger particulates as well. A small impact of particulate COD on EBPR in municipal AS plants has been observed, although some impact of particulate COD on biomass growth and denitrification was shown as well (Drewnowski and Makinia, 2014; Jabari et al., 2016). In AGS, the contribution of particulates to EBPR is probably lower than in AS due a limited substrate-sludge contact.

### 5.4.3 | Considerations on granule stability

The slow hydrolysis of proteins in domestic wastewater, and the resulting limited anaerobic conversion, imply that proteins are likely present in the aerobic stage too. Hence, proteins will be partly hydrolysed aerobically, which could be problematic for granule morphology (de Kreuk et al., 2010; Pronk et al., 2015a). The rbCOD made available aerobically due to protein hydrolysis can be estimated from the anaerobic protein uptake rates measured in this study, assuming protein hydrolysis rates to be similar between anaerobic and aerobic conditions (Goel et al., 1998b). Considering, again, 8 g VSS/L of granules and a soluble protein concentration of 200 mg COD/L in the bulk liquid, around 32 mg COD/L of proteins could be hydrolysed during a 4 hour long aerobic period. A more realistic soluble protein concentration of 20 mg COD/L in the bulk liquid during the aeration phase, would only result in 4 mg COD/L of rbCOD released aerobically during 4 hours of aeration, assuming first order kinetics. Some additional rbCOD will likely be released by particulate proteins, but with an even lower rate. Moreover, there is increasing evidence that the stability of aerobic granules is determined by the proportion of COD that is stored anaerobically, rather than by the absolute aerobic COD consumption (Campo et al., 2020; Haaksman et al., 2020; Sguanci et al., 2019; van Dijk et al., 2022). Aerobic utilization of proteins is unlikely to pose a threat to the stability of AGS treating municipal wastewater, as long as enough COD is stored anaerobically. When a large fraction of rbCOD is stored by PAO and GAO, these



organisms will still outcompete ordinary heterotrophs, even if some rbCOD is available during the subsequent aerobic phase (Haaksman et al., 2020). The results of this study evidence that aerobic granules are suited to take up a large variety of substrates, which would act together with VFA as granule-forming substrates. In this scenario, aerobic uptake of the COD slowly produced from proteins would only lead to marginal growth of filamentous organisms on the granule surfaces, and to the proliferation of a flocculent biomass fraction, easily controlled through selective sludge discharge (Haaksman et al., 2020; van Dijk et al., 2022).

In some scenarios, however, aerobic conversion of polymers could be of concern. For instance, in very low-strength wastewaters, or wastewaters containing unusually low VFA concentrations. Then, it will be important to stimulate anaerobic hydrolysis and uptake of hydrolysates. To maximise anaerobic hydrolysis, the length of the anaerobic feeding phase should be increased, and possibly the feeding strategy adjusted, to enhance the contact between substrate and granules during anaerobic conditions. Sguanci (2019) and Campo (2020) achieved stable operation and smooth granules with very low COD concentrations, by increasing the anaerobic feeding time and adding an anaerobic mixed phase after plug-flow feeding, to maximize anaerobic COD storage (Campo et al., 2020; Sguanci et al., 2019). In case of low-strength wastewater, polymeric substrates could not only be harmless, but also beneficial for EBPR if the appropriate operation conditions are applied.

## 5.5 | CONCLUSION

Our batch tests highlight the versatility of AGS in terms of substrate uptake. A wide range of monomeric substrates, including VFA, organic acids and amino acids, can be stored under anaerobic conditions and potentially contribute to EBPR and granule formation. Some substrates, like carbohydrates, can still contribute to AGS stability without supporting EBPR, by selecting for slow-growing organisms. Polymeric substrates as proteins may be consumed by AGS microorganisms and contribute to EBPR too. Yet, low hydrolysis rates were measured at the protein concentrations similar to those found in most domestic wastewaters. The anaerobic uptake of proteins will therefore be modest, but the low consumption rates also imply that their aerobic consumption will not challenge granule stability in most scenarios.

## SUPPLEMENTARY INFORMATION

### Supplementary information 1: Total COD uptake, P release and PHB production in all the assays performed.

The anaerobic substrate uptake assays described in this article were performed in different days, using granules from different samplings. The activity of the granules varied between days, and therefore the uptake of all the substrates tested was normalized against the uptake of acetate to allow comparison across days and simplify visualizations. In this section, the absolute values of COD uptake, P release, and PHB production are presented.

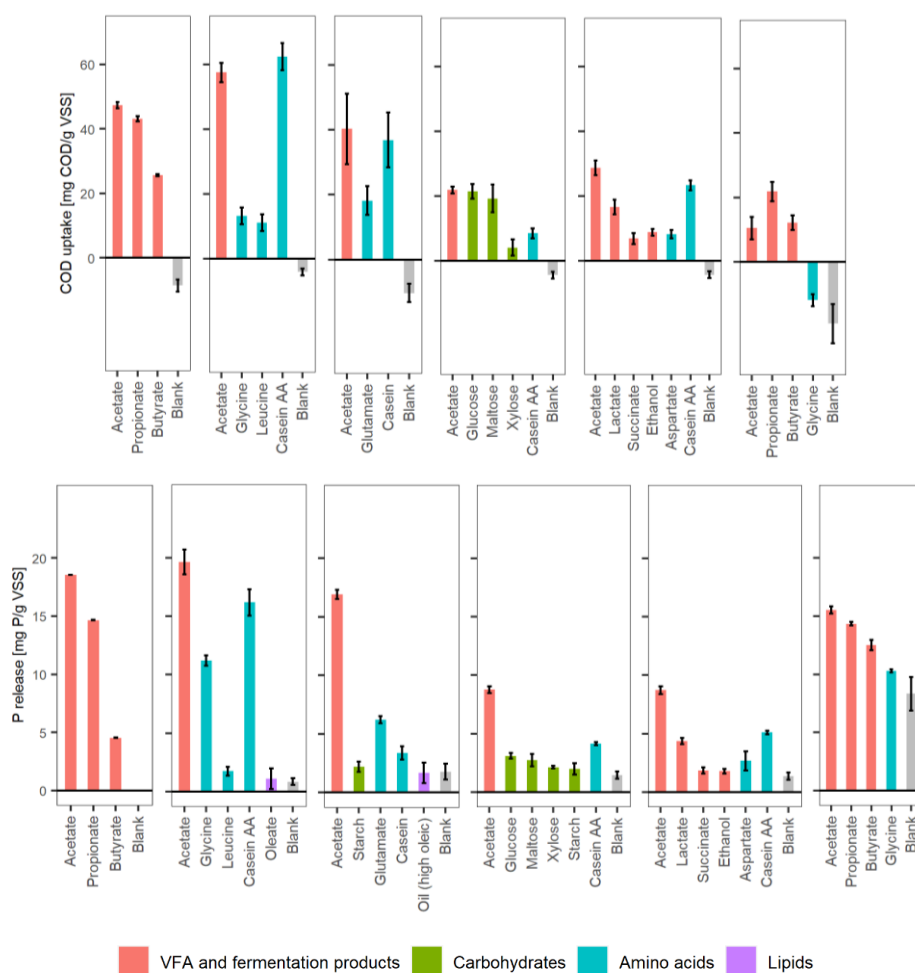


**Figure S5.1.1.** COD uptake (top) and P release (bottom) of aerobic granules incubated with different C sources for 2 hours. The plot is separated in 6 sections, delimiting 6 different assays,

performed with sludge sampled in different days. Acetate samples were analysed in every assay, and the corresponding C uptake and P release values are shown in the first position of each section. The colors in the axis text indicate the type of C source (red = VFA and fermentation products; green = carbohydrates; blue = amino acids and proteins; orange = lipids).

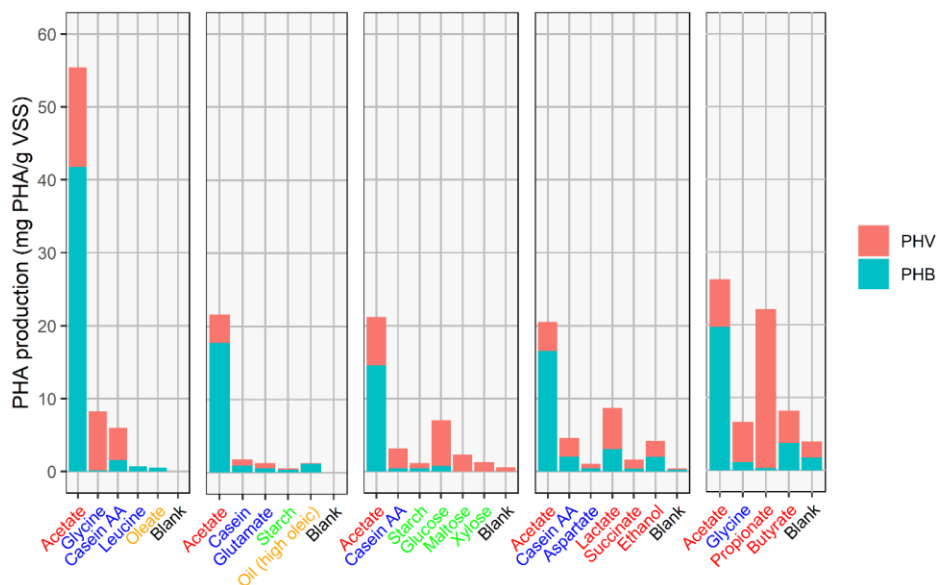


**Fig S5.1.2.** PHB production upon incubation with different C sources for 2 hours. The plot is separated in 5 sections, delimiting 5 different assays, performed with sludge sampled in different days. Acetate samples were analysed in every assay, and the corresponding PHB production values are shown in the first position of each section. The colors in the axis text indicate the type of C source (red = VFA and fermentation products; green = carbohydrates; blue = amino acids and proteins; orange = lipids).

**Table S5.1.** COD uptake capacity of AGS and the associated P release and PHA production in each of the performed assays.

Assay date	Substrate	COD uptake mg COD/g VSS	P release mg P/g VSS	PHB production mg PHB/g VSS	PHV production mg PHV/g VSS
13-07-20	Acetate	47.35	18.54		
	Propionate	43.07	14.66		
	Butyrate	25.62	4.54		
	Blank	-8.64	0		
20-10-20	Acetate	57.58	19.64	41.76	13.66
	Glycine	13.21	11.22	0.16	8.08
	Leucine	11.16	1.74	0.70	-1.86
	Casein AA	62.48	16.18	1.55	4.44
	Oleate	n/a	1.11	0.53	-2.16
	Blank	-4.08	0.85	-0.17	-2.43
01-12-20	Acetate	40.29	16.93	17.73	3.90
	Glutamate	18.17	6.23	0.59	0.70
	Starch	n/a	2.20	0.42	0.14
	Casein	36.84	3.40	0.94	0.87
	Oil (high oleic)	n/a	1.67	1.21	0.07
	Blank	-10.29	1.79	-0.09	-0.40
21-09-21	Acetate	21.93	8.76	14.54	6.64
	Glucose	21.51	3.10	0.77	6.25
	Maltose	19.30	2.73	-0.03	2.36
	Starch	n/a	1.97	0.44	0.70
	Xylose	4.10	2.12	-0.05	1.28
	Casein AA	8.51	4.14	0.45	2.76
	Blank	-4.39	1.44	-0.01	0.58
28-09-21	Acetate	28.74	8.72	16.54	3.98
	Lactate	16.69	4.36	3.07	5.66
	Succinate	6.94	1.85	0.39	1.22
	Ethanol	8.84	1.79	1.99	2.19
	Aspartate	8.21	2.67	0.41	0.64
	Casein AA	23.35	5.09	2.05	2.56
	Blank	-4.25	1.35	0.25	0.21
15-12-21	Acetate	10.54	15.52	19.74	6.54
	Propionate	21.86	14.34	0.33	21.82
	Butyrate	12.20	12.52	3.77	4.47
	Glycine	-11.87	10.28	1.10	5.55
	Blank	-19.15	8.32	1.74	2.24

## Supplementary information 2: $\text{PO}_4^{3-}$ and $\text{NH}_4^+$ profiles measured during anaerobic substrate uptake tests

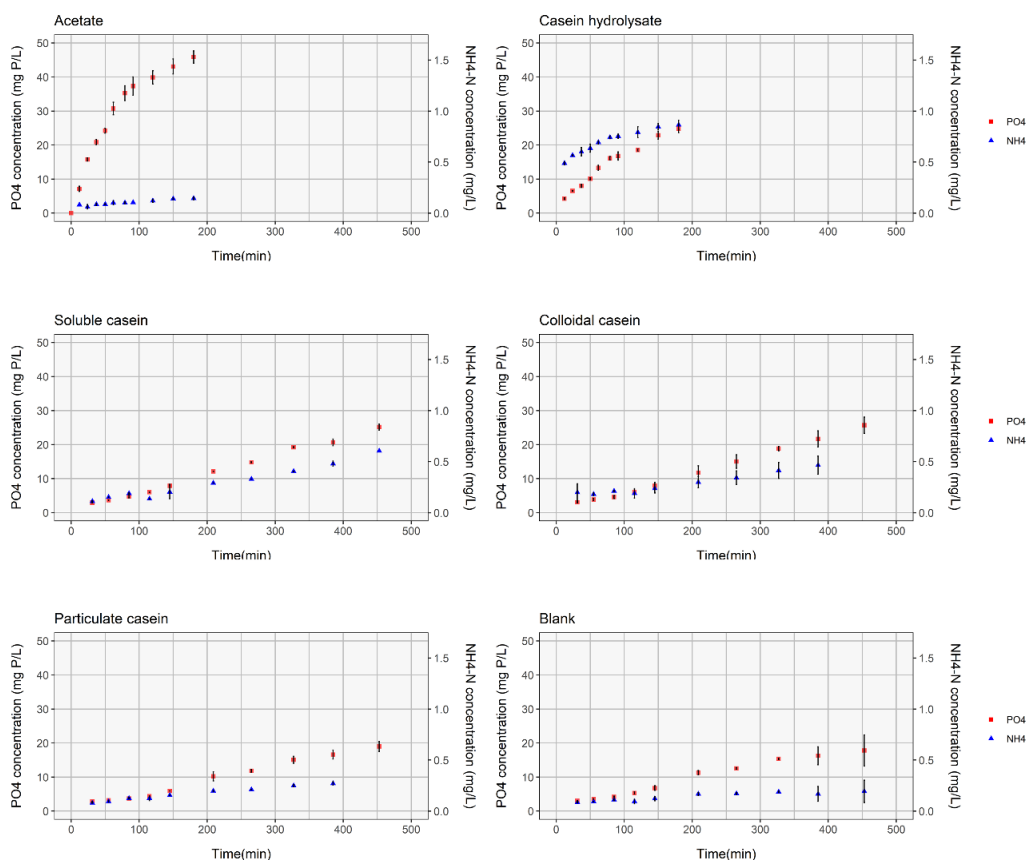


**Figure S5.2.**  $\text{PO}_4$ -P and  $\text{NH}_4$ -N release in anaerobic batch tests. The assays were performed with acetate, casein hydrolysate, soluble casein, colloidal casein and particulate casein. A blank was also analysed to account for endogenous P and N release. Each of the data points in the graphs is the average of triplicate samples; error bars indicate standard deviation between triplicates.





# 6

## Outlook



## 6.1 | FOREWORD

The goal of this thesis was to assess the ability of aerobic granules to convert polymeric substrates, and evaluate the significance of these substrates for granule stability and nutrient removal during the treatment of domestic wastewater. In this section, the insights gained throughout the previous chapters are combined to draw a general picture of polymeric substrate degradation in AGS. The remaining research gaps are discussed and future research directions are proposed.

## 6.2 | ANAEROBIC CONVERSION OF POLYMERIC SUBSTRATES

A main objective of this thesis was to evaluate if polymeric substrates can be converted and stored anaerobically by AGS microorganisms, to be used for granule growth and nutrient removal. Considering hydrolysis to be the rate limiting step in the biodegradation of polymeric substrates, the emphasis was put on the location and the rate of hydrolysis. The hydrolytic activity assays described in chapters 2 and 3 localized the activity of four large enzyme groups (protease, lipase, and  $\alpha$ - and  $\beta$ - glucosidases) in the AGS bed. They revealed that hydrolysis mainly occurred associated to the biomass, rather than in the bulk liquid, similar to previous studies on activated sludge (Confer and Logan, 1998a; Frølund et al., 1995; Karahan et al., 2006). As a consequence, conversion is influenced by the transport of polymers from the bulk to the biofilm, where they can be hydrolysed. Polymeric substrates diffuse slowly due to their high molecular weights, and depending on their size they might even be excluded from the granule matrix (van den Berg et al., 2022b). Hence, the available surface area of the biomass is determinant for the hydrolysis rates that can be achieved in AGS reactors. The increase in biomass-specific hydrolytic activity with decreasing granule size, as reported in chapter 4, reflects this surface area dependency of hydrolysis. Also the flocs, with their open structure, harbour high hydrolysis capacities compared to the other biomass fractions.

The anaerobic conversion of polymeric substrates by the AGS biomass fractions should be assessed considering the specific hydrodynamic conditions during feeding, i.e. mixing of the reactor content is minimized and the sludge bed is settled and stratified (van Dijk et al., 2020). Most likely, only the particulates that are hydrolysed by granules can be used by the micro-organisms within these granules during the anaerobic phase. For this reason, the measured hydrolytic activity of the granules is of significance for the AGS system, even if their biomass-specific activity is lower than that of flocculent sludge. In the SBR cycle commonly applied in AGS reactors, the anaerobic feeding phase is short (typically 1 hour), and thus high hydrolysis rates are needed to provide a significant

anaerobic COD storage by PAO or GAO, when polymeric substrates are supplied. The results of this thesis provide an insight on the magnitude of the hydrolysis rates that are attainable at different substrate concentrations (Table 6.1). Hydrolysis rates were measured under anaerobic conditions, but similar rates are expected aerobically, based on previous studies that found no effect of redox conditions in hydrolysis rates (Boczar et al., 1992; Goel et al., 1998b).

**Table 6.1.** Hydrolysis rates measured in this thesis.

Substrate type	Substrate concentration in the assay (mg COD/L)	WWTP	Measurement method	Hydrolysis rate (mg COD/g VS/h)	Total substrate hydrolysable during 1 h of feeding (mg COD/L)
Lipase	15225	Garmerwolde	Colorimetric	30.8	653
	15225	Epe	Colorimetric	16.5	403
$\beta$ -glucosidase	339	Garmerwolde	Colorimetric	6.2	164
$\alpha$ -glucosidase	339	Garmerwolde	Colorimetric	2.9	76
	339	Utrecht	Colorimetric	1.8	31
Amylase	79.1	Utrecht	Fluorescent	2.8	48
	2740	Garmerwolde	Colorimetric	31.0	573
	2740	Epe	Colorimetric	36.7	896
Protease	2740	Utrecht	Colorimetric	38.8	653
	219	Utrecht	Colorimetric	4.2	71
	200	Utrecht	P release	0.7	17
	22	Utrecht	Fluorescent	0.4	7
	4.1	Utrecht	Fluorescent	0.2	3

The influent concentration of polymeric substrates, and especially soluble polymers, in domestic wastewater is low, as measured in chapter 5 and reported in previous studies. An average of 37 mg COD/L of soluble proteins (median 38 mg COD/L) and 25 mg COD/L of soluble carbohydrates (median 10 mg COD/L) have been reported (Table 5.2). The attainable hydrolysis rate with those substrate concentrations is too low to significantly contribute to anaerobic COD storage, but particulate and colloidal substrates could supplement some COD when hydrolysed anaerobically. The micro-organisms within the

granules are able to take up a wide range of C-sources which would derive from the hydrolysis of polymeric substrates (saccharides, amino acids, organic acids) (Chapter 5). Moreover, PAO and GAO were found near hydrolysis sites, indicating that they might have access to hydrolysis products (Chapter 4). Overall, the results presented in the different chapters indicate that granules have the enzymatic and metabolic potential to convert, and store, polymeric substrates anaerobically. The actual utilization will be mainly limited by hydrolysis rates, which heavily depend on substrate concentration and substrate-sludge contact.

The conclusions of the assays with model substrates may be complemented with studies using more complex substrate mixtures, such as real wastewater or complex synthetic wastewaters (e.g. the synthetic wastewater recipe developed by Gonzalez-Ortega et al (Gonzalez et al., 2021)). The substrate uptake in these complex influents could be studied using indirect techniques such as respirometry or P release tests, similar to those applied in chapter 5. Furthermore, a detailed description of substrate concentration-dependent hydrolysis kinetics would enable a better prediction of hydrolysis rates as a function of wastewater strength. In addition, the fate of particulates should be studied further, given that they are more abundant than soluble polymers in domestic wastewater. An important aspect to elucidate is how significantly particles interact with granules during the anaerobic feeding phase, which has yet only been addressed by a very limited number of studies (M. Layer et al., 2020; Ranzinger et al., 2020). These studies suggest that particulate attachment is minimal during plug-flow, which would greatly limit the anaerobic storage of particulate COD. However, more research is needed to comprehend the behaviour of different particulates in the AGS granule bed. Not only during the plug flow; the attachment of substrates to granules during turbulent flow conditions is also not well understood. Substrates attached during aeration could also be hydrolysed and stored during the subsequent anaerobic phase, if they are not fully converted within one SBR cycle.

### 6.3 | AEROBIC CONVERSION OF POLYMERIC SUBSTRATES

Three full-scale AGS plants treating domestic wastewater were described in this thesis. Moreover, the full-scale WWTP of Epe was studied during two periods, with different wastewater compositions that mainly differed in the fraction of particulate substrates. In all these plants, AGS operation was stable, the granule beds consisted of large average granule diameters, and granules only exhibited a few irregularities on their surface. During the full-scale study of WWTP Epe, higher denitrification rates were observed during increased particulate COD loading, suggesting that particulate COD could support denitrification. A high proportion of particulate COD did not correlate with irregular

granules or unstable performance of the full-scale AGS process. Unstable granule growth in the presence of particulates is attributed to the low concentrations of rbCOD available during aeration (de Kreuk et al., 2010). Even though our assays targeted anaerobic conversions of polymeric substrates, the determined low uptake rates indicate that polymeric substrates will be available during the aerobic period as well. Therefore, granule stability issues could have been expected, and yet no such thing was observed. There are a number of hypotheses that could explain why the granules remained stable even at elevated sbCOD availability during the aeration phase:

- I. The aerobic substrate loading is low in real wastewater. Hydrolysis usually follows first order or Michaelis-Menten kinetics, and polymers are found in low concentrations in domestic wastewater. The polymeric substrate concentration will even be further reduced due to the mixing of the reactor content at the beginning of the aeration phase. Considering a typical exchange ratio of 30%, the concentration in the reactor is diluted three times at the start of the aeration. Hence, low aerobic hydrolysis rates can be expected. In Chapter 5, casein was used as a reference polymer; possibly, many of the polymeric substrates in domestic wastewater would reveal a different biodegradability. A detailed characterization of the size, composition and biodegradability of wastewater particles could help to evaluate the extent of their aerobic degradation and thus their contribution to possible irregular granule growth.
- II. Moderate aerobic COD consumption is tolerable. As long as enough COD is stored anaerobically, slow-growing organisms are favoured over OHOs. Haaksman et. al cultivated lab-scale AGS, with varying concentrations of soluble COD available during the aerobic phase. They concluded that the granule structure remains stable with an aerobic supply of up to 20% of the COD, which would mean that the aerobic hydrolysis of a moderate pCOD fraction is compatible with stable granulation. In their study, acetate was supplied continuously to mimic a slow release of COD. The COD distribution may be somewhat different when COD is released from particulate hydrolysis. Moreover, the hydrolysis of influent particulates renders other products than VFA, especially in aerobic conditions where fermentation is less likely. These compounds might be taken up by microorganisms with a different maximum growth rate and hence have a different impact on granule structure. Overall, more research is needed to evaluate what percentage of aerobically available COD is permissible in order to maintain the structural stability of aerobic granules.
- III. Particulates are captured by protozoa, reducing the amount of particulates that are available in granule surfaces. Early research on AGS found protozoa to significantly take up particulates in the granule surfaces (N. Schwarzenbeck et al., 2004; Norbert

Schwarzenbeck et al., 2004). Various AGS studies have since reported a strong protozoa presence in AGS fed with high particulate concentrations (Barrios-Hernández et al., 2020; de Kreuk et al., 2010; Li et al., 2013; Weber et al., 2007). Schwarzenbeck et al. (2004) followed fluorescent tracer particles in AGS, and found that they were almost completely taken up by the protozoa attached to the granule surface; particles did not reach the biofilm surface. They employed high influent COD concentrations (1.7 g/L on average), and the granules were completely covered in protozoa. Protozoa are generally less abundant in full-scale granules, but they are present in most granules and likely graze on particles, reducing the availability of particles on the granule surface during aeration. Chapter 2 also described an observed increase in protozoa concentration upon an increase in influent particulate concentration. Moreover, protozoa were fluorescently labelled after incubating granules with BODIPY-casein (Figure 6.1). The conversions of particulates by protozoa have not been studied in detail and their contribution to particulate removal has not been quantified. Given their ubiquity and their possible relation with granule stability, protozoa activity deserves further attention.

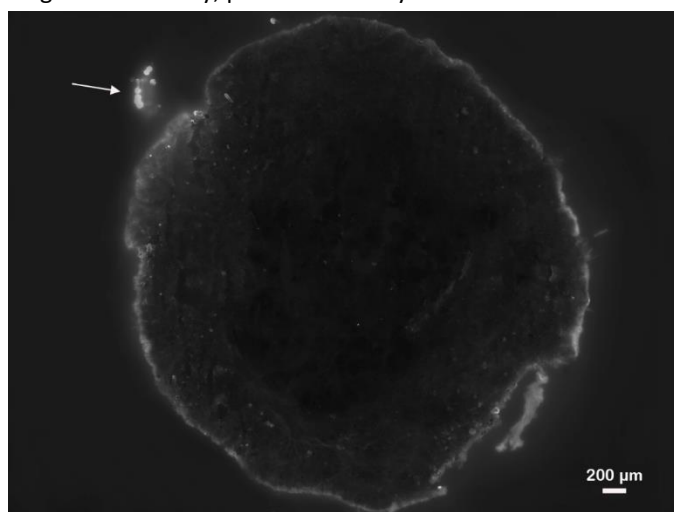


**Figure 6.1.** Cross-section of a Bodipy-casein stained granule, imaged by epifluorescence microscopy. Fluorescent areas indicate protease activity. The arrow points to a fluorescently labelled stalk of protozoa attached to the granule surface.

- IV. Flocs could also contribute to capturing particulate substrates. It has been speculated that flocs are important for AGS stability after consistently finding a floc fraction accompanying granules in reactors fed with complex substrates (Derlon et al., 2016; Layer et al., 2019; Liu et al., 2010). The presence of flocs enhances the

retention of suspended solids in AGS reactors (M. Layer et al., 2020), and the flocs discharged via the selective spill contain a high biogas potential similar to that of primary sludge, indicating a significant unconverted particulate COD content (Guo et al., 2020). This thesis found a high hydrolytic activity in flocs, which also increased in response to increased influent particulate concentrations. Flocs appeared to be more adapted for the degradation of particulate substrates than granules. Their contribution to sbCOD removal is probably most relevant during aeration, when the reactor contents are mixed and the influent substrates are accessible to all sludge fractions. Not only capturing the sbCOD by flocculent sludge, also their high hydrolytic capacity and limited mass-transfer resistance allow them to consume aerobically available rbCOD at a higher rate than granules. Thus, flocs probably indirectly improve granule stability, similarly as protozoa, by consuming the aerobically available COD and limiting its access to granules. They might also utilize particulate substrates for denitrification, improving biological nutrient removal. For a better understanding of the function of flocs in AGS, their physical interaction with particulates and their nutrient removal behaviour should be clarified.

Even though this study did not find detrimental effects of polymeric and particulate substrates in mature full-scale AGS, there are some scenarios in which these compounds could be of concern. For instance, in settings where the VFA loading from the influent wastewater is low, aerobic growth on polymeric substrates could be a challenge to AGS stability. In these cases, anaerobic hydrolysis should be stimulated, as discussed in chapter 5. Another special condition would be start-up. During the initial phases of start-up (lag phase), more attention should be given to the selection of granules over flocs (van Dijk et al., 2022). van Dijk et al. (2022) predicted that ample floc formation during the lag phase, causes spillage of proto-granules before they grow into small granules that can preferentially be retained in the reactor. In this context, preferential growth of flocculent sludge due to high hydrolytic activity and preferential capturing of polymers and particulates, will slow down the granule formation process. This hypothesis is underlined by the observation made at Garmerwolde WWTP, where biomass-specific hydrolysis was at least twice as high in flocs compared to granules (Chapter 3). To overcome the challenges of granulating with wastewaters with a large fraction of slowly biodegradable COD, readily biodegradable COD could be supplemented anaerobically. That may be done by including a pre-fermentation tank for the influent, or by dosing VFA temporarily during start-up, for example from an external waste source or locally produced by fermentation of a fine sieved influent cellulose fraction. Another strategy would be seeding the reactor with (a fraction of) granules, to skip the lag phase and therefore avoid having to select proto-granules formed from flocs (Sguanci et al., 2019).

## 6.4 | THE ROLE OF HYDROLYTIC ENZYMES IN THE GRANULE CORE

Even though hydrolysis is generally mass-transfer limited, and the model substrates used were only hydrolysed in the outer layer of aerobic granules, hydrolytic enzymes were localized throughout the granules (chapter 4). Hydrolytic activity visualisation was used in this work as an indicator of where influent substrates are degraded. Nevertheless, it is unlikely that the enzymes in the granule core have access to substrates from the influent. First, small polymeric substrates are not very abundant in domestic wastewater, and the diffusion of larger particulates is most likely very limited (van den Berg et al., 2022b). Second, even when diffusible substrates are present in relatively high concentrations, they are degraded at the granule surface due to higher conversion than transport rates. Thus, the total hydrolytic potential of aerobic granules should not be regarded as a measure of their ability to degrade influent polymers, since not all the hydrolytic enzymes might be accessible to influent substrates.



**Figure 6.2.** Light and fluorescence microscope images of Utrecht granule sections containing inclusions in their matrix. The first and third images were taken with bright field microscope. The second and fourth show intrinsically fluorescent areas in granules, seemingly fibers and other inclusions, captured with an epifluorescence microscope at Ex/Em 546/575-640 nm.

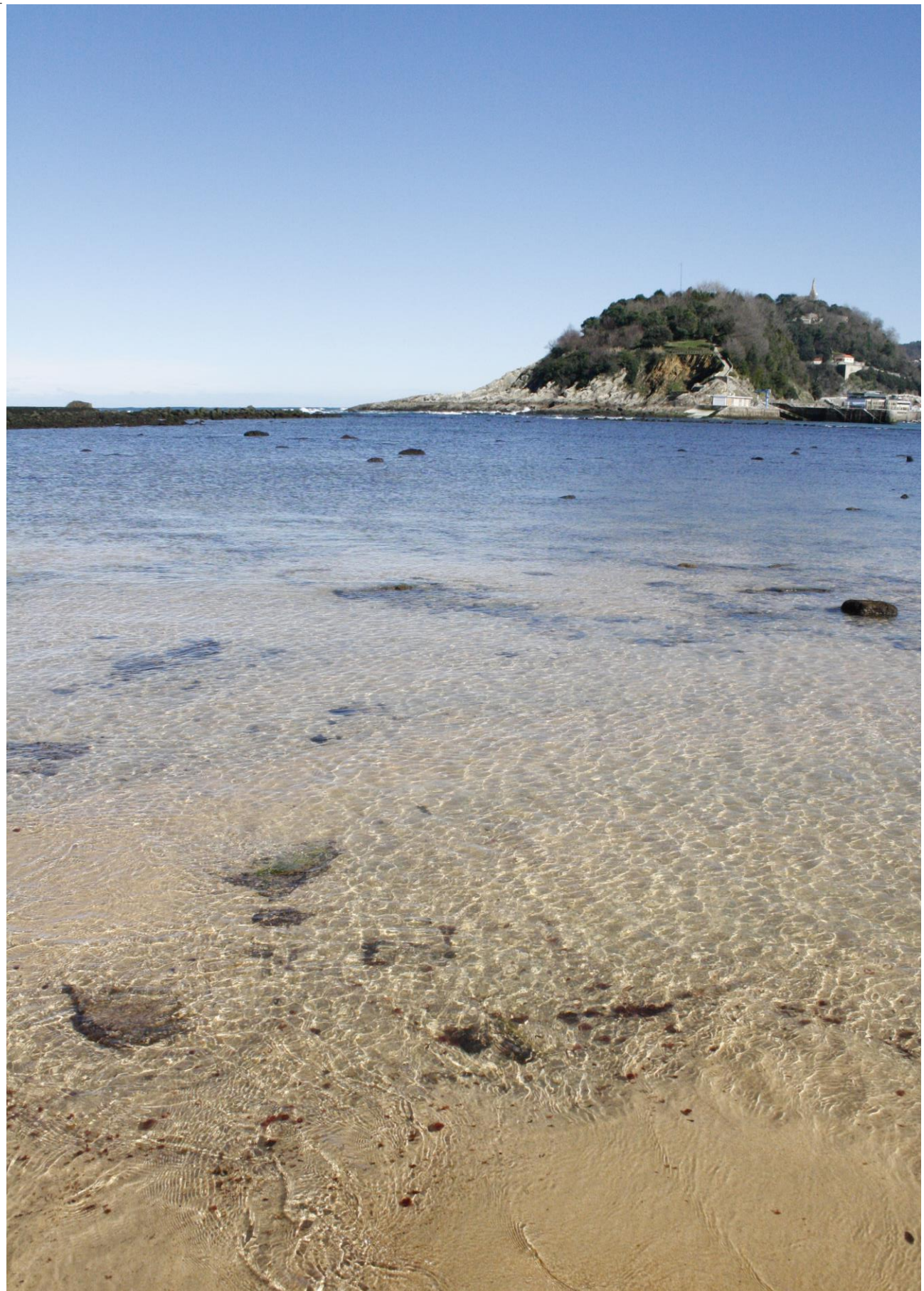
It is possible that extracellular enzymes located deeper in the granules degrade some of the particulates in wastewater if those were overgrown by biomass. It is not uncommon to find fibres and other inclusions embedded in granules (Figure 6.2). Most likely, the hydrolytic enzymes located deeper in the granules are also involved in the degradation of cell decay products and extracellular polymeric substances (EPS) (Seviour et al., 2019). The EPS composition of AGS remains poorly understood, due to its complexity and the limitations of the commonly used characterization methods. In order to advance towards a circular economy and improve biofilm control strategies, it is essential to characterize the synthesis and composition of EPS (Seviour et al., 2019). In this context,

the extracellular enzymes and their potential to transform EPS components should not be overlooked.

Extracellular enzymes could be researched further in full-scale AGS, but a lab-scale setup would offer a more simplified scenario to study the synthesis and activity of these enzymes in detail. Lab-scale reactors allow monitoring hydrolytic activity changes as a response to changes in influent particulate concentrations, in a more controlled setting than in full-scale reactors (as the one described in chapter 2). More advanced analytical methods than those employed in this study would contribute to characterize hydrolytic enzymes in aerobic granules. For instance, FTIR imaging, Raman microscopy, or CLSM (combined with lectin or antibody staining) could be used to co-localize EPS compounds with respect to hydrolytic enzymes (Lin et al., 2018; Neu and Kuhlicke, 2017; Seviour et al., 2019; Wagner et al., 2009). Genomic and proteomic analyses would provide more detailed characterization of hydrolytic enzymes in AGS (Zhang et al., 2015). The metabolism of hydrolysers can be researched through *in situ* physiology approaches (e.g. MAR, qSIP, NanoSIMS, BONCAT), and linked to their identity by FISH or genomics (Hatzenpichler et al., 2020; Neu et al., 2010). These techniques would contribute to clarifying the metabolism of different microorganisms in AGS without long-term lab-scale reactor operation. For instance, the activity of PAO and GAO may be assessed, to study the differences between classical genera (*Ca. Accumulibacter*, *Ca. Competibacter*) and their fermentative counterparts (*Tetrasphaera*, *Propionivibrio*, *Dechloromonas*, *Micropruina*).

Overall, this thesis indicates that polymeric substrates in domestic wastewater pose a low threat to AGS stability. In most scenarios, low hydrolysis rates can be expected in granules, leading to low aerobic substrate loading. Still, the microbial community and hydrolytic enzyme content of AGS enables the utilization of diverse polymeric substrates. Polymeric substrates in domestic wastewaters, however, comprise a heterogeneous group of compounds, and their degradation extent will be impacted by various factors, such as their molecule type, concentration and substrate-sludge contact. The earned knowledge about the capacity and location of polymeric substrate conversion can guide future research into how to control the degradation of this slowly biodegradable wastewater fraction. Combining assays based on model labelled substrates, and assays that measure substrate uptake indirectly (*via* P and N measurements, sludge production, storage polymer formation, etc.) constitutes an effective approach to study polymeric and particulate substrate conversions in AGS systems.





## References

- Abu-Ghararah, Z.H., Randall, C.W., 1991. The effect of organic compounds on biological phosphorus removal, in: *Water Science and Technology*. IWA Publishing, pp. 585–594. <https://doi.org/10.2166/wst.1991.0508>
- Adav, S.S., Lee, D.J., Lai, J.Y., 2009. Proteolytic activity in stored aerobic granular sludge and structural integrity. *Bioresour. Technol.* 100, 68–73. <https://doi.org/10.1016/j.biortech.2008.05.045>
- Adav, S.S., Lee, D.J., Tay, J.H., 2008. Extracellular polymeric substances and structural stability of aerobic granule. *Water Res.* 42, 1644–1650. <https://doi.org/10.1016/j.watres.2007.10.013>
- Albertsen, M., Karst, S.M., Ziegler, A.S., Kirkegaard, R.H., Nielsen, P.H., 2015. Back to Basics – The Influence of DNA Extraction and Primer Choice on Phylogenetic Analysis of Activated Sludge Communities. *PLoS One* 10, e0132783. <https://doi.org/10.1371/journal.pone.0132783>
- Ali, M., Wang, Z., Salam, K.W., Hari, A.R., Pronk, M., van Loosdrecht, M.C.M., Saikaly, P.E., 2019. Importance of Species Sorting and Immigration on the Bacterial Assembly of Different-Sized Aggregates in a Full-Scale Aerobic Granular Sludge Plant. *Environ. Sci. Technol.* 53, 8291–8301. <https://doi.org/10.1021/acs.est.8b07303>
- Alves, O.I.M., Araújo, J.M., Silva, P.M.J., Magnus, B.S., Gavazza, S., Florencio, L., Kato, M.T., 2022. Formation and stability of aerobic granular sludge in a sequential batch reactor for the simultaneous removal of organic matter and nutrients from low-strength domestic wastewater. *Sci. Total Environ.* 843, 156988. <https://doi.org/10.1016/j.scitotenv.2022.156988>
- Amann, R.I., Binder, B.J., Olson, R.J., Chisholm, S.W., Devereux, R., Stahl, D.A., 1990. Combination of 16S rRNA-targeted oligonucleotide probes with flow cytometry for analyzing mixed microbial populations. *Appl. Environ. Microbiol.* 56, 1919–1925. <https://doi.org/10.1128/aem.56.6.1919-1925.1990>
- Amir, A., McDonald, D., Navas-Molina, J.A., Kopylova, E., Morton, J.T., Zech Xu, Z., Kightley, E.P., Thompson, L.R., Hyde, E.R., Gonzalez, A., Knight, R., 2017. Deblur Rapidly Resolves Single-Nucleotide Community Sequence Patterns. *mSystems* 2. <https://doi.org/10.1128/msystems.00191-16>
- Amorim de Carvalho, C. de, Ferreira dos Santos, A., Tavares Ferreira, T.J., Sousa Aguiar Lira, V.N., Mendes Barros, A.R., Bezerra dos Santos, A., 2021. Resource recovery in aerobic granular sludge systems: is it feasible or still a long way to go? *Chemosphere* 274, 129881. <https://doi.org/10.1016/j.chemosphere.2021.129881>
- Andersen, K.S., Kirkegaard, R.H., Karst, S.M., Albertsen, M., 2018. ampvis2: An R package to analyse and visualise 16S rRNA amplicon data. *bioRxiv*. <https://doi.org/10.1101/299537>
- Anderson, M.J., 2001. A new method for non-parametric multivariate analysis of variance. *Austral Ecol.* 26, 32–46. <https://doi.org/10.1111/j.1442-9993.2001.01070.pp.x>
- APHA, 2005. *Standard methods for the examination of water and wastewater*, 21st ed. American Public Health Association, Washington, DC.
- Avella, A.C., Görner, T., de Donato, P., 2010. The pitfalls of protein quantification in wastewater treatment studies. *Sci. Total Environ.* 408, 4906–4909. <https://doi.org/10.1016/j.scitotenv.2010.05.039>
- Balmat, J.L., 1957. Biochemical Oxidation of Various Particulate Fractions of Sewage. *Sewage Ind. Waste.* 29, 757–761. <https://doi.org/10.2307/25033376>
- Barrios-Hernández, M.L., Buenaño-Vargas, C., García, H., Brdjanovic, D., van Loosdrecht, M.C.M., Hooijmans, C.M., 2020. Effect of the co-treatment of synthetic faecal sludge and wastewater in an aerobic granular sludge system. *Sci. Total Environ.* 741, 140480. <https://doi.org/10.1016/j.scitotenv.2020.140480>

- Bassin, J.P., Kleerebezem, R., Dezotti, M., van Loosdrecht, M.C.M., 2012. Simultaneous nitrogen and phosphate removal in aerobic granular sludge reactors operated at different temperatures. *Water Res.* 46, 3805–3816. <https://doi.org/10.1016/j.watres.2012.04.015>
- Bassin, J.P., Pronk, M., Muyzer, G., Kleerebezem, R., Dezotti, M., van Loosdrecht, M.C.M., 2011. Effect of elevated salt concentrations on the aerobic granular sludge process: Linking microbial activity with microbial community structure. *Appl. Environ. Microbiol.* 77, 7942–7953. <https://doi.org/10.1128/AEM.05016-11>
- Begum, S.A., Batista, J.R., 2014. Impact of butyrate on microbial selection in enhanced biological phosphorus removal systems. *Environ. Technol. (United Kingdom)* 35, 2961–2972. <https://doi.org/10.1080/09593330.2014.927531>
- Bengtsson, S., de Blois, M., Wilén, B.-M., Gustavsson, D., 2018. Treatment of municipal wastewater with aerobic granular sludge. *Crit. Rev. Environ. Sci. Technol.* 48, 1–48. <https://doi.org/10.1080/10643389.2018.1439653>
- Benneouala, M., Bareha, Y., Mengelle, E., Bounouba, M., Sperandio, M., Bessiere, Y., Paul, E., 2017. Hydrolysis of particulate settleable solids (PSS) in activated sludge is determined by the bacteria initially adsorbed in the sewage. *Water Res.* 125, 400–409. <https://doi.org/10.1016/J.WATRES.2017.08.058>
- Beun, J.J., Van Loosdrecht, M.C.M., Heijnen, J.J., 2002. Aerobic granulation in a sequencing batch airlift reactor. *Water Res.* 36, 702–712. [https://doi.org/10.1016/S0043-1354\(01\)00250-0](https://doi.org/10.1016/S0043-1354(01)00250-0)
- Beun, J.J., Van Loosdrecht, M.C.M., Heijnen, J.J., 2000. Aerobic granulation, in: *Water Science and Technology*. Int Water Assoc, pp. 41–48. <https://doi.org/10.2166/wst.2000.0423>
- Björnsson, L., Hugenholtz, P., Tyson, G.W., Blackall, L.L., 2002. Filamentous Chloroflexi (green non-sulfur bacteria) are abundant in wastewater treatment processes with biological nutrient removal. *Microbiology* 148, 2309–2318. <https://doi.org/10.1099/00221287-148-8-2309>
- Boczar, B.A., Begley, W.M., Larson, R.J., Creek, M., 1992. Characterization of enzyme activity in activated sludge using rapid analyses for specific hydrolases. *Water Environ. Res.* 64, 792–797.
- Boltz, J.P., La Motta, E.J., 2007. Kinetics of Particulate Organic Matter Removal as a Response to Bioflocculation in Aerobic Biofilm Reactors. *Water Environ. Res.* 79, 725–735. <https://doi.org/10.2175/106143007x156718>
- Boltz, J.P., La Motta, E.J., 2006. A model for simultaneous particulate and dissolved substrate removal in a biofilm reactor. *Environ. Eng. Sci.* 23, 886–896. <https://doi.org/10.1089/ees.2006.23.886>
- Bolyen, E., Rideout, J.R., Dillon, M.R., Bokulich, N.A., Abnet, C.C., Al-Ghalith, G.A., Alexander, H., Alm, E.J., Arumugam, M., Asnicar, F., Bai, Y., Bisanz, J.E., Bittinger, K., Brejnrod, A., Brislawn, C.J., Brown, C.T., Callahan, B.J., Caraballo-Rodríguez, A.M., Chase, J., Cope, E.K., Da Silva, R., Diener, C., Dorrestein, P.C., Douglas, G.M., Durall, D.M., Duvallet, C., Edwardson, C.F., Ernst, M., Estaki, M., Fouquier, J., Gauglitz, J.M., Gibbons, S.M., Gibson, D.L., Gonzalez, A., Gorlick, K., Guo, J., Hillmann, B., Holmes, S., Holste, H., Huttenhower, C., Huttley, G.A., Janssen, S., Jarmusch, A.K., Jiang, L., Kaehler, B.D., Kang, K. Bin, Keefe, C.R., Keim, P., Kelley, S.T., Knights, D., Koester, I., Kosciulek, T., Kreps, J., Langille, M.G.I., Lee, J., Ley, R., Liu, Y.X., Loftfield, E., Lozupone, C., Maher, M., Marotz, C., Martin, B.D., McDonald, D., McIver, L.J., Melnik, A. V., Metcalf, J.L., Morgan, S.C., Morton, J.T., Naimey, A.T., Navas-Molina, J.A., Nothias, L.F., Orchanian, S.B., Pearson, T., Peoples, S.L., Petras, D., Preuss, M.L., Priesse, E., Rasmussen, L.B., Rivers, A., Robeson, M.S., Rosenthal, P., Segata, N., Shaffer, M., Shiffer, A., Sinha, R., Song, S.J., Spear, J.R., Swafford, A.D., Thompson, L.R., Torres, P.J., Trinh, P., Tripathi, A., Turnbaugh, P.J., Ul-Hasan, S., van der Hooft, J.J.J., Vargas, F., Vázquez-Baeza,

- Y., Vogtmann, E., von Hippel, M., Walters, W., Wan, Y., Wang, M., Warren, J., Weber, K.C., Williamson, C.H.D., Willis, A.D., Xu, Z.Z., Zaneveld, J.R., Zhang, Y., Zhu, Q., Knight, R., Caporaso, J.G., 2019. Reproducible, interactive, scalable and extensible microbiome data science using QIIME 2. *Nat. Biotechnol.* <https://doi.org/10.1038/s41587-019-0209-9>
- Caluwé, M., Goossens, K., Suazo, K.S., Tsertou, E., Dries, J., 2022. Granulation strategies applied to industrial wastewater treatment: from lab to full-scale. *Water Sci. Technol.* 85, 2761–2771. <https://doi.org/10.2166/wst.2022.129>
- Campo, R., Sguanci, S., Caffaz, S., Mazzoli, L., Ramazzotti, M., Lubello, C., Lotti, T., 2020. Efficient carbon, nitrogen and phosphorus removal from low C/N real domestic wastewater with aerobic granular sludge. *Bioresour. Technol.* 305, 122961. <https://doi.org/10.1016/j.biortech.2020.122961>
- Carlson, G., Silverstein, J., 1998. Effect of molecular size and charge on biofilm sorption of organic matter. *Water Res.* 32, 1580–1592. [https://doi.org/10.1016/S0043-1354\(97\)00354-0](https://doi.org/10.1016/S0043-1354(97)00354-0)
- Cetin, E., Karakas, E., Dulekgurgen, E., Ovez, S., Kolukirik, M., Yilmaz, G., 2018. Effects of high-concentration influent suspended solids on aerobic granulation in pilot-scale sequencing batch reactors treating real domestic wastewater. *Water Res.* 131, 74–89. <https://doi.org/10.1016/j.watres.2017.12.014>
- Chen, G.-H., van Loosdrecht, M.C.M., Ekama, G.A., Brdjanovic, D., 2020. *Biological Wastewater Treatment : Principles, Modelling and Design*, 2nd editio. ed. IWA Publishing.
- Coates, J.D., Ellis, D.J., Gaw, C. V., Lovley, D.R., 1999. *Geothrix fermentans* gen. nov., sp. nov., a novel Fe(III)-reducing bacterium from a hydrocarbon-contaminated aquifer. *Int. J. Syst. Bacteriol.* 49, 1615–1622. <https://doi.org/10.1099/00207713-49-4-1615>
- Coma, M., Verawaty, M., Pijuan, M., Yuan, Z., Bond, P.L., 2012. Enhancing aerobic granulation for biological nutrient removal from domestic wastewater. *Bioresour. Technol.* 103, 101–108. <https://doi.org/10.1016/j.biortech.2011.10.014>
- Confer, D.R., Logan, B.E., 1998a. Location of protein and polysaccharide hydrolytic activity in suspended and biofilm wastewater cultures. *Water Res.* 32, 31–38. [https://doi.org/10.1016/S0043-1354\(97\)00194-2](https://doi.org/10.1016/S0043-1354(97)00194-2)
- Confer, D.R., Logan, B.E., 1998b. A conceptual model describing macromolecule degradation by suspended cultures and biofilms. *Water Sci. Technol.* 37, 231–234. <https://doi.org/10.2166/wst.1998.0631>
- Crocetti, G.R., Hugenholtz, P., Bond, P.L., Schuler, A., Keller, J., Jenkins, D., Blackall, L.L., 2000. Identification of polyphosphate-accumulating organisms and design of 16S rRNA-directed probes for their detection and quantitation. *Appl. Environ. Microbiol.* 66, 1175–82. <https://doi.org/10.1128/AEM.66.3.1175-1182.2000>
- Crocetti R., G., Banfield F., J.F., Keller, J., Bond, P.L., Blackall, L.L., 2002. Glycogen-accumulating organisms in laboratory-scale and full-scale wastewater treatment processes. *Microbiology.* <https://doi.org/10.1099/00221287-148-11-3353>
- Daims, H., Brühl, A., Amann, R., Schleifer, K.H., Wagner, M., 1999. The domain-specific probe EUB338 is insufficient for the detection of all bacteria: Development and evaluation of a more comprehensive probe set. *Syst. Appl. Microbiol.* 22, 434–444. [https://doi.org/10.1016/S0723-2020\(99\)80053-8](https://doi.org/10.1016/S0723-2020(99)80053-8)
- Daims, H., Nielsen, J.L., Nielsen, P.H., Schleifer, K.H., Wagner, M., 2001. In Situ Characterization of Nitrospira-Like Nitrite-Oxidizing Bacteria Active in Wastewater Treatment Plants. *Appl. Environ. Microbiol.* 67, 5273–5284. <https://doi.org/10.1128/aem.67.11.5273-5284.2001>
- de Bruin, L.M.M., de Kreuk, M.K., van der Roest, H.F.R., Uijterlinde, C., van Loosdrecht, M.C.M., 2004. Aerobic granular sludge technology: An alternative to activated sludge? *Water Sci.*

- Technol. 49, 1–7.
- de Graaff, D.R., van Loosdrecht, M.C.M., Pronk, M., 2020. Stable granulation of seawater-adapted aerobic granular sludge with filamentous Thiothrix bacteria. *Water Res.* 175, 115683. <https://doi.org/10.1016/j.watres.2020.115683>
- De Kreuk, M.K., 2006. Aerobic granular sludge : scaling up a new technology. Delft University of Technology.
- de Kreuk, M.K., Heijnen, J.J., van Loosdrecht, M.C.M., 2005. Simultaneous COD, nitrogen, and phosphate removal by aerobic granular sludge. *Biotechnol. Bioeng.* 90, 761–769. <https://doi.org/10.1002/bit.20470>
- de Kreuk, M.K., Kishida, N., Tsuneda, S., van Loosdrecht, M.C.M., 2010. Behavior of polymeric substrates in an aerobic granular sludge system. *Water Res.* 44, 5929–5938. <https://doi.org/10.1016/j.watres.2010.07.033>
- de Kreuk, M.K., Kishida, N., van Loosdrecht, M.C.M., 2007. Aerobic granular sludge - State of the art. *Water Sci. Technol.* 55, 75–81. <https://doi.org/10.2166/wst.2007.244>
- de Kreuk, M.K., van Loosdrecht, M.C.M., 2004. Selection of slow growing organisms as a means for improving aerobic granular sludge stability. *Water Sci. Technol.* 49, 9–17. <https://doi.org/https://doi.org/10.2166/wst.2004.0792>
- Derlon, N., Wagner, J., da Costa, R.H.R., Morgenroth, E., 2016. Formation of aerobic granules for the treatment of real and low-strength municipal wastewater using a sequencing batch reactor operated at constant volume. *Water Res.* 105, 341–350. <https://doi.org/10.1016/J.WATRES.2016.09.007>
- Dockx, L., Caluwé, M., De Vleeschauwer, F., Dobbeleers, T., Dries, J., 2021. Impact of the substrate composition on enhanced biological phosphorus removal during formation of aerobic granular sludge. *Bioresour. Technol.* 337, 125482. <https://doi.org/10.1016/j.biortech.2021.125482>
- Drewnowski, J., Makinia, J., 2014. The role of biodegradable particulate and colloidal organic compounds in biological nutrient removal activated sludge systems. *Int. J. Environ. Sci. Technol.* 11, 1973–1988. <https://doi.org/10.1007/s13762-013-0402-1>
- DuBois, M., Gilles, K.A., Hamilton, J.K., Rebers, P.A., Smith, F., 1956. Colorimetric Method for Determination of Sugars and Related Substances. *Anal. Chem.* 28, 350–356. <https://doi.org/https://doi.org/10.1021/ac60111a017>
- Ekama, G.A., Wentzel, M.C., van Loosdrecht, M.C.M. (Eds.), 2020. Nitrogen removal, in: *Biological Wastewater Treatment: Principles, Modeling and Design*. IWA Publishing, pp. 161–238. [https://doi.org/10.2166/9781789060362\\_0161](https://doi.org/10.2166/9781789060362_0161)
- Elahinik, A., Haarsma, M., Abbas, B., Pabst, M., Xevgenos, D., van Loosdrecht, M.C.M., Pronk, M., 2022. Glycerol conversion by aerobic granular sludge. *Water Res.* 227. <https://doi.org/10.1016/j.watres.2022.119340>
- Espíndola, S.P., Pronk, M., Zlopasa, J., Picken, S.J., van Loosdrecht, M.C.M., 2021. Nanocellulose recovery from domestic wastewater. *J. Clean. Prod.* 280, 124507. <https://doi.org/10.1016/j.jclepro.2020.124507>
- Feinstein, L.M., Woo, J.S., Blackwood, C.B., 2009. Assessment of bias associated with incomplete extraction of microbial DNA from soil. *Appl. Environ. Microbiol.* 75, 5428–5433. <https://doi.org/10.1128/AEM.00120-09>
- Felz, S., Vermeulen, P., van Loosdrecht, M.C.M., Lin, Y.M., 2019. Chemical characterization methods for the analysis of structural extracellular polymeric substances (EPS). *Water Res.* 157, 201–208. <https://doi.org/10.1016/j.watres.2019.03.068>
- Ferenci, T., 1980. The Recognition of Maltodextrins by *Escherichia coli*. *Eur. J. Biochem.* 108, 631–



636. <https://doi.org/10.1111/j.1432-1033.1980.tb04758.x>
- Frølund, B., Griebe, T., Nielsen, P.H., 1995. Enzymatic activity in the activated-sludge floc matrix. *Appl. Microbiol. Biotechnol.* 43, 755–761. <https://doi.org/10.1007/BF00164784>
- Gich, F., Garcia-Gil, J., Overmann, J., 2001. Previously unknown and phylogenetically diverse members of the green nonsulfur bacteria are indigenous to freshwater lakes. *Arch. Microbiol.* 177, 1–10. <https://doi.org/10.1007/s00203-001-0354-6>
- Giesen, A., de Bruin, L.M.M., Niermans, R.P., van der Roest, H.F., 2013. Advancements in the application of aerobic granular biomass technology for sustainable treatment of wastewater. *Water Pract. Technol.* 8, 47–54. <https://doi.org/10.2166/wpt.2013.007>
- Giesen, A., van Loosdrecht, M., de Buin, B., 2014. Full-scale Experiences with Aerobic Granular Biomass Technology for Treatment of Urban and Industrial Wastewater. *Proc. Water Environ. Fed.* 2014, 2347–2357. <https://doi.org/10.2175/193864714815942512>
- Goel, R., Mino, T., Satoh, H., Matsuo, T., 1998a. Comparison of hydrolytic enzyme systems in pure culture and activated sludge under different electron acceptor conditions. *Water Sci. Technol.* 37, 335–343. <https://doi.org/10.2166/wst.1998.0659>
- Goel, R., Mino, T., Satoh, H., Matsuo, T., 1998b. Enzyme activities under anaerobic and aerobic conditions in activated sludge sequencing batch reactor. *Water Res.* 32, 2081–2088. [https://doi.org/10.1016/S0043-1354\(97\)00425-9](https://doi.org/10.1016/S0043-1354(97)00425-9)
- Gonzalez, A., van Lier, J.B., de Kreuk, M.K., 2021. The role of growth media on composition, bioconversion and susceptibility for mild thermal pre-treatment of waste activated sludge. *J. Environ. Manage.* 298, 113491. <https://doi.org/10.1016/j.jenvman.2021.113491>
- Gujer, W., Henze, M., Mino, T., Loosdrecht, M. van, 1999. Activated sludge model No. 3. *Water Sci. Technol.* 39, 183–193. [https://doi.org/10.1016/S0273-1223\(98\)00785-9](https://doi.org/10.1016/S0273-1223(98)00785-9)
- Guo, H., van Lier, J.B., de Kreuk, M., 2020. Digestibility of waste aerobic granular sludge from a full-scale municipal wastewater treatment system. *Water Res.* 173, 115617. <https://doi.org/10.1016/j.watres.2020.115617>
- Gupta, N., Rath, P., Gupta, R., 2002. Simplified para-nitrophenyl palmitate assay for lipases and esterases. *Anal. Biochem.* 311, 98–99. [https://doi.org/10.1016/S0003-2697\(02\)00379-2](https://doi.org/10.1016/S0003-2697(02)00379-2)
- Haaksman, V.A., Mirghorayshi, M., van Loosdrecht, M.C.M., Pronk, M., 2020. Impact of aerobic availability of readily biodegradable COD on morphological stability of aerobic granular sludge. *Water Res.* 116402. <https://doi.org/10.1016/j.watres.2020.116402>
- Hatzenpichler, R., Krukenberg, V., Spietz, R.L., Jay, Z.J., 2020. Next-generation physiology approaches to study microbiome function at single cell level. *Nat. Rev. Microbiol.* <https://doi.org/10.1038/s41579-020-0323-1>
- Henze, M., Comeau, Y., 2008. Wastewater characterization, in: *Biological Wastewater Treatment: Principles, Modelling and Design*. pp. 33–52. [https://doi.org/10.2166/9781780408644\\_001](https://doi.org/10.2166/9781780408644_001)
- Henze, M., Grady, C.P.L., Gujer, W., Marais, G. v. R., Matsuo, T., 1986. Activated sludge model No.1, IAWPRC Scientific and Technical Report No.1. London.
- Henze, M., Gujer, W., Mino, T., Matsuo, T., Wentzel, M.C., Marais, G. v. R., Van Loosdrecht, M.C.M., 1999. Activated Sludge Model No.2d, ASM2D. *Water Sci. Technol.* 39, 165–182. <https://doi.org/10.2166/wst.1999.0036>
- Hollender, J., van der Krol, D., Kornberger, L., Gierden, E., Dott, W., 2002. Effect of different carbon sources on the enhanced biological phosphorus removal in a sequencing batch reactor. *World J. Microbiol. Biotechnol.* 18, 359–364. <https://doi.org/10.1023/A:1015258308460>
- Hollibaugh, J.T., Azam, F., 1983. Microbial degradation of dissolved proteins in seawater. *Limnol. Oceanogr.* 28, 1104–1116. <https://doi.org/10.4319/lo.1983.28.6.1104>
- How, S.W., Sin, J.H., Wong, S.Y.Y., Lim, P.B., Aris, A.M., Ngoh, G.C., Shoji, T., Curtis, T.P., Chua,

- A.S.M., 2020. Characterization of slowly-biodegradable organic compounds and hydrolysis kinetics in tropical wastewater for biological nitrogen removal. *Water Sci. Technol.* 81, 71–80. <https://doi.org/10.2166/wst.2020.077>
- Hvitved-Jacobsen, T., Raunkjaer, K., Nielsen, P.H., 1995. Volatile fatty acids and sulfide in pressure mains. *Water Sci. Technol.* 31, 169–179. [https://doi.org/10.1016/0273-1223\(95\)00334-J](https://doi.org/10.1016/0273-1223(95)00334-J)
- Hvitved-Jacobsen, T., Vollertsen, J., Haaning Nielsen, A., 2013. Sewer processes: Microbial and chemical process engineering of sewer networks, *Sewer Processes: Microbial and Chemical Process Engineering of Sewer Networks*, Second Edition. CRC Press. <https://doi.org/10.1201/b14666>
- Hvitved-Jacobsen, T., Vollertsen, J., Tanaka, N., 1999. Wastewater quality changes during transport in sewers — An integrated aerobic and anaerobic model concept for carbon and sulfur microbial transformations. *Water Sci. Technol.* 39, 233–249. [https://doi.org/10.1016/S0273-1223\(99\)80036-5](https://doi.org/10.1016/S0273-1223(99)80036-5)
- Jabari, P., Yuan, Q., Oleszkiewicz, J.A., 2016. Potential of Hydrolysis of Particulate COD in Extended Anaerobic Conditions to Enhance Biological Phosphorous Removal 113, 2377–2385. <https://doi.org/10.1002/bit.25999>
- Janning, K.F., Le Tallec, X., Harremoës, P., 1998. hydrolysis of organic Waste Water particles in laboratory and pilot scale biofilm reactors munder anoxic and aerobic conditions. *Water Sci. Technol.* 38, 179–188.
- Janning, K.F., Mesterton, K., Harremoës, P., 1997. Hydrolysis and degradation of filtrated organic particulates in a biofilm reactor under anoxic and aerobic conditions. *Water Sci. Technol.* [https://doi.org/10.1016/S0273-1223\(97\)00335-1](https://doi.org/10.1016/S0273-1223(97)00335-1)
- Jenkins, D., Wanner, J., 2014. *Activated Sludge - 100 Years and Counting*. IWA Publishing.
- Jones, M.D., Singleton, D.R., Sun, W., Aitken, M.D., 2011. Multiple DNA extractions coupled with stable-isotope probing of anthracene-degrading bacteria in contaminated soil. *Appl. Environ. Microbiol.* 77, 2984–2991. <https://doi.org/10.1128/AEM.01942-10>
- Karahan, O., Martins, A., Orhon, D., van Loosdrecht, M.C.M., 2006. Experimental Evaluation of Starch Utilization Mechanism by Activated Sludge. *Biotechnol. Bioeng.* 93, 964–970. <https://doi.org/10.1002/bit>
- Kleikamp, H.B.C., Grouzdev, D., Schaasberg, P., Valderen, R. van, Zwaan, R. van der, Wijgaart, R. van de, Lin, Y., Abbas, B., Pronk, M., Loosdrecht, M.C.M. van, Pabst, M., 2022. Comparative metaproteomics demonstrates different views on the complex granular sludge microbiome. *bioRxiv* 2022.03.07.483319. <https://doi.org/10.1101/2022.03.07.483319>
- Koch, H., van Kessel, M.A.H.J., Lücker, S., 2019. Complete nitrification: insights into the ecophysiology of comammox Nitrospira. *Appl. Microbiol. Biotechnol.* <https://doi.org/10.1007/s00253-018-9486-3>
- Kommedal, R., Milferstedt, K., Bakke, R., Morgenroth, E., 2006. Effects of initial molecular weight on removal rate of dextran in biofilms. *Water Res.* 40, 1795–1804. <https://doi.org/10.1016/j.watres.2006.02.032>
- Kong, Y., Nielsen, J.L., Nielsen, P.H., 2005. Identity and ecophysiology of uncultured actinobacterial polyphosphate-accumulating organisms in full-scale enhanced biological phosphorus removal plants. *Appl. Environ. Microbiol.* 71, 4076–4085. <https://doi.org/10.1128/AEM.71.7.4076-4085.2005>
- Kong, Y., Xia, Y., Nielsen, J.L., Nielsen, P.H., 2007. Structure and function of the microbial community in a full-scale enhanced biological phosphorus removal plant. *Microbiology* 153, 4061–4073. <https://doi.org/10.1099/mic.0.2007/007245-0>
- Kragelund, C., Levantesi, C., Borger, A., Thelen, K., Eikelboom, D., Tandoi, V., Kong, Y., Van Der



- Waarde, J., Krooneman, J., Rossetti, S., Thomsen, T.R., Nielsen, P.H., 2007. Identity, abundance and ecophysiology of filamentous Chloroflexi species present in activated sludge treatment plants. *FEMS Microbiol. Ecol.* 59, 671–682. <https://doi.org/10.1111/j.1574-6941.2006.00251.x>
- Krasnits, E., Beliaevski, M., Tarre, S., Green, M., 2014. The contribution of suspended solids to municipal wastewater PHA-based denitrification. *Environ. Technol.* 35, 313–21. <https://doi.org/10.1080/09593330.2013.827728>
- Krasnits, E., Beliaevski, M., Tarre, S., Green, M., 2013. PHA based denitrification: Municipal wastewater vs. acetate. *Bioresour. Technol.* 132, 28–37. <https://doi.org/10.1016/j.biortech.2012.11.074>
- Kristiansen, R., Thi, H., Nguyen, T., Saunders, A.M., Lund Nielsen, J., Wimmer, R., Le, V.Q., Mcilroy, S.J., Petrovski, S., Seviour, R.J., Calteau, A., Lehmann Nielsen, K., Nielsen, P.H., 2013. A metabolic model for members of the genus *Tetrasphaera* involved in enhanced biological phosphorus removal. *ISME J.* 7136, 543–554. <https://doi.org/10.1038/ismej.2012.136>
- Kwok, W.K., Picioreanu, C., Ong, S.L., Van Loosdrecht, M.C.M., Ng, W.J., Heijnen, J.J., 1998. Influence of biomass production and detachment forces on biofilm structures in a biofilm airlift suspension reactor. *Biotechnol. Bioeng.* 58, 400–407. [https://doi.org/10.1002/\(SICI\)1097-0290\(19980520\)58:4<400::AID-BIT7>3.0.CO;2-N](https://doi.org/10.1002/(SICI)1097-0290(19980520)58:4<400::AID-BIT7>3.0.CO;2-N)
- Langeveld, J.G., Clemens, F.H.L.R., Van Der Graaf, J.H.J.M., 2003. Interactions within the wastewater system: Requirements for sewer processes modelling, in: *Water Science and Technology*. IWA Publishing, pp. 101–108. <https://doi.org/10.2166/wst.2003.0231>
- Lanham, A.B., Ricardo, A.R., Albuquerque, M.G.E., Pardelha, F., Carvalho, M., Coma, M., Fradinho, J., Carvalho, G., Oehmen, A., Reis, M.A.M., 2013. Determination of the extraction kinetics for the quantification of polyhydroxyalkanoate monomers in mixed microbial systems. *Process Biochem.* 48, 1626–1634. <https://doi.org/10.1016/J.PROCBIO.2013.07.023>
- Lanham, A.B., Ricardo, A.R., Coma, M., Fradinho, J., Carvalho, M., Oehmen, A., Carvalho, G., Reis, M.A.M., 2012. Optimisation of glycogen quantification in mixed microbial cultures. *Bioresour. Technol.* 118, 518–525. <https://doi.org/10.1016/J.BIORTECH.2012.05.087>
- Larsen, T.A., Harremoës, P., 1994. Degradation mechanisms of colloidal organic matter in biofilm reactors. *Water Res.* 28, 1443–1452. [https://doi.org/10.1016/0043-1354\(94\)90312-3](https://doi.org/10.1016/0043-1354(94)90312-3)
- Layer, M., Adler, A., Reynaert, E., Hernandez, A., Pagni, M., Morgenroth, E., Holliger, C., Derlon, N., 2019. Organic substrate diffusibility governs microbial community composition, nutrient removal performance and kinetics of granulation of aerobic granular sludge. *Water Res.* X 4, 100033. <https://doi.org/10.1016/J.WROA.2019.100033>
- Layer, M., Bock, K., Ranzinger, F., Horn, H., Morgenroth, E., Derlon, N., 2020. Particulate substrate retention in plug-flow and fully-mixed conditions during operation of aerobic granular sludge systems. *Water Res.* X 9, 100075. <https://doi.org/10.1016/j.wroa.2020.100075>
- Layer, Manuel, Villodres, M.G., Hernandez, A., Reynaert, E., Morgenroth, E., Derlon, N., 2020. Limited simultaneous nitrification-denitrification (SND) in aerobic granular sludge systems treating municipal wastewater: Mechanisms and practical implications. *Water Res.* X 7, 100048. <https://doi.org/10.1016/j.wroa.2020.100048>
- Levine, A.D., Tchobanoglous, G., Asano, T., 1991. Size distributions of particulate contaminants in wastewater and their impact on treatability. *Water Res.* 25, 911–922. [https://doi.org/10.1016/0043-1354\(91\)90138-G](https://doi.org/10.1016/0043-1354(91)90138-G)
- Li, J., Ma, L., Wei, S., Horn, H., 2013. Aerobic granules dwelling vorticella and rotifers in an SBR fed with domestic wastewater. *Sep. Purif. Technol.* 110, 127–131.

- <https://doi.org/10.1016/j.seppur.2013.03.022>
- Lin, Y., Reino, C., Carrera, J., Pérez, J., van Loosdrecht, M.C.M., 2018. Glycosylated amyloid-like proteins in the structural extracellular polymers of aerobic granular sludge enriched with ammonium-oxidizing bacteria. *Microbiol. Open* 7, e00616. <https://doi.org/10.1002/mbo3.616>
- Liu, Y., Wang, Z.-W., Liu, Y.-Q., Qin, L., Tay, J.-H., 2008. A Generalized Model for Settling Velocity of Aerobic Granular Sludge. *Biotechnol. Prog.* 21, 621–626. <https://doi.org/10.1021/bp049674u>
- Liu, Y.Q., Moy, B., Kong, Y.H., Tay, J.H., 2010. Formation, physical characteristics and microbial community structure of aerobic granules in a pilot-scale sequencing batch reactor for real wastewater treatment. *Enzyme Microb. Technol.* 46, 520–525. <https://doi.org/10.1016/j.enzmictec.2010.02.001>
- Loy, A., Horn, M., Wagner, M., 2003. Probase: An online resource for rRNA-targeted oligonucleotide probes. *Nucleic Acids Res.* <https://doi.org/10.1093/nar/gkg016>
- Lundstedt, T., Seifert, E., Abramo, L., Thelin, B., Nyström, Å., Pettersen, J., Bergman, R., 1998. Experimental design and optimization. *Chemom. Intell. Lab. Syst.* 42, 3–40. [https://doi.org/10.1016/S0169-7439\(98\)00065-3](https://doi.org/10.1016/S0169-7439(98)00065-3)
- Marques, R., Santos, J., Nguyen, H., Carvalho, G., Noronha, J.P., Nielsen, P.H., Reis, M.A.M., Oehmen, A., 2017. Metabolism and ecological niche of *Tetrasphaera* and *Ca. Accumulibacter* in enhanced biological phosphorus removal. *Water Res.* 122, 159–171. <https://doi.org/10.1016/j.watres.2017.04.072>
- Martins, A.M.P., Karahan, Ö., van Loosdrecht, M.C.M., 2011. Effect of polymeric substrate on sludge settleability. *Water Res.* 45, 263–273. <https://doi.org/10.1016/j.watres.2010.07.055>
- McIlroy, S.J., Albertsen, M., Andresen, E.K., Saunders, A.M., Kristiansen, R., Stokholm-Bjerregaard, M., Nielsen, K.L., Nielsen, P.H., 2014. ‘Candidatus Competibacter’-lineage genomes retrieved from metagenomes reveal functional metabolic diversity. *ISME J.* 8, 613–624. <https://doi.org/10.1038/ismej.2013.162>
- McIlroy, S.J., Onetto, C.A., McIlroy, B., Herbst, F.-A., Dueholm, M.S., Kirkegaard, R.H., Fernando, E., Karst, S.M., Nierychlo, M., Kristensen, J.M., Eales, K.L., Grbin, P.R., Wimmer, R., Nielsen, P.H., 2018. Genomic and in Situ Analyses Reveal the *Micropruina* spp. as Abundant Fermentative Glycogen Accumulating Organisms in Enhanced Biological Phosphorus Removal Systems. *Front. Microbiol.* 9, 1004. <https://doi.org/10.3389/fmicb.2018.01004>
- McMurdie, P.J., Holmes, S., 2013. phyloseq: An R Package for Reproducible Interactive Analysis and Graphics of Microbiome Census Data. *PLoS One* 8, e61217. <https://doi.org/10.1371/journal.pone.0061217>
- McSwain, B.S., Irvine, R.L., Hausner, M., Wilderer, P.A., 2005. Composition and distribution of extracellular polymeric substances in aerobic flocs and granular sludge. *Appl. Environ. Microbiol.* 71, 1051–1057. <https://doi.org/10.1128/AEM.71.2.1051-1057.2005>
- Metcalf & Eddy, 2003. *Wastewater Engineering: Treatment and Reuse*, 4th editio. ed. McGraw-Hill, Boston, USA.
- Meunier, C., Henriot, O., Schroonbroodt, B., Boeur, J.M., Mahillon, J., Henry, P., 2016. Influence of feeding pattern and hydraulic selection pressure to control filamentous bulking in biological treatment of dairy wastewaters. *Bioresour. Technol.* 221, 300–309. <https://doi.org/10.1016/j.biortech.2016.09.052>
- Mishima, K., Nakamura, M., 1991. Self-immobilization of aerobic activated sludge - A pilot study of the Aerobic Upflow Sludge Blanket Process in municipal sewage treatment, in: *Water Science and Technology*. IWA Publishing, pp. 981–990.

- <https://doi.org/10.2166/wst.1991.0550>
- Morales, N., Figueroa, M., Fra-Vázquez, A., Val Del Río, A., Campos, J.L., Mosquera-Corral, A., Méndez, R., 2013. Operation of an aerobic granular pilot scale SBR plant to treat swine slurry. *Process Biochem.* 48, 1216–1221. <https://doi.org/10.1016/j.procbio.2013.06.004>
- Morgenroth, E., Kommedal, R., Harremoës, P., 2002. Processes and modelling of hydrolysis of particulate organic matter in aerobic wastewater treatment - a review. *Water Sci. Technol.* 45(6), 25–40.
- Morgenroth, E., Sherden, T., Van Loosdrecht, M.C.M., Heijnen, J.J., Wilderer, P.A., 1997. Aerobic granular sludge in a sequencing batch reactor. *Water Res.* 31, 3191–3194. [https://doi.org/10.1016/S0043-1354\(97\)00216-9](https://doi.org/10.1016/S0043-1354(97)00216-9)
- Mosquera-Corral, A., de Kreuk, M.K., Heijnen, J.J., van Loosdrecht, M.C.M., 2005. Effects of oxygen concentration on N-removal in an aerobic granular sludge reactor. *Water Res.* 39, 2676–2686. <https://doi.org/10.1016/j.watres.2005.04.065>
- Mosquera-Corral, A., Monrás, A., Heijnen, J.J., van Loosdrecht, M.C.M., 2003. Degradation of polymers in a biofilm airlift suspension reactor. *Water Res.* 37, 485–492. [https://doi.org/10.1016/S0043-1354\(02\)00309-3](https://doi.org/10.1016/S0043-1354(02)00309-3)
- Narkis, N., Henefeld-Fourrier, S., Rebhun, M., 1980. Volatile organic acids in raw wastewater and in physico-chemical treatment. *Water Res.* 14, 1215–1223. [https://doi.org/10.1016/0043-1354\(80\)90179-7](https://doi.org/10.1016/0043-1354(80)90179-7)
- Neu, T., Kuhlicke, U., 2017. Fluorescence Lectin Bar-Coding of Glycoconjugates in the Extracellular Matrix of Biofilm and Bioaggregate Forming Microorganisms. *Microorganisms* 5, 5. <https://doi.org/10.3390/microorganisms5010005>
- Neu, T.R., Manz, B., Volke, F., Dynes, J.J., Hitchcock, A.P., Lawrence, J.R., 2010. Advanced imaging techniques for assessment of structure, composition and function in biofilm systems. *FEMS Microbiol. Ecol.* 72, 1–21. <https://doi.org/10.1111/j.1574-6941.2010.00837.x>
- Nguyen, H.T.T., Kristiansen, R., Vestergaard, M., Wimmer, R., Nielsen, P.H., 2015. Intracellular Accumulation of Glycine in Polyphosphate-Accumulating Organisms in Activated Sludge, a Novel Storage Mechanism under Dynamic Anaerobic-Aerobic Conditions. *Appl. Environ. Microbiol.* 81, 4809–18. <https://doi.org/10.1128/AEM.01012-15>
- Nguyen, H.T.T., Le, V.Q., Hansen, A.A., Nielsen, J.L., Nielsen, P.H., 2011. High diversity and abundance of putative polyphosphate-accumulating Tetrasphaera-related bacteria in activated sludge systems. *FEMS Microbiol. Ecol.* 76, 256–267. <https://doi.org/10.1111/j.1574-6941.2011.01049.x>
- Nguyen Quoc, B., Wei, S., Armenta, M., Bucher, R., Sukapantharam, P., Stahl, D.A., Stensel, H.D., Winkler, M.K.H., 2021. Aerobic granular sludge: Impact of size distribution on nitrification capacity. *Water Res.* 188, 116445. <https://doi.org/10.1016/j.watres.2020.116445>
- Ni, B.-J., Xie, W.-M., Liu, S.-G., Yu, H.-Q., Wang, Y.-Z., Wang, G., Dai, X.-L., 2009. Granulation of activated sludge in a pilot-scale sequencing batch reactor for the treatment of low-strength municipal wastewater. *Water Res.* 43, 751–761. <https://doi.org/10.1016/J.WATRES.2008.11.009>
- Nielsen, J.L., Nguyen, H., Meyer, R.L., Nielsen, P.H., 2012. Identification of glucose-fermenting bacteria in a full-scale enhanced biological phosphorus removal plant by stable isotope probing. *Microbiology* 158, 1818–1825. <https://doi.org/10.1099/mic.0.058818-0>
- Nielsen, P.H., McIlroy, S.J., Albertsen, M., Nierychlo, M., 2019. Re-evaluating the microbiology of the enhanced biological phosphorus removal process. *Curr. Opin. Biotechnol.* <https://doi.org/10.1016/j.copbio.2019.03.008>
- Nielsen, P.H., Mielczarek, A.T., Kragelund, C., Nielsen, J.L., Saunders, A.M., Kong, Y., Hansen, A.A.,

- Vollertsen, J., 2010. A conceptual ecosystem model of microbial communities in enhanced biological phosphorus removal plants. *Water Res.* 44, 5070–5088. <https://doi.org/10.1016/j.watres.2010.07.036>
- Nierychlo, M., Andersen, K.S., Xu, Y., Green, N., Jiang, C., Albertsen, M., Dueholm, M.S., Nielsen, P.H., 2020. MiDAS 3: An ecosystem-specific reference database, taxonomy and knowledge platform for activated sludge and anaerobic digesters reveals species-level microbiome composition of activated sludge. *Water Res.* 182, 115955. <https://doi.org/10.1016/j.watres.2020.115955>
- Nittami, T., Speirs, L.B.M., Yamada, T., Suzuki, I., Fukuda, J., Kurisu, F., Seviour, R.J., 2017. Quantification of Chloroflexi Eikelboom morphotype 1851 for prediction and control of bulking events in municipal activated sludge plants in Japan. *Appl. Microbiol. Biotechnol.* 101, 3861–3869. <https://doi.org/10.1007/s00253-016-8077-4>
- Nybroe, O., Jørgensen, P.E., Henze, M., 1992. Enzyme activities in waste water and activated sludge. *Water Res.* 26, 579–584. [https://doi.org/10.1016/0043-1354\(92\)90230-2](https://doi.org/10.1016/0043-1354(92)90230-2)
- Oehmen, A., Lemos, P.C., Carvalho, G., Yuan, Z., Keller, J., Blackall, L.L., Reis, M.A.M., 2007. Advances in enhanced biological phosphorus removal: From micro to macro scale. *Water Res.* <https://doi.org/10.1016/j.watres.2007.02.030>
- Oehmen, A., Zeng, R.J., Yuan, Z., Keller, J., 2005. Anaerobic metabolism of propionate by polyphosphate-accumulating organisms in enhanced biological phosphorus removal systems. *Biotechnol. Bioeng.* 91, 43–53. <https://doi.org/10.1002/bit.20480>
- Palatsi, J., Affes, R., Fernandez, B., Pereira, M.A., Alves, M.M., Flotats, X., 2012. Influence of adsorption and anaerobic granular sludge characteristics on long chain fatty acids inhibition process. *Water Res.* 46, 5268–5278. <https://doi.org/10.1016/J.WATRES.2012.07.008>
- Picioreanu, C., van Loosdrecht, M.C.M., Heijnen, J.J., 2000a. A theoretical study on the effect of surface roughness on mass transport and transformation in biofilms. *Biotechnol. Bioeng.* 68, 355–369. [https://doi.org/10.1002/\(SICI\)1097-0290\(20000520\)68:4<355::AID-BIT1>3.0.CO;2-A](https://doi.org/10.1002/(SICI)1097-0290(20000520)68:4<355::AID-BIT1>3.0.CO;2-A)
- Picioreanu, C., van Loosdrecht, M.C.M., Heijnen, J.J., 1998. Mathematical modeling of biofilm structure with a hybrid differential-discrete cellular automaton approach. *Biotechnol. Bioeng.* 58, 101–116. [https://doi.org/10.1002/\(SICI\)1097-0290\(19980405\)58:1<101::AID-BIT11>3.0.CO;2-M](https://doi.org/10.1002/(SICI)1097-0290(19980405)58:1<101::AID-BIT11>3.0.CO;2-M)
- Picioreanu, C., Van Loosdrecht, M.C.M., Heijnen, J.J., 2000b. Effect of diffusive and convective substrate transport on biofilm structure formation: A two-dimensional modeling study. *Biotechnol. Bioeng.* 69, 504–515. [https://doi.org/10.1002/1097-0290\(20000905\)69:5<504::AID-BIT5>3.0.CO;2-S](https://doi.org/10.1002/1097-0290(20000905)69:5<504::AID-BIT5>3.0.CO;2-S)
- Pronk, M., Abbas, B., Al-zuhairy, S.H.K., Kraan, R., Kleerebezem, R., van Loosdrecht, M.C.M., 2015a. Effect and behaviour of different substrates in relation to the formation of aerobic granular sludge. *Appl. Microbiol. Biotechnol.* 99, 5257–5268. <https://doi.org/10.1007/s00253-014-6358-3>
- Pronk, M., de Kreuk, M.K., de Bruin, B., Kamminga, P., Kleerebezem, R., van Loosdrecht, M.C.M., 2015b. Full scale performance of the aerobic granular sludge process for sewage treatment. *Water Res.* 84, 207–217. <https://doi.org/10.1016/j.watres.2015.07.011>
- Pronk, M., Giesen, A., Thompson, A., Robertson, S., van Loosdrecht, M., 2017. Aerobic granular biomass technology: advancements in design, applications and further developments. *Water Pract. Technol.* 12, 987–996. <https://doi.org/10.2166/wpt.2017.101>
- Qiu, G., Liu, X., Saw, N.M.M.T., Law, Y., Zuniga-Montanez, R., Thi, S.S., Ngoc Nguyen, T.Q., Nielsen, P.H., Williams, R.B.H., Wuertz, S., 2020. Metabolic Traits of Candidatus Accumulibacter

- clade IIF Strain SCELSE-1 Using Amino Acids As Carbon Sources for Enhanced Biological Phosphorus Removal. *Environ. Sci. Technol.* 54, 2448–2458. <https://doi.org/10.1021/acs.est.9b02901>
- Qiu, G., Zuniga-Montanez, R., Law, Y., Thi, S.S., Nguyen, T.Q.N., Eganathan, K., Liu, X., Nielsen, P.H., Williams, R.B.H., Wuertz, S., 2019. Polyphosphate-accumulating organisms in full-scale tropical wastewater treatment plants use diverse carbon sources. *Water Res.* 149, 496–510. <https://doi.org/10.1016/J.WATRES.2018.11.011>
- Ranzinger, F., Matern, M., Layer, M., Guthausen, G., Wagner, M., Derlon, N., Horn, H., 2020. Transport and retention of artificial and real wastewater particles inside a bed of settled aerobic granular sludge assessed applying magnetic resonance imaging. *Water Res. X* 7, 100050. <https://doi.org/10.1016/j.wroa.2020.100050>
- Raunkjær, K., Hvitved-Jacobsen, T., Nielsen, P.H., 1994. Measurement of pools of protein, carbohydrate and lipid in domestic wastewater. *Wat. Res.* 28, 251–262. [https://doi.org/https://doi.org/10.1016/0043-1354\(94\)90261-5](https://doi.org/https://doi.org/10.1016/0043-1354(94)90261-5)
- Ravndal, K.T., Opsahl, E., Bagi, A., Kommedal, R., 2018. Wastewater characterisation by combining size fractionation, chemical composition and biodegradability. *Water Res.* 131, 151–160. <https://doi.org/10.1016/J.WATRES.2017.12.034>
- Rocktäschel, T., Klarmann, C., Ochoa, J., Boisson, P., Sørensen, K., Horn, H., 2015. Influence of the granulation grade on the concentration of suspended solids in the effluent of a pilot scale sequencing batch reactor operated with aerobic granular sludge. *Sep. Purif. Technol.* 142, 234–241. <https://doi.org/10.1016/j.seppur.2015.01.013>
- Roy, S., Guanglei, Q., Zuniga-Montanez, R., Williams, R.B., Wuertz, S., 2021. Recent advances in understanding the ecophysiology of enhanced biological phosphorus removal. *Curr. Opin. Biotechnol.* <https://doi.org/10.1016/j.copbio.2021.01.011>
- Rubio-Rincón, F.J., Welles, L., Lopez-Vazquez, C.M., Abbas, B., van Loosdrecht, M.C.M., Brdjanovic, D., 2019. Effect of Lactate on the Microbial Community and Process Performance of an EBPR System. *Front. Microbiol.* 10, 125. <https://doi.org/10.3389/fmicb.2019.00125>
- Rudelle, E., Vollertsen, J., Hvitved-Jacobsen, T., Nielsen, A.H., 2011. Anaerobic Transformations of Organic Matter in Collection Systems. *Water Environ. Res.* 83, 532–540. <https://doi.org/10.2175/106143010X12681059116699>
- Saunders, A.M., Albertsen, M., Vollertsen, J., Nielsen, P.H., 2016. The activated sludge ecosystem contains a core community of abundant organisms. *ISME J.* 10, 11–20. <https://doi.org/10.1038/ismej.2015.117>
- Schwarzenbeck, N., Borges, J.M., Wilderer, P.A., 2005. Treatment of dairy effluents in an aerobic granular sludge sequencing batch reactor. *Appl. Microbiol. Biotechnol.* 66, 711–718. <https://doi.org/10.1007/s00253-004-1748-6>
- Schwarzenbeck, Norbert, Erley, R., Mc Swain, B.S., Wilderer, P., Irvine, R.L., 2004. Treatment of malting wastewater in a granular sludge sequencing batch reactor (SBR). *Acta Hydrochim. Hydrobiol.* 32, 16–24. <https://doi.org/10.1002/ahch.200300517>
- Schwarzenbeck, N., Erley, R., Wilderer, P. a., 2004. Aerobic granular sludge in an SBR-system treating wastewater rich in particulate matter. *Water Sci. Technol.* 49, 41–46.
- Seviour, T., Derlon, N., Dueholm, M.S., Flemming, H.C., Girbal-Neuhauser, E., Horn, H., Kjelleberg, S., van Loosdrecht, M.C.M., Lotti, T., Malpei, M.F., Nerenberg, R., Neu, T.R., Paul, E., Yu, H., Lin, Y., 2019. Extracellular polymeric substances of biofilms: Suffering from an identity crisis. *Water Res.* <https://doi.org/10.1016/j.watres.2018.11.020>
- Sguanci, S., Lubello, C., Caffaz, S., Lotti, T., 2019. Long-term stability of aerobic granular sludge for the treatment of very low-strength real domestic wastewater. *J. Clean. Prod.* 222, 882–890.

- <https://doi.org/10.1016/j.jclepro.2019.03.061>
- Sophonsiri, C., Morgenroth, E., 2004. Chemical composition associated with different particle size fractions in municipal, industrial, and agricultural wastewaters. *Chemosphere* 55, 691–703. <https://doi.org/10.1016/j.chemosphere.2003.11.032>
- Stes, H., Caluwé, M., Dockx, L., Cornelissen, R., de Langhe, P., Smets, I., Dries, J., 2021. Cultivation of aerobic granular sludge for the treatment of food-processing wastewater and the impact on membrane filtration properties. *Water Sci. Technol.* 83, 39–51. <https://doi.org/10.2166/wst.2020.531>
- Stewart, P.S., 1998. A review of experimental measurements of effective diffusive permeabilities and effective diffusion coefficients in biofilms. *Biotechnol. Bioeng.* 59, 261–272. [https://doi.org/10.1002/\(SICI\)1097-0290\(19980805\)59:3<261::AID-BIT1>3.0.CO;2-9](https://doi.org/10.1002/(SICI)1097-0290(19980805)59:3<261::AID-BIT1>3.0.CO;2-9)
- Stokholm-Bjerregaard, M., McIlroy, S.J., Nierychlo, M., Karst, S.M., Albertsen, M., Nielsen, P.H., 2017. A Critical Assessment of the Microorganisms Proposed to be Important to Enhanced Biological Phosphorus Removal in Full-Scale Wastewater Treatment Systems. *Front. Microbiol.* 8, 718. <https://doi.org/10.3389/fmicb.2017.00718>
- Tian, Y., Chen, H., Chen, L., Deng, X., Hu, Z., Wang, C., Wei, C., Qiu, G., Wuertz, S., 2022. Glycine adversely affects enhanced biological phosphorus removal. *Water Res.* 209, 117894. <https://doi.org/10.1016/j.watres.2021.117894>
- Tijhuis, L., Hijman, B., Van Loosdrecht, M.C.M., Heijnen, J.J., 1996. Influence of detachment, substrate loading and reactor scale on the formation of biofilms in airlift reactors. *Appl. Microbiol. Biotechnol.* 45, 7–17. <https://doi.org/10.1007/s002530050641>
- Toh, S.K., Tay, J.H., Moy, B.Y.P., Ivanov, V., Tay, S.T.L., 2003. Size-effect on the physical characteristics of the aerobic granule in a SBR. *Appl. Microbiol. Biotechnol.* 60, 687–695. <https://doi.org/10.1007/s00253-002-1145-y>
- Toja Ortega, S., Pronk, M., de Kreuk, M.K., 2021a. Anaerobic hydrolysis of complex substrates in full-scale aerobic granular sludge: enzymatic activity determined in different sludge fractions. *Appl. Microbiol. Biotechnol.* 105, 6073–6086. <https://doi.org/10.1007/s00253-021-11443-3>
- Toja Ortega, S., Pronk, M., de Kreuk, M.K., 2021b. Effect of an Increased Particulate COD Load on the Aerobic Granular Sludge Process: A Full Scale Study. *Processes* 9, 1472. <https://doi.org/10.3390/pr9081472>
- Toja Ortega, S., van den Berg, L., Pronk, M., de Kreuk, M.K., 2022. Hydrolysis capacity of different sized granules in a full-scale aerobic granular sludge (AGS) reactor. *Water Res. X* 16, 100151. <https://doi.org/10.1016/j.wroa.2022.100151>
- Ubukata, Y., 1997. Kinetics of polymeric substrate (dextrin or peptone) removal by activated sludge: hydrolysis of polymers to monomers is the rate-determining step. *Water Sci. Technol.* 36, 159–167. [https://doi.org/10.1016/S0273-1223\(97\)00716-6](https://doi.org/10.1016/S0273-1223(97)00716-6)
- van den Berg, L., Pronk, M., van Loosdrecht, M.C.M., de Kreuk, M.K., 2022a. Density measurements of aerobic granular sludge. *Environ. Technol.* 1–11. <https://doi.org/10.1080/09593330.2021.2017492>
- van den Berg, L., Toja Ortega, S., van Loosdrecht, M.C.M., de Kreuk, M.K., 2022b. Diffusion of soluble organic substrates in aerobic granular sludge: Effect of molecular weight. *Water Res. X* 16, 100148. <https://doi.org/10.1016/j.wroa.2022.100148>
- van der Roest, H.F., de Bruin, L.M.M., Gademan, G., Coelho, F., 2011. Towards sustainable waste water treatment with Dutch Nereda® technology. *Water Pract. Technol.* 6. <https://doi.org/10.2166/wpt.2011.059>
- van Dijk, E., Pronk, M., van Loosdrecht, M., 2020. A settling model for full-scale aerobic granular

- sludge. *Water Res.* 186, 116135. <https://doi.org/10.1016/j.watres.2020.116135>
- van Dijk, E.J.H., Haaksman, V.A., van Loosdrecht, M.C.M., Pronk, M., 2022. On the mechanisms for aerobic granulation - model based evaluation. *Water Res.* 216, 118365. <https://doi.org/10.1016/j.watres.2022.118365>
- van Dijk, E.J.H., Pronk, M., van Loosdrecht, M.C.M., 2018. Controlling effluent suspended solids in the aerobic granular sludge process. *Water Res.* 147, 50–59. <https://doi.org/10.1016/J.WATRES.2018.09.052>
- Van Gaelen, P., Springael, D., Smets, I., 2020. A high-throughput assay to quantify protein hydrolysis in aerobic and anaerobic wastewater treatment processes. *Appl. Microbiol. Biotechnol.* 104, 8037–8048. <https://doi.org/10.1007/s00253-020-10751-4>
- van Loosdrecht, M.C.M., Eikelboom, D., Gjaltema, A., Mulder, A., Tijhuis, L., Heijnen, J.J., 1995. Biofilm structures. *Water Sci. Technol.* 32, 35–43. <https://doi.org/10.2166/wst.1995.0258>
- Wagner, J., Weissbrodt, D.G., Manguin, V., Ribeiro da Costa, R.H., Morgenroth, E., Derlon, N., 2015. Effect of particulate organic substrate on aerobic granulation and operating conditions of sequencing batch reactors. *Water Res.* 85, 158–166. <https://doi.org/10.1016/j.watres.2015.08.030>
- Wagner, M., Ivleva, N.P., Haisch, C., Niessner, R., Horn, H., 2009. Combined use of confocal laser scanning microscopy (CLSM) and Raman microscopy (RM): Investigations on EPS - Matrix. *Water Res.* 43, 63–76. <https://doi.org/10.1016/j.watres.2008.10.034>
- Wang, L., Liu, J., Oehmen, A., Le, C., Geng, Y., Zhou, Y., 2021. Butyrate can support PAOs but not GAOs in tropical climates. *Water Res.* 193, 116884. <https://doi.org/10.1016/j.watres.2021.116884>
- Wang, N., Peng, J., Hill, G., 2002. Biochemical model of glucose induced enhanced biological phosphorus removal under anaerobic condition. *Water Res.* 36, 49–58. [https://doi.org/10.1016/S0043-1354\(01\)00236-6](https://doi.org/10.1016/S0043-1354(01)00236-6)
- Weber, S.D., Ludwig, W., Schleifer, K.H., Fried, J., 2007. Microbial composition and structure of aerobic granular sewage biofilms. *Appl. Environ. Microbiol.* 73, 6233–6240. <https://doi.org/10.1128/AEM.01002-07>
- Weissbrodt, D.G., Neu, T.R., Kuhlicke, U., Rappaz, Y., Holliger, C., 2013. Assessment of bacterial and structural dynamics in aerobic granular biofilms. *Front. Microbiol.* 4. <https://doi.org/10.3389/fmicb.2013.00175>
- Weissbrodt, D.G., Shani, N., Holliger, C., 2014. Linking bacterial population dynamics and nutrient removal in the granular sludge biofilm ecosystem engineered for wastewater treatment. *FEMS Microbiol. Ecol.* 88, 579–595. <https://doi.org/10.1111/1574-6941.12326>
- Wentzel, M.C., Comeau, Y., Ekama, G.A., van Loosdrecht, M.C.M., Brdjanovic, D., 2008. Enhanced biological phosphorus removal, Biological wastewater treatment: principles, modelling and design. <https://doi.org/10.1080/00986449808912728>
- Winkler, M. K.H., Bassin, J.P., Kleerebezem, R., van der Lans, R.G.J.M., van Loosdrecht, M.C.M., 2012. Temperature and salt effects on settling velocity in granular sludge technology. *Water Res.* 46, 3897–3902. <https://doi.org/10.1016/j.watres.2012.04.034>
- Winkler, Mari K.H., Kleerebezem, R., Khunjar, W.O., de Bruin, B., van Loosdrecht, M.C.M., 2012. Evaluating the solid retention time of bacteria in flocculent and granular sludge. *Water Res.* 46, 4973–4980. <https://doi.org/10.1016/j.watres.2012.06.027>
- Winkler, U.K., Stuckmann, M., 1979. Glycogen, hyaluronate, and some other polysaccharides greatly enhance the formation of exolipase by *Serratia marcescens*. *J. Bacteriol.* 138, 663–670. <https://doi.org/10.1128/jb.138.3.663-670.1979>
- Xia, Y., Kong, Y., Nielsen, P.H., 2008a. In situ detection of starch-hydrolyzing microorganisms in

- activated sludge. *FEMS Microbiol. Ecol.* 66, 462–471. <https://doi.org/10.1111/j.1574-6941.2008.00559.x>
- Xia, Y., Kong, Y., Nielsen, P.H., 2007. In situ detection of protein-hydrolysing microorganisms in activated sludge. *FEMS Microbiol. Ecol.* 60, 156–165. <https://doi.org/10.1111/j.1574-6941.2007.00279.x>
- Xia, Y., Kong, Y., Thomsen, T.R., Halkjaer Nielsen, P., 2008b. Identification and ecophysiological characterization of epiphytic protein-hydrolyzing saprospiraceae ("Candidatus Epiflobacter" spp.) in activated sludge. *Appl. Environ. Microbiol.* 74, 2229–38. <https://doi.org/10.1128/AEM.02502-07>
- Yilmaz, G., Lemaire, R., Keller, J., Yuan, Z., 2008. Simultaneous nitrification, denitrification, and phosphorus removal from nutrient-rich industrial wastewater using granular sludge. *Biotechnol. Bioeng.* 100, 529–541. <https://doi.org/10.1002/bit.21774>
- Yu, C., Wang, K., Tian, C., Yuan, Q., 2021. Aerobic granular sludge treating low-strength municipal wastewater: Efficient carbon, nitrogen and phosphorus removal with hydrolysis-acidification pretreatment. *Sci. Total Environ.* 792, 148297. <https://doi.org/10.1016/j.scitotenv.2021.148297>
- Yun, Z., Yun, G.H., Lee, H.S., Yoo, T.U., 2013. The variation of volatile fatty acid compositions in sewer length, and its effect on the process design of biological nutrient removal. *Water Sci. Technol.* 67, 2753–2760. <https://doi.org/10.2166/wst.2013.192>
- Zeng, R.J., Lemaire, R., Yuan, Z., Keller, J., 2003. Simultaneous nitrification, denitrification, and phosphorus removal in a lab-scale sequencing batch reactor. *Biotechnol. Bioeng.* 84, 170–178. <https://doi.org/10.1002/bit.10744>
- Zengin, G.E., Artan, N., Orhon, D., Chua, A.S.M., Satoh, H., Mino, T., 2010. Population dynamics in a sequencing batch reactor fed with glucose and operated for enhanced biological phosphorus removal. *Bioresour. Technol.* 101, 4000–4005. <https://doi.org/10.1016/j.biortech.2010.01.044>
- Zhang, P., Shen, Y., Guo, J.-S., Li, C., Wang, H., Chen, Y.-P., Yan, P., Yang, J.-X., Fang, F., 2015. Extracellular protein analysis of activated sludge and their functions in wastewater treatment plant by shotgun proteomics. *Sci. Rep.* 5, 12041. <https://doi.org/10.1038/srep12041>







**Acknowledgements**

**Curriculum Vitae**

**List of Publications**

## Acknowledgements

This book would not have been finished without the guidance and support of so many good colleagues and friends, whom I would like to thank here.

First of all, thank you **Merle** for entrusting me with this project and giving me counsel and encouragement when I needed them. Your enthusiasm about AGS was contagious, and you always held an open door to discuss, vent, get inspired, and celebrate. You created a safe and supportive environment, and gave me plenty of opportunities to develop myself (only to mention some, participating in the AGS course, encouraging me to learn microbial community analysis, or enabling my stay in MSU). You've been an excellent role model. **Mario**, I have been lucky for having you involved in my project; your ideas and experience gave so much value to this thesis. It was always fun to chat with you and our meetings flew by. And I learned to deal with the "Dutch directness"! Too bad that since the Covid months our meetings became sparser.

**Lenno**, thank you for being my accomplice during this adventure. It was really fun to have you on my team, and I very much enjoyed our conversations in the lab, during our meetings, in the coffee corner or in the office. You've been a great source of inspiration too, and with your critical and challenging attitude you always pushed me a little bit further. I'm excited to see where life takes you and I hope our paths cross again.

I would like to thank my paranymp, roommate and friend **Magela**. You contributed to my feeling of a home away from home with your friendship, our discussions over PhD and life, your delicious parrilladas and heated discussions about how to speak Spanish correctly. You also amazed me with your karaoke singing skills. Academically we also had some valuable exchange, part of which led to our shared meme group. **Javier**, also founding member of such group, it's been very fun to see you craft in the lab, discuss about all sorts of interesting topics, and also to share chill PSOR nights which ended up with us closing the bar. You also helped a lot in the lab, thank you! Also **Pamela** thank you for being always ready to help out and for the good memories of our time in Delft. I'll gladly open pressure reactors for you anytime. **Antonella**, you've been a great support and really contributed to a cozy lab and office with your music and joy. With the special contribution of **Carina** and **Emiel**, I could see a little ray of sunshine when I crossed your office and always looked forward to hanging out with you. **Víctor**, carnal, it was a pleasure sharing so many nice moments, like making a lab piñata; **Hongxiao**, thanks for being such a caring and fun office mate; **Bruno**, you've got an ease to draw a smile on people's faces, eskerrik asko! I also thank my Water Management colleagues:

**Niels, Adrian, Bayardo, César, Guilherme, Dhavissen, Rogelio, Hamed, Ka Leung, Steef, Shreya, Mrinal, Mona, Job, Diana, Max, Lihua, Mingliang, Bin Lin, Sophie, Simon, Roos** and everyone in the department who made this journey enriching and fun.

My work would not have been possible without the invaluable help of the Water Management staff: **Armand, Mohammed, Patricia, Jane, Jasper, Sabrina, Mariska, Tamara** and **Riëlle**; thank you for making our lives easier! Thank you also **Astrid** for helping in the cryostat and making it so accessible for me. Thank you **Ben, Roel, Zita** and **Cor** for all the help in the EBT labs, and PhD colleagues at the EBT department for being so welcoming and always ready to help. Thank you **Edward** for introducing me in RHDHV projects and sharing full-scale data and advice. Thanks **Mark** for the help in Utrecht, the gezelligheid and the Dutch practice. I also would like to thank the colleagues at the CBE for having me in the final months of my PhD; specially **Cat** and **Kylie**. I loved the time in Bozeman, it was so enriching and fun.

I taught some but I certainly learnt a lot with my students, **Chiara, Samyuktha, Dante**, and **Nadia**. Thank you for your contributions to this project – and to my growth! Thanks **Quentin** too for your help in Garmerwolde, and **Mingyue** for collaborating with me in this project, even with the difficulties you encountered to work in the lab.

I would also like to thank those who opened the doors of this adventure for me: **José Luis**, for sparking my interest for water treatment and connecting me with TU Delft; **Jules** for welcoming me in the group, and **Julián** for being my first mentor in the Water Management department and assessing me over my career.

My sanity would not have lasted much without my friends and flatland climber crew, so you deserve a warm thank you too: **Carlos** and **Coco**, my family in NL, **David**, you're like the little brother (although older than me); **Jorge, Joan**, whom my car is named after; **Spyros, Nikolas, Domingos, Hannah, Fer, Philippe, Isa**. You all allowed me to free up some headspace when I needed it most. **Jeroen**, you've been the greatest support, always believing in me and pushing me to do so too. You were there in all the happy and sad moments, and brought me so much peace. **Wo**, a dear roommate and friend, thanks for making it feel like home! And thanks all the other friends that, even if not in the Netherlands, have been there through the years by my side.

Finalmente, no podría haber llegado hasta aquí sin el apoyo incondicional de mis padres y hermano. Siempre me habéis estimulado a desarrollarme tanto en lo académico como en lo personal. Durante el doctorado, habéis compartido mis éxitos y fracasos, siempre alentándome a seguir adelante. Buena parte de la escritura de esta tesis se dio en casa, en un sitio acogedor y alentador. Poco más se puede pedir. ¡Gracias!

## Curriculum Vitae

Sara Toja Ortega was born in Galdakao, Spain, on September 6<sup>th</sup>, 1993. From 2011 until 2015 she studied a Bachelor's degree in Biochemistry and Molecular Biology in the University of the Basque Country (UPV/EHU). She spent her graduation year in Queen's University, Ontario, Canada, through the exchange program TASSEP.



In 2016 she obtained an MSc degree in Microbiology in the Autonomous University of Madrid (UAM). She specialized in environmental microbiology, and completed her graduation work in the laboratory of microbiology of anaerobic environments, under the supervision of Prof. José Luis Sanz. There, she studied the conversion of glycerol to useful by-products (1,3-Propanediol, ethanol, hydrogen) in UASB reactors, testing different operating conditions. The interest in employing bioreactors to treat waste streams drove her to seek an internship in the Water Management Department of the Delft University of Technology (the Netherlands) after her MSc degree. She spent three months working on the project BioXtreme, treating phenol-containing wastewater using anaerobic membrane bioreactors. Afterwards, she continued in the Water Management Department to pursue her PhD under the supervision of Prof. Dr. Merle de Kreuk and Dr. Mario Pronk, and in collaboration with Lenno van den Berg. The aim of her PhD project was to understand the fate of polymeric substrates in aerobic granular sludge (AGS) and their effect on biofilm structure and process performance. In her final PhD year, she participated in the organization of the professional education (ProfEd) course "Aerobic granular sludge technology for wastewater treatment". She also spent five months on an exchange in the Center for Biofilm Engineering (CBE) in the Montana State University (MSU), continuing her PhD work. In the CBE, she applied bioorthogonal non-canonical amino acid tagging (BONCAT) and confocal microscopy to study active microorganisms in AGS under different feeding conditions.

Currently, Sara is seeking job opportunities to keep developing her career in environmental microbiology and biotechnology.

# List of Publications

## Publications

**Toja Ortega, S.**, Pronk, M., & De Kreuk, M. K. (2021). Anaerobic hydrolysis of complex substrates in full-scale aerobic granular sludge: enzymatic activity determined in different sludge fractions. *Applied Microbiology and Biotechnology*, 105(14-15), 6073-6086. DOI: 10.1007/s00253-021-11443-3

**Toja Ortega, S.**, Pronk, M., & De Kreuk, M. K. (2021). Effect of an increased particulate cod load on the aerobic granular sludge process: A full scale study. *Processes*, 9(8), 1472. DOI: 10.3390/pr9081472

Van den Berg, L., **Toja Ortega, S.**, Van Loosdrecht, M. C. M., & De Kreuk, M. K. (2022). Diffusion of soluble organic substrates in aerobic granular sludge: Effect of molecular weight. *Water Research X*, 16, 100148. DOI: 10.1016/j.wroa.2022.100148

**Toja Ortega, S.**, Van den Berg, L., Pronk, M., & De Kreuk, M. K. (2022). Hydrolysis capacity of different sized granules in a full-scale aerobic granular sludge (AGS) reactor. *Water Research X*, 16, 100151. DOI: 10.1016/j.wroa.2022.100151

## Conference contributions

**Toja Ortega, S.**, Pronk, M., & De Kreuk, M. K. (2020, February 12-14). Evolution of full scale aerobic granular sludge upon addition of a particulate-rich influent stream. [Oral presentation]. IWA Young Water Professionals Conference, Luxembourg, Luxembourg.

**Toja Ortega, S.**, Pronk, M., & De Kreuk, M. K. (2019, November 12-15). Localization of hydrolytic activity in aerobic granular sludge. [Oral presentation]. Young Water Professionals (YWP) Spanish chapter, Madrid, Spain.